Lysosomal Storage Disorders and Neurodegenerative Disease; related Mechanisms of Pathogenesis and identification of Novel Therapeutic Targets.

Luke J. Haslett

Ph.D 2015

Abstract

Lysosomal storage disorders (LSDs) are rare diseases caused by inherited mutations in genes coding for proteins of the endolysosomal system. The lysosome is an organelle responsible for the degradation of dysfunctional organelles and for the catabolism, and subsequent recycling, of macromolecules within the cell. When this process becomes defective the substrates of lysosomal catabolism accumulate; these can include lipids, proteins, polysaccharides, nucleotides and diverse combinations of all three. The phenotypic spectrum of these diseases in isolation, and even more so as a group, is extremely broad but an almost universal consequence of lysosomal dysfunction is severe, early onset neurodegeneration. Neurodegenerative diseases of ageing such as Alzheimer's disease, Parkinson's disease and Huntington's disease represent a major challenge to the provision of human healthcare in light of an ageing global population. Whilst some commonalities exist between these three diseases a myriad of hypotheses for the onset of pathology has been proposed. There is growing evidence for involvement of the lysosome in all three of these diseases.

We have been looking at specific lysosomal pathologies such as lipid storage, endocytosis and Ca^{2+} dysregulation in forms of these three neurodegenerative diseases of ageing whilst using LSDs as models to inform our study. We have found that lysosomal alkalisation in familial models of Alzheimer's disease results in changes to lipid and Ca^{2+} homeostasis in this compartment and identified a lysosomal ion channel, transient receptor potential cation channel, mucolipin subfamily, member 1 (TRPML1), as a key constituent of this process. Our study of models of Huntington's disease have implicated the Niemann-Pick type C1 protein (NPC1) in the pathogenesis of this disease and identified ways in which this could be therapeutically targeted. Finally, we have found evidence of Ca^{2+} dyshomeostasis throughout the cell in genetic models of Parkinson's disease which have defects in lysosomal proteins. Taken together, these studies strengthen the evidence for lysosomal involvement in neurodegenerative diseases of ageing, albeit with different mechanisms in each case, whilst expanding on the molecular basis for these processes. Accordingly, our understanding of the mechanisms underlying the pathogenesis of these diseases has improved and new therapeutic targets have been identified by these studies.

Acknowledgments

This Ph. D. studentship was funded by the BBSRC with supplementary funding from the MRC.

First up, I'd like to thank Emyr for his constant enthusiasm, dedication and camaraderie. The time has flown by. I'd also like to thank everyone who has been through the Lloyd-Evans lab, I've been there since it began and had the privilege to work with many great people as it has grown, even Maguire. Paramount among these though – Mat!!. oh Mat.

Thanks to Sun, Polly and Natalie for their help working with the neurons, the HD project wouldn't have gone anywhere without them. Likewise Profs Allen and Kemp for getting behind the project. Thanks also to the many students who have helped drive projects forward. Also thanks to our collaborator in the States from the Nixon lab. Hope I did something useful.

Also a special mention for my friend on the second floor – always a solid companion.

I'd like to thank my parents for always being supportive and motivating me to pursue my interests.

Finally, I'd like to thank Rachael for her love, understanding and support throughout the time I have been working towards this Ph. D. She has always been there when I needed her.

Table of Contents

Figures

Chapter 1

Chapter 2

Chapter 3

Abbreviations

7-DHC : 7 - Dehydrocholesterol
Aβ : Amyloid beta protein
ABCD 4 : ATP binding cassette, subfamily D, member 4
ACMA : 9-amino-6-chloro-2-methoxyacridine
AD : Alzheimer's Disease
ACerase : Acid ceramidase
ALS : Amyotrophic lateral sclerosis
AM : Acetoxymethyl ester
AMD : age related macular degeneration
AnA2 : Annexin A2
ANOVA : Analysis of variance
apH-1 : Anteriorpharynx defective 1
APOE : Apolipoprotein E
APOE4 : Apolipoprotein E4
APP : Amyloid precursor protein
ASM : Acid sphingomyelinase
ATP : Adenosine triphosphate
BBB : Blood brain barrier
BCA : Bicinchoninic acid
BD : Blastocyst-derived
BDNF : Brain derived neurotrophic factor
BM : bone marrow
BOD-LacCer : BODIPY - Lactosylceramide
BSA : Bovine serum albumin
cADPR : cyclic ADP ribose
CatB : Cathepsin B
CatC : Cathepsin C
CatD : Cathepsin D
CatL : Cathepsin L
CBE : Conduritol-β-epoxide
Cer : Ceramide
CERT : Ceramide ER transfer protein
CHMP2B : Charged multivesicular body protein 2B
Chol : Cholesterol

CICR : Ca^{2+} induced Ca^{2+} release

CLN1 : Ceroid lipofuscinosis, neuronal 1

CLN3 : Ceroid-lipofuscinosis, neuronal 3

CLN5 : Ceroid-lipofuscinosis, neuronal 5

CLN10 : Ceroid-lipofuscinosis, neuronal 10

CMA : Chaperone mediated autophagy

CMT : Charcot Marie Tooth

CNS : Central nervous system

Co-IP : co-immunoprecipitation

ConA : Concanamycin A

CSF : Cerebro-spinal fluid

CT : Computerised tomography

CTF : C-terminal fragment

CtxB : Cholera toxin B subunit

DA : Dopaminergic

DMEM : Dulbecco's modified Eagle's medium

DMEM/F12 : Dulbecco's modified Eagle's medium, F12 modification

DPBS : Dulbecco's phosphate buffered saline

DS : Down's syndrome

ECL : Enhanced chemiluminescence

EGF : Epidermal growth factor

EM : Electron microscopy

EMA : European medicines agency

EOAD : Early-onset Alzheimer's disease

ER : Endoplasmic reticulum

ERT : Enzyme replacement therapy

ESCRT : Endosomal sorting complexe required for transport

EU : European Union

FAD : Familial Alzheimer's Disease

FCS : Foetal calf serum

FGF : Fibroblast growth factor

FITC : Fluorescein isothiocyanate

FITC-SphO : FITC-tagged sphingosine

FTD : Frontotemporal dementia

GABA : Gamma-Aminobutyric acid

GalCer : Galactosylceramide

GCase : Glucocerebrosidase

GlcCer : Glucosylceramide

GlcSph : Glucosylsphingosine

GSL : Glycosphingolipid

GPN : Glycyl-L-phenylalanine 2-napthylamide

GWAS : Genome wide association study

HBSS : Hank's balanced salt solution

HD : Huntington's disease

HIP1 : Huntingtin interacting protein 1

HF : Human fibroblast

HIV : Human immunodeficiency virus

HPβCD : Hydroxy-propyl-β-cyclodextrin

HPTLC : High-performance thin layer chromatography

HSC70 : Heat-shock cognate protein 70

HTT : Huntingtin

IgG : Immunoglobulin G

IP_3 : Inositol triphosphate

iPSC : induced pluripotent stem cell

iTRAQ : isobaric tags for relative and absolute concentration

KRS : Kufor-Rakeb syndrome

LacCer : Lactosylceramide

LAL : Lysosomal acid-lipase

LAMP 1 : Lysosome associated membrane protein 1

LAMP 2 : Lysosome associated membrane protein 2

LAMP2A : Lysosome associated membrane protein 2A

LBPA : Lysobisphosphatidic acid

LC3 : Microtubule-associated protein 1A/1B-light chain 3

LDL : Low-density lipoprotein

LED : Light-emitting diode

LGE : Lateral ganglionic emergence

LIEV : Luminal intraendosomal vesicles

LIMP-2 : Lysosome membrane protein 2

LOAD : Late-onset Alzheimer's Disease

LRRK2 : Leucine rich repeat kinase 2

LSD : Lysosomal storage disorder

M6P : Mannose-6-phosphate

M6PR : Mannose-6-phosphate receptor

MAPT : Microtubule associated protein Tau

MCOLN1 : Mucolipin 1

MEF : Mouse embryonic fibroblast

mHTT : mutant Huntingtin

MLIV : Mucolipidosis type IV

MLN64 : metastatic lymph node 64 protein

ML-SA1 : Mucolipin synthetic agonist 1

MPS : Mucopolysaccharidosis

MR CatB : Magic red cathepsin B substrate

MR Cat L : Magic red cathepsin L substrate

MRI : Magnetic resonance imaging

mTORC : mammalian Target of rapamycin complex

MVB : Multivesicular body

NAADP : nicotinic acid adenine dinucleotide phosphate

NAADP-AM : nicotinic acid adenine dinucleotide phosphate acetoxy methyl ester

***N*B-DNJ :** *N*-butyl-deoxynojirimycin

NCL : Neuronal ceroid lipofuscinoses

NFT : Neurofibrillary tangle

NPC : Niemann-Pick type C

NPC1 : Niemann-Pick type C1

NPC2 : Niemann-Pick type C2

NSC : Neural stem cell

ORAI : Calcium release-activated calcium channel protein 1

PA : Phytic acid

PDL : Poly-D-lysine

PEN : Presenilin enhancer protein

PET : Positron emission tomography

PFA : Paraformaldehyde

PGRN : Progranulin

PI : Phosphoinositol

PI(3,5)P2 : Phosphoinisitol 3,5-bisphosphate

PL : Phospholipid

polyQ : Poly-glutamine

PS : Presenilin

PS1 : Presenilin 1

PS1/2 : Presenilin 1 and 2

PS2 : Presenilin 2

PTFE : Polytetrafluoroethylene

PVDF: Polyvinylidene fluoride

Rab 5 : Ras-related protein Rab-5

Rab 7 : Ras-related protein Rab-7

Rab11 : Ras-related protein Rab-11

REST : RE1-silencing transcription factor

ROI : Region of interest

RPE : Retinal pigment epithelium

RyR : Ryanodine Receptor

S-1-P : Sphingosine-1-phosphate

SERCA2 : Sarcoplasmic endoplasmic reticulum ATPase 2

SERCA3 : Sarcoplasmic endoplasmic reticulum ATPase 3

SLOS : Smith-Lemli-Opitz Syndrome

SNARE : Soluble NSF Attachment Protein receptor

SNpc : Substantia Nigra pars compacta

SOCE : Store-operated Ca^{2+} entry

SphB : Sphingoid base

SphM : Sphingomyelin

SphO : Sphingosine

SRT : Substrate reduction therapy

STD : Standard

STIM : stromal interaction molecule

TFEB : Transcription factor EB

TLC : Thin layer chromatography

TMED4 : Transmembrane emp24 protein domain containing

TMEM106B : Transmembrane protein 106B

TPC2 : Two-pore channel 2

TRND : Therapeutics for rare and neglected diseases

TRPM8 : Transient receptor potential cation channel, subfamily M, member 8

TRPML1 : Transient receptor potential cation channel, mucolipin subfamily, member 1

TRPML3 : Transient receptor potential cation channel, mucolipin subfamily, member 3

UCH-L1 : Ubiquitin carboxyl-terminal estrase L1

UPS : Ubiquitin proteasomal system

vATPase : Vacuolar ATPase

VSP10 : Vacuolar sorting protein 10

VTA : Ventral tegmental area

WT : Wild type

Chapter 1

Introduction

1.1. – The Lysosome

Lysosomes are membrane bound organelles with an acidic lumen primarily responsible for macromolecular degradation and recycling within cells. Present in all mammalian cell types, with the exception of mature red blood cells, they were initially characterised as a 'cellular stomach', situated at the terminus of the endocytic system where they digest macromolecules delivered by endocytosis, phagocytosis and autophagy (Appleqvist et al., 2013). More recently, however, they have increasingly been recognised as important signalling compartments (Morgan et al., 2011); mediators of secretion and plasma membrane repair (Andrews et al., 2014); key players in energy metabolism and lipid homeostasis (Settembre et al., 2014) and interactors with other cellular compartments (Penny et al., 2015). Accordingly lysosomes are now recognised as vital contributors to, and potential therapeutic targets for, a myriad of diseases such as cancer (White, 2015), cardiovascular disease (Mei et al., 2015) and neurodegenerative conditions (Nixon, 2013) in addition to the lysosomal storage disorders (LSDs) which are caused by a loss of function in lysosomal proteins (Cox and Chachon Gonzalez, 2012).

Lysosomes were discovered, somewhat serendipitously, by Christian De Duve after a study of enzymes present in different fractions of liver homogenate, separated by centrifugation, revealed an interesting phenomenon. In freshly prepared fractions the activity assay of the liver enzyme, non-specific acid phosphatase, appeared abnormally low but recovered when samples stored in a refrigerator for 5 days were re-assayed. Further experimentation involving biochemical activation of the enzyme suggested that the acid phosphatase must be enclosed within membranous sacs. Utilising this enzyme activity assay De Duve and colleagues were able to study which cellular fractions the enzyme was present in; in doing so they found a distribution pattern spread between mitochondrial and microsomal fractions. From this they established that the enzyme was probably associated with a novel group of particles different from both mitochondria and microsomes. Accordingly, they developed a more selective five-fraction centrifugation procedure and discriminated between the organelles present in these particles by using enzyme markers. Using this process five additional enzymes were found to be concentrated in the same fraction as acid-phosphatase. Four of these were hydrolases with acidic pH optimum sharing the latency properties of acid-phosphatase. The fifth was non-latent and was later traced to another new cytoplasmic particle with similar physical properties to

lysosomes which De Duve and colleagues named the peroxisome. Due to the presence of five acid hydrolases in the same membrane limited cytoplasmic particle, a digestive function was proposed for these structures and the term lysosome (Greek for 'digestive bodies') was coined (Applemans et al., 1955; de Duve et al., 1955; de Duve, 2005).

Further electron microscopy (EM) studies showed that lysosomes were electron dense organelles of heterogeneous shape and size which contribute about 5% to the overall volume of the cell (Luzio et al., 2007). The general structure of a lysosome is shown in figure 1.1.1.

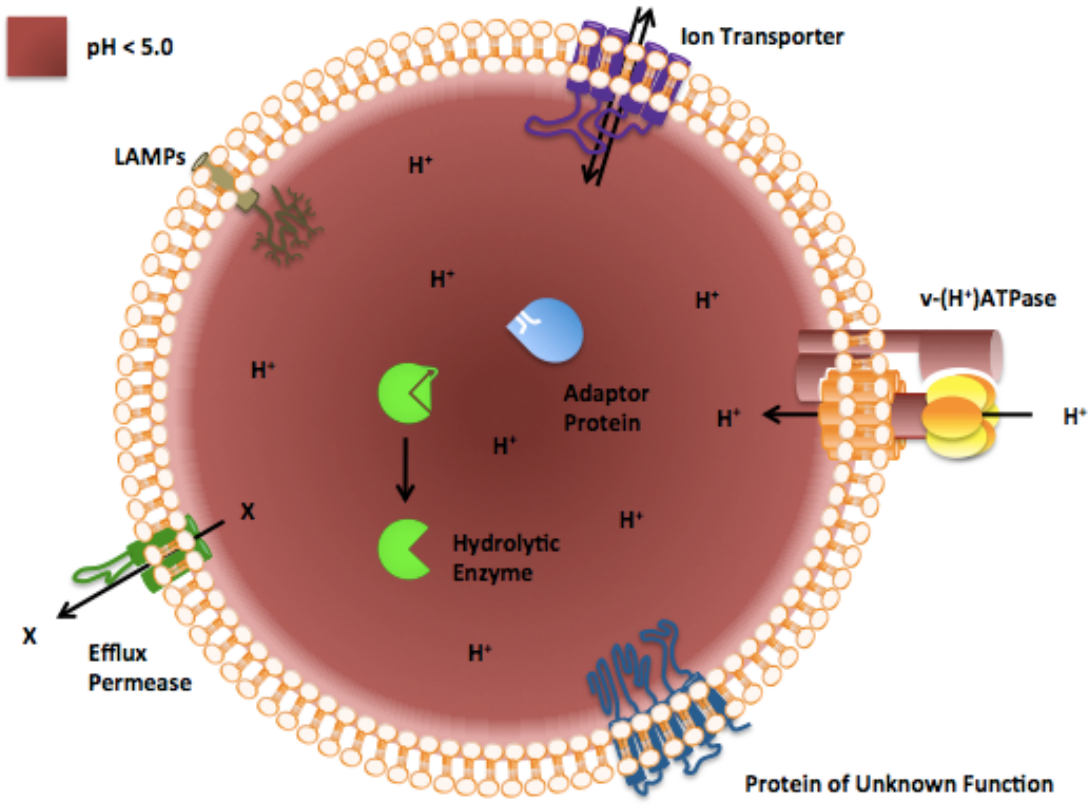

Figure 1.1. – Basic characteristics of the lysosome*. The soluble proteins such as hydrolytic enzymes and adaptor proteins are detailed alongside transmembrane proteins of a variety of functions. The lumen is maintained at low pH by active translocation of proteins facilitated by the vATPase protein complex. X is a generalised representation of a specific transport substrate.*

1.1.1. – The lysosomal membrane and lysosomal transmembrane proteins

The lysosomal membrane has a heavily glycosylated inner lumen referred to as the glycocalyx which is mainly composed of lysosomal membrane associated proteins 1 and 2 (LAMP1 and 2). These transmembrane glycoproteins help to prevent the lysosome from self-digestion thus maintaining lysosomal integrity (Schwake et al., 2013). This role is illustrated by a study which showed increased lysosome mediated cell death in response to chemotherapeutic agents in tumour cells which had decreased levels of LAMP1 and LAMP2 (Fehrenbacher et al., 2008).

In addition to the LAMP proteins there are at least 50 other lysosomal transmembrane proteins which are targeted to this compartment by dileucine or tyrosine motifs (Schwake et al., 2013). A number of these transmembrane proteins are known to be vital to the correct function of lysosomes as inherited mutations in the genes which code these proteins cause LSDs (eg. The Niemann-Pick type C1 disease protein or NPC1) (Carstea et al., 1997). Although a vast array of research has been conducted into these proteins many of their functions still remain elusive. In fact a prominent reason for the identification of many of these proteins is that the genes coding for them were identified as mutated in patients with LSDs.

A subset of lysosomal transmembrane proteins, such as the lysosomal cobalamin transporter ATP-binding cassette, subfamily D, member 4 (ABCD4), function as efflux permeases to allow the recycling of substrates produced by degredative processes in the synthesis of new macromolecules (Coelho et al., 2012). The coupling of hydrolytic enzymes and efflux permeases form a salvage pathway, which leads into the synthesis of macromolecules in an energetically favourable fashion when compared to *de novo* synthesis (Kitatani et al., 2008).

Ion transport into and out of lysosomes is facilitated by an array of specific transporters and channels. Concerted action of these proteins maintain metal ion homeostasis vital for proper lysosomal function. Transition metal ions arrive in the lysosomal lumen after endocytic degradation of macromolecules such as the plasma protein ceruloplasmin which carries divalent copper ions (Cu^{2+}). Chemically active ions such as Cu^{2+} combined with the acidic environment of the lysosome promotes Fenton-like chemical reactions which generate free radicals and lead to lysosomal membrane damage (Kurz et al., 2010). Extrusion of Cu^{2+} from the lysosomal lumen is

facilitated by copper-transporting ATPase 2 in order to prevent such processes (Guggilla et al., 2015). Other chemically active ions such as Fe^{2+}, Fe^{3+}, Mn^{2+}, Zn^{2+} and Co^{2+} can also cause damage to lysosomal membranes so must be removed from the lumen. Various proteins facilitate this although, not all the pathways have been delineated and a number of these proteins appear to be selective for more than one ion (Kiselyov et al., 2011). As such, these pathways and the diseases which arise or are compounded by their deregulation remain a major area of research.

In addition to ion export, lysosomes require appropriate concentrations of ions that are important in cellular signalling, such as Ca^{2+}, for normal function. This is particularly important in relation to fusion with other endocytic vesicles (Luzio et al., 2007). Accordingly, some ion transporters in the lysosomal membrane are responsible for the import of these ions. These will be discussed in section 1.3.

1.1.2. – Proteins of the lysosomal lumen

Hydrolytic enzymes are situated in the lysosomal lumen and drive catabolism. These enzymes, which have acidic pH optima, degrade a wide variety of macromolecules such as proteins, carbohydrates, lipids, RNA and DNA often in a sequential and stepwise manner into their constituent parts (Schroder et al., 2010). As these enzymes are synthesised in the endoplasmic reticulum (ER), transport pathways are required for the enzymes to be delivered to the lysosome where proteolytic removal of propeptides from the proenzyme is the final step in the production of active enzyme (Braulke and Bonifacino, 2009).

1.1.3 – Transport of functional proteins to the lysosome

The majority of lysosomal proenzymes are delivered by the mannose-6-phosphate (M6P) receptor pathway. This begins with addition of a mannose containing oligosaccharide to proteins in the ER before the translocation to the *cis*-Golgi alongside other proteins of the secretory pathway. Here a specific phosphotransferase facilitates the specific addition of GlcNac-1-phosphate to specific mannose residues on the protein. The resultant phosphodiester-tagged protein is translocated to the trans Golgi and the M6P tag is exposed by phosphodiesterase mediated removal of GlcNac residues (Braulke and Bonifacino, 2009).

Lysosomal proenzymes can now bind to the M6P receptor (M6PR) and the complex translocates to the endolysosomal system due to presence of dileucine motifs, a process which utilises adaptor proteins such as adaptor protein 2 (AP2), on the cytoplasmic tails of M6PRs (Mattera et al., 2011). M6PRs have the greatest affinity for the bound proenzymes at pH 6-7, accordingly, as the complex progresses through the endolysosomal system to more acidic compartments dissociation of the proenzyme occurs. The M6PR is recycled to the Golgi from the late-endosome, whilst the proenzyme progresses to the lysosome where it is cleaved and activated by enzymes such as cathepsin D (Braulke and Bonifacino, 2009).

Some lysosomal proenzymes utilise M6P independent pathways to reach the lysosome. A particular example of this is lysosomal membrane protein 2 (LIMP2) which transports β-glucosidase proenzyme from the Golgi to the lysosome (Zachos et al., 2012). β-glucosidase, like many lysosomal enzymes, is 'tethered' to membranes by specific post-translational glycosylation. This brings β-glucosidase to an area where it can associate with LIMP2 in a pH-dependant manner similar to M6PR-proenzyme binding. LIMP2 has transmembrane domains, one of which has a short cytoplasmic tail containing a dileucine motif, which allows the complex to translocate to the endosome and the proenzyme can dissociate in the more acidic compartments (Blanz et al., 2015). Cathepsin-mediated cleavage then mediates conversion from proenzyme to enzyme.

A final characterised pathway for transport of proteins to the lysosome utilises Vacuolar sorting protein 10 (VSP10) family members including sortilin and SorlA (sortilin-related receptor). These are suggested to be multifunctional receptors capable of transporting numerous proteins such as the adaptor protein prosaposin (Canuel et al., 2009) and lysosomal enzymes such as cathepsin D in a manner that does not require glycosylation (Canuel et al., 2008).

1.1.4. – Lysosomal activator proteins

In order for proper function of hydrolytic enzymes, particularly those which degrade complex lipids, a class of soluble proteins called activator proteins are required. These proteins solubilise and present specific substrates to their companion enzymes for example Saposin C presents glucosylceramide to β-glucosidase in an

energetically favourable orientation to allow efficient catabolism (figure 1.1.). Saposin C is one of four homologous proteins produced by sequential proteolytic cleavage of prosaposin (Vaccaro et al., 1997). An illustration of the importance of these proteins comes from the observation that loss of function can lead to lysosomal storage phenotypes virtually indistinguishable from loss of function in the specific acid hydrolase they interact with (Grabowski and Horowitz 1997).

1.1.5. – Lysosomal pH maintenance

The entire array of lysosomal proteins are reliant on the correct pH in the lysosome which is typically between 4.5 – 5.0 dependant upon cell type (Wolfe et al., 2013). As such, the vacuolar-type H^+ ATPase (vATPase) enzyme complex responsible for transporting H^+ ions into the lysosome is a 'master regulator' of lysosomal function. The mammalian vATPase enzyme complex consists of 13 subunits which can be sub-divided into 8 peripheral proteins (V1 proteins) and 5 membrane intrinsic proteins (V0) many of which have various isoforms that exhibit cell-specific expression profiles (Toei et al., 2010). Functionally the vATPase can be divided into subdomains (Muench et al., 2011). The ATP catalytic subdomain is a heterohexameric structure which utilises ATP hydrolysis to power the central rotor. This motion is then transferred to the ion pump subunit which takes the form of a rotating ring constructed from multiple subunits and can transfer protons into the lysosomal lumen against the concentration gradient (Saroussi and Nelson, 2009). Whilst the vATPase is the best understood regulator of lysosomal acidification the less well characterised Cl^-/H^+ antiporter CLC-7 also provides key contributions to lysosomal pH homeostasis (Graves et al., 2009) and further study of the interplay between both of these remains an important field of research.

From discussion of the major protein classes responsible for lysosomal function we can see that the lysosome is an intricately regulated organelle which is not only optimised as the degredative centre of the cell but can interact with various other cellular organelles and metabolic pathways. The intricate regulation of lysosomal activity also illustrates how dysfunction in a single protein in the lysosome can lead to a myriad of complex pathologies within the lysosome and as a result within cells and organisms.

1.2. – The greater lysosomal system

Although lysosomes are commonly presented as a defined organelles they are dynamic compartments constantly fusing with other compartments and remodelling as they separate again. Accordingly, viewing lysosomes as just a store of acid hydrolases, without appreciation of the cycles of fusion and fission with late endosomes and autophagosomes, prevents the full appreciation of its role as an important hub in cellular homeostasis. It also prevents a thorough understanding of how dysfunction within this hub can impact the entire cell. As such we must view lysosomes within the greater lysosomal system (figure 1.2.) and take into account the interactions that occur between it and the major cellular pathways such as endocytosis (Pryor et al., 2009), autophagy (Nixon, 2013), proteasomal degradation (Ryhanen et al., 2009), signalling and Ca^{2+} homeostasis (Morgan et al., 2011). This interdependence between lysosomes and the pathways which contribute to the greater lysosomal system is exemplified by the discovery of a gene regulatory network linking the greater lysosomal system at the transcriptional level. This 471 gene CLEAR (Co-ordinated Lysosomal Expression and Regulation) network is governed by the master gene transcription factor EB (TFEB) (Settembre et al., 2015).

1.2.1 - Endocytosis

Endocytosis is an important cellular pathway responsible for the internalisation of cell surface and extracellular material which is a vital process linking a cell to its external environment. An example of this is neurons of the central nervous system (CNS) utilising endocytosis in order to recycle neurotransmitters, a process which contributes to both signalling and neuroplasticity (Melikian 2004).

The canonical representation of the endocytic pathway progresses from the plasma membrane proceeding through increasingly acidic endosomal compartments, the early then late endosomes, to the lysosome. The initial stages of this pathway are characterised by the molecular components of the initial membrane invaginations resulting in two major pathways: clathrin-dependent endocytosis and clathrin-independent endocytosis (Mayor and Pagano, 2007). Clathrin-dependent endocytosis utilises clathrin coated pits on the plasma membrane to internalise receptor/cargo complexes. The resultant small (~100 nm) vesicles are sorted at the early endosome where a proportion are recruited back to the plasma membrane as

recycling endosomes or progress to the lysosome for degradation and subsequent recycling of products (Mousavi et al., 2004). Clathrin-independent endocytosis often occurs at small (50nm) flask-like invaginations in the plasma membrane named caveolae which in concert with the endosomal system organise membrane microdomains which are vital to cell signalling (Mayor and Pagano 2007). Other forms of clathrin-independent endocytosis are macropinocytosis, which forms large vesicles up to 5μm consisting of extracellular debris suspended in fluid, and phagocytosis in specialised cells (Lim and Gleeson 2007).

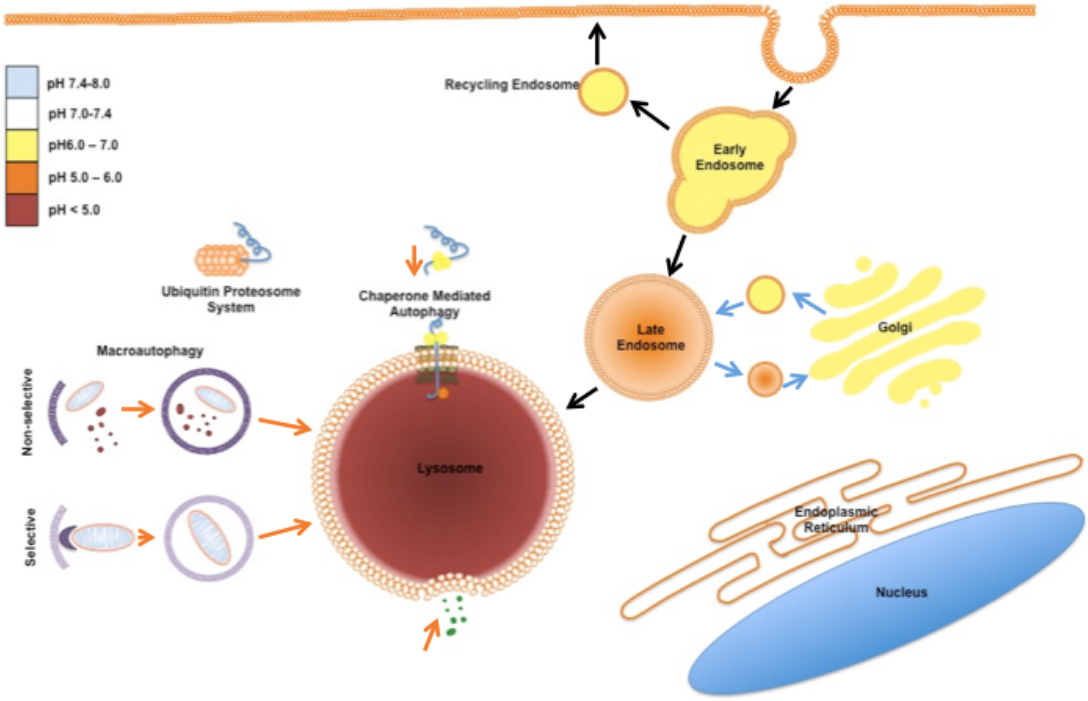

Figure 1.2. – The greater endolysosomal system. *Endocytic pathways are detailed by black arrows, autophagic processes by orange arrows and interactions with the Golgi by blue arrows. pH is shown by the key on the left hand side of the image.*

Beyond the initial invagination of defined regions of plasma membrane and subsequent scission to generate the early endocytic vesicles which fuse to form early endosomes (Huotari and Helenius, 2011) there are common steps in the onward transport of cargo. These are membrane budding to form nascent vesicles and transport to a defined destination followed by docking and fusion with the target membrane (Scott et al., 2014). These processes are facilitated by various protein families which interact with the endocytic vesicles manipulating them accordingly (Cullen 2008).

The Annexin proteins, such as Annexin A2, are one of these families. Annexin A2 is a Ca^{2+}-dependent phospholipid binding protein which interacts with actin in order to regulate the location of endocytic vesicles (Babiychuk et al., 2006). Rab proteins are a family of 40 or so small GTPases which play a vital role in endocytic processes; particularly vesicle tethering (Zerial and McBride 2001). For example Rab5A helps facilitate tethering of early and late endosomes (Porteryaev et al., 2010) and Rab7 is a key mediator of tethering between late-endosomes and lysosomes (Vanlandingham and Ceresa 2009). Tethering allows SNARE complex formation, the constituents of which are dependant upon the types of tethered vesicles. Once the SNARE complex forms, fusion can be initiated by release of Ca^{2+} from the vesicle lumen and a hybrid organelle is formed from the late-endosome and lysosome (Luzio et al., 2007).

As the hybrid organelle contains the full complement of lysosomal enzymes, and appropriate pH, it is proposed to be the site of macromolecule degradation. In this situation the lysosome itself is fundamentally an enzyme storage granule which periodically undergoes fusion with the late-endosome to form the hybrid organelle which is the degradative compartment. The lysosomes must then reform in a complex process that appears to require the retromer complex, lumenal Ca^{2+} sequestration (Pryor et al., 2000) and the endolysosomal cation channel TRPML1.

In addition to the hybrid organelles, multi-vesicular bodies are present as a subset of the compartments constituting the endolysosomal system. These contain membrane bound intraluminal vesicles which result from membrane invagination. These can also fuse with lysosomes and are extremely important in lipid catabolism (Wang et al., 2011).

However, as the processes governing fusion and fission of these compartments and their constant state of flux, the majority of the literature (particularly that describing disease processes), still employs the classical description of the late endosome and lysosome as separate compartments with the major degradative processes occurring in the lysosome. For clarity this model, shown in figure 1.2., will be used in this thesis.

With these different methods of internalisation and scope for deviation from the degredative pathway the endocytic system can co-ordinate recycling of cell surface receptors, deliver signalling ligands to the correct locations within the cell and

internalise and reorganise membrane components (Scott et al., 2014). As these activities are tightly regulated within the endocytic system it can easily be understood that correct lysosomal function is necessary to maintain the availability of the many constituents required for the cell to orchestrate these pathways.

1.2.2. – Autophagy

As shown in figure 1.2.1. the lysosome is also the endpoint for the various autophagic pathways within cells. There are three of these 'self-eating' pathways currently characterised and in concert they are vital for the maintenance of cellular energy and metabolic homeostasis (Nixon 2013).

The simplest of these pathways in microautophagy during which the lysosome remodels its membrane in order to directly engulf cytosolic material by pinocytosis. This is generally a non-specific process although micropexophagy, piecemeal microautophagy of the nucleus, and micromitophagy can be activated in response to specific cellular stresses (Li et al., 2012).

Chaperone mediated autophagy (CMA) is a selective form of proteolysis which degrades specific cytoplasmic proteins after direct translocation across the lysosomal membrane. Proteins targeted for CMA contain a pentapeptide KFERQ motif which is recognised by the cytosolic chaperone heat shock cognate protein of 70kD (HSC70). Substrate bound HSC70 interacts with lysosomal-associated membrane protein 2A (LAMP-2A) and the substrate unfolds before active translocation across the lysosomal membrane and subsequent proteolytic degradation (Cuervo and Wong., 2014).

Macroautophagy involves the formation of double-membrane vesicles which sequester regions of the cytosol into structures known as autophagosomes, which are mildly acidic and can be characterised by the presence of the phosphatidylethanolamine lipidated protein, LC3-II (Kabeya et al., 2000). This process is most often associated with clearance of dysfunctional organelles such as aged mitochondria but it may also be used for the degradation of lipids, carbohydrates, polyubiquinated proteins and RNA (Eskelinen and Saftig, 2009). The majority of these are subject to non-selective microautophagy however a number of selective pathways are present such as mitophagy (for the degradation of

mitochondria) and pexophagy (for the degradation of superfluous peroxisomes) (Farre et al., 2013). Regardless of the method of induction the end-point is fusion with the endolysosomal system before degradation of the autophagosomal cargo. Accordingly, optimal lysosomal function is essential for the efficient clearance of autophagosomes and a reduction of autophagosomal flux is observed in most LSDs (Ballabio and Gieselmann 2009; Raben et al., 2009). It is interesting to note that a reduction in autophagosomal flux is also associated with ageing and neurodegenerative disease (Nixon, 2013).

1.2.3 - The ubiquitin proteasomal system

Although the ubiqutin proteasomal system (UPS) does not directly involve transit of substrates through the lysosome it is the major degredative pathway for short-lived cytosolic proteins and, as such, co-ordinates some of its proteolytic activities with autophagic pathways which are directly lysosomal dependant. Autophagic induction has been observed in response to proteasome inhibition (Ryhanen et al., 2009) suggesting a compensatory role. This is further evidenced by an increase in polyubiquinated proteins, the primary substrate for proteasome degradation, in response to inhibition of autophagy (Lilienbaum, 2013). It has been suggested that the UPS may compensate for the reduced autophagic flux observed in neurodegenerative disease states (Nedelsky et al., 2008). This remains a potentially interesting area for further research.

1.2.4 - Interaction with other cellular compartments

In addition to the other constituents of the lysosomal system the lysosome also must interact with other cellular organelles beyond their degradation (mitophagy, pexophagy) and trafficking of enzymes to the lysosome from the ER via the Golgi (discussed in 1.1.3). An area of particular interest is lysosome and ER membrane contact sites which may play roles in lipid trafficking and Ca^{2+} homeostasis. These membrane contact sites are regions of close apposition (<20nm) between organelles and it has been predicted that around 82% of lysosomes are in contact with the ER in human fibroblasts (Penny et al., 2015). With such a high proportion of lysosomes in contact with the ER these microdomains have emerged as an interesting new area of research which also extend to other compartments in the endocytic system.

Lysosomes also play a key role as mediators of plasma membrane repair. In response to 'cell wounding' (survivable disruption to the plasma membrane) Ca^{2+} influx induces lysosomal exocytosis and lysosomes from a specific pool fuse with the breach. This results in the luminal epitopes of lysosomal proteins such as LAMP-1 being exposed to antibodies applied to non-permeabilised cells (Andrews et al.,2014).

Considering lysosomes as part of the greater endolysosomal system and their interaction with other cellular compartments and organelles, the necessity for intricate regulation becomes obvious. Correct homeostasis of the important signalling ion, Ca^{2+}, is vital for this.

1.3 – Ca^{2+} regulation in the endolysosomal system

With the appreciation of the lysosome as a dynamic compartment situated at the hub of a pathway which is vital to cellular homeostasis has come an understanding that strict molecular regulatory systems must govern the interaction of all components of the endocytic system. After it was recognised that the endolysosomal system represented a significant reservoir of intracellular Ca^{2+} (Morgan et al., 2011), and given the role of Ca^{2+} in regulating vesicular fusion and trafficking, lysosomes emerged as a key regulator of endolysosomal function (Luzio et al., 2007). Known Ca^{2+} concentrations along with key proteins involved in endolysosomal Ca^{2+} regulation are shown in figure 1.3.

1.3.1. – The endolysosomal system as a Ca^{2+} store

When endocytosis occurs at the plasma membrane, delivering material to the early endosome, the cell also takes in a large amount of extracellular fluid which contains a high concentration of Ca^{2+} (1mM) (Lloyd-Evans et al., 2010). A study of early-endosomal Ca^{2+} levels using endocytosed Ca^{2+} and pH probes revealed that Ca^{2+} was lost from the endosome within a few minutes during which time endosomal acidification took place. Interestingly the acidification of endosomes was inhibited by reductions in extracellular Ca^{2+} and Ca^{2+} loss from the endosomes was blocked by inhibition of the vATPase suggesting an interaction between these two aspects of early-endosomal function (Gerasimenko et al., 1998). The protein underlying this reaction is transient receptor potential cation channel, mucolipin subfamily, member

3 (TRPML3) – a Ca^{2+} release channel located in the early endosomal membrane which allows Ca^{2+} to flow from the early endosomal lumen to the cytosol at a mildly acidic pH (Martina et al., 2009).

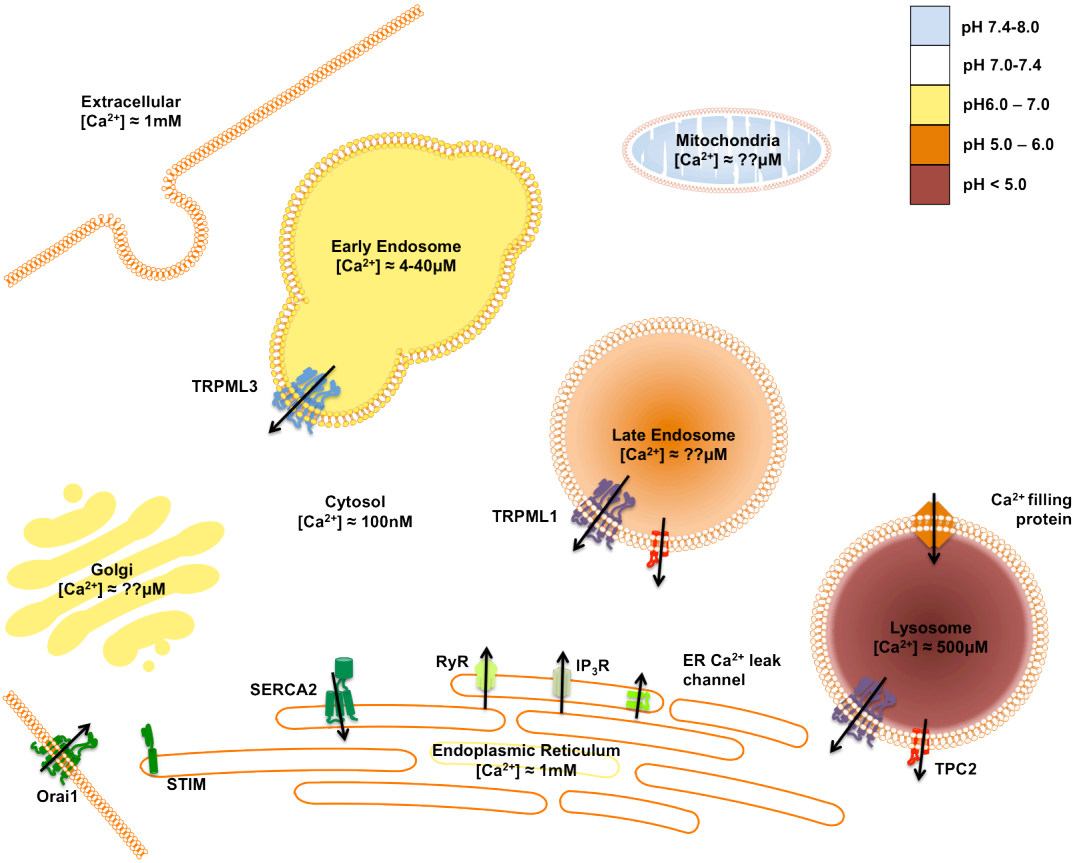

Figure 1.3. – Cellular Ca^{2+} stores with illustrations of important channels for Ca^{2+} flux. *Defined Ca^{2+} concentrations of various stores are shown, pH of different compartments is illustrated by the key on the right of the diagram. The direction of Ca^{2+} movement through channels is shown by arrows. Adapted from Lloyd- Evans et al., 2010*

Shortly after endocytosis, material is contained within endosomes of low Ca^{2+} concentration (4-40 μM) and a mildly acidic pH (pH~6). Subsequent studies have shown that lysosomal Ca^{2+} is approximately 500 μM (pH 4-4.5) (Lloyd-Evans et al., 2008). This shows that past a certain point in the endolysosomal system, Ca^{2+} efflux is abolished and the store actively fills with Ca^{2+}. Currently it remains unclear at what point in the endocytic system this occurs and the concentration of Ca^{2+} in the late endosome has not yet been characterised (Lloyd-Evans et al. 2010). The presence of putative leak channels, such as transient receptor potential cation channel, mucolipin subfamily, member 1 (TRPML1), which are active at around pH 5 (similar to late endosomal pH) (Raychowdhury et al., 2004) suggests that late-endosomal Ca^{2+} concentration is below that of the lysosome and that reduction in the levels of

Ca^{2+} in the homotypic organelle is required for the subsequent fission and return to discrete compartments.

1.3.2 - Endolysosomal Ca^{2+} influx channels

Another unknown in Ca^{2+} regulation in the endocytic system is the identity of the proteins which regulate Ca^{2+} influx. Information from *Saccharomyces cerevisiae* and *Arabidopsis thaliana* reveal two types of protein capable of transporting Ca^{2+} into the vacuole - the approximate equivalent of the lysosome in these organisms. Whilst the first type of protein (H^+/Ca^{2+} exchangers) are not present in mammals (Lloyd-Evans et al., 2010) Ca^{2+} ATPases, the other type of protein, have been observed in mammals. In addition to this, Ca^{2+} ATPase activity has been reported in lysosomal preparations and a specific isoform of the sarcoplasmic/endoplasmic reticulum Ca^{2+} ATPase (SERCA) SERCA3a has been identified as the protein responsible for Ca^{2+} entry into platelet dense-core granules (a lysosome related organelle) (Lopez et al., 2005). Further information comes from the reserve granule of sea urchin egg homogenate – another approximate equivalent to the lysosome. In this system Ca^{2+} entry required a proton gradient and ATP but was only slightly sensitive to vanadate – suggestive of ATPase function but not that of a P-type ATPase as these proteins are inhibited by Vanadate (Churchill et al., 2002). It still remains to be seen if either or indeed both of these classes of channel are present within lysosomal membranes.

Although much work is still required to investigate endolysosomal Ca^{2+} influx channels, a number of endolysosomal Ca^{2+} efflux channels have been identified, although the precise function and ion selectivity of many of these channels remain a subject of spirited debate. Two channels important to the work contained in this thesis are discussed below.

1.3.2.1 – TRPML1

TRPML1 (also known as mucolipin 1, MCOLN1) is a selective cation channel found in the late endosomes and lysosomes. It is required for correct functioning of these compartments as evidenced by the studies of cells from patients with Mucolipidosis type IV (section 1.5.3.) who have mutations in the gene *MCOLN1* which codes for TRPML1 (Sun et al., 2000).

It has long been established that TRPML1 is permeable to Ca^{2+} however various studies have also reported outward permeability (from the lumen to the cytoplasm) to K^{+}, Na^{+}, Fe^{2+} and Zn^{2+} (Kiselyov et al., 2009; Dong et al., 2009). A potential confounding factor in these studies is that they are often made under non-physiological conditions either adding high concentrations of the ions in question or utilising lysosomes which are expanded by treatment with vacuolin-1 a cell-permeable triazine. Vacuolin-1 recruits various compartments of the endolysosomal system to create a fused compartment the majority of which is composed of early endosomes, which have low levels of lumenal Ca^{2+} (Gerasimenko et al., 1998; Cerny et al., 2004). Importantly, only the permeability to Ca^{2+} has been replicated by various groups under different experimental conditions (Raychowdhury et al., 2004) suggesting that TRPML1 is indeed permeable to Ca^{2+} in an outward direction.

TRPML1 open probability and, therefore, Ca^{2+} release is modulated in two ways. The first of these is due to a change in pH. Raychowdhury *et al.* demonstrated that reductions in pH reduced the open probability of TRPML1 but this did not occur in TRPML1 channels with mild disease causing mutations (Raychowdhury et al., 2004). This data is suggestive of a role for TRPML1 in Ca^{2+} release from late endosomes. Secondly, agonists for TRPML1 have been characterised. The first is Phosphoinositol (3,5)-bisphosphate ($PI(3,5)P_2$) a lipid present in low concentrations within cells mainly localised in the endolysosomal system. The enzyme Fab1/PIKfyve is responsible for the synthesis of $PI(3,5)P_2$ from PI(3)P and this lipid can then act as an endogenous ligand of TRPML1 by increasing the open probability of the channel (Dong et al., 2010). This process is thought to be important to the fission of late-endosomes and lysosomes vital for correct endocytic function (Luzio et al., 2007). A synthetic agonist of Mucolipin, Mucolipin Synthetic Agonist 1 (ML-SA1) has also recently been discovered (Shen et al., 2012) and this has allowed further study of TRPML1. This was identified by chemical screening of a known agonist of the related channel TRPML3 and it has been noted that care needs to be taken when using this agonist as it can activate related channels (TRPML2 and TRPML3). It is also interesting to note that there are differences in channel activation in response to MLSA1 dependant upon the species of TRPML1 being investigated. For example ML-SA1 can activate murine TRPML1 in the absence of $PI(3,5)P_2$ (Shen et al., 2012) whereas ML-SA1 increases the sensitivity to $PI(3,5)P_2$ in *D.melanogaster*. (Feng et al., 2014). Accordingly, experiments using this agonist must be carefully controlled.

There is also debate as to whether or not nicotinic acid adenine dinucleotide phosphate (NAADP), one of the major intracellular messengers promoting Ca^{2+} release, invokes Ca^{2+} release from TRPML1 (Zhang et al., 2011). This finding remains to be confirmed by multiple research groups as NAADP stimulation of a different lysosomal Ca^{2+} efflux channel, TPC2, has been.

1.3.2.2. – TPC2

Two-pore segment channel 2 (TPC2) has been shown to localise to the late-endosomes and lysosomes and contain the dileucine motifs required to target proteins to this locale (Brailoiu et al. 2010). A concerted period of study suggested TPC2 as the target for Ca^{2+} release from acidic stores in response to NAADP after overexpression and knockdown studies produced the expected changes in NAADP response (Ruas et al., 2015). More specific recordings of TPC2 in lipid bilayers and patch-clamped methods revealed Ca^{2+} permeability and gating by NAADP, a study by Pitt *et al.* used immunopurified TPC2 incorporated into a lipid bilayer to provide additional data regarding the pH range in which TPC2 is activated (Pitt et al., 2010). This study showed that TPC2 is a dual sensor of luminal Ca^{2+} and pH and that at low pH it binds NAADP reversibly to TPC2 allowing for sustained Ca^{2+} release, whereas at neutral pH NAADP becomes irreversibly bound preventing subsequent activation.

There has been some recent controversy suggesting that TPC2 is an NAADP-independent Na^{2+} channel stimulated instead by $PI(3,5)P_2$ (Wang et al., 2012). This study may have been influenced by the complication that experimentally manipulating a single protein within the endolysosomal system tends to have implications for the function of other proteins. Recently it has been shown that this study also utilised a mouse model as a TPC2 knockout when 90% of the protein was still present and subsequent experiments were used to show that TPC2 is indeed a Ca^{2+} permeable channel stimulated by NAADP (Ruas et al., 2015).

1.3.3. – The endolysosomal system in relation to cellular Ca^{2+} homeostasis

As with the degredative aspects of lysosomal function, the lysosome and endolysosomal Ca^{2+} regulation cannot be correctly considered without appreciation of the impact of other cellular Ca^{2+} stores.

The most abundant of these Ca^{2+} stores is the ER which has a luminal Ca^{2+} concentration of ~1mM (Lloyd-Evans et al., 2012). This store has been extensively characterised as the location of Ca^{2+} release in response to the two other major intracellular Ca^{2+} release messengers; inositol triphosphate (IP_3) and cyclic adenosine triphosphate ribose (cADPR) (Verkhratsky, 2002). The study of ER Ca^{2+} has also benefitted from extensive pharmacological manipulation of the store by inhibition and stimulation of key Ca^{2+} uptake and release proteins. One example of this is thapsigargin mediated inhibition of SERCA2, leading to an increase in cytosolic Ca^{2+}, as the inward pumping of Ca^{2+} ions by this Ca^{2+} ATPase prevents filling of the ER Ca^{2+} store, leading to the unmasking of Ca^{2+} leak channels such as Presenilin 1 (Bezprozvanny, 2009). This causes subsequent Ca^{2+} induced Ca^{2+} release (CICR) from ryanodine receptors and IP_3 receptors (Shoback et al., 1995). Another mechanism is specific stimulation of the ryanodine receptor family of Ca^{2+} release channels by ryanodine, crucial in processes such as neurotransmission, which is also inhibitory at higher concentrations (Lloyd-Evans et al., 2003).

As previously mentioned, lysosome-ER membrane contact sites have been suggested to play important roles in Ca^{2+} homeostasis (Penny et al., 2015). Interestingly, release of Ca^{2+} from lysosomes by osmotic swelling in response to the glycyl-L-phenylalanine 2-napthylamide (GPN), an agent commonly used to induce lysosomal Ca^{2+} release, generates subsequent Ca^{2+} release from the ER by CICR (Kilpatrick et al., 2013). CICR has been recapitulated after stimulation of TPC2 by NAADP and both pheneomena may centre around lysosome-ER membrane contact sites. Due to this, CICR must always be considered when measuring lysosomal Ca^{2+} release as the ER Ca^{2+} store is more concentrated and of a larger volume than the lysosome. Accordingly, this secondary release, which is difficult to resolve temporally, may overwhelm lysosomal Ca^{2+} release and prevent correct analysis of the lysosomal Ca^{2+} store.

1.4. – Lipids and the endolysosomal system

Another key regulator of endolysosomal function is correct lipid composition throughout the different compartment membranes. This is not only important as lipids are highly bioactive molecules which can mediate and/or modulate a great deal of protein function but also because lysosomes are the centres for lipid catabolism and

as such must be able to efficiently process large amounts of lipid (Kolter and Sandhoff, 2005). Due to this, an understanding of lipid biochemistry, including biosynthesis and breakdown, is required to properly understand lysosomal function and to investigate the causes and consequences of lysosomal dysfunction. The most well studied class of lipids associated with the endolysosomal system are the sphingolipids, although given the fact the 'sphingo' moniker was given to this class of lipids to reflect their enigmatic nature it is unsurprising that, there still remains a great deal to learn about these lipids (Hannun, 2008).

1.4.1. – Sphingolipid Biosynthesis

The *de novo* biosynthesis of sphingolipids begins on the cytosolic face of the ER with serine palmitoyl transferase facilitating the condensation of L-serine and palmitoyl CoA to generate 3-ketosphinganine. This is reduced to sphinganine by 3-ketosphinganine reductase followed by sphinganine *N*-acyl transferase mediated acylation to form dihydroceramide. In mammals, this step is carried out by 1 of 6 ceramide synthases which are expressed in a tissue specific manner to provide sphingolipids with appropriate chain lengths for that tissue. Dihydroceramide is subsequently reduced by dihydroceramide desaturase to form ceramide, the hydrophobic membrane anchor of sphingolipids which now contains a sphingosine backbone (Gault, et al., 2010).

Further metabolism, to either sphingomyelin (SphM) or glycosphingolipid (GSL), ceramide must be transported by either the ceramide ER transfer protein (CERT) or secretory vesicle flow to the cytosolic leaflet of the Golgi Apparatus. Here a glucose moiety may be added to ceramide to form the simplest of the glycosphingolipids glucosylceramide (GlcCer) by glucosylceramide synthase. The subsequent addition of a galactose moiety to form lactosylceramide (LacCer) is performed by lactosylceramide synthase which is situated within the Golgi lumen where GlcCer must be transported by either multidrug transporters or the GlcCer transporter protein four-phosphate adaptor protein 2 (FAPP2) (Gault et al., 2010). The sialylation (addition of a sialic acid group) of LacCer by GM3 synthase on the *cis*-Golgi produces the simple ganglioside, GM3, from which concurrent sialylation reactions produce firstly GD3 and the subsequently GT3. In turn GM3, GD3 and GT3 are the Ganglioside precursors of the o, a and b series of gangliosides. Using the a series as an example GM3 has a GalNac group added by a glycosyltransferase to form GM2

which undergoes a subsequent glycosylation to add a further galactose moiety forming GM1a before sialylation of the terminal galactose forms GD1a. These terminal steps of Ganglioside biosynthesis occur at the trans Golgi where cell type specific differential expression of multiple sialylases and glycosylases form the myriad of glycosphingolipids (GSLs) produced (Simpson et al., 2004). After biosynthesis these complex GSLs reach the outer leaflet of the plasma membrane, where they generate membrane heterogeneity and facilitate transmembrane signalling events via the secretory system (Gault et al., 2010).

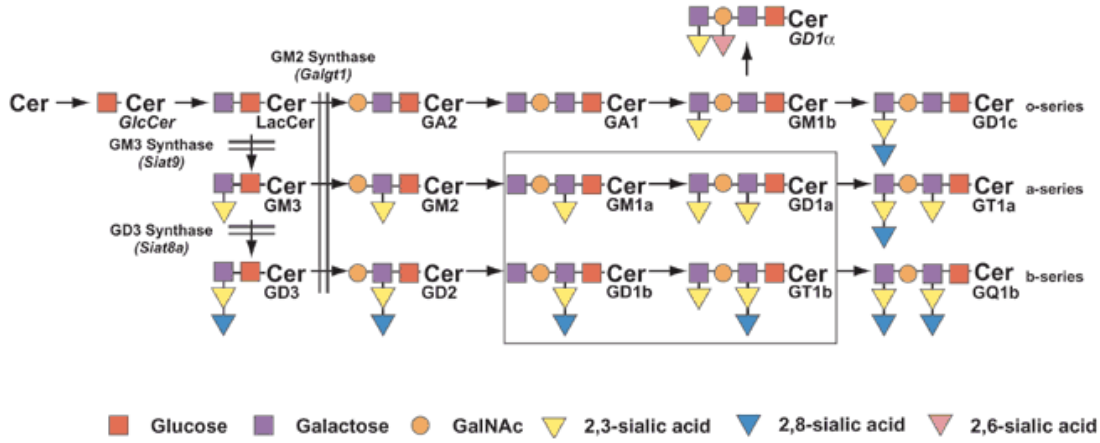

Figure 1.4. – The ganglioside biosynthetic pathway. *Sugar constituents are described in the key below the figure. Ganglioside biosynthetic enzymes linked to disease are also shown. Image taken from Simpson et al., 2004.*

The important membrane lipid sphingomyelin is formed on either the cytoplasmic side of the trans-Golgi or at the plasma membrane where the transferase sphingomyelin synthase joins ceramide with phosphatidylcholine (Gault et al., 2010. *De novo* production of sphingolipids from first principles is often not the major production route as in some cell types salvage pathways, predominantly lysosomal salvage of sphingosine, contribute up to 90% of GSL generation (Schulze and Sandhoff, 2011). Accordingly, correct sphingolipid catabolism is vitally important to cells.

1.4.2. – Sphingolipid Catabolism

Sphingolipids, primarily located in the outer leaflet of the plasma membrane, are degraded in lysosomes after internalisation by the endolysosomal system although some sphingolipids present in other membranes may reach the lysosomes as a result of autophagy. Within the endolysosomal system lipids are internalised to

luminal intraendosomal vesicles (LIEVs) generated by budding and fission events under the control of the endosomal sorting complex required for transport (ESCRT). It is thought that LIEVs are targeted for degradation in the lysosome by a lipid sorting process beginning early on in the endolysosomal system (Schulze and Sandhoff, 2011).

LIEVs are platforms for sphingolipid catabolism as they separate lipids from the glycocalyx and expose them to the aqueous interface required for the function of adaptor proteins and hydrolytic enzymes both of which are water soluble. As previously mentioned, the enzymes and adaptor proteins work in concert to degrade GSLs in a stepwise manner by removal of terminal sugar residues (Schulze and Sandhoff, 2011). As illustrated in figure 1.5., the loss of activity in either the enzyme or adaptor protein required for each step results in a lysosomal storage disorder in which the sphingolipid preceding this step is the primary storage substrate.

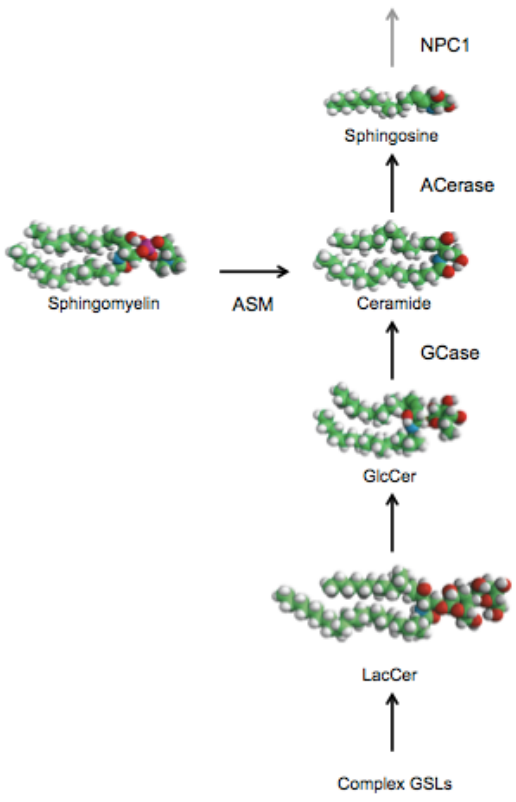

Figure 1.5. – Lysosomal sphingolipid catabolism. *Selected lysosomal catabolic pathways which lead into the production of ceramide and subsequently the sphingoid base sphingosine. Lysosomal catabolism is indicated by black arrows, grey arrow indicates the efflux of lipids from the lysosome. Degredative enzymes are as follows: ACerase (acid ceramidase), ASM (acid sphingomyelinase), GCase (glucocerebrosidase). The NPC1 protein is also indicated as it is required for lysosomal sphingosine efflux.*

In addition to the presence of the activated proteins in an acidic environment, anionic lipids are required for sphingolipid degradation. This was demonstrated by the *in vitro* observation that GM2 was not degraded by the enzyme, hexosaminidase, in liposomal membranes which did not contain anionic lipids – subsequent addition of

the anionic phospholipid, lysobisphosphatidic acid (LBPA), was required to stimulate the reaction. It is interesting to note that in liposomes with greater than 10 mol% anionic phospholipids, GlcCer can be degraded by its specific catabolic enzyme glucocerebrosidase in the absence of saposin C. When the concentrations of luminal cholesterol and LBPA in the endolysosomal system are compared, cholesterol concentrations decrease with pH while the LBPA concentrations increase. The result of this is that LIEVs in the lysosome are cholesterol-depleted and LBPA-rich resulting in a structure of high membrane fluidity and curvature optimised for sphingolipid degradation by hydrolytic enzymes. This process of LIEV formation predominantly takes place in the multivesicular bodies where the highly unsaturated phospholipid LBPA is required to generate curvature of membranes (Schulze and Sandhoff, 2011).

As previously mentioned, salvage pathways are able to remove certain degradation products from the catabolic pathway to feed back into biosynthesis of new GSLs. Complete GSL degradation results in the simplest of these, ceramide. Ultimately by the action of acid ceramidase this is degraded to the sphingoid base sphingosine (Park and Schuchman, 2006). This can leave the lysosome by an undefined mechanism where it can be utilised by ceramide synthases to produce ceramide and is the classical example of sphingolipid recycling (Gault et al., 2010). Sphingosine, however, may also be converted to sphingosine-1-phosphate by specific phosphatases; which is a critical signalling molecule, and this process illustrates how lysosomal catabolism and efflux of substrates can impact upon multiple other cellular pathways (Kunkel et al., 2013). Turnover of this molecule and the sugar constituents of GSLs is a vital energy saving measure for the cell as it is estimated by *in vitro* experiments that half the plasma membrane is endocytosed per hour, although not all this material is degraded but a significant amount is recycled to the membrane by lipid transport pathways (Schulze and Sandhoff, 2011)

1.4.3. – Endolysosomal Sphingolipid Transport Pathways

From discussion of lipid catabolic pathways we can see that lysosomal lipid transport is vital for cell membrane homeostasis. For sphingolipids, the transport of ganglioside GM1 is well studied using fluorescent or radiolabelled analogues. These lipids are internalised by endocytosis of the plasma membrane although it does not appear to be reliant on a specific endocytic pathway. The majority of GM1 is sorted in the early

endosome and recycled back to the plasma membrane without metabolic processing by vesicles budding from late endosomal compartments. Those gangliosides not immediately recycled are transported to the Golgi apparatus in healthy cells, where they can be trafficked to the plasma membrane by secretory vesicle flow with or without further modification (Pagano et al., 2000). It is unclear which endolysosomal vesicles these lipids pass through and at what point they leave the endocytic system. Evidently some of these gangliosides traverse the entire endocytic system and are targeted to lysosomes for degradation (Pagano et al., 2003). What is clear about this pathway, however, is that it is dysregulated in LSDs as discussed in section 1.5. When deregulated, it is hypothesised that sphingolipids can 'escape' the endolysosomal system and be transferred to the ER. Although this pathway remains hypothetical, the results of sphingolipid interference with ER processes such as Ca^{2+} homeostasis has been widely reported (Vitner et al., 2010; Lloyd-Evans et al., 2003).

From the above discussion it is clear that sphingolipid processing in the endolysosomal system is intrinsically linked to correct cell function and, when defective, is a cause of disease. While the array of proteins illustrate the complex protein network required for sphingolipid processing, biophysical interactions with other lipids are also key. The importance of the anionic phospholipid LBPA has been described, however, the biosynthetic and degredative pathways controlling levels of this lipid remain elusive (Chevallier et al., 2008). The delivery of another lipid, cholesterol, which interacts biophysically with sphingolipids in the endolysosomal system is better understood but questions still remain as to how it is distributed from this system.

1.4.4. – Cholesterol and the Endolysosomal System

Cholesterol is internalised in cells by clathrin-dependant endocytosis of low density lipoprotein (LDL) complexed to the LDL receptor until acidification of the endosomal system promotes dissociation in late endosomes (Chang et al., 2006). While the LDL receptor is recycled back to the plasma membrane, free cholesterol is liberated from LDL by the enzyme acid lipase, inherited dysfunction in which is the basis of the LSD Wolman's disease (Du et al., 2013; Hoffman et al., 1993). Free cholesterol can then be transported to the ER in a dynamin-dependant process where it is effluxed to the plasma membrane or to mitochondria for the production of steroid hormones (Robinet et al., 2006; Miller, 2013). Beyond disruption to LIEV membrane fluidity this

efflux is important as it impacts upon cholesterol intake and efflux in addition to the regulation of cholesterol synthesis by negative feedback (Bjorkhem et al., 2010).

The redistribution of cholesterol to the plasma membrane involves vesicular transport under the control of Rab11 and MLN64 mediated cholesterol transport to mitochondria (Hollta-Vuori and Ikonen, 2006). As the biophysical properties of cholesterol allow 'flip-flop' translocation within lipid bilayers without assistance from proteins it is entirely possible that cholesterol efflux may occur as a result of membrane dynamics at ER-lysosome contact sites (Hamilton 2003). Another proposed mechanism suggests cholesterol is effluxed by an, as yet undefined, transport protein to cytosolic sterol carrier proteins. A candidate for the cholesterol transporter arose from study of the LSD Niemann-Pick type C after cells from patients with this disease were observed to have endolysosomal free cholesterol accumulation (Carstea et al. 1997). Two proteins are associated with this disease, further discussed in section 1.5.2., a late-endosomal and lysosomal transmembrane protein, NPC1, and a soluble lysosomal glycoprotein NPC2 (Scott and Ioannou, 2004;Infante et al., 2003). It has been shown experimentally that NPC2 can bind cholesterol in the lysosomal lumen and that the N-terminus of NPC1 can also bind cholesterol (Infante et al., 2003, Kwon et al., 2009). This led to the proposal that NPC2 removes cholesterol from LIEVs before 'handing-off' cholesterol to NPC1 for efflux from the endolysosomal system. Whilst this proposal still remains an elegant solution it has not been proved, despite considerable effort, that NPC1 can transport cholesterol. Other contentions remain to be addressed, which will be discussed in section 1.5.2. (Lloyd-Evans and Platt, 2010). More recently, the lysosomal membrane protein LIMP-2 has been shown to be capable of functioning as a cholesterol efflux channel (Neculai et al., 2013).

Discussion of the endolysosomal system has revealed the inherent complexity that is associated with this important cellular pathway. Accordingly it remains unsurprising that loss of function in proteins active within this system, leading to LSDs, result in severe cellular dysfunction and complex disease pathology.

1.5. – Lysosomal Storage Disorders

Lysosomal storage disorders (LSDs) are a group of 70 or so genetically distinct inborn conditions with a combined frequency estimated to be between 1 in 5000 and 1 in 7500 live births (Cox and Chacon Gonzalez, 2012) although this may be higher when misdiagnosed or undiagnosed cases are accounted for (Platt et al., 2012) and new technologies such as whole exome sequencing provide insight which may pertain to milder variants of disease (Wassif et al., 2015). Interestingly, LSDs are also prevalent in the animal kingdom with naturally occurring variants of human diseases identified in animals from mice (Lopez and Scott, 2008) to flamingos (Zeng, 2008.).

LSDs are predominantly caused by loss of function mutations in lysosomal enzymes or late-endosomal and lysosomal transmembrane proteins. As a result macromolecular storage occurs which can include accumulation of glycosaminoglycans (Coutinho et al., 2012), glycosphingolipids, cholesterol (Lloyd-Evans et al., 2010) and lipofuscin (Seehafer and Pearce, 2006); a heterogeneous storage material associated with the majority of neurodegenerative diseases and ageing (Ottis et al., 2012). Although the primary storage material in some LSDs is clearly defined, controversy exists with regard to which molecule is stored first in others (Lloyd-Evans and Platt, 2010). Further complexity is added to this situation by significant overlap in secondary storage materials between LSDs. As a result it is also extremely difficult to determine which storage material, or materials, trigger different aspects of pathogenesis (Vitner et al., 2010).

The further subdivision of LSDs into classes is fraught with difficulty due to convergent storage profiles, defects in proteins of unknown function and in some cases such as the ‘enigmatic lysosomal disorders’, known as lipofuscinoses, where genetic defects are present in apparently unrelated genes not all of which are present in the endolysosomal pathway although in all cases lipofuscin is stored (Platt et al., 2012). However, the classical subdivision of LSDs by storage substrate still remains useful. These major classes of LSDs are shown in the table below with some specific LSDs important to this thesis detailed.

Primary Class	Sub-class	Disease	Protein deficiency	Primary storage material	Secondary storage materials	Other organelles affected	Inheritance	Gene symbol and localisation
Lipidoses	Sphingolipidoses	Gaucher Disease	β-Glucosidase	GlcCer, GlcSph	Chol (ER)	ER	Autosomal recessive	*GBA1* 1q21
			Saposin C	GlcCer, GlcSph	Chol (ER)	ER	Autosomal recessive	*PSAP* 10q21-q22
		Niemann-Pick type C	NPC1	SphO	Chol, GSLs, LBPA, SphM	Mitochondria	Autosomal recessive	*NPC1* 18q11-q12
			NPC2		Chol, GSLs, LBPA, SphO, SphM	Mitochondria	Autosomal recessive	*NPC2* 14q24.3
	Mucolipidoses	Mucolipidosis type IV	TRPML1	Unknown	Lipofuscin			*MCOLN1 19p13.2*
Mucopolysaccharidoses		MPS diseases	Glycoamnoglcan degredative enzymes	GAGs	GSLs		Majority autosomal recessive, one X-linked recessive	
Lipofuscinoses		NCL diseases	Various lysosomal and some non-lysosomal proteins	Unknown	Disparate group of diseases characterised by lipofuscin accumulation	ER	Autosomal recessive	

Table 1.1. – General classification of lysosomal storage disorders. LSDs important to this thesis are detailed. *GlcCer = glucosylceramide, GlcSph = glucosylsphingosine, GSLs = Glycosphingolipids, SphO = Sphingosine, SphM = Sphingomyelin, Chol = Cholesterol, GAGs = glycosaminoglycans. (Matha and Winchester, 2012)*

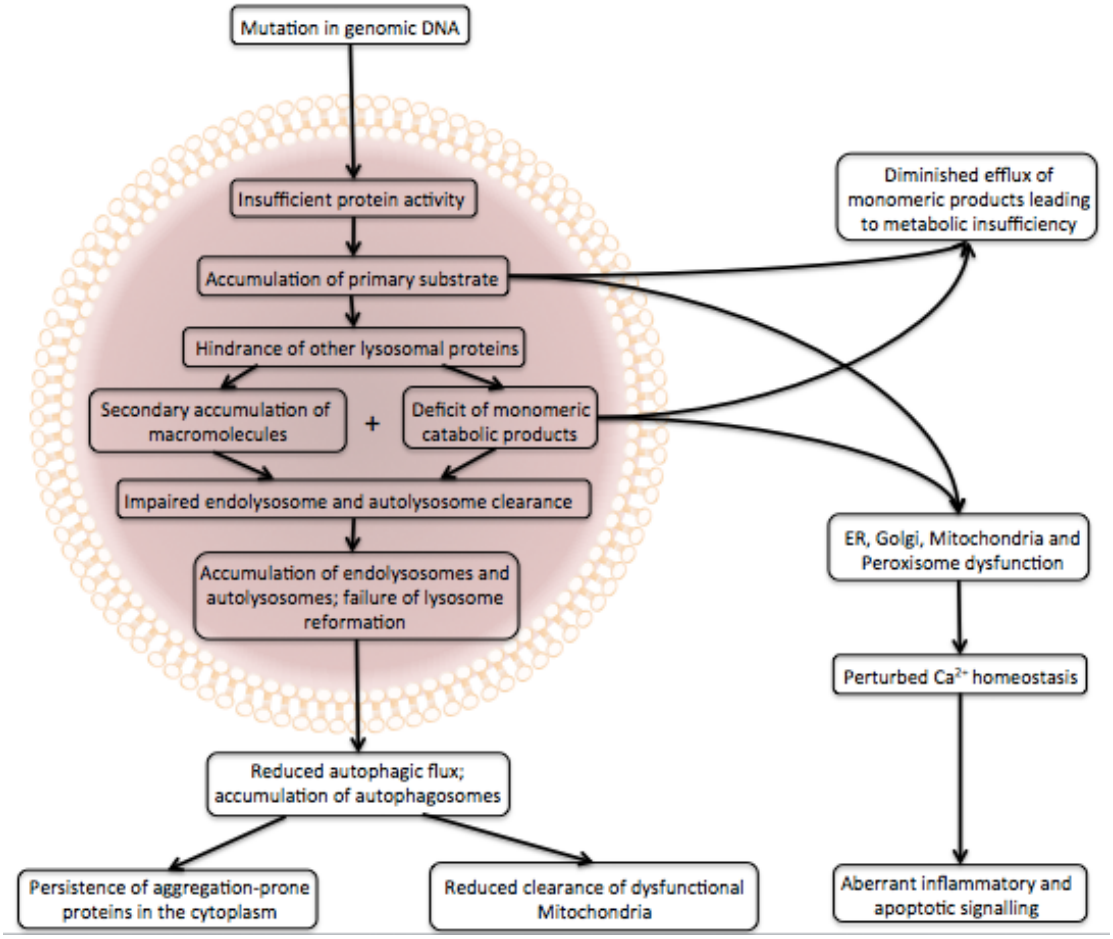

Figure 1.5. – Generalised schematic illustrating hypothetical disease cascades present in lysosomal storage disorders. *Adapted from Platt et al., 2012*

Despite relative simplicity in terms of causative gene defect, monogenic conditions commonly of autosomal recessive inheritance, the pathogenic cascades which lead to the final clinical phenotypes in LSDs remain complex (Cox and Chacon Gonzalez, 2012). As previously mentioned macromolecular storage is not always clearly temporally defined and in addition to this other organelles are often affected by the, initially lysosomal, storage (Platt et al., 2012). Attempts to reconcile these observations has lead to the proposal of a hypothetical cascade of events in LSD pathology (figure 1.5.) which includes processes observed in a number of LSDs although it does not necessarily apply to all LSDs (Platt et al., 2012). This generalised scheme will be further illustrated by discussion of three LSDs. One of these has a defect in a lysosomal hydrolase - Gaucher Disease; and two have defects in endolysosomal transmembrane proteins - Niemann-Pick type C disease and Mucolipidosis type IV.

1.5.1. – Gaucher Disease

Gaucher disease is the most common LSD with a predicted carrier frequency of around 1 in 100 and is most common in Ashkenazi Jewish populations (Chen and Wang 2008; Grabowski, 2012). It is caused by autosomal recessive inheritance of mutations in the *GBA1* gene, which codes for the lysosomal enzyme glucocerebrosidase (GCase). GCase is a lysosomal hydrolase which catabolises the simplest glycosphingolipid glucosylceramide (GlcCer) into ceramide by removal of the glucose moiety after it has been presented in an energetically favourable confirmation by the adaptor protein, saposin C (Grabowski et al., 2012), as discussed in section 1.4.2. this is also influenced by lipid composition with low levels of cholesterol and higher levels of LBPA helping to facilitate catabolism (Shulze and Sandhoff, 2011). Accordingly, mutations in saposin C also lead to Gaucher disease although this is characterised as an atypical form (Horowitz and Zimran, 1994).

This accumulation of lipid causes a broad phenotypic spectrum with wide variation in age of onset and neurological manifestations. Gaucher can be sub-classified into type 1, 2 and 3; a process largely dependant upon age of onset and neurological involvement (Pastores et al., 2000). Type 1 Gaucher is the mildest and most prevalent form accounting for around 95% of cases; it is considered 'non-neuropathic' with an average age of onset in the early 20's, although this can vary widely and some patients never present with symptoms (Pastores et al., 2000). This strongly suggests that there are a number of disease modifying genes for Gaucher (Grabowski, 2008). Type 2 Gaucher, also known as infantile Gaucher, is an extremely severe disorder with neurological manifestations in infants, which commonly leads to death before 2 years of age. Type 3 is known as the sub-acute neuropathic form, and previously as 'juvenile Gaucher', is symptomatic early in life and although some patients die in childhood others can live beyond middle age. Type 1 Gaucher may be extremely mild and as such remain undiagnosed, however, the most frequent clinical sign is an enlarged spleen due to lipid storage which may also extend to the liver (splenomegaly/hepatosplenomegaly) but other more specific symptoms may be noticed such as the characteristic Ehrlenmeyer flask deformity of the thigh bones (Pastores et al, 2000; Faden et al., 2009)). Although type 1 Gaucher is considered non-neuropathic recent evidence linking GBA1 mutations as a genetic risk factor for Parkinson's disease is suggestive of milder neuronal impairment in these patients (Sidransky et al., 2009). For patients with type 1 Gaucher Disease it is well established that enzyme replacement therapy (ERT) is an effective and safe

treatment. This treatment was pioneered by Roscoe Brady using enzyme purified from human placenta and,although this has since been superseded by treatment with recombinant enzyme, it was very effective in terms of reducing hepatosplenomegaly and ameliorating skeletal pathology(Brady et al., 1974; Brady, 2006). An unfortunate clinical limitation of ERT is that enzymes do not cross the blood-brain barrier to any significant extent so it cannot treat CNS disease, this limits clinical outcomes when treating the neuropathic forms of Gaucher (Scarpa et al., 2015). This is particularly true of type 2 Gaucher where severe neurological pathogenesis is life-threatening early on in a patient's life (Pastores et al., 2000).

Neurological pathology in Gaucher can often begin with either hyperextension of the neck and dysphagia or supranuclear gaze palsy although not all patients present this way and a variety of other clinical features including ataxia, neuropathic pain and seizures may be observed (Pastores et al., 2000).

In human cases and mouse models of neuropathic Gaucher there is specific neuronal loss in cortical layers III and V (Wong et al., 2004) and this pathology has been further described in mouse models to be most pronounced in motor and somatosensory regions (Farfel-Becker, 2011). Hippocampal neuron loss is also observed in both patients and mice but this was shown to manifest later than the cortical phenotypes in mouse models. In the inducible Karlsson mouse model of Gaucher astrogliosis, neuroinflammation and microglial activation have been observed prior to neuronal loss and markers of these processes correlate with neuron loss in post-mortem human brain samples (Farfel-Becker et al., 2011). The localisation of inflammation and progressive neuron loss is reflective of clinical presentation.

Due to the unsuitability of ERT for treatment of the CNS, a different therapeutic approach has been utilised for neuropathic forms of Gaucher – substrate reduction therapy (SRT). Miglustat (chemical name *N*-butyl-deoxynorjirimycin, trade name Zavesca, Actelion Pharmaceuticals Ltd. Allschwill, Switzerland) is an orally available iminosugar which reversibly inhibits glucosylceramide synthase (Ficicioglu, 2008, Platt et al., 2004) preventing the synthesis of glucosylceramide and thus reducing the accumulation of undigested substrate. Miglustat is blood-brain barrier (BBB) permeable and has shown therapeutic benefit in treating neuropathic Gaucher and patients who are unsuitable for ERT.

It is interesting to consider that although the levels of the primary storage substrate GlcCer have been shown to be elevated in patients, and are reduced in response to beneficial therapy (Aerts et al., 2011), there are multiple studies which report that levels of the lysosomally derived de-acylated analogue of GlcCer, glucosylsphingosine (GlcSph), correlate more closely with disease severity. This may be particularly relevant for neurological phenotypes of Gaucher as it has been reported that GlcSph is significantly elevated in the brains of type 2 and 3 Gaucher patients but elevated to a much lesser extent in the brains of type 1 patients (Dekker et al., 2012; Mirzaian et al., 2015).

When it is considered that the primary pathogenic substrate has not been confirmed it is unsurprising that the pathogenic cascade of events has not been clearly delineated. Various proposals of pathogenic mechanisms involving autophagic dysfunction (Liebermann et al., 2012) and mitochondrial defects (de la Mata et al., 2015) have been made but perhaps the most well studied affect of the lysosomal dysfunction in Gaucher on another organelle is that which impacts the ER – particularly in relation to Ca^{2+} homeostasis. ER Ca^{2+} dyshomeostasis has been reported in a number of the sphingolipidoses although the specific mechanisms which lead to this differ in each LSD (Vitner et al., 2010). In Gaucher it has been shown that pharmacologically elevated intracellular GlcCer leads to increased Ca^{2+} store release in cultured neurons and that this was a result of stimulation of ryanodine receptors (RyR, one of the ER Ca^{2+} release channels, section 1.3.3.). It was further confirmed that only specific sphingolipids had this effect with only GlcCer, galactosylceramide (GalCer) and GlcSph causing ER Ca^{2+} release. This pathology was also confirmed in ER microsomes prepared from the brain of a type 2 Gaucher patient when compared to those prepared from a control brain in the same study (Lloyd-Evans et al., 2003) and similar results have been recapitulated in iPSC derived neurons containing mutations in *GBA1* which are known to cause neuropathic Gaucher (Schondorf et al., 2014).

Recently, the link between mutations in *GBA1* and Parkinson's disease have been the source of much interest in the field (Sidransky et al., 2009; Nalls et al., 2013). This will be further discussed in chapter 5.

The complexity arising from loss of function mutations in a simple gene and the intriguing link to Parkinson's (Sidransky et al., 2009) disease highlights the need for

further study into this LSD. It is also worth noting that disease complexity increases when dysfunction arises in transmembrane proteins.

1.5.2. – Niemann-Pick type C Disease

Niemann-Pick type C (NPC) is a neurovisceral lysosomal storage disorder in which multiple lipids are stored within the late-endosomes and lysosomes of cells (Vanier, 2010). The disease is estimated to have an incidence of approximately 1 in 90,000 (Wassif et al., 2015).

Patients with NPC suffer from severe neurodegeneration with a pronounced ataxic phenotype caused by the selective loss of cerebellar Purkinje neurons. A variety of other phenotypes falling within a broad phenotypic spectrum may also be observed. In the viscera the lipid storage within the liver and spleen cause hepatosplenomegaly; respiratory dysfunction and dysphagia may also become problematic leading to aspiration pneumonia which is a prevalent cause of death (Vanier 2010).

In the classical presentation of NPC, clumsiness and gait disturbance become evident in middle to late childhood and are often the first evidence of neurodegeneration although abnormalities in saccadic eye movements may be present before this (Rottach et al., 1997). As the disease progresses, cognitive impairment becomes increasingly evident alongside psychiatric problems, epilepsy, sleep disturbances and loss of speech. Death of these patients generally occurs at around 15 - 25 years (Vanier et al., 2010). Although this classical presentation of NPC accounts for around 60-70% of all cases the age of presentation varies from the perinatal period to over 50 years. There is also a variant form of NPC in which patients do not have cholesterol storage and present with the disease much later (Vanier, 2010).

NPC is inherited in an autosomal recessive fashion and is predominantly (95% of cases) caused by mutations in the *NPC1* gene, the protein product of which is a transmembrane protein, NPC1, situated in the limiting membrane of the late endosome. This is a large, 1278 amino acid, protein with 13 transmembrane domains and large hydrophilic intraluminal loops (Ioannou, 2005). The remaining 5% of cases are caused by mutations in the *NPC2* gene which codes for the soluble

lysosomal 151 amino acid protein, NPC2 (Ioannou, 2005). It is known that NPC2 can bind and transport luminal cholesterol exchanging it with the N-terminus of NPC1 (Infante et al., 2003,), the function of which remains enigmatic (Lloyd-Evans et al., 2010). Recently analysis of massively parallel exome sequencing datasets has suggested that common variants in NPC1 may be much more prevalent than previously expected suggesting a previously unanticipated late-onset form of NPC disease (Wassif et al., 2015). Whilst this remains to be confirmed by clinical studies it may be interesting to analyse other LSDs in this way in order to ascertain if late-onset forms of this class of disease are prevalent.

Due to the fact mutations in either *NPC1* or *NPC2* result in the same clinical features and cellular phenotypes, it is clear that they act within the same pathway to maintain lysosomal function (Sleat et al., 2004). NPC1 contains a sterol-sensing domain similar to proteins such as patched, which is a cholesterol regulated protein and accordingly this is suggestive of NPC2-transported cholesterol (Bablola et al., 2007), or other sterols such as the cholesterol precursor 7-DHC (Platt et al., 2014), being a regulator of NPC1 function (Lloyd-Evans et al., 2010). The remainder of the NPC1 protein consists of a predicted 13 transmembrane domains with a number of large loops projecting into the late-endosomal lumen and the challenge remains to determine what the primary function of this protein is. Interestingly the yeast homologue of NPC1, Ncr1p, is capable of correcting lipid storage phenotypes in mammalian cell lines in which NPC1 has been knocked out suggesting a evolutionarily ancient function (Malathi et al., 2004).

When either of the NPC proteins become dysfunctional a complex array of lipids including cholesterol, sphingomyelin, various glycosphingolipids and the primary constituent of sphingolipids, sphingosine, become stored within the late-endosomes and lysosomes of cells in which they can be observed as punctate staining by microscopy (Lloyd-Evans et al., 2010). In 2008, Lloyd-Evans *et al.* temporally delineated the onset of lipid storage after inactivation of NPC1 finding that the primary lipid to accumulate was sphingosine followed by the accumulation of cholesterol, sphingomyelin and glycosphingolipids. In this study they characterised depletion of the late-endosomal and lysosomal Ca^{2+} store as the subsequent event following sphingosine accumulation, as mentioned previously, endolysosomal Ca^{2+} homeostasis is required for correct endocytic trafficking (Luzio et al., 2007) and in the absence of this, transport defects occur. The authors concluded that this was responsible for the eventual accumulation of more complex lipid species within the

endolysosomal system. This accumulation of lipids was recapitulated in control cells in which the lysosomal Ca^{2+} had been specifically chelated (Lloyd-Evans et al., 2008).

The fact that sphingosine is the initial substrate stored after NPC1 interaction, may provide information as to the primary function of the NPC1 protein. Within the acidic environment of the late-endosome and lysosome sphingosine becomes protonated upon the amino group gaining a net-positive charge, the only lipid accumulating in NPC to do so. As such, a specific transporter would be required to extrude sphingosine from the lysosome and a transporter capable of this has not yet been characterised, whereas transporters for the other species of storage lipid have been (Lloyd-Evans et al., 2010). A class of transporter protein highly conserved in evolution which can transport charged amines such as sphingosine is the RND permease family of transporters. In 2004, Scott *et al.* proposed that NPC1 was the only known mammalian member of this family and it has been subsequently shown that NPC1 can transport known substrates of this family such as acriflavine, and is inhibited by hydrophobic amphiphilic amines such as U18666a and can be stimulated by amines such as imidazole (Scott et al., 2004). Accordingly, NPC1 may be a multi-substrate efflux pump responsible for the extrusion of charged amines such as sphingosine from the late-endosomal and lysosomal lumen. This however does not exclude a cholesterol transporting function and currently there is no evidence for the direct transport of any molecule across the lysosomal membrane, accordingly the function of NPC1 remains enigmatic (Lloyd-Evans et al., 2010).

In the European Union (EU), miglustat has been approved for the treatment of neurological manifestations of NPC disease and this has shown some improvement in saccadic eye movement velocity and swallowing capacity, alongside slower deterioration in ambulatory index (Patterson et al., 2007; Patterson et al., 2015). Although the exact mechanism for therapeutic benefit after miglustat treatment in NPC has not been confirmed the inhibition of complex glycosphingolipid (GSL) formation (Platt et al., 1994) and reduction in sphingosine, both of which accumulate in NPC disease is thought to be important (Haslett et al., Unpublished). Another treatment option for NPC is supplementation with the nutraceutical curcumin. As a weak SERCA2 antagonist, curcumin reduces Ca^{2+} uptake by the ER, which results in increased cytosolic Ca^{2+}. In turn, this can help overcome the lysosomal Ca^{2+} release defect in NPC cells which helps rectify lipid mistrafficking phenotypes and subsequently reduces lysosomal storage. The effectiveness of curcumin has been

demonstrated in the mouse model of NPC which benefits from an increased lifespan and outcomes in behavioural testing (Lloyd-Evans et al., 2008) although it has been difficult to confirm these benefits in patients due to the variety of curcumin supplements which have been utilised – particularly as these supplements vary greatly in both curcumin concentration and additional constituents (Maguire *et al.* submitted).

A further therapeutic option for NPC disease is 2-hydroxypropyl-β-cyclodextrin (HPβCD), which has been developed for the clinic by the NIH led Theraputics for Rare and Neglected Diseases (TRND) program after initial discovery by academic researchers (Davidson et al., 2009) and initial reports of compassionate use in patients (Matsuo et al., 2013). HPβCD is a cyclic oligosaccharide commonly used to increase solubility and dissolution rate of poorly water soluble drugs, as such it has been extensively tested for use as an excipient and is well tolerated by a variety of animals (Ottinger et al., 2014). Accordingly HPβCD has been tested in NPC mouse and cat models and has been shown to reduce intracellular storage, promote Purkinje neuron survival and extend lifespan when either injected into the spinal canal (intrathecal injection) or directly onto the brain (intracerbroventricularly) (Davidson et al., 2009; Vite et al., 2015).

Despite the clinical interest, the mechanism of HPβCD action has not been well defined. In addition to the *in vitro* observation that intracellular cholesterol storage is reduced, a study by Chen *et al.* proposed that this was due to HPβCD stimulating Ca^{2+}-enhanced lysosomal exocytosis (Chen, 2010). It is also interesting to note that HPβCD does not reduce storage and ameliorate neurological symptoms in other LSDs including a sphingolipidosis suggesting an NPC specific mechanism of action (Davidson et al., 2009). Finally and, perhaps, most compelling of all is the observation that peripheral administration of HPβCD can reduce brain lipid storage despite a lack of significant BBB permeability (Pontikis et al., 2013). Further research is required to resolve these issues and in doing so may provide avenues for rational improvement of HPβCD as a therapy for NPC.

Recent studies indicate that the development of NPC therapies may also benefit research and treatment of other diseases, some of which are much more commonly occurring. These include the implication of the NPC1 protein in endolysosomal cholesterol mistrafficking in Smith-Lemli-Opitz Syndrome, a disease of cholesterol biosynthesis (Platt et al., 2014); inhibition of the NPC1 protein by mycobacterium

tubercolosis to facilitate survival within the endolysosomal system by preventing phagosome-lysosome fusion (Lloyd-Evans et al., Unpublished); and, reports of Alzheimer's disease phenotypes in NPC patients (Malnar et al., 2014).

NPC disease is arguably the most thoroughly researched LSD caused by a transmembrane protein, and yet, the protein function still remains elusive. Nevertheless the delineation of storage events which follow protein loss of function has provided valuable insights which have allowed for rational therapy design. In the majority of other LSDs caused by the loss of function of a transmembrane protein this has not yet been achieved, and presents additional difficulty when studying diseases such as Mucolipidosis type IV.

1.5.3. – Mucolipidosis type IV

Mucolipidosis type IV (MLIV) is an extremely rare LSD, caused by mutations in the gene *MCOLN1,* with severe neurodevelopmental and neurodegenerative phenotypes. Originally associated with the Ashkenazi-Jewish population this autosomal recessive disorder has since been shown to be pan-ethnic (Bach, 2001) with an estimated incidence that has been difficult to determine accurately due to a number of mutations causing only mild phenotypes which are likely misdiagnosed (Wakabayashi et al., 2011). Two mutations are commonly found in patients of Ashkenzi-Jewish ancestry, both of which reduce expression of TRMPL1 at the level of mRNA. Additional missense mutations have been reported in conserved regions of the TRPML1 protein, which are particularly interesting as they may be associated with milder disease phenotypes involving partial protein dysfunction (Wakabayashi et al., 2011.)

The protein product of the gene is TRPML1, a six transmembrane domain protein of 580 amino acids, with intraluminal N and C termini (LaPlante et al, 2002; Nilius et al., 2007). Without TRPML1 function cells accumulate a wide variety of substrates in the lysosomes including lipofuscin, phospholipids, gangliosides and glycosaminoglycans, alongside a cellular vacuolation phenotype (Wakabayashi et al., 2011). This storage is likely the result of profound endocytic mistrafficking (Fares and Greenwald, 2001) caused by the loss of luminal Ca^{2+} homeostasis which is mediated by TRPML1 (section 2.3.2.1.). Recently, Ca^{2+} release from TRPML1 has been associated with the regulation of autophagy and induction of lysosome biogenesis by TFEB although the

impact of this on disease phenotypes has not yet been established (Medina et al., 2015).

Diagnosis of MLIV remain a challenge as a lack of characteristic neurological findings may result in misdiagnosis as cerebral palsy of spastic paraplegia. It is often the eye abnormalities such as corneal clouding progressing to visual degeneration alongside severe cognitive impairment that define the 'typical' MLIV patient (Wakabayashi et al., 2011). Considering the lipofuscin accumulation in the endolysosomal system and the 'enigmatic' nature of MLIV's cellular phenotypes and clinical signs, this disease may arguably be better characterised as a lipofuscinosis (Carcel-Trullols et al., 2015). Regardless of the merits of classifying this disease as either a lipofuscinosis or mucolipidosis, it does serve to highlight the difficulties presented by the classification and subdivision of LSDs.

Unfortunately, the above considerations may be key contributing factors to the lack of a specific therapy for MLIV, with only symptomatic amelioration currently a therapeutic option.

1.6. – Convergent themes in the study of LSDs

The hypothetical cascade of LSD pathogenesis as shown in figure 1.5.1. and the subsequent examples of LSDs have illustrated the complexity borne out of the loss of a single functional protein. Considering the three diseases discussed in detail, and LSDs in general, several convergent themes emerge. These are lipid dyshomeostasis, neurodegeneration and the impact of these upon therapy.

1.6.1. – Lipid Dyshomeostasis

A large number of the LSDs are primary lipid disorders caused by defects in primary lipid catabolic enzymes within the endolysosomal system (Platt, 2014). However the impact of lipid storage on LSD pathology can be expanded when it is considered that lipid storage is observed in many LSDs, which do not have a primary lipid catabolic defect (Kreutz et al., 2013). A clear example of this is ganglioside storage observed in mucopolysaccharidosis type 1 (Hurler syndrome). The primary defect in this LSD is in an enzyme which catabolises glycosaminoglycans, alpha-L-iduronidase. It is proposed that structural similarity between glycoasminoglycans and the terminal

glycosylation present on certain gangliosides can inhibit enzymes such as hexosaminidase resulting in ganglioside GM2 accumulation (Heinecke et al., 2011). This is a clear example of steric hindrance contributing to secondary substrate storage illustrated in figure 1.5.1.

A similar pathological process that can cause further lipid storage is endocytic mistrafficking of sphingolipids. As discussed in section 1.4.3., sphingolipids are endocytosed and those not recycled back to the plasma membrane are sorted to either the Golgi or lysosomes. Although the mechanisms for this sorting are not well defined, the accumulation of sphingolipid in the endosomal system as a result of mistrafficking is a clearly defined phenotype in many LSDs (Pagano et al., 2000). This has been assayed by either the addition of fluorescently tagged sphingolipid or the addition of fluorescently tagged protein such as cholera toxin subunit B (CtxB) which bind specifically to ganglioside GM1 (Blank et al., 2007; Benktander et al., 2013) in the plasma membrane, triggering internalisation and subsequent transport. The amount of fluorescently tagged probe that accumulates in cells from different LSDs varies (Pagano, 2003). As with the mechanistic basis of this trafficking, it is not entirely understood how sphingolipid mistrafficking occurs although the distribution of cholesterol and maintenance of Ca^{2+} homeostasis in the endolysosomal system appears to be important (Pagano, 2003; Choudhury et al., 2004; Luzio et al., 2007). Nevertheless, the distribution of fluorescent analogues added to cells to assay this system remain a useful method for the examination of lysosomal dysfunction by inhibitory compounds or the benefit mediated by therapies designed to reduce endolysosomal dysfunction.

Lipids and in particular sphingolipids are a particularly bioactive class of macromolecule and as such when levels are higher than usual or they are not localised appropriately they can cause a myriad of defects in areas of the cell outside of the endolysosomal system (Platt, 2014). An intriguing example of this is the action of sphingolipids which accumulate in LSDs on the ER. In Gaucher, and some other sphingolipidoses, the accumulating substrates can escape the endolysosomal system by an undefined mechanism and modulate ER Ca^{2+} channels (Lloyd-Evans et al., 2013). The mechanisms underlying this ‘escape’ are not well defined but may involve membrane contact points (Penny et al., 2015). Conversely, to this situation of excessive lipids being redistributed to other membranes and organelles, the lack of lipids due to their sequestration in endolysosomal compartments may be disruptive to

some cellular pathways. This appears to be particularly important in neurons and will be further discussed in 1.6.2.

1.6.2. – Neurodegeneration

Consideration of the LSDs discussed is section 1.5 and the broader range of LSDs reveals that the majority are neuropathic and profound neurodegeneration is a major phenotype (Cox and Chacon Gonzalez, 2012). Whilst this is a major challenge for the treatment of LSDs they do provide a unique model for the study of neurodegeneration as compromised lysosomal function causes neuronal death by apoptosis or necrosis – features which are found in common neurodegenerative disease such as Alzheimer's disease (Okouchi et al., 2007; Troulinaki et al.,2012).

As with the cellular pathology of LSDs, discussed above, the neuropathology of LSDs is a complex cascade which may be reliant upon primary storage substrates, secondary storage substrates or subsequent dysfunction in other cellular organelles and pathways. Due to this complex pathology neuropathology in LDSs may include any number of the following: disruption of neuronal architecture, abnormal inflammatory response, increased oxidative stress, dysregulated Ca^{2+} homeostasis, lipid mistrafficking, abnormal proteolysis and evidence of decreased autophagic flux. (Pagano, 2003; Farfel-Becker et al., 2011; Platt et al., 2012; Nixon, 2013; Schondorf et al.,2014)

1.6.2.1. – Changes to neuronal architecture

Some of the most striking CNS pathology of LSDs is the observation of meganeurites, axonal spheroids and ectopic dendrites. Meganeurites are hugely enlarged axonal hillocks containing storage bodies most often containing the primary storage substrate and thus considered disease specific (Walkley and James, 1984). Axonal spheroids are more variable, containing an array of material in enlargements distal to the axon initial segment region and are considered more similar across different storage disorders. Ectopic dendritogenesis, which does not occur in mouse models of LSDs, is the phenomenon of increased proliferation of malformed dendrites from neurons although the consequences of this remain unclear although the presence of dysfunctional synapses and subsequent neuronal injury caused by

these has been proposed as a pathological mechanism (Walkley et al., 1990; Walkley, 1998).

1.6.2.2. – Neuroinflammation

A common neuropathalogical event in the brains of LSD patients is the presence of 'activated' microglia with pathological secretion of cytokines. This activation of microglia has been shown to correlate with levels of storage and onset of symptoms in animal models of LSDs such as Gaucher mice. In these mice, extensive elevation of markers of oxidative stress were also present, a process observed in a number of other animal models of LSDs (Farfel-Beker et al., 2011). It is suggested the initiating events that cause the onset of chronic inflammation and increased oxidative stress are caused by the accumulation of different substrates, whether primary or secondary, in different LSDs before the pathways converge later on in the pathogenic cascade. Nevertheless, they represent a significant challenge for the treatment of CNS pathology in LSDs and may provide links to the pathology observed in more common neurodegenerative diseases (Vitner et al., 2010).

1.6.2.3. – Protein aggregation

Protein aggregation and inclusion body formation are cardinal features of the more common neurodegenerative diseases which most commonly onset in later life. In Alzheimer's disease extracellular plaques of beta-amyloid (Aβ) protein are observed alongside intracellular neurofibriliary tangles comprised of aberrantly phosphorylated Tau. The presence of amyloid plaques or pathogeneic changes to Aβ levels have been reported in a range of LSDs (Martins et al., 2015) including NPC (Maulik et al., 2013). The mechanisms leading to such pathology are not well defined although defects in endocytosis, proteolysis and autophagy are thought to play an important role (Nixon, 2005; Nixon 2013). The defined protein aggregate most strongly related to Parkinson's disease are Lewy bodies (although these can also be present in other forms of dementia including Alzheimer's disease variants); and intracellular protein aggregates primarily composed of α-synuclein (Sardi et al., 2015). Recently it has been ascertained that *GBA1* plays a greater role in the genetic aetiology of dementia with Lewy bodies than it does for Parkinson's disease (Nalls et al., 2013). This suggests that there is a mechanistic link between either loss of function of GCase or

increased GlcCer and α-synuclein aggregation and this remains an area of intense research (Mazzulli et al., 2011). It is important to consider, however, that protein aggregation may be a protective response which is initiated to sequester toxic soluble proteins as such the contribution of aggregates to pathogenic cascades particularly early on in disease pathogenesis is debated (Arasante et al., 2004).

1.6.2.4. – Ca^{2+} dyshomeostasis

Within the CNS, correct homeostasis of Ca^{2+} homeostasis becomes increasingly important as excitable cells such as neurons utilise Ca^{2+} for many signalling events (Surmeier et al., 2011) and Ca^{2+} is also used by astrocytes to regulate growth factor secretion and neurotransmitter uptake and release (Volterra et al., 2014). A result of this high dependence upon Ca^{2+} is a vulnerability to Ca^{2+} overload, which is toxic to neurons, activating nitric oxide synthesis generation of free radicals and apoptosis. The most well characterised from of excitotoxicity is induced by the major excitatory neurotransmitter of the mammalian CNS – glutamate (Wang and Qin, 2010). Dysfunction in the endolysosomal pathway associated with decreased autophagic flux can play an important role in excitotoxic neuron death, so it is not surprising that a number of LSDs are thought to be susceptible to this process (Kovacs et al., 2006). This is especially true when we consider that elevated intracellular Ca^{2+} levels are, in part, reduced by buffering from intracellular Ca^{2+} stores such as the ER and mitochondria. When we consider that LSDs such as Gaucher have dysregulated ER Ca^{2+} stores it would be surprising if excitotoxic neuron death did not play a role in pathology (Lloyd-Evans et al., 2003; Schondorf et al., 2014). Increased levels of Ca^{2+} in cells also increase mitochondrial stress which can initiate caspase dependant apoptosis pathways (Kiselyov et al., 2007). Ca^{2+} excitotoxicity has been implicated in Huntington's disease, Alzheimer's disease and Parkinson's disease and may be a common pathway to pathology in diseases where neurons are lost (Wang and Qin, 2010).

In addition to neuronal Ca^{2+} levels being important in the brain, astrocytic Ca^{2+} responses are also vital to correct brain function. Although the contribution of these responses to spatial and temporal regulation of neural signalling is less well understood, it is becoming an increasing area of study. A particularly interesting area of study is the implication of dysregulated astrocytic Ca^{2+} signalling in Alzheimer's

disease models where it has been observed early in pathogenesis (Vincent et al., 2010).

1.6.2.5. – Decreased autophagic flux

The excitable nature of neurons means that they also have high energy demands, particularly in the areas surrounding synapses where active transport processes and high rates of protein turnover place high demands on metabolism. This is particularly important when we consider that neurons are post-mitotic cells and as such become increasingly susceptible to the build up of dysfunctional organelles and toxic proteins as they age. Co-ordinated action of mitophagy, macroautophagy and chaperone mediated autophagy is therefore of vital importance for the maintenance of correct neuronal function by preventing the accumulation dysfunctional organelles and toxic proteins (Nixon, 2013). The reduced autophagic flux observed in the majority of LSDs result in increased susceptibility to such toxic processes driving the formation of dystrophic neurites (Boland et al., 2008). Essentially in situations where lysosomal function is compromised and autophagy is subsequently reduced neurons become dysfunctional at a very early age leading to the early-onset neurodegeneration observed in LSDs (Liebermann et al., 2012).

1.7. – Summary

This discussion of LSDs has served to highlight the complexity arising from these monogenic disorders and the detrimental effects they can have on patients with profound neurodegeneration one of the most common and severe patient outcomes (Cox and Chacon Gonzalez, 2012). We have also observed that milder forms of lysosomal disease are potentially more prevalent than currently recognised (Wassif et al., 2015) and that those originally not considered to have neurodegenerative pathology may result in a predisposition to more common neurodegenerative diseases (Sidransky et al., 2009). Accordingly, the study of lysosomal pathology and the involvement of proteins which are the primary defects in LSDs is an area of intense interest in neurodegenerative disease research. Hopefully, by applying our knowledge of pathogenic cascades following lysosomal dysfunction we can identify new therapeutic targets in diseases such as Alzheimer's, Huntington's and Parkinson's

1.8. – Aims

In chapter 3 of this thesis we will investigate lysosomal dysfunction in cells which do not have functional Presenilin proteins. Mutations in these proteins are known to cause familial Alzheimer's and lysosomal dysfunction leading to reduced autophagic flux has been suggested to be important in this pathogenesis (Nixon, 2013). Although lysosomal dysfunction is an established observation in presenilin cells the molecular basis of this remains to be clarified with both disruption of lysosomal pH (Lee et al., 2010; Coffey et al., 2015) and lysosomal Ca^{2+} (Coen et al., 2012) having been implicated. Accordingly we will utilise cells in which presenilin proteins have been knocked out to investigate lysosomal dysfunction in a simple model of presenilin deficiency in order to establish molecular targets which could be used to investigate more patient relevant models of familial Alzheimer's.

The specific aims of chapter 3 are to:

- Investigate whether $PS1^{-/-}$ cells had phenotypes mimicking NPC1 disease
- Determine whether the lysosomal Ca^{2+} defect observed in $PS1^{-/-}$ cells could be recapitulated using our laboratories extensive expertise in the area.
- If a lysosomal Ca^{2+} defect in $PS1^{-/-}$ cells is confirmed we will investigate the mechanisms underlying this defect.

In chapter 4 we will investigate the expanding area of interest which relates to the accumulation of lysosomes in models of Huntington's disease (Castiglioni et al., 2012; Camniaso et al., 2012; Erie et al., 2015). As there is also evidence of dysregulation of lipid levels and endocytic trafficking defects in these cells we are interested to see if any of the lysosomal phenotypes which are present are reminiscent of any LSDs. This study ha the potential to highlight new therapeutic targets. In order to do this we will utilise cellular models of Huntingtons created from well characterised animal models of the disease alongside emerging iPSC-derived patient models of the disease.

The specific aims of chapter 4 are to:

- Perform a robust phenotyping of various Huntington's cell lines to determine the extent of lysosomal dysfunction in the disease.

- Investigate the potential mechanism leading to lysosomal dysfunction in Huntington's.
- Determine any therapeutic intervention points which have the potential to correct lysosomal dysfunction in Huntington's cells.

In chapter 5 we will investigate whether cellular Ca^{2+} dysregulation which has been implicated in the pathogenesis of Parkinson's (Surmeier etal., 2011) is prevalent in genetic models of Parkinson's disease. Recently it has been suggested that changes to lysosomal Ca^{2+} signalling may be an initiating factor in this Ca^{2+} dysregulation (Hockey et al., 2015). To study this we will utilise fibroblasts from KRS patients who carry mutations in the lysosomal protein ATP13A2 and suffer from a form of early onset Parkinson's (Ramirez et al., 2006). As this protein is both lysosomal and proposed to be involved in ionic transport these cells represent an ideal model in which we can investigate if Ca^{2+} dysregulation is widespread in genetic models of Parkinson's disease. We will also study primary astrocytes in which Gaucher disease phenotypes have been induced by either genetic or pharmacological means in order to see if the Ca^{2+} dysregulation reported in models of Gaucher (Lloyd-Evans et al., 2003; Schondorf et al., 2014) is present and what impact this has upon astrocytic Ca^{2+} signalling.

The specific aims of chapter 5 are to:

- Determine if the loss of ATP13A2 function results in changes to lysosomal Ca^{2+} homeostasis.
- Determine what impact these Ca^{2+} changes, if any, may have on other cellular Ca^{2+} stores
- Investigate what effects the induction of Gaucher phenotypes has on Ca^{2+} signalling within astrocytes.

Chapter 2

Materials and Methods

All chemicals were obtained from Sigma Aldrich, Poole, UK unless otherwise stated.

2.1. – Cell Culture

2.1.1. – Blastocyst-derived cells

WT and PS1$^{-/-}$ mouse blastocyst-derived (BD) cells were obtained from Dr. Ralph Nixon, Nathan Kline Institute, USA. These cells were maintained in sub-confluent conditions in Dulbecco's Modified Eagle's Medium (DMEM) with 10% Foetal Calf Serum (FCS) and 2mM L-Glutamine at 37°C and 5% CO_2 in a humidified incubator. These cells have previously been used in the study of lysosomal phenotypes by Lee et al. (2010).

2.1.2. – Mouse Embryonic Fibroblasts

WT, PS1$^{-/-}$ and PS1/2$^{-/-}$ mouse embryonic fibroblasts (MEFs) were obtained from Dr. Ralph Nixon, Nathan Kline Institute, USA. These cells were maintained in sub-confluent conditions in DMEM with 10% FCS and 2mM L-Glutamine at 37°C and 5% CO_2 in a humidified incubator. These have previously been used for the study of lysosomal Ca^{2+} by Coen et al. (2012).

2.1.3. – Down's syndrome Human Fibroblasts

Human fibroblasts (HF) with trisomy of chromosome 21 along with an age matched control cell line were obtained from Dr. Ralph Nixon, Nathan Kline Institute, USA. These cell have been previously described in Jiang et al. (2010). All cells were maintained in sub-confluent conditions in DMEM with 10% heat inactivated foetal calf serum and 2mM L-Glutamine at 37°C and 5% CO_2 in a humidified incubator.

2.1.4. – Induced pluripotent stem cell derived neural stem cells

HD patient induced pluripotent stem cell (iPSC) derived neural progenitor cells (NPCs) were obtained from Prof. Nick Allen, Cardiff University, UK. In this study they are referred to as neural stem cells (NSCs) in order to avoid confusion with the

Niemann-Pick type C (NPC) proteins. These cells have 180 polyQ repeats in the huntingtin (HTT) protein and were the starting point for neuronal differentiation in the HD iPS consortium study (HD iPSC Consortium, 2012). The control cells used in this study were H9 neural stem cells. Cells were maintained as a near confluent monolayer on a laminin coated growth surface in Advanced DMEM/F12 medium (Life Technologies, Warrington, UK) with 20ng/ml epidermal growth factor (EGF), 20ng/ml fibroblast growth factor (FGF) and 5µg/ml heparin at 37°C and 5% CO_2 in a humidified incubator.

2.1.5. – ST14A embryonic striatal cells

Conditionally immortalised ST14A from cells expressing fragments of human HTT corresponding to amino acids 1-548 with different degrees of poly Q expansion (Q15 and Q120) were obtained from the Coriell Cell Repository, Coriell Institute for Medical Research, New Jersey, USA. These cells are a well-characterised line originally derived from day 14 embryonic rat striatal primordia. All cells were maintained in sub-confluent conditions in DMEM with 10% heat inactivated FCS and 2mM L-glutamine at 33°C and 5% CO_2 in a humidified incubator. These cells have been studied in numerous publications pertaining to Huntington's disease (Ehrlich et al., 2001; Valenza et al., 2005; Maglione et al., 2010; Marullo et al., 2012).

2.1.6. – PC12 pheochromocytoma cells

PC12 cells with inducible expression of full length human HTT with different degrees of polyQ expansion (Q23 and Q145).were obtained from the Coriell Cell Repository, Coriell Institute for Medical Research, New Jersey, USA. These cells are a well characterised Huntington's model originally generated from a rat pheochromocytoma (Edwardson, 2003). Cells were maintained in partial suspension culture in DMEM F12 with 15% Horse serum (Life Technologies), 2.5% FCS, 1% penicillin/ streptomycin, 0.2 mg/ml Zeocin (Invivogen, San Diego, USA) and 0.2 mg/ml G418 (Invivogen).

2.1.7. – Differentiation of iPS derived Neural Stem Cells into neurons

The iPSC derived cell lines 21n1, 33n1, 60n5 and 109n4; examined in the HD iPS consortium study were differentiated into neurons representative of the lateral ganglionic eminence (LGE). Each cell line has a poly-glutamine repeat length as described by the first number in the cell line with the number following n the clone number. All cell cultures are grown at 37°C and 5% CO_2 in a humidified incubator utilising methods adapted from (HD iPSC Consortium, 2012; Rushton et al. 2013).

iPSC neural progenitor cultures greater than 70% confluent grown in matrigel (BD, Oxford, UK) coated vessels were selected for differentiation. For the first 3 days, cells were grown in SLI media, consisting of Advanced DMEM F12 (Life Technologies) with 1% Glutamax (Life Technologies), 1% penicillin/streptomycin, 2% MACS neurobrew without retinoic acid (Milteyni, Bisley, UK), 10μM SB431542 (AbCam, Cambridge, UK), 1μM LDN193189 (Stemgent, Lexington, USA) and 1.5μM IWR1 (Tocris, Bristol, UK), which was changed daily. Cells were passaged by 1:1.5 split after 4 days using Accutase (Life technologies) in the presence of 10μM the ROCK inhibitor Y-27632 (AbCam) and plated onto matrigel coated 6 well plates and grown in SLI medium which is changed daily. At 8 days, cells were again passaged by the same method but maintained in LI medium (Advanced DMEM F12 with 1% Glutamax, 1% penicillin/streptomycin, 2% MACS neurobrew without retinoic acid, 1μM LDN193189 and 1.5μM IWR1), which is again changed daily. At day 16, these cultures can either be further expanded for cryopreservation or passaged for LGE neural differentiation. Cells were obtained from Sun Yung (Allen lab, Cardiff University) at this stage.

For neural differentiation, a single cell suspension was obtained by Accutase treatment in the presence of 10μM Y-27632 and cells were counted then the volume of cell solution adjusted to $1X10^6$ cells/ml. 80μl of this cell suspension was then plated onto glass coverslips or Ibidi 8 well μ-slides coated with PDL and matrigel to achieve a final cell number of 80,000/coverslip. After 1 hr incubation at 37°C and 5% CO_2 in a humidified incubator each well was gently flooded with SCM1 medium consisting of Advanced DMEM F12 with 1% Glutamax, 1% penicillin/streptomycin, 2% MACS neurobrew with retinoic acid (Milteyni), 2μM PDO332991 (Tocris), 10μM DAPT (Tocris), 10ng/ml BDNF (Milteyni), 0.5μM LM22A4 Tocris), 10μM Forskolin (Tocris), 3μM CHIR 99021 (Tocris), 0.3mM GABA (Tocris), 1.8mM $CaCl_2$ and 0.2mM Ascorbic acid. This media was changed every 2-3 days until day 23 when the cells

were changed into SCM2 medium. SCM2 medium consists of Advanced DMEM F12 with 1% Glutamax, 1% penicillin/streptomycin, 2% MACS neurobrew with retinoic acid, PDO332991 2μM, 10ng/ml BDNF, LM22A4 0.5μM, CHIR 99021 3μM, $CaCl_2$ 1.8mM and 0.2mM Ascorbic acid 0.2mM. Cells were then maintained in this medium with media changes every 2-3 days until 30 - 44 days after initiation of the protocol as determined by the experiment. At this stage, cells have been characterised as mature LGE neurons by DARPP32 staining and were used for experimentation as appropriate.

All neuronal differentiations were performed either by, or with assistance from Dr. Sun Yung (Allen Lab, Cardiff University).

2.1.8. – Kufor-Rakeb Syndrome Human Fibroblasts

Human fibroblasts with mutations in the ATP13A2 protein were obtained from Prof. Christine Klein, Lubeck, Germany. Patient 1 is identified as L6025 and Patient 2 as L3292, these cells are described in Dehay et al. (2012). Both cell lines contain mutations which lead to misfolded protein which is retained in the ER (Ramirez et al., 2006). The control cell line GM05399 was obtained from Coriell Cell Repositories, New Jersey, USA. All cells were maintained in sub-confluent conditions in Dulbecco's modified Eagle's medium (DMEM) with 10% heat inactivated foetal calf serum (FCS) and 2mM L-Glutamine at 37°C and 5% CO_2 in a humidified incubator.

2.1.9. – GD Mouse Model Primary Astrocytes

WT and Gaucher murine astrocytes were isolated from post-natal day 1 Gaucher mice utilising a method adapted from Hirst et al. (1998). Briefly, brains were taken from the pups and meninges removed before dissociation by trypsinisation (0.25% w/v) for 15 min at 37°C followed by passage through a 23g needle. After centrifugation at 100rpm for 5 minutes to remove trypsin solution cells were resuspended in DMEM with 10% FCS, 2mM L-Glutamine and 1% penicillin/streptomycin and the preperations from each brain were plated in a $25cm^2$ tissue culture flask. Cells were maintained in culture in DMEM with 10% FCS, 2mM L-Glutamine and 1% penicillin/streptomycin at 37°C and 5% CO_2 with at least 2 passages occurring prior to use. Subsequently, these cells were maintained in DMEM with 10% FCS, 2mM L-Glutamine and 1% penicillin/streptomycin at 37°C and

5% CO_2 as a near confluent monolayer in a humidified incubator. This nestin – flox/flox mouse model does not express *Gba1* in neurons and astrocytes and is used to model neurodegenerative Gaucher disease (Farfel-Becker., 2011).

2.1.10. – Control primary astrocytes

Primary astrocytes were isolated from post-natal day 1 C57BL/6 mice by Jenny Lange (King's College, London). These cells were maintained in DMEM with 10% FCS, 2mM L-Glutamine and 1% penicillin/streptomycin at 37°C and 5% CO_2 as a near confluent monolayer in a humidified incubator. These cells were treated with conduritol β epoxide (CβE) to pharmacologically induce GlcCer storage (Das et al., 1987). and model Gaucher disease for experiments independent to those in which the cells prepared in 2.1.9. were utilised.

2.1.11. – Summary table of cell lines

A summary of all the cell lines utilised in this thesis detailing the chapters they were used in is provided below.

Cell Line	Origin	Genetic Change	Relevant Disease	Utilised in Chapter	Described in Section
Blastocyst-derived (BD) cells	Mouse	PS1$^{-/-}$	Alzheimer's	3	2.1.1.
Mouse embryonic fibroblast (MEF) cells	Mouse	PS1$^{-/-}$ and PS1/2$^{-/-}$	Alzheimer's	3	2.1.2.
Down's syndrome patient fibroblasts	Human	Trisomy 21	Alzheimer's	3	2.1.3.
iPSC-derived neural stem cells (NSCs)	Human	*HTT* polyQ expansion	Huntington's	4	2.1.4.
ST14A cells	Rat	Q120 human HTT overexpression	Huntington's	4	2.1.5.
PC12 cells	Rat	Q145 human HTT	Huntington's	4	2.1.6.
iPSC-derived neurons	Human	*HTT* poly Q expansion	Huntington's	4	2.1.7.
Kufor-Rakeb syndrome patient fibroblasts	Human	*ATP13A2* mutation	Parkinson's	5	2.1.8.
GD mouse model primary astrocytes	Mouse	GBA1$^{-/-}$	Parkinson's	5	2.1.9.
Control primary astrocytes	Mouse	N/A	Parkinson's	5	2.1.10.

Table 2.1. – Summary of cell lines utilised in this thesis. *The species the cell line originated from, genetic change and neurodegenerative disease of relevance are detailed along with the chapter the cell were used in and the section of this chapter they were described in.*

2.2 . – Pharmacological modulation of cell lines

2.2.1. – U18666a treatment

BD cells on glass coverslips or Ibidi 8 well µ-slides as appropriate were left to adhere overnight then treated with 2µg/ml U18666a in growth medium for 20 – 24 hr as appropriate. U18666a has been extensively characterised as a pharmacological inducer of NPC disease phenotypes (Lloyd-Evans et al. 2008).

2.2.2. – Concanamycin A treatment

BD cells in tissue culture tanks or Ibidi 8 well µ-slides as appropriate were left to adhere overnight then treated with 50nM Concanamycin A for 9 – 12 hr as appropriate. Concanamycin A is a well characterised inhibitor of vATPase (Coen et al. 2012).

2.2.3. – Ned19 inhibition of TPC2

Ned19 (Enzo, Exeter, UK), an inhibitor of Ca^{2+} release mediated by NAADP was used to model lysosomal Ca^{2+} release phenotypes observed in $PS1^{-/-}$ cells. BD cells were treated with Ned-19 at 0.5µM for 24 hr. (Naylor et al., 2009).

2.2.4. – YM201636 inhibition of PIKfyve

BD cells on Ibidi 8 well µ-slides were left to adhere overnight then treated with 10µM YM201636 in growth medium for 1 hr. YM201636 is a potent inhibitor of mammalian phosphatidylinositol phosphate kinase (PIKfyve), the enzyme required for biosynthesis of phosphatidylinositol (3,5) bis-phosphate (PI(3,5)P2) which is the endogenous activator of TRPML1. (Jefferies et al. 2008).

2.2.5. – Inhibition of TRPML1 using anti TRPML1 antibody

BD cells on Ibidi 8 well µ-slides were left to adhere overnight then treated with 5 µg/ml of polyclonal anti-TRPML1 (Sigma) in growth medium for 16 hr. This antibody

had been titrated to a level where increased Lysotracker staining was observed in HF cells (Lloyd-Evans, Unpublished). This phenotype is observed in MLIV cells were TRPML1 function is lost and was used as evidence of inhibition of this lysosomal channel. Other anti TRPML1 antibodies were tested on HF cells but no increase in Lysotracker staining was observed (Lloyd-Evans, Unpublished). This method has previously been used to inhibit TRPML1 (Zhang et al., 2012).

2.2.6. – Hydroxypropyl-β-Cyclodextrin Treatment

BD cells grown in the conditions described above conditions were treated with 0.4 mg/ml Hydroxypropyl-β-Cyclodextrin (HPβCD) in growth medium for 24 hr as per Chen et al., 2010) HPβCD has been established to reduce cholesterol accumulation in cell models of NPC1 disease and improve phenotypes in animal models of NPC1 (Davidson et al., 2009; Vite et al., 2015).

2.2.7. – Miglustat Treatment

ST14A cells or iPSC derived neurons grown in appropriate conditions were treated with 50μM Miglustat (Enzo) in growth medium for 5 days. Miglustat (*N*-butyl-denojirimycin, *N*B-DNJ) is an approved treatment for the neurological manifestations of NPC disease in the European Union and these treatment conditions have been established as beneficial in cell models of NPC disease (Haslett *et al.* Unpublished). It is a form of substrate reduction therapy (SRT) which reduces levels of glycosphingolipids by inhibition of the biosynthetic enzyme glucosylceramide synthase (Platt et al., 1994; Patterson et al., 2015).

2.2.8. – Phytic acid Treatment

HF cells on glass coverslips or Ibidi 8 well μ-slides as appropriate were left to adhere overnight then treated with 1mM Phytic acid in growth medium for 7-15 days as appropriate. Phytic acid is a non-specific chelator of heavy metal cations effective in acidic microenvironments (Maguire *et al.* Unpublished).

2.2.9. – Conduritol β epoxide treatment of primary astrocytes

Control primary astrocytes (3.1.10) grown in six well plates were treated with 200μM conduritol β epoxide (CβE) (Matreya LLC, State College, USA) in astrocyte growth medium for five days prior to plating in Ibidi 8-well μ-slides. Medium was changed every 2 days. CβE is a specific, irreversible inhibitor of GCase and is commonly used to pharmacologically model Gaucher disease (Das et al., 1987; Manning-Bog., 2009).

2.3. – Cell Biology

2.3.1. – Fixed cell biology

2.3.1.1. – Paraformaldehyde fixation of cells

Cells plated on glass coverslips had growth media removed and were washed once in DPBS before incubation with 4% paraformaldehyde (PFA) for 8 min at room temperature. Post incubation cells were washed once with DMEM containing 10% FCS in order to prevent over fixation before 3 further washes in DPBS. Fixed cells were stored in DPBS at 4°C until staining.

2.3.1.2. – Methanol fixation of cells

Cells plated on glass coverslips had growth media removed and were washed once in DPBS before incubation with methanol for 5 min at -20°C. Post incubation cells were washed 3 times in DPBS. Fixed cells were stored in DPBS at 4°C until staining.

2.3.1.3. – Blocking Buffer

1% bovine serum albumin (BSA) to prevent non-specific antibody interactions and 0.01% saponin to aid permeabilisation of cells in DPBS. This was stored in aliquots at -20°C until use.

2.3.1.4. – Primary Antibodies for Immunocytochemistry

Primary antibodies utilised in the studies described in this these are listed below in alphabetical order.

2.3.1.4.1. – Annexin A2

Visualisation of levels of Annexin A2 (AnA2) was used as an indication of endocytic trafficking dysfunction as a result of Ca^{2+} dyshomeostasis. In healthy cells plasma membrane localisation of AnA2 is observed whereas a small perinuclear cluster of AnA2 is observed in cells where endolysosomal Ca^{2+} dyshomeostasis is dysregulated. PFA fixed cells were incubated with a 1:200 dilution of mouse monoclonal anti-AnA2 (Novus, Oxford, UK) in blocking buffer overnight a 4°C.

2.3.1.4.2. – LAMP-2

LAMP-2 was used as a marker of late-endosomal and lysosomal morphology and expansion. Methanol fixed cells were incubated with 2% FCS and 2% BSA in PBS for 30 min at room temperature. Cells were then incubated for 30 min at room temperature with rat monoclonal anti-mouse LAMP-2 ABL-93 (developmental studies hybridoma bank, University of Iowa, USA) or anti-human LAMP-2 H4B4 (developmental studies hybridoma bank) at a 1:100 dilution in 2% FCS and 2% BSA in PBS.

2.3.1.4.3. – LBPA

Visualisation of levels and localisation of lysobisphosphatidic acid (LBPA/BMP) was used to determine lipid levels and localisation. PFA fixed cells were incubated with a 1:1000 dilution mouse monoclonal anti-ZPLBPA (Echelon, Salt Lake City, USA) in blocking buffer overnight a 4°C.

2.3.1.4.4. – NPC1

Visualisation of levels and localisation of the Niemann-Pick C1 (NPC1) protein was used to study lipid trafficking dysfunction in the late-endosome and lysosome. PFA fixed cells were incubated with a 1:200 dilution rabbit polyclonal anti-NPC1 (Novus) in blocking buffer overnight a 4°C.

2.3.1.4.5. – NPC2

Visualisation of levels and localisation of the Niemann-Pick C2 (NPC2) protein was used to study lipid trafficking dysfunction in the lysosome and as a lysosomal marker where appropriate. PFA fixed cells were incubated with a 1:200 dilution rabbit polyclonal anti-NPC2 (Sigma) in blocking buffer overnight a 4°C.

2.3.1.4.6. – SERCA2

Visualisation of levels of the sarco/endoplasmic reticulum Ca^{2+} ATPase (SERCA2) was used as an indication of ER density and to investigate changes, which may lead to Ca^{2+} dyshomeostasis. PFA fixed cells were incubated with a 1:200 dilution of mouse monoclonal [IID8] to SERCA2 ATPase (Abcam) in blocking buffer overnight at 4°C.

2.3.1.4.7. – TMED4

Visualisation of levels of Transmembrane Emp24 Protein Transport Domain Containing 4 (TMED4) was used as an indication of ER stress. In healthy cells Golgi localised staining of TMED4 is evident, in cells with ER stress lightly punctate extra-Golgi staining is evident. PFA fixed cells were incubated with a 1:200 dilution of TMED4 (Novus) in blocking buffer overnight at 4°C.

2.3.1.5. – Secondary Antibodies for Immunocytochemistry

Post incubation with primary antibodies, cells were washed 3 x 5 min in Dulbecco's phosphate buffered saline (DPBS). They were then incubated for 30 min at room temperature with epitope compatible Dylight 488 secondary antibody (Vector) or Dylight 594 secondary antibody (Vector, Peterborough, UK) at a 1:200 dilution in blocking buffer. Cells were washed in DPBS 3 x. Secondary antibody controls were performed on all cell lines and during initial experiments with primary antibodies.

2.3.1.6. – Filipin staining

Visualisation of levels and localisation of un-esterified cholesterol was achieved using the autofluorescent polyene antibiotic filipin which is widely used as a histochemical stain. (Vanier., 2015). PFA fixed cells were incubated in a 125µg/ml

solution of filipin in DMEM with 10% FCS for 30 min at room temperature before three washes in DPBS.

2.3.1.7. – Lysenin staining

Lysenin is a protein isolated from the coelomic fluid of the earthworm *Eisenia foetida* which binds specifically to sphingomyelin; as such it was used to visualise levels and localisation of sphingomyelin within cells. (Taskir., 2012). PFA fixed cells were incubated in a 33ng/ml solution of Lysenin toxin (Peptides International, Louisville, USA) in blocking buffer overnight a 4°C before 3 x 5 min washes in DPBS. Cells were then incubated with primary anti-lysenin antibody (Peptides International) at a 1:1000 dilution in blocking buffer for 1 hr at room temperature. After 3 x 5 min washes in DPBS cells were incubated with a Dylight 594 anti-rabbit IgG (Vector) as described in 2.2.4.

2.3.1.8. – FITC-Cholera Toxin B subunit staining

The cholera toxin B subunit binds to Ganglioside GM1 and can be visualised by the FITC-tag applied to the protein (Blank et al., 2007). PFA fixed cells were incubated in a 1µg/ml solution of FITC- Cholera Toxin B subunit (CtxB) in blocking buffer overnight a 4°C before 3 washes in PBS.

2.3.1.9. – Nuclear Co-Staining

Nuclei were visualised by 10 min incubation with 2µg/ml Hoechst 33342 trihydrochloride trihydrate in DPBS.

2.3.1.10. – Coverslip Mounting

Coverslips were mounted onto glass slides in 0.4 g/ml mowiol 4-88 in DPBS and left to dry in the dark at room temperature for at least 16 hr prior to imaging.

2.3.2. – Live Cell Staining

2.3.2.1. – Imaging Buffer

Hank's balanced salt solution (HBSS) with 1mM HEPES, 1mM $MgCl_2$ and 1mM $CaCl_2$, all live cell analysis was conducted in this buffer unless otherwise stated.

2.3.2.2. – Autofluorescence

Cells grown in Ibidi µ well microscope slides were washed once in imaging buffer then imaged live. All excitation wavelengths were imaged to check levels of autofluorescence and then multiple pictures were taken after excitation at 470nm to image the autofluorescence observed in cells and post mortem analysis of patients with lysosomal storage diseases such as the neuronal ceroid lipofuscinoses (Di Guardo., 2015).

2.3.2.3. – Lysotracker

Lysotracker green DND-26 or lysotracker red DND-99 (Life Technologies) was used to investigate the volume of acidic compartments (pH < 5.5) within cells. Cells grown in Ibidi µ well microscope slides were washed once in imaging buffer then incubated with 200nM lysotracker in imaging buffer for 15 min at room temperature. Cells were washed once more in imaging buffer then imaged live.

2.3.2.4. – ER tracker

ERtracker blue-white DPX (Life Technologies) was used to investigate the volume of the ER within cells. Cells grown in Ibidi µ well microscope slides were washed once in imaging buffer then incubated with 200nM ER tracker in imaging buffer for 15 min at room temperature. Cells were washed once more in imaging buffer then imaged live.

2.3.2.5. – Cholera toxin B trafficking assay

When applied to live cells CtxB binds to ganglioside GM1 in the plasma membrane (Blank et al., 2007; Benktander et al., 2013) and is internalised by retrograde endocytic transport to the Golgi apparatus in healthy cells (Singh et al., 2003). A well

characterised defect in lysosomal storage diseases is incomplete trafficking of sphingolipids resulting in retention within the endocytic system (Pagano E., 2003).

Cells grown on coverslips had growth medium replaced with ice cold growth medium containing 1µg/ml FITC CtxB and incubated for 30 min at room temperature, medium was kept ice cold to prevent premature internalisation. Pulse medium was then removed and cells were incubated in pre-warmed normal growth medium for a chase period calibrated for each cell line at 37°C and 5% CO_2. Three 10 min back exchanges were then carried out in ice cold growth medium supplemented with 2% BSA and 0.1mg/ml heparin sulphate. These back exchanges remove non-specifically bound GM1 from the plasma membrane. Cells were washed once in DPBS and PFA fixed.

During microscopy representative images of field of cells were taken and in subsequent analysis the subcellular localisation of the FITC tagged protein was identified and each cell was scored for either correct trafficking to the Golgi, defective endo-lysosomal trafficking or an intermediate between the two states.

2.3.2.6. – Magic Red cathepsin assays

To examine the *in situ* activities of cathepsin B and L in cells specific fluorescent probes for each enzyme were used. These are substrates specific for cathepsin B or L and fluoresce upon cleavage.

Cells grown in Ibidi µ well microscope slides were washed once in imaging buffer then incubated with Magic Red cathepsin B (MR Cat B) or Magic Red cathepsin L (MR Cat L) (Immunocytochemistry technologies) for 15 min at 37°C and 5% CO_2 or 30 min at 33°C and 5% CO_2. Dependant upon the normal growth conditions of the cell. Cells were washed once more in imaging buffer then imaged live.

2.3.2.7. – FITC Sphingosine transport assay

FITC-tagged sphingosine (FITC-SphO) has previously been shown to adopt a punctate localisation in cells which have disrupted activity of NPC1 (Lloyd-Evans *et al.,* unpublished). Importantly, the tagged SphO utilised in this study has been shown to cause NPC disease cellular phenotypes when applied to cells as has been

observed with un-modified SphO; this strongly suggests that the addition of a FITC tag to SphO does not disrupt the protein interactions.

Cells treated with 1μM FITC-SphO for 10 min were examined by microscopy to ensure a punctate distribution of FITC-SphO representing traffic to acidic organelles and initial retention in these compartments due to the pKa of SphO, this has been confirmed by lysotracker co-staining (Lloyd-Evans *et al*., Unpublished). Cells were then left in growth medium for 24 hr before re-imaging to determine the final location of FITC-SphO and analyse the cells for either diffuse or punctate distribution.

2.3.2.8. – Glutamate induced Ca^{2+} dyshomeostasis in neurons

iPSC derived neurons grown as described in 2.1.7. for 37 - 44 days had BDNF withdrawn from growth media for 24 hr prior to loading with Fura2-AM (Life Technologies) in growth medium for 30 min at 37°C and 5% CO_2. Before removal of the staining solution and 15 min incubation at room temperature in external cell solution for these experiments. This consisted of 135mM NaCl, 5mM KCl, %mM HEPES, 10mM glucose, 1.2mM $MgCl_2$ and 1.25mM $CaCl_2$.

The method was adapted from that described in the HD iPSC Consortium report (2012). Briefly, coverslips were transferred to a perfusion chamber on an inverted microscope (Olympus, Southend-on-Sea, UK) with monochrome based fluorimiter (Cairn Research, Faversham, UK) and continuously perfused using a rapid perfusion system (BioLogic science instruments, Claix, France). Fura2 was alternately excited at 340 and 380nm and images recorded every 2 seconds using a CCD camera (Hamamatsu, Hamamatsu City, Japan). Cell body regions of interest were defined and all values recorded were adjusted for background fluorescence. Cells were then perfused with 60mM KCl to induce depolarization and confirm cell viability. Subsequently cells were perfused with 300μM glutamate and 30μM glycine for 5 min before 5 min washout in external cell solution. This process was repeated 5 times before a prolonged pulse of 300μM glutamate and 30μM glycine was added to cells for 2 hr. Subsequently external cell solution wash out was performed and cells were subjected to a final 10mM KCl perfusion.

Cells were counted as having lost Ca^{2+} homeostasis when the Fura2 ratio exceeded that of the 1 min prolonged pulse baseline (plateau) and did not return. Subsequently survival curves were plotted with the loss of Ca^{2+} homeostasis counted as a 'death'

event. These experiments were all performed by, or with assistance from Polina Yarova (Kemp lab, Cardiff University) who also analysed the data subsequently.

2.4. - Microscopy

2.4.1. – Fluorescence microscopy

All fluorescence microscopy was performed on an inverted AX10 inverted microscope (Zeiss, Cambridge, UK) with LED lightsource and Colibri controller (Zeiss). Images were taken in monochrome with a Axiocam MRm CCD digital camera (Zeiss) using Axiovision software release 4.7.1 (Zeiss). Pseudocolouring was added to images using Photoshop CS3 (Adobe, California, USA). Subsequent image analysis was performed using ImageJ (NIH, Bethesda, USA). In all cases cells from different genotypes and treatments were imaged alongside control cells and identical LED power and exposure time were applied to all images. Subsequent image analysis was performed with identical adjustments.

2.4.2. – Thresholding image analysis

For experiments in which the level of brightness of a probe was being compared a thresholding procedure was used to determine if there were any differences between cell lines. Representative images of field of cells taken during microscopy underwent identical alterations in brightness and contrast in photoshop CS3. In ImageJ, images were changed to 8-bit monochrome and the total number of cells were counted using the cell counter plugin. Subsequently the threshold was adjusted so that approximately 50% of cells from control experimental populations were highlighted. All images were then subjected to these settings and the cell counter plugin was used to count the number of cells above the threshold value. Accordingly cells could be analysed in a semi-quantitative manner. Greater than 30 cells were analysed per experimental repeat.

2.5. – Ca^{2+} measurements

2.5.1. – Cytosolic Ca^{2+} probe loading

Cells were plated on Ibidi µ-Slide 8 well imaging dishes and left to adhere overnight. Post incubation, cells were loaded with either 5µM Fluo3-AM (Stratech Scientific LTD, Newmarket, UK; Life Technologies) or 5µM Fura2-AM (Teflabs, Austin, USA) in DMEM with 1% BSA and 0.025% Pluronic acid F127 for 1 hr at room temperature then washed in imaging buffer and left for 10 min at room temperature to allow de-esterification of the calcium probe. Imaging buffer was adapted to exclude Ca^{2+} where this was required for experimental considerations.

2.5.2. – Cellular Ca^{2+} measurement

Intracellular Ca^{2+} responses were recorded using a Colibri LED microscope system with an Axiocam Mrm CCD camera and Axiovision software version 4.7 with the additional physiology module for live cell Ca^{2+} imaging (Zeiss). Cytoplasmic regions of interest (ROIs) were drawn over the cell and a minimum number of 5 cells were analysed per field of view per experiment. Prior to agonist addition recordings of the Ca^{2+} probe baseline was used to provide comparative basal Ca^{2+} measurements of cells within the same experiment. All agonist-induced Ca^{2+} responses were compared by peak height. Data was subsequently analysed using Graphpad Prism. Experiments utilising Fluo3 were converted to % of control against the control cell line (WT BD cells in all cases). This was to make the experiments comparable in the absence of a loading control. This was not necessary for Fura2 as a loading control is present as part of this probe making experiments comparable.

2.5.3. – Lysosomal Ca^{2+} release measurements

Release of lysosomal Ca^{2+} was measured using methods adapted from those previously described (Lloyd-Evans et al., 2008). Post loading with a cytosolic Ca^{2+} probe addition of 300µM GPN (Sigma, Alfa Aesar,Ward Hill, USA; Cayman, Ann Arbor, USA) was used to induce lysis of the lysosome, 100-250nM NAADP-AM (synthesised according to Parkesh et al., 2008) was used to release Ca^{2+} from the TPC2 channel and 5mM NH_4Cl was used to de-protonate the lysosome and

subsequently release Ca^{2+} as required for the experiment. In later experiments 10μM Nigericin was used to induce Ca^{2+} release from the lysosome due to the action of nigericin as a Ca^{2+} - K^{+} antiporter. This change in protocol was due to inconsistent observations of lysosomal lysis in response to some batches of GPN from Alfa Aesar and Cayman. This was observed during the time experiments in chapter 5 were taking place and was also used in 3.2.3.11. and 3.2.3.15. In order to prevent the release of Ca^{2+} from other cellular stores as a result of Ca^{2+} induced Ca^{2+} release (CICR) in some experiments cells were pre-treated with either 1 μM or 5μM thasigargin (Sigma) to prevent ER release, or 2 μM or 5 μM ionomycin (Calbiochem) to prevent release from all other cellular Ca^{2+} stores.

2.5.4. – ML-SA1 induced Ca^{2+} release measurements

ML-SA1 (Calbiochem) is a synthetic agonist which induces Ca^{2+} release from TRPM1 as described in (Shen et al., 2012) To study Ca^{2+} release in response to ML-SA1 cells were treated with 20μM ML-SA1 (BD blastocysts) or 50μM ML-SA1 (Human fibroblasts). All experiments with ML-SA1 were conducted in he absence of Ca^{2+} in imaging buffer.

2.5.5. – ER Ca^{2+} release measurements

Release of ER Ca^{2+} was measured by addition of between 1μM and 5μM thapsigargin (Sigma), dependant upon cell type, or 10μM ryanodine post loading with a cytosolic Ca^{2+} probe. In order to evaluate if cells were more susceptible to Ca^{2+} release decreased concentrations (0.1μM thapsigargin) of antagonist was used. Thapsigargin is a non-competitive inhibitor of SERCA2 which actively transports Ca^{2+} into the ER; at the concentrations used thapsigargin causes ER Ca^{2+} channel unmasking releasing Ca^{2+} from Ca^{2+} leak channels causing subsequent CICR from ryanodine and IP3 receptors on the ER. It is not necessary to remove other Ca^{2+} stores when measuring ER Ca^{2+} release as it is the largest cellular Ca^{2+} store so the input from other Ca^{2+} stores is negligible when this experiment is conducted in the absence of extracellular Ca^{2+}. In some experiments 10μM ryanodine was used to induce Ca^{2+} release from the ryanodine receptors (RyRs) on the ER.

2.5.6. – Mitochondrial Ca^{2+} release measurements

Mitochondrial Ca^{2+} release was induced by de-polarisation of mitochondria by 10μM rotenone post loading with a cytosolic Ca^{2+} probe. Prevention of release from other Ca^{2+} stores was not possible for this store as it would either cause mitochondrial release (ionomycin) or raise mitochondrial Ca^{2+} levels due to the uptake of cytosolic Ca^{2+} released from other stores such as the ER.

2.5.7. – Store operated Ca^{2+} entry measurements

Cells loaded with cytosolic Ca^{2+} probe in Ca^{2+} free imaging buffer were induced to release ER Ca^{2+} with 1-5 μM thapsigargin. This activates STIM proteins which translocate from the ER to the plasma membrane where they bind ORAI to facilitate plasma membrane Ca^{2+} entry. Accordingly when the Ca^{2+} release induced by thapsigargin has returned to baseline 1mM Ca^{2+} is added to the imaging medium and response are measured.

2.6. – Biochemistry

2.6.1. – Thin Layer Chromatography

Lipid species within cells were quantified using a thin layer chromatography method adapted from Maue et al. (2012).

2.6.1.1. – Lipid Extraction

Cells were harvested from tissue culture flasks by trypsinisation before pelleting by centrifuge and 3 washes in DPBS. Cell pellets were subjected to 3 rounds of freeze-thaw and homogenised by 50 strokes in a PTFE coated glass pestle and mortar homogeniser on ice. Homogenate was centrifuged at 1000rpm for 5 min at 4°C and a small aliquot of supernatant taken for BCA protein assay (conducted as per manufacturers instructions). Aliquots of samples were then taken from the entire homogenate equal to the maximum amount of protein (<1mg) available across all the desired samples. Volumes were equalised with MilliQ water and lipids were extracted

by adding 5 original volumes of chloroform:methanol 1:2 to each sample before gentle agitation by roller for 16 hr at 4°C. Samples were then centrifuged at 3000rpm for 10 min at 20°C and the supernatant collected. The pellet was re-extracted with 5 original volumes of chloroform:methanol 1:2 and agitated gently by roller for 3 hr at room temperature. Samples were again centrifuged at 3000rpm for 10 min at 20°C and supernatant collected. Combined supernatant was then dried down under a stream of N_2.

To remove excessive salt from the samples resuspension by vigorous vortexing in 2 ml of chloroform:methanol 1:2 was followed by the addition of 3ml of PBS and 3ml of chloroform:methanol 1:2 and samples vortexed then centrifuged at 500rpm for 2 min at 20°C to give a clear phase separation. The aqueous upper phase was removed and the remaining organic lipid containing lower phase after this process was dried down under nitrogen.

2.6.1.3. – Preparation of standards for TLC

A total lipid brain extract (Avanti Polar lipids, Alabaster, USA) was solubilised in chloroform:methanol 1:1. The lipid species present in this extract have been verified using standard preparations of different lipids (Avanti Polar Lipids, Sigma, Matreya). 150 µg of brain extract was loaded per cm of lane onto each plate.

2.6.1.2. – TLC separation of lipid species

A pre-dried silica gel HPTLC plate (Merck, Kenilworth, USA) was used to separate the lipid species, samples were resuspended in chloroform:methanol 1:1 by vortexing and sonication and applied at the nottom of the plate in lanes of a size dependant upon the starting amount of material extracted (approx. 0.3cm for samples below 0.5mg protein, 0.5 cm for samples between 0.5-1mg of protein and 1cm for samples between 1-2mg protein). Loaded plates were ran in a pre-equilibrated TLC tank with a mobile phase of chloroform:methanol:water 65:25:5 until the solvent front was 1cm from the top edge of the TLC plate. This mobile phase was changed to chloroform:methanol:water 80:10:5 if separation of cholesterol and ceramide was required.

2.6.1.4. – Development of separated lipid species

Plates for general lipid analysis were dried under a stream of hot air prior to spraying with p-Anisaldehyde spray reagent consisting of 50ml glacial acetic acid, 1ml concentrated sulphuric acid and 0.5ml p-Anisaldehyde. Plates were sprayed until saturation. Saturated plates were then charred by gradual warming up to 95°C.

2.6.1.5. – Analysis of lipid species

Post heating plates were scanned immediately in both grayscale and colour. Coloured images were used to assist with lipid species identification and grayscale images were used for densiometric analysis using ImageJ. In order to do this the gel analysis plugin was utilised in order to plot the grayscale values from bands on the TLC. These plots were used to calculate the area under the curve of each of the bands relating to known lipids, baseline decay was taken into account when defining the extent of these peaks.

2.6.2. – Western blotting

Homogenised samples from cell pellets corresponding to 5µg of protein (determined by BCA assay, as per manufacturers instructions) was denatured in sample buffer SDS containing sample buffer for 1hr at 60°C. Denatured protein samples were separated by gel electrophoresis across a 10% SDS-PAGE gel at 160V for 2 hr. Proteins were then transferred onto PVDF transfer membrane soaked in methanol (Merck-Millipore, Billerica, USA) using a semi-dry transfer method at 40mA for 2 hr.

Transfer membranes were then blocked overnight at 4°C in 5% milk powder solution. Before incubation with anti-TRPML1 primary antibody (Santa Cruz, Dallas, USA) at 1:1000 dilution overnight at 4°C in 5% milk powder solution. After repeated washing in TBS buffer with 0.05% TWEEN-20 an anti-rabbit secondary antibody was applied at a 1:10000 dilution. Subsequently transfer membranes were washed in ECL development solution and exposed onto X-ray film (Santa Cruz) prior to development.

Bands were analysed utilising the same methodology described for TLC analysis above.

2.7. – Statistical analysis

For statistical analysis each n refers to an experiment initiated from an independent plating of cells, for microscopy or Ca^{2+} analysis, or an independent cell culture, for western blot or TLC analysis.

T tests were performed for experiments in which values from 2 conditions were being compared. In relation to Ca^{2+} analysis and threshold counting, these values were experimental means from individual measurements. With respect to western blotting and TLC analysis these were individual bands from these studies these were generated from independently prepared cell cultures. One way ANOVA with Bonferroni post test were used to analyse experiments in which 3 or more conditions were present. The data used in this analysis was as described above for T tests. Analysis of survival curves was conducted by Logrank test. All these tests were performed using in Graphpad Prism version 4.0c.

For experiments in which groups of cells within a cell culture were being compared Chi^2 (X^2) tests were used. In these tests the expected value was generated from the mean of the groups in the cell culture that was being compared against. As standard error of the mean (SEM) was small (<10%) in all the experiments these tests were utilised to compare this remains robust. Individual X^2 values were calculated for each experimental repeat of these experiments and are shown in the text. For experiments in which 5 or more repeats had been conducted X^2 values are presented as a mean of the individual values +/- SEM. X^2 values were calculated in Microsoft excel.

Statistical test for each experiment are shown in figure legends, as are indicators of significance which are as follows: * = $P < 0.05$, ** = $P < 0.01$, *** = $P < 0.001$, **** = $P < 0.0001$.

Chapter 3

How do Ca^{2+} and lipid dyshomeostasis in the endolysosomal system contribute to familial Alzheimer's disease?

3.1. – Introduction

3.1.1. – Alzheimer's disease

Alzheimer's disease is the most common neurodegenerative disease in North America and Europe, worldwide a new case is estimated to be reported every 7 seconds (Cornutiu, 2015). It is a form of slowly progressing dementia which often begins with subtle, symptoms, which may go unrecognised. Commonly patients present with the disease around the 6th decade of life with symptoms such as short term memory loss which progresses to incapacitation over an average course of 8-10 years. During this time, patients may suffer from a variety of symptoms including confusion, poor judgment, language disturbance, agitation, withdrawal and hallucinations (Mckhann et al., 2011). As with other forms of dementia, the incidence of Alzheimer's increases markedly with age and a combination of subtle initial symptoms and convergent phenotypes with other forms of dementia mean that many cases remain undiagnosed (Bird, 1998).

In addition to the clinical presentation of dementia, Alzheimer's patients are also observed to have gross cerebral atrophy by computed tomography scan (CT) or magnetic resonance imaging (MRI) and diffuse cerebral hypometabolism by positron emission tomography (PET) (Bird, 1998; Weiner, M.W., 2015). In the post-mortem brain extracellular plaques consisting of the protein β-amyloid (Aβ) and intraneuronal tangles of aberrantly phosphorylated tau protein are observed and analysis of patient cerebro-spinal fluid (CSF) reveals alterations in the levels of these proteins (Snider et al., 2009). Lewy bodies consisting of α-synuclein may also be present in the amygdala in some cases highlighting the convergent pathology observed in various form of dementia (Bird, 1998; Popescu et al., 2004;).

The majority of Alzheimer's cases, approximately 95%, are considered idiopathic. Currently there are no known environmental agents which have been proved to be directly involved in Alzheimer's although twin studies have implicated both genes and environment (Bird, 1998). Recently, there has been a concerted effort within the Alzheimer's research community to identify predisposing genetic variation using large datasets in the hope of identifying disease modifiers (Escott-Price et al., 2014; Lambert et al., 2013).

3.1.2 - Familial Alzheimer's disease

The remaining approximately 5% of Alzheimer's patients are considered to have familial Alzheimer's disease (FAD) as two or more cases have been observed in directly related individuals. Of all Alzheimer's cases 95% are classified as late-onset (LOAD) as symptoms begin to manifest in the sixth decade of life; the remaining 5% experience symptoms prior to this age and are considered early-onset (EOAD) (Raux et al., 2005).

The first gene linked to Alzheimer's by investigation of families presenting with EOAD was *APP* which codes for the β-amyloid precursor protein (Goate et al., 1991). This protein is the precursor of β-amyloid (Aβ) which had been isolated from the brain of a patient with Down's syndrome and was originally linked to Alzheimer's due to the universal presence of Alzheimer's in patients with trisomy 21 (Masters et al., 1985). With this suggestion of chromosome 21 as the location for a causative Alzheimer's gene, and another study showing duplication of the *APP* locus was present in sporadic Alzheimer's patients (Delebar et al., 1987), mutations in *APP* were identified as a cause of EOAD (Goate et al., 1991) and subsequent publications corroborated these findings (Chartier-Harlin et al., 1991; Murrel et al., 1991; Mullan et al., 1992). A combination of these studies helped establish the amyloid hypothesis of Alzheimer's disease Hardy and Allsop, 1991; Hardy and Higgins, 1992). This entailed five major predictions: (i) Other kindreds with Alzheimer's would be identified with APP mutations, (ii) Aβ is a normal product of APP metabolism and that the mutations would influence Aβ production, (iii) other Alzheimer's genes would be identified and these would influence Aβ production, (iv) regulatory variants in APP would predispose to LOAD, (v) Aβ deposition is a central event in the pathogenesis of Alzheimer's (Goate and Hardy, 2012).

Initially, these predictions seemed to bear weight with Presenilin genes (*PSEN1*/*PSEN2*) identified as another cause of familial EOAD and the demonstration that Presenilin formed the catalytic core of the complex capable of metabolising APP, thus affecting Aβ production. Such observations have lead to the development of Alzheimer's disease animal models and informed therapeutic study. Confirmation of predictions iv and v have proven more elusive; variants predisposing to LOAD have, as yet, not been directly linked to APP regulation. For example, the most common variant predisposing to LOAD is the ε4 allele of Apolipoprotein E (APOε4), which causes a dose-dependant increase in risk and decrease in age of onset of

Alzheimer's. This gene influences cholesterol metabolism, and although this has been linked to changes in Aβ clearance, it is not directly implicated in APP regulation. The final prediction of the amyloid hypothesis remains unproven, as Aβ lowering therapies have not proven efficacious in the treatment of Alzheimer's, accordingly the role of Aβ, APP and the amyloid hypothesis remains debatable (Goate and Hardy, 2012).

As previously mentioned, the other 'hallmark' of post-mortem Alzheimer's pathology is the intracellular accumulation of aberrantly phosphorylated tau protein in structures known as neurofibrillary tangles (NFTs) (Liu et al., 2015). Tau proteins are highly expressed in the neurons where they assist in the stabilization of microtubules and are encoded by *MAPT*, alternative mRNA splicing of which provides the six tau isoforms present in human brains (Goedert et al., 1989). Tau has been implicated in LOAD (Gerrish et al., 2012) where the presence of NFTs correlates well with neuronal loss (Gomez-Isla et al., 1997). In Alzheimer's, tau protein becomes hyperphosphorylated and accumulates in the form of paired helical filaments which accumulate in the form of larger filaments of around 10nm. It has been suggested that a 'tau protein hypothesis' may better explain Alzheimer's pathogenesis that the amyloid hypothesis (Maccioni et al., 2010) however most studies now agree that an interplay between hyperphosphorylaed tau and Aβ underlie this process. It is hypothesised that a dual pathway model may exist with the intracellular presence of Aβ as smaller aggregates, such as oligomers, as an initiating factor driving subsequent pathology including tau hyperphosphorylation (Walsh and Selkoe, 2007). Although such a pathway remains to be proven it would implicate the endolysosomal system in Alzheimer's pathogenesis, as both early processing of Aβ and the clearance of hyper-phosphorylated tau is dependent upon the endolysosomal system (Lin et al., 2014; Wang et al., 2009).

Recently, genome-wide association studies (GWAS) have utilised advances in sequencing technology in order to assess common genetic variability at the level of the whole genome between large groups of patients and controls. Such studies have identified over 20 genetic loci which, in isolation, impart a low risk of late-onset Alzheimer's disease (LOAD) upon patients. Interestingly, these genetic loci partition into a small number of distinct biological pathways with the predominant effects upon three main processes: the immune system and inflammatory responses, cholesterol and lipid metabolism and endolysosomal vesicle trafficking (Escott-Price et al., 2014; Lambert et al., 2013). Accordingly the implication of genes such as *BIN1*, *PICALM*

(Lambert et al., 2013) and *SORL1* (Nicholas et al., 2015) provide further evidence that the endolysosomal system is important to the pathogenesis of Alzheimer's disease.

3.1.3. – The endolysosomal system in Alzheimer's disease

As previously mentioned the processes which occur within the endolysosomal system may be central to the pathogenesis of the various forms of Alzheimer's. Changes to this system within neurons have also been reported to be one of the primary pathogenic events in Alzheimer's. This has been observed in patients with Down's syndrome decades before the onset of Alzheimer's and has been proposed as an initiating factor underlying changes leading to the elevation of Aβ levels in patients with sporadic Alzheimer's (Cataldo et al., 1997; Cataldo et al., 2000).

One of the primary links between the endolysosomal system and Alzheimer's is the importance of this pathway for the processing of APP. Glycosylated APP situated at the plasma membrane is subject to continuous turnover by two well-delineated mechanisms although other mechanisms may be involved in this processing. One mechanism begins with α-cleavage of APP by aspartyl proteases at a site within the extracellular domain to generate a large soluble N-terminal fragment which enters the extracellular milieu and a C-terminal fragment (CTF) which remains membrane associated. The alternate mechanism is initiated when plasma membrane APP is internalised within early endosomes prior to β-cleavage to generate a smaller soluble N-terminal fragment than α-cleavage and accordingly a larger CTF. The aspartyl protease which cleaves these β-CTFs, γ secretase, requires an acidic pH optimum and is predominantly present in the endolysosomal system. Aβ can be generated from β-CTFs by intramembrane γ-cleavage to yield mainly 40 aa Aβ (Aβ40) with a smaller amount of 42 aa Aβ (Aβ42). Changes in the ratio of Aβ42:Aβ40 are considered to be one of the better biomarkers of Alzheimer's (Nixon, 2005; Spies et al., 2010). Inhibition of endocytosis in model systems have been shown to decrease Aβ generation with the converse true of acceleration (Koo et al., 1994; Grbovic et al., 2003). γ-cleavage of APP is mediated by the γ-secretase complex which consists the proteins presenilin 1 (PS1) and 2 (PS2), nicastrin, anterior pharynx defective 1 (apH-1) and presenilin-enchancer protein (PEN) (Edbauer., 2003; Nixon., 2005). The various components of this complex have been identified throughout the autophagic and endolysosomal system clearly implicating this system in APP processing and

highlighting how dysfunction in this pathway can impact upon Aβ production (Pasternak et al., 2003).

Interestingly, the well established risk factors for Alzheimer's disease such as APoE alleles (Ji et al., 2006) and the causes of faimilial Alzheimer's such as APP and PS1 have all also been further implicated in lysosomal dysfunction particularly disruption of lysosomal proteolysis (Lee et al., 2010). When the effect of other contributors to Alzheimer's pathogenesis such as Aβ peptide, oxidised lipids and lipoproteins have also been shown to disrupt lysosomal proteolysis (Glabe 2001) and increase the substrates entering this system by Rab5 upregulation (Grbovic et al., 2003) it is not surprising that these phenotypes remain an area of intense study. The implications of impaired lysosomal proteolysis particularly in relation to defects in autophagic processes will be discussed in section 3.1.4.

A variety of other proteins in the endolysosomal system including both transmembrane proteins from various organelles and soluble lysosomal hydrolases have also been implicated in Alzheimer's pathogenesis. A number of these identified lysosomal hydrolases such as lysosomal acid lipase (LAL) (von Trotha., 2006), identified by linkage analysis, and acid sphingomyelinase (ASM), identified as a potential therapeutic target in animal models of familial Alzheimer's, link lysosomal catabolism and endocytosis to cholesterol and lipid homeostasis (Grimm et al., 2005; Lee et al., 2014.), another pathway implicated in LOAD by GWAS studies (Lambert et al., 2013). It is interesting to note that there is significant interplay between these two pathways as previously described.

Endolysosomal transmembrane proteins such as TRPML1 and NPC1 have also been implicated in Alzheimer's pathogenesis. The recent connection to TRPML1 has been identified in a preclinical model of HIV infection used to investigate the premature deficits in cognition often experienced by HIV-infected patients who have responded to anti-retroviral therapy (Bae et al., 2014). Conversely the connection between NPC1 and Alzheimer's is long established even to the degree where NPC disease is referred to as 'childhood Alzheimer's' partially due to the presence of NFTs in post-mortem patient brains, it is interesting that this is not strongly associated with the presence of plaques; a rare occurrence (Love et al., 2005; Saito et al., 2002; Nixon 2005). As discussed in section 1.5.2. loss of function in the NPC1 protein is associated with the lysosomal accumulation of a variety of lipids and the resultant effect of cholesterol storage in NPC1 models upon APP processing,

including the accumulation of APP-CTFs (Jin et al., 2004; Boland et al., 2010) and redistribution of presenilin to the early endocytic system has been studied (Burns et al., 2003). Given that the accumulation of other lipids including sphingolipids, which have been implicated in Alzheimer's disease pathogenesis (Grimm et al., 2010) also accumulate in NPC1 deficient lysosomes further work may be necessary to determine whether endocytic dysfunction or lipid dysregulation is the preliminary pathogenic event underlying Alzheimer's phenotypes in models of NPC disease. Yet further complexity is added to this situation when the presence of NFTs in NPC patients is considered, particularly, as it is one of only a small number of disorders where NFTs can be robustly observed in the absence of tau mutations and, in some cases, Aβ deposition (Love et al., 2005; Saito et al., 2002; Nixon 2005). Interestingly, tau mutation have been shown to exacerbate NPC phenotypes suggesting an interaction between the two proteins (Malnar et al., 2014). Given that a myriad of lysosomal defects have been found within Alzheimer's disease patients and models it is perhaps somewhat surprising that few genetic links directly implicating the lysosome in pathogenesis have been discovered. Nevertheless, it remains an important area of study as increasing numbers of genes and pathways which predispose individuals to Alzheimer's disease are shown to either cause or be compounded by endolysosomal dysfunction (Lambert et al., 2014). It may transpire that the role of the lysosome as a hub for the many cellular pathways which comprise the greater lysosomal system (section 1.2) and the importance of these pathways to neuronal cell function (1.6.2.) underlies this potential link.

3.1.4. – Autophagy and Alzheimer's disease

One pathway which forms part of the greater lysosomal system and terminates at the lysosome that has been extensively studied in relation to Alzheimer's is autophagy (Nixon, 2005; Nixon, 2013). The architecture of neurons places particular strain on this system as dysfunctional organelles must be transported large distances by retrograde transport of autophagosomes to reach the cell body where the majority of lysosomes are located. In young neurons, this task and the subsequent clearance of autophagic substrates such as dysfunctional organelles proceeds efficiently, however as neurons age this process begins to slow and as terminally differentiated cells they are not aided by reductions in these substrates due to cell division. Accordingly they are vulnerable to the accumulation of autophagic substrates (Boland et al., 2008); a

process which has been strongly linked to the accumulation of protein aggregates observed in many neurodegenerative diseases (Nixon, 2013).

In a number of Alzheimer's disease models and post-mortem samples from Alzheimer's patients dystrophic neurites, reminiscent of the meganeurites observed in LSDs, filled with autophagic vacuoles have been reported (Walkley et al., 1990). Although some of this accumulation may be caused by increases in the induction of autophagy, a lack of clearance of these organelles due to defects in the lysosome has been proposed as the major contributing factor. This proposal is supported by observations detailing LSD-like accumulations of autophagic vacuoles, particularly autolysosomes, when lysosomal proteolysis is disrupted in wild-type mice and the compounding of these phenotypes when the same disruptions in mouse models of Alzheimer's (Boland et al., 2008; Yang et al., 2008; Lee et al., 2011). The further study of these phenotypes in presenilin deficient cell lines and animal models of familial Alzheimer's have revealed some interesting mechanistic suggestions (Lee et al., 2010).

3.1.5. – Endolysosomal dysfunction in presenilin deficient models of Alzheimer's

In 2010, Lee *et al.* proposed that decreases in lysosomal proteolysis observed in cells deficient in PS1 was the result of lysosomal alkalisation and cathepsin activation, resulting from improper targeting of the V0a1 subunit of v-ATPase to the lysosome. As discussed in section 1.1.5., this protein complex is responsible for lysosomal acidification. The targeting defect was the result of defective N-glycosylation of V0a1 due to the removal of a selective binding event with PS1, which is necessary to facilitate the interaction of the unglycosylated protein with the Sec61 alpha/oligosaccharyltransferase complex. The resulting autophagic pathology and the accumulation of pathogenic protein aggregates was proposed to result from this initial event (Lee et al., 2010). Although lysosomal alkalisation was also observed in fibroblasts from Alzheimer's patients and have been reported by a number of other groups, this phenotype has been the subject of contention (Avrahami et al., 2013; Coen et al., 2012; Wolfe et al., 2013). Some aspects of this contention may be that correct measurement of lysosomal pH is technically difficult which may be best illustrated by a recent paper by Coffey et al. (2014) which showed lysosomal

alkalisation in fibroblasts from familial Alzheimer's patients in the region of 0.2 - 0.3 pH units.

Subsequently, a paper which contends the findings of Lee *et al*. was published. In this paper Coen *et al*. (2012) propose that lysosomal alkalisation is not present and that the accumulation of autophagic vacuoles is the result of reduction in lysosomal Ca^{2+} preventing the fusion of autophagic vacuoles with lysosomes (Coen et al., 2012). Although the authors did not provide a mechanism for this process it has been suggested that reduced ER Ca^{2+} leak results in less ability for the lysosome to fill with Ca^{2+}(Bezprozvanny, 2012).

3.1.6. – Ca^{2+} dyshomeostasis in Presenilin 1 deficient cells.

This study expands observations of Ca^{2+} dyshomeostasis in familial Alzheimer's to the lysosome. Previously studies on Ca^{2+} dyshomeostasis in Alzheimer's have focussed on the ER and the proposal that PS1 is a Ca^{2+} leak channel in this compartment (Tu et al., 2006; Popugaeva et al., 2013). A summary of the findings relating to Ca^{2+} dyshomeostasis in cells deficient in Presenilin 1 is shown in figure 3.1.

It is proposed that the loss of PS1-mediated Ca^{2+} leak from the ER leads to elevation in the Ca^{2+} content of this store. As a compensatory mechanism, the activity of ER Ca^{2+} release channels such as the ryanodine receptor (RyR) and IP_3 receptor (IP_3R) are potentiated and release more Ca^{2+}. This is accompanied by downregulation of store-operated Ca^{2+} entry (SOCE) (Popugaeva et al., 2013). There are varied reports of the result this has on cytosolic Ca^{2+} (Brunello et al., 2009; Tu et al., 2006) although the varied levels, including transient elevations in Ca^{2+} from the ER, are thought to lead to increased mitochondrial buffering of Ca^{2+} and subsequently the increased levels of Ca^{2+} in this organelle (Huang., 2014; Zampese., 2011). The recent addition of the lysosome to stores which are deregulated in $PS1^{-/-}$ cells is also shown. If reductions in Ca^{2+} release from lysosomal Ca^{2+} channels such as TPC2 and TRPML1 are present then this may result in lack of vesicular fusion and, therefore, autophagic impairment.

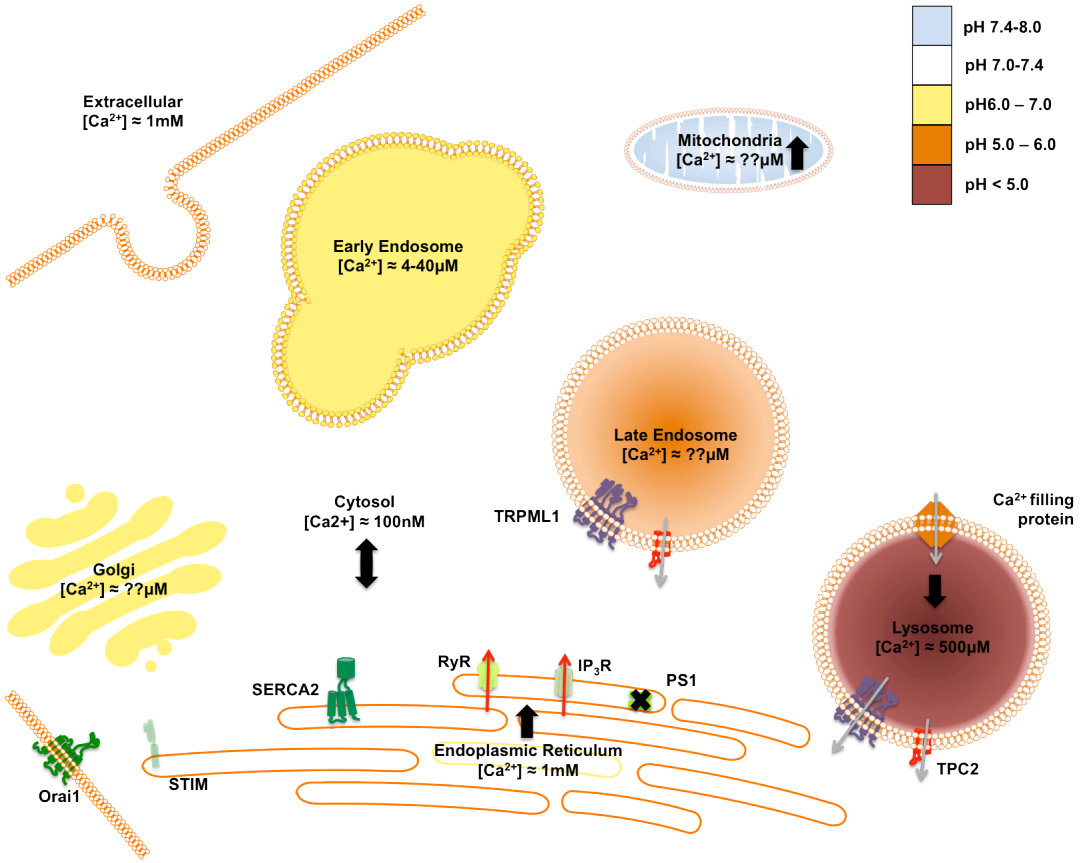

Figure 3.1. – Ca^{2+} dyshomeostasis in cell as a result of loss of function in PS1. *Changes to Ca^{2+} stores are shown by black arrows, pathogenically changes to Ca^{2+} releases are shown by thin arrows, red arrows indicate elevated release, grey arrows indicate reduced release. Protein loss of function is indicated by black crosses. Adapted from Popugaeva et al., 2013 and Lloyd-Evans et al., 2010.*

Of particular interest here is the similarity of this phenotype to that in NPC disease, a condition strongly linked to Alzheimer's-like pathology. It is also interesting to note that punctate staining with the cholesterol probe, filipin, has been observed in cells deficient in both PS1 and PS2 (Thimiri Govinda Raj., et al 2011), a phenotype which has also been observed in patient fibroblasts with the E693del *APP* mutation (Nomura et al., 2013). As this phenotype and reduced lysosomal Ca^{2+} are observed in NPC disease we are interested in investigating if presenilin deficiency has any further NPC phenotypes.

3.2. – Procedures

In section 3.3.1. we will investigate lipid phenotypes observed in cellular models of NPC1 disease using $PS1^{-/-}$ blastocyst-derived (BD) cells (2.1.1.) and $PS1^{-/-}$ and $PS1/2^{-/-}$ MEF cells (2.1.2.). Lipid phenotypes will be examined using the cell biology techniques described in 2.3.1. followed by biochemical quantification of lipid levels using thin-layer chromatography (2.6.1.). Subsequently, in section 3.3.2. we will use the most suitable of these two cell lines (identified by the studies in 3.3.1.) to conduct an examination of other cellular phenotypes observed in NPC1 disease models. These will include endolysosomal trafficking assays (2.3.2.5.) and analysis of cell for the storage of autofluorescent material (2.3.2.2.).

We will then undertake a thorough examination of lysosomal Ca^{2+} homeostasis using the techniques described in section 2.5 (section 3.3.3.). Where possible at least 3 independent plating replicates will be used in these experiments and appropriate statistical analysis will be performed as detailed in individual figure legends. In instances where 3 independent plating replicates were not performed, due to unavailability of cells or time restrictions this will be shown in the figure legend. These studies will include numerous controls to confirm the specificity of agonists, such as ML-SA1, utilised in this study.

Finally, is section 3.3.4, we will apply a combination of these techniques to study if any phenotypes we have identified are present in a different model utilised for Alzheimer's research, Down's syndrome patient fibroblasts.

Statistical analyses as described in section 2.7 have been performed on all these experiments as appropriate, details of these are given in individual figure legends.

3.3. – Results

3.3.1. – Lipid dyshomeostasis in Presenilin 1 deficient cells suggests complex lysosomal pathology

As discussed in section 3.1.5. a number of recent studies have suggested that disruption of PS function in cells can lead to a number of phenotypes which are suggestive of NPC1 dysfunction (Coen et al., 2012; Thimiri Govinda Raj., et al 2011). Currently most of these analyses have involved the visualisation of cholesterol within cells so we were interested to see if other lipids known to accumulate in NPC1 (Lloyd-Evans et al., 2008) disease do so in PS1$^{-/-}$ cells.

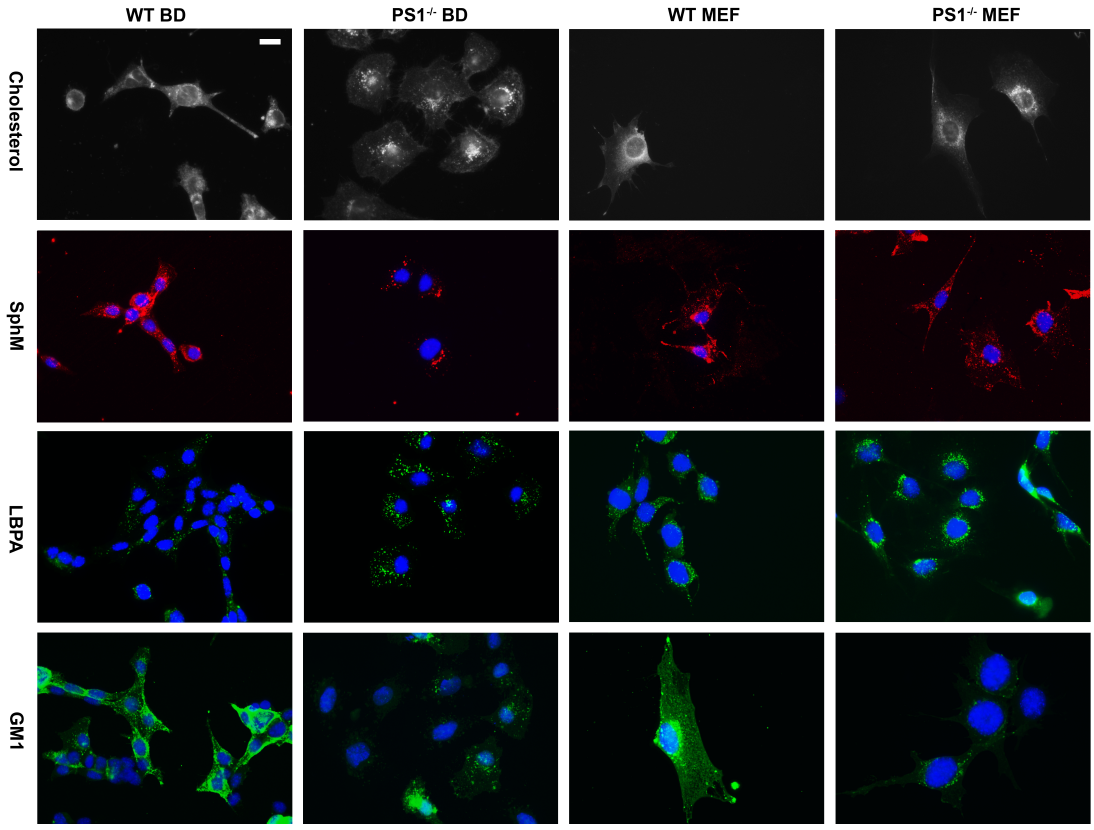

Figure 3.3.1. – Sphingolipid, phospholipid and cholesterol distribution in PS1$^{-/-}$ cell lines*. Representative microscopy images of wild-type (WT) and PS1$^{-/-}$ BD cells alongside wild-type (WT) and PS1$^{-/-}$ MEFs showing levels of cholesterol (white) visualised by filipin, sphingomyelin (SphM, red) visualised by IHC against the lysenin toxin, LBPA (green) visualised by IHC and ganglioside GM1 (GM1, green) visualised by FITC-tagged CtxB. Hoechst 33342 stained nuclei are shown in blue. n = 3. Scale bar = 7.5µm.*

Accordingly, we visualised cholesterol with filipin staining, the sphingolipid sphingomyelin with lysenin toxin, the phospholipid lysobisphospatidic acid (LBPA) with an antibody and the glycosphingolipid, ganglioside GM1, utilising cholera toxin B

subunit. All these lipids accumulate in cells with NPC1 disease phenotypes and as such we would expect elevated levels of all those lipids accompanied by redistribution to a punctate distribution indicative of lysosomal accumulation if NPC1 phenotypes were present in $PS1^{-/-}$ cells (Lloyd-Evans et al., 2008).

As figure 3.3.1. demonstrates, this is not observed in either of the $PS1^{-/-}$ cell lines investigated. Although there appears to be some accumulation of cholesterol in punctate bodies this is not accompanied by the concomitant increase in sphingomyelin and ganglioside observed in NPC disease, these lipids can instead be seen to decrease. There is an accumulation of LBPA, which is somewhat reminiscent of NPC disease, however, this lipid becomes elevated as compartment size in the endolysosomal system increases, a phenotype likely to occur in cells with any deficiency in clearance of substrates from the lysosomal system. As such, this increase appears to be a non-specific phenotype resulting from expansion of the endolysosomal system in $PS1^{-/-}$ cells.

It is interesting to note that the lipid phenotypes observed in $PS1^{-/-}$ BD cells seem to be more severe than those observed in $PS1^{-/-}$ MEF cells. In preliminary experiments, MEF cells with a double knockout of PS1 and PS2 were more similar to the results obtained in BD cells. This is suggestive of greater redundancy in MEF cells with regard to the knockout of either PS1 or PS2 alone in these cells perhaps explaining why $PS1/2^{-/-}$ MEF cells are commonly used to study presenilin deficiency. For clarity, and more relevance to patient phenotypes, we continued to perform most subsequent experiments in $PS1^{-/-}$ BD cells as they represent a robust phenotype without the loss of function of multiple proteins – a situation not observed in familial Alzheimer's.

As some hallmarks of NPC1 disease still remain in these cells we decided to further investigate lipid phenotypes in $PS1^{-/-}$ BD blastocysts alongside the same cells in which we had pharmacologically induced NPC1 disease phenotypes using the well-characterised molecule U18666a. This induces robust NPC1 phenotypes which relate temporally to the onset of cellular dysfunction in NPC1 disease (Lloyd-Evans et al., 2008).

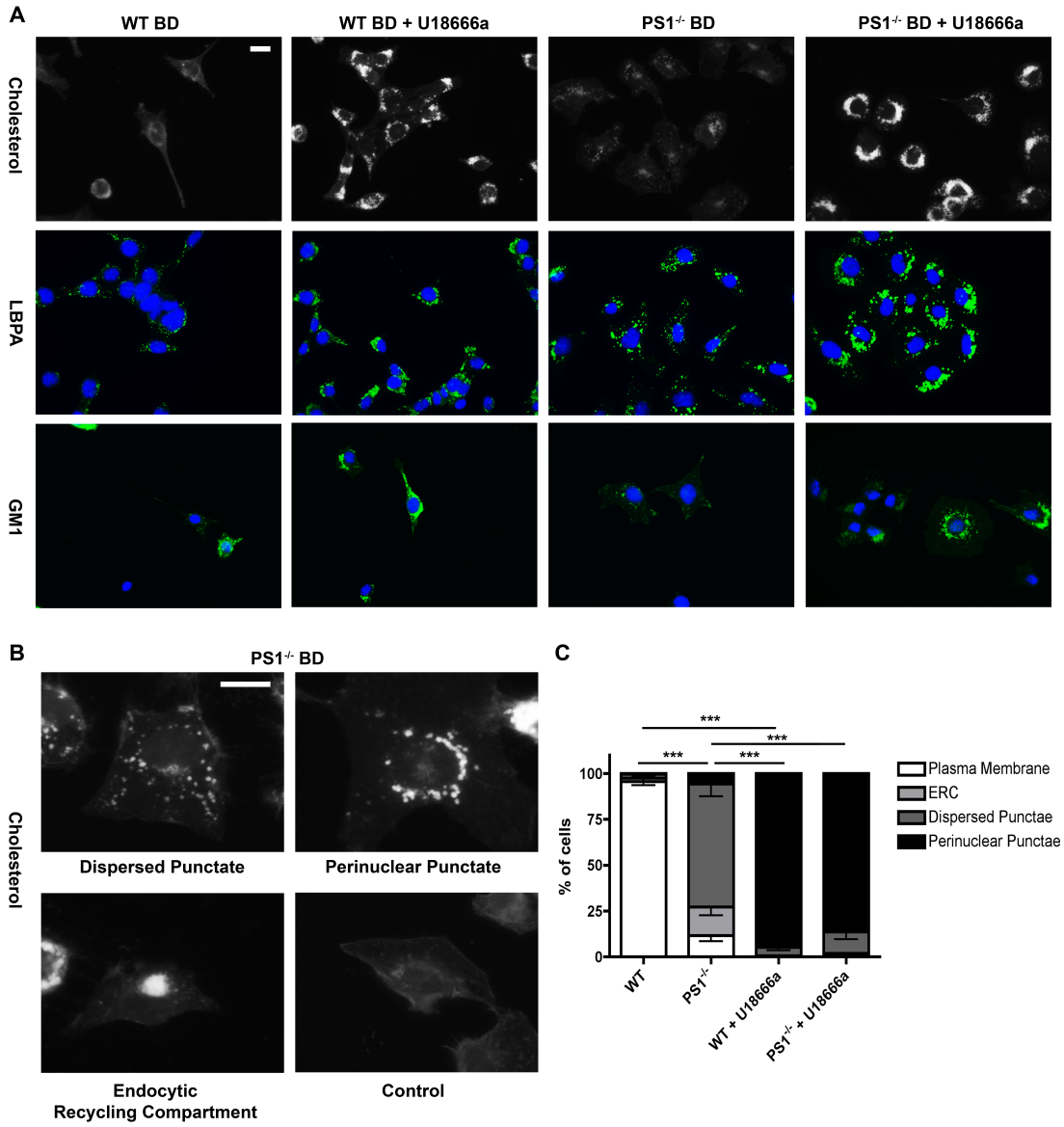

Figure 3.3.2. – Sphingolipid and cholesterol distribution changes in PS1$^{-/-}$ BD cells lines compared to NPC-like lipid storage phenotypes. A *– Representative microscopy images of wild-type (WT) and PS1$^{-/-}$ BD cells alongside cells treated with 2µg/ml U18666a as a positive control for NPC lipid storage. Images show levels of cholesterol visualised by filipin (white), LBPA (green) visualised by IHC and ganglioside GM1 (GM1, green) visualised by FITC-tagged CtxB. Hoechst 33342 stained nuclei are shown in blue. n = 3. Scale bar = 7.5µm.* ***B*** *– Images demonstrating the different cholesterol distributions observed in PS1$^{-/-}$ BD blastocysts visualised by filipin (white).* ***C*** *– Quantification of the percentage of cells in each cell population which have the different cholesterol distributions. Error bars = SEM, n = 8 for all conditions apart from PS1$^{-/-}$ + U18666a where n = 5. Scale bar = 7.5µm. *** = P<0.001 by X^2 test.*

When PS1$^{-/-}$ cells are compared to cells in which NPC1 disease phenotypes have been induced it is clearly evident that the cellular disease phenotypes are clearly distinct. The accumulation of cholesterol and LBPA observed in PS1$^{-/-}$ cells is not only lower than in cells in which NPC1 disease phenotypes have been induced, it is also spatially distinct. Less punctate staining is observed in the perinuclear regions of cells with individual punctae much more evenly distributed throughout the cells in a

diffuse pattern. The clear decrease in ganglioside GM1 is partially reversed by U18666a treatment suggesting that different cellular pathways lead to the alterations in levels of this lipid.

When the distribution of cholesterol is analysed in $PS1^{-/-}$ cells there are four different distribution patterns observed. Predominating among these, is a diffuse punctate distribution distinct from cells with an induced NPC phenotype, although some cells demonstrate the perinuclear punctate distribution which predominates in NPC cells. Another population of cells show cholesterol in a perinuclear location reminiscent of the endocytic recycling compartment (ERC) whilst others do not show any overt cholesterol accumulation (figure 3.3.2. B). Quantification of these distribution patterns (figure 3.3.2. C) further highlights the difference between WT cells and $PS1^{-/-}$ cells ($P < 0.001$, $X^2 = 1879.55 +/- 90.51$ (SEM), df =2), and also those that have had $PS1^{-/-}$ cells and NPC1 phenotypes induced by treatment of WT cells with U18666a ($P < 0.001$, $X^2 = 1505.97 +/- 24.21$ (SEM), df = 2). It can also be observed that NPC1-like phenotypes can be induced in $PS1^{-/-}$ cells by U18666a treatment ($P < 0.001$, $X^2 = 1226.89 +/- 49.56$ (SEM), df = 2). This analysis was conducted using the means of the first cell line in the comparison as the expected value and comparing individual experimental repeats of the second cell line to this, in this instance the mean X^2 value is then provided for brevity. As inter-repeat variation was low (SEM < 2.5%) in these experiments this analysis remains robust.

As chelation of lysosomal Ca^{2+} to reduce the levels that can be released by the cell also creates identical lipid storage phenotypes to those observed in NPC1 disease (Lloyd-Evans et al., 2008) it is unlikely that the phenotype of reduced endolysosomal Ca^{2+} is causing the lipid changes observed in $PS1^{-/-}$ cells. From initial inspection the distribution of LBPA also reflects the distribution of cholesterol showing the differences in distribution are likely to be not solely specific to cholesterol implicating changes in endocytic vesicle trafficking in this redistribution.

As the analyses described above do not provide quantification of lipid levels we were interested to see if these changes could be validated by biochemical quantification.

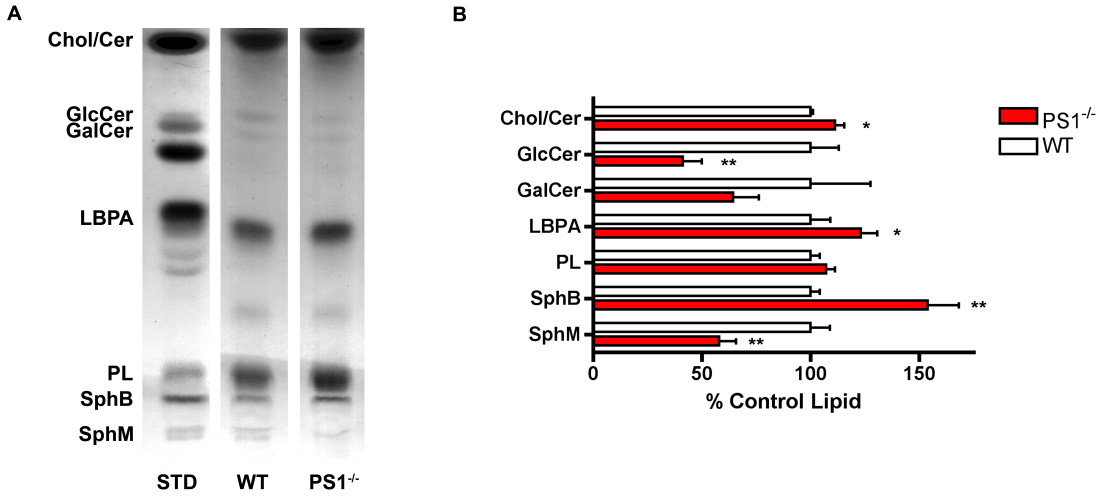

Figure 3.3.3. – Biochemical quantification of sphingolipids, sterols and phospholipids in PS1$^{-/-}$ BD cells. A – *Representative images of thin-layer chromatography analysis of various lipids in wild-type (WT) and PS1$^{-/-}$ BD cells (PS1$^{-/-}$) ran alongside identified lipid standards (STD). Chol/Cer = combined levels of cholesterol and ceramide, GlcCer = glucosylceramide, GalCer = galactosylceramide, LBPA = lysobisphosphatidic acid, PL = phospholipids, S SphL = simple sphingolipids and SphM = sphingomyelin.* ***B –*** *Densiometric quantification of lipid levels in PS1$^{-/-}$ BD blastocysts as a percentage of the lipid levels in control BD blastocysts. Lipid species are labeled as in A. Error bars = SD. n = 3.** = P < 0.01, * = P < 0.05 calculated by T test.*

Biochemical quantification of lipid species supports the lipid alterations observed by cell biology. An accumulation of cholesterol ($P < 0.05$, $t = 4.544$, $df = 4$, $F_{2,2} = 16.95$) and LBPA ($P < 0.05$, $t = 3.339$, $df = 4$, $F_{2,2} = 1.429$) is accompanied by reductions in sphingomyelin ($P < 0.01$, $t = 6.153$, $df = 4$, $F_{2,2} = 1.310$) and simple glycosphingolipids such as GlcCer ($P < 0.01$, $t = 6.509$, $df = 4$, $F_{2,2} = 2.150$, figure 3.3.3.). This, previously reported (Mutoh et al., 2012), reduction may help to explain why levels of gangliosides such as GM1 are reduced as GlcCer is the first GSL synthesised within cells and is required for the synthesis of more complex GSLs. It is interesting that most GSLs are synthesized from the recycling of their various constituent molecules as opposed to *de novo* synthesis (Schulze and Sandhoff, 2011). This may be indicative of lower activity in lysosomal hydrolytic enzymes although this would be accompanied by punctate lipid accumulation when the distribution of lipids is visualised, this remains to be further investigated and defective biosynthesis may be the sole cause of this phenotype.

Interestingly, there is also evidence of increased phospholipid accumulation, although this was not statistically significant, within PS1$^{-/-}$ cells. Phospholipidosis phenotypes are associated with lysosomal alkalisation (Nujic et al., 2012) and are not observed in genetic models of NPC1. There is evidence of phospholipid

accumulation in cells treated over long periods of time with U18666a however this is a non-specific phenotype observed after the onset of NPC disease phenotypes (Waller-Evans *et al*., Unpublished). In preliminary experiments, using a probe for phospholipidosis, no increase was seen in PS1$^{-/-}$ cells in relation to control cells, however, it is anticipated this is due to lower loading of the probe in PS1$^{-/-}$ cells due to trafficking defects (figure 3.3.8.).

Robust accumulation of sphingoid bases ($P < 0.01$, $t = 6.267$, $df = 4$, $F_{2,2} = 11.40$, figure 3.3.3.) is also observed in PS1$^{-/-}$ cells. These lipids would include sphingosine the most simple of sphingolipids, and, the substrate shown to accumulate first in NPC1 disease (Loyd-Evans et al., 2008). This method does not, however, differentiate between this lipid and biosynthetic sphingoid bases such as sphinganine, the important signaling lipid sphingosine-1-phosphate and lysosphingolipids such as lyso-sphingomyelin. Accordingly, a number of processes may contribute the increase in this band and these phenotypes should be further investigated.

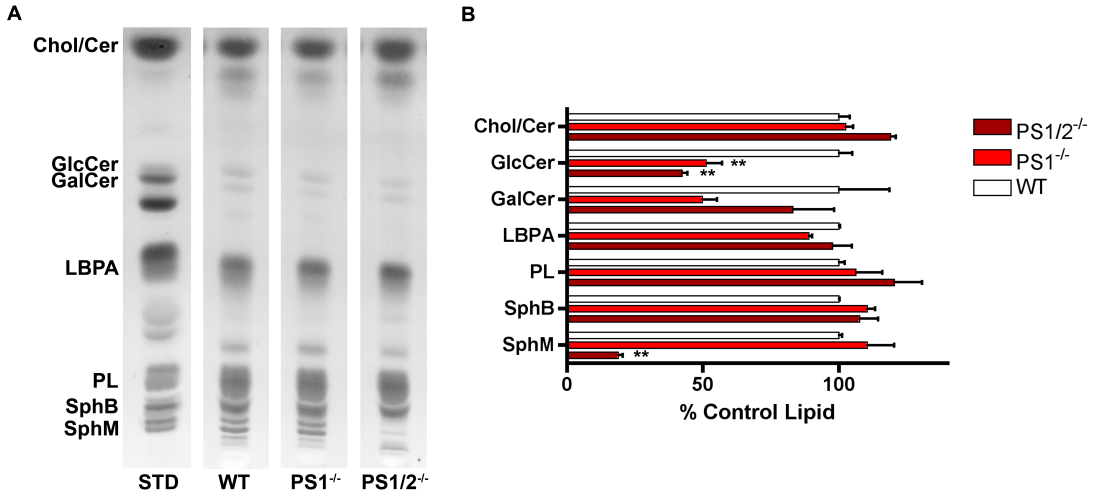

Figure 3.3.4. – Biochemical quantification of sphingolipids, sterols and phospholipids in PS1$^{-/-}$ and PS1 and PS2$^{-/-}$ MEF cells. A – *Representative images of thin-layer chromatography analysis of various lipids in wild-type (WT) and PS1$^{-/-}$ MEFs (PS1$^{-/-}$) and PS1$^{-/-}$ and PS2$^{-/-}$ MEFs (PS1/2$^{-/-}$) ran alongside identified lipid standards (STD). Chol/Cer = combined levels of cholesterol and ceramide, GlcCer = glucosylceramide, GalCer = galactosylceramide, LBPA = lysobisphosphatidic acid, PL = phospholipids, S SphL = simple sphingolipids and SphM = sphingomyelin.* ***B –*** *Densiometric quantification of lipid levels in PS deficient MEFs as a percentage of the lipid levels in control MEFs. Lipid species are labeled as in A. Error bars = SD. n = 2. ** = P<0.01, calculated by one way ANOVA with Bonferroni post test.*

As expected from the investigation of lipids in PS1$^{-/-}$ MEFs by cell biology (figure 3.3.1.) similar phenotypes are observed in PS deficient MEFs although they are not

as robustly observed until both PS1 and 2 are removed. This is particularly evident in the levels of sphingomyelin observed in cells. In $PS1^{-/-}$ MEFs there is actually a trend towards increased sphingomyelin predominantly through increases in the lower band of this lipid before both species become significantly reduced to around 20% in $PS1/2^{-/-}$ cells ($P < 0.01$, $t = 1.773$, $df = 1$).

The band observed below sphingomyelin on the TLC in figures 3.3.4. is most likely to be a species of ganglioside which has not yet been defined. Initial TLC analysis of ganglioside levels in all of the cell lines discussed above show the reductions in ganglioside GM1 observed in these cell lines by cholera toxin B analysis and disruption in many other ganglioside species although this class of lipids remains to be fully analysed.

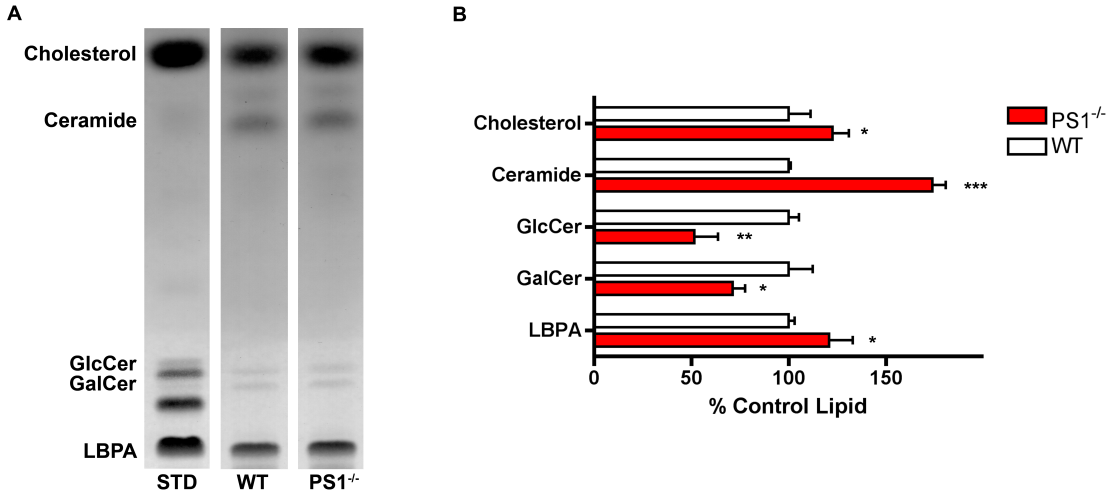

Figure 3.3.5. – Biochemical quantification of cholesterol, ceramide, LBPA and glycosphingolipids in $PS1^{-/-}$ BD cells. A – *Representative images of thin-layer chromatography analysis of various lipids in wild-type (WT) and $PS1^{-/-}$ BD cells ($PS1^{-/-}$) ran alongside identified lipid standards (STD) in a mobile phase designed to optimize the separation of cholesterol and ceramide. Chol = cholesterol, Cer = ceramide, GlcCer = glucosylceramide, GalCer = galactosylceramide and LBPA = lysobisphosphatidic acid.* ***B –*** *Densiometric quantification of lipid levels in $PS1^{-/-}$ BD blastocysts as a percentage of the lipid levels in control BD blastocysts. Lipid species are labeled as in A. Error bars = SD. n = 3 from three independent cell cultures. *** = P < 0.001, ** = P < 0.01, * = P < 0.05 calculated by T test.*

Adaption of the TLC performed in figures 3.3.3 and 3.3.4 by modulation of the mobile phase to separate cholesterol and ceramide reveals that both lipids are increased in these cells ($P < 0.05$, $t = 2.797$, $df = 4$, $F_{2,2} = 1.750$ and $P < 0.001$, $t = 19$, $df = 4$, F2,2 = 38.66). The elevation of cholesterol is as expected from filipin staining of these cells (figure 3.3.1 and figure 3.3.2.) and the changes in other species of lipid glycosphingolipids ($P < 0.05$, $t = 3.597$, $df = 4$, $F_{2,2} = 3.683$ for GalCer and P <

0.01, t = 6.311, df = 4, $F_{2,2}$ = 5.683 for GlcCer) and LBPA (P < 0.05, t = 2.865, df = 4, $F_{2,2}$ = 16.60) are confirmed. It is interesting that ceramide is also robustly increased to 150% of control levels in these cells. This is a phenotype observed in a variety of cellular and animal models of Alzheimer's along with clinical samples (Haughey et al., 2010). Ceramide elevation has not been reported in models of NPC1 disease further highlighting the divergent phenotypes between cells from this disease and $PS1^{-/-}$ cells.

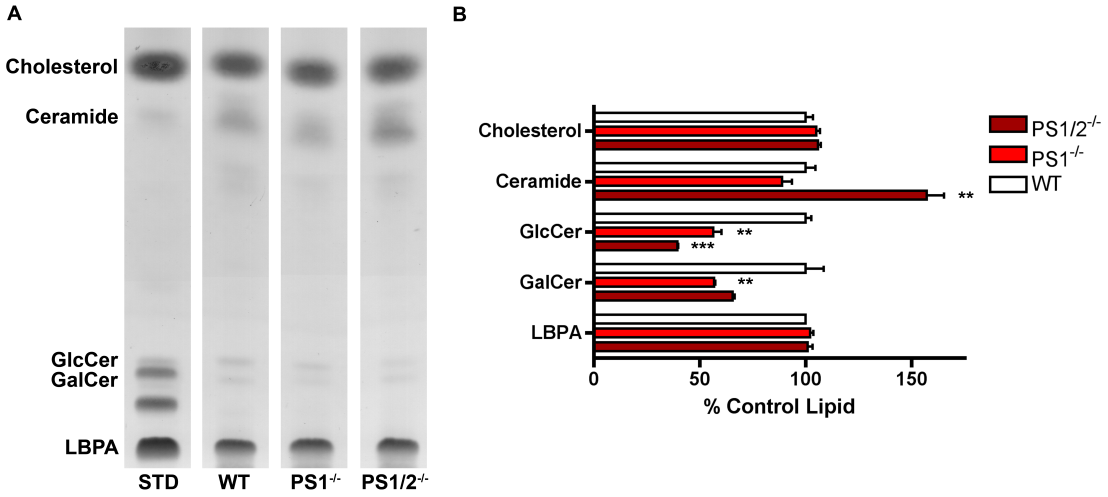

Figure 3.3.6 – Biochemical quantification of cholesterol, ceramide, LBPA and glycosphingolipids in $PS1^{-/-}$ and PS1 and $PS2^{-/-}$ MEF cells. A – *Representative images of thin-layer chromatography analysis of various lipids in wild-type (WT) and $PS1^{-/-}$ MEFs ($PS1^{-/-}$) and $PS1^{-/-}$ and $PS2^{-/-}$ MEFs ($PS1/2^{-/-}$) ran alongside identified lipid standards (STD) in a mobile phase designed to optimize the separation of cholesterol and ceramide. Chol = cholesterol, Cer = ceramide, GlcCer = glucosylceramide, GalCer = galactosylceramide and LBPA = lysobisphosphatidic acid.* ***B –*** *Densiometric quantification of lipid levels in PS deficient MEFs as a percentage of the lipid levels in control BD blastocysts. Lipid species are labeled as in A. Error bars = SD. n = 2 from two independent cell cultures. *** = P<0.001, ** = P<0.01, * = P<0.05 calculated by one way ANOVA with Bonferroni post test.*

Subsequent assay of these phenotypes in MEF cells deficient in PS1 reveal the expected pattern of alterations in lipid levels suggested by previous analyses (figure 3.3.4 and figure 3.3.5.). The decrease in GSLs is further exacerbated in PS1 and $PS2^{-/-}$ cells reducing to less than 50% of control levels for GlcCer (P < 0.01, t = 22.37, df = 1). Accumulation of cholesterol and LBPA is not especially evident in these cells as suggested by cellular staining for these lipids (figure 3.3.1.). The levels of ceramide are the converse of the pattern observed for sphingomyelin levels (P < 0.001, t = 9.505, df = 1, figure 3.3.4) suggesting that the decrease in this lipid is a result of conversion to ceramide by sphingomyelinase enzymes. This is particularly interesting as reduction in the activity of the member of this family active in the lysosomes, acid sphingomyelinase (ASM) has been shown to improve autophagic

defects in mouse models of FAD (Lee et al, 2014). This is potentially a target for further investigation, as increases in levels of ceramide induce apoptosis so this phenotype may be a major cause of neuronal loss.

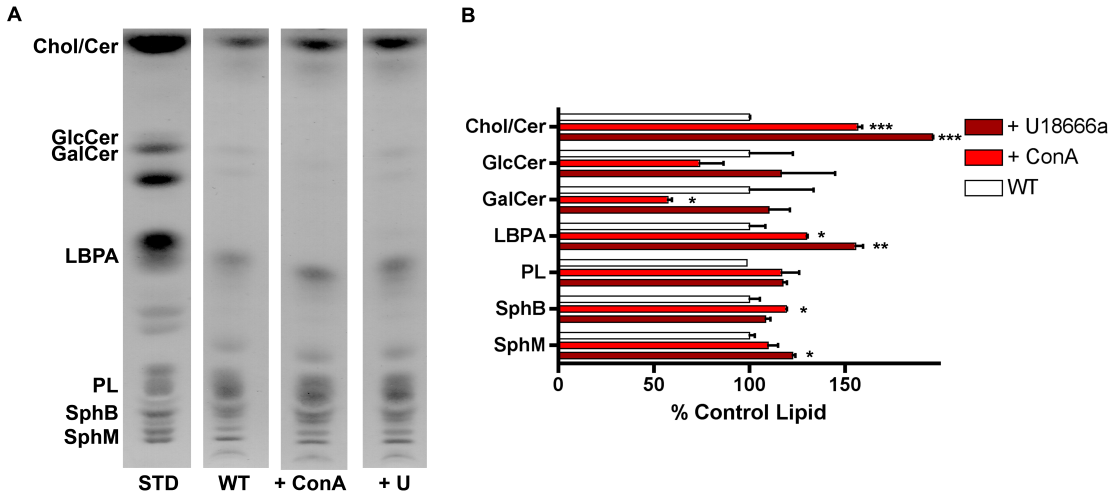

Figure 3.3.7 – Changes in levels of sphingolipids, phospholipids and cholesterol in PS1$^{-/-}$ cells in response to vATPase inhibition and NPC-like phenotype induction. A – *Representative images of thin-layer chromatography analysis of various lipids in untreated wild-type (WT) blastocysts and those treated with 50nM Concanamycin A for 12 hr used to inhibit vATPase alkalising lysosomes or 24hr 2ug/ml treatment of U18666a to induce an NPC phenotype ran alongside identified lipid standards (STD. Chol/Cer = combined levels of cholesterol and ceramide, GlcCer = glucosylceramide, GalCer = galactosylceramide, LBPA = lysobisphosphatidic acid, PL = phospholipids, S SphL = simple sphingolipids and SphM = sphingomyelin.* ***B –*** *Densiometric quantification of lipid levels in treated and untreated BD blastocysts as a percentage of the lipid levels in untreated BD blastocysts. Lipid species are labeled as in A. Error bars = SD. n = 2. *** = P < 0.001, ** = P < 0.01, * = P < 0.05 calculated by one way ANOVA with Bonferroni post test.*

The induction of NPC1 phenotypes using U18666a in BD cells leads to the expected increase in lipids seen in models of this disease with at least trends towards increases in cholesterol, LBPA, GSLs and sphingomyelin all observed (figure 3.3.7.). As seen in figures 3.3.3. – 3.3.6. this lipid profile is distinctly different to that observed in cells deficient in PS1 as they have reduced GSLs and sphingomyelin. Interestingly, lysosomal alkalisation using the specific inhibitor of vATPase (Coen et al., 2012) results in a much more similar profile to that observed in these cells. It can be seen that lipids such as LBPA are increased ($P < 0.05$, $t = 5.576$, $df = 1$) and there is a trend towards reduction of GSLs. The cholesterol and ceramide band is also increased on this TLC ($P < 0.001$, $t = 37.39$, $df = 1$) which likely reflects accumulation of cholesterol as there has been no decrease in sphingomyelin levels which appears to result in ceramide increase as observed in figures 3.3.5 and 3.3.6. Interestingly, there is a redistribution of the sphingomyelin band reminiscent of that seen in PS1$^{-/-}$ MEFs. As this seems to be an intermediate phenotype between WT MEFs and

PS1/2$^{-/-}$ cells it would be interesting to increase the short time, 12 hr, that cells are exposed to concanamycin A and then see if sphingomyelin reductions are observed and ceramide levels increase.

Figures 3.3.1. – 3.3.7. show that consideration of lipid phenotypes in Presenilin deficient cell lines clearly demonstrates that NPC1 disease phenotypes are not present in these cells. Accordingly, it is strongly suggestive that, if present lysosomal Ca^{2+} reductions are not the only form of lysosomal dysfunction in these cells. Further, it illustrates that a more likely explanation for the changes in lipid levels and distribution observed in these cells is lysosomal alkalisation, this warrants further investigation.

3.3.2. – Endolysosomal defects in Presenilin deficient cells reveal further complexity

A number of other assays can be used to study lysosomes and potentially provide more information as to what processes are defective in the lysosome. As a result of our findings with respect to changes in lipids observed in cells, particularly the large increases in ceramide accompanied by reductions in sphingomyelin, we are continuing to use BD cells for these assays. A particularly interesting process in cells which can be used to investigate the result of changes to lipids and endolysosomal Ca^{2+} homeostasis is the endocytic trafficking of lipids from the cell membrane. A useful tool for this analysis is fluorescently tagged cholera toxin B subunit which binds to ganglioside GM1 in cell membranes and is internalised to the Golgi in healthy cells. Defects in this process are observed in the majority of LSDs and have been shown to contribute to lipid storage in diseases such as NPC1.

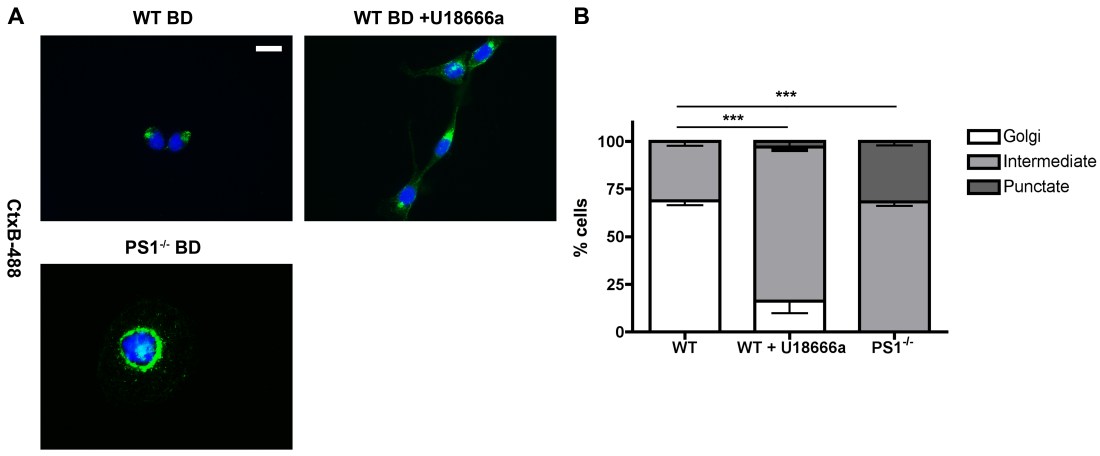

Figure 3.3.8. – Endolysosomal sphingolipid trafficking in PS1$^{-/-}$ BD cells. A – *Representative microscopy images of WT and PS1$^{-/-}$ BD cells pulse (30 min) and chased (90 min) with FITC-tagged cholera toxin B subunit (CtxB-488), green, co-labelled with the nuclear marker Hoechst 33342. In control cells CtxB is internalised to the Golgi. 24hr 2ug/ml treatment of U18666a is used as a positive control for sphingolipid mistrafficking and NPC phenotypes.* ***B –*** *Qualitative quantification of CtxB-488 localisation as Golgi, punctate or intermediate between the two states in PS1$^{-/-}$ BD blastocysts as a percentage of the total cell population. Error bars = SD. n = 3 for WT and PS1$^{-/-}$ cells and n= 2 for WT cells + U18666a. Scale bar = 7.5μm. *** = P < 0.001 calculated by X^2 test.*

Analysis of this the endocytosis of CtxB bound ganglioside GM1 in PS1$^{-/-}$ cells reveals an endolysosomal sphingolipid trafficking defect of unexpected severity. U18666a was used as a positive control in this experiment as NPC1 disease has been shown to have a sphingolipid trafficking defect which is considered to be more severe than many other LSDs (Pagano et al., 2000). Surprisingly, PS1$^{-/-}$ cells had a trafficking defect which was more pronounced (figure 3.3.8 A). Quantification of this trafficking defect shows that virtually all PS1$^{-/-}$ cells retained FITC-tagged CtxB in the endolysosomal system demonstrated by the, at least partial, punctate distribution of probe within cells. This was significantly different from WT cells treated with U18666a to induce trafficking defects ($P < 0.001$, $X^2 = 27.79$, 26.80 and 31.11 for each individual experimental repeat, df = 2). U18666a treated cells showed a phenotype intermediate between PS1$^{-/-}$ and untreated WT cells ($P < 0.001$, $X^2 = 107.43$ and 166.02 for each individual experimental repeat, df = 2, figure 3.3.8. B). This analysis was carried out using the means from each cellular condition as inter-repeat variation was low (SEM < 5%).

This severe trafficking defect is suggestive of fundamental dysfunction in the endolysosomal system of these cells as this assay was performed under conditions predisposing all cells to show transport of the probe to the Golgi, this was achieved by increasing the chase time after cell were pulsed with CtxB to 90 minutes and

explains why U18666a treated cells showed a more intermediate distribution than previously reported.

Another way of studying dysfunction in the endocytic system is by determining the localisation of annexin A2 within cells. In healthy cells this Ca^{2+} dependent phospholipid binding protein should be evenly distributed at the plasma membrane. Figure 3.3.9. clearly shows this is not the case in $PS1^{-/-}$ cells.

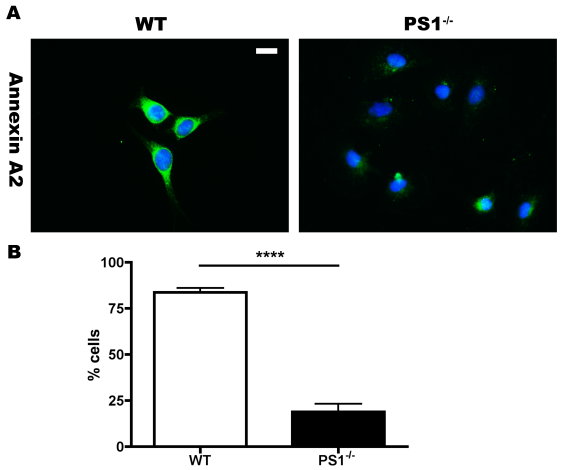

Figure 3.3.9. – Distribution of Annexin A2 in $PS1^{-/-}$ BD cells. A – *Representative microscopy images of WT and $PS1^{-/-}$ BD cells showing Annexin A2 distribution by IHC.* ***B –*** *Quantification of Annexin A2 levels by threshold analysis in $PS1^{-/-}$ BD cells as a percentage of the total cell population. Error bars = SD. Data calculated from three independent plating replicates. Scale bar = 7.5μm. **** = P < 0.0001 by T test.*

In $PS1^{-/-}$ cells, levels of annexin A2 appear to be vastly reduced as demonstrated by threshold analysis of these images ($P < 0.0001$, $t = 22.53$, $df = 4$, $F_{2,2} = 3.297$). The remaining annexin A2 appears to be mislocalised and is retained in the perinuclear region of cells (figure 3.3.9. A.). This phenotype has previously been reported in cellular models of NPC1 where this redistribution was attributed to the low levels of lysosomal Ca^{2+}(Lloyd-Evans et al., 2008). Taken together both of these assays of endolysosomal trafficking appear to indicate the Ca^{2+} dyshomeostasis may be present in the endolysosomal system of $PS1^{-/-}$ cells although the severity of these trafficking abnormalities suggests that more than low levels of lysosomal Ca^{2+} may be contributing to this.

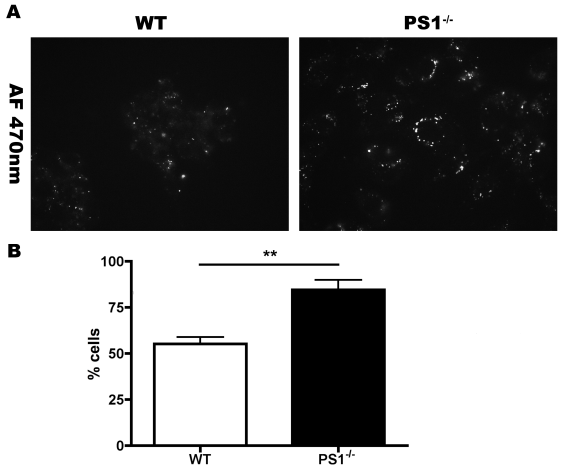

Figure 3.3.10. – Autofluorescent material in $PS1^{-/-}$ BD cells. A – *Representative microscopy images of WT and $PS1^{-/-}$ BD cells showing autofluorescence at 470nm which may be indicative of lipofuscin accumulation.* ***B –*** *Quantification of autofluorescence at 470nm by threshold analysis in $PS1^{-/-}$ BD blastocysts as a percentage of the total cell population. Error bars = SD. Data calculated from three independent plating replicates. Scale bar = 7.5μm. ** = P < 0.01 by T test.*

A final phenotype that can be easily investigated in cells is the presence of punctate autofluorescence which indicate endolysosomal accumulation of lipofuscin. Interestingly autofluorescence at 470nm was increased in $PS1^{-/-}$ cells ($P < 0.01$, $t = 7.731$, $df = 4$, $F_{2,2} = 2.173$). This phenotype has been reported in a number of lysosomal diseases including those such as CLN10 where proteolytic activity in cells is reduced due to the loss of functional Cathepsin D and other diseases in which endolysosomal Ca^{2+} dyshomeostasis has been observed such as MLIV. Whilst it is not a phenotype which specifically implicates a particular type of lysosomal dysfunction it has not been widely reported in cells which have low levels of lysosomal Ca^{2+} or lipid accumulation; but would be expected in cells which have proteolytic defects (Guha et al., 2014). This phenotype is also often hard to visualise in cells which turn over quickly, even those where accumulation of autofluorescent material is considered a hallmark of the disease, accordingly it is interesting that it appears to be a robust phenotype in these cells. Again this suggests a profound defect may be present in the endolysosomes of these cells.

The increasing complexity revealed by the endolysosomal defects assayed above suggest that either multiple forms of dysfunction are present within this system or a new pathological mechanism is taking place in these cells. Due to this, a complete investigation of endolysosomal Ca^{2+} homeostasis is required as many of the phenotypes described above are indicative of dysfunction within this system.

3.3.3. – Presenilin 1 maintains lysosomal Ca^{2+} homeostasis by regulating vATPase mediated lysosomal acidification

As described in section 3.3.1. and 3.3.2., $PS1^{-/-}$ BD cells are the most suitable cell line in which to perform a thorough investigation of endolysosomal Ca^{2+} homeostasis changes which result from loss of presenilin function. This is due to the robust phenotypes observed in these cells without the need to remove the function of multiple proteins.

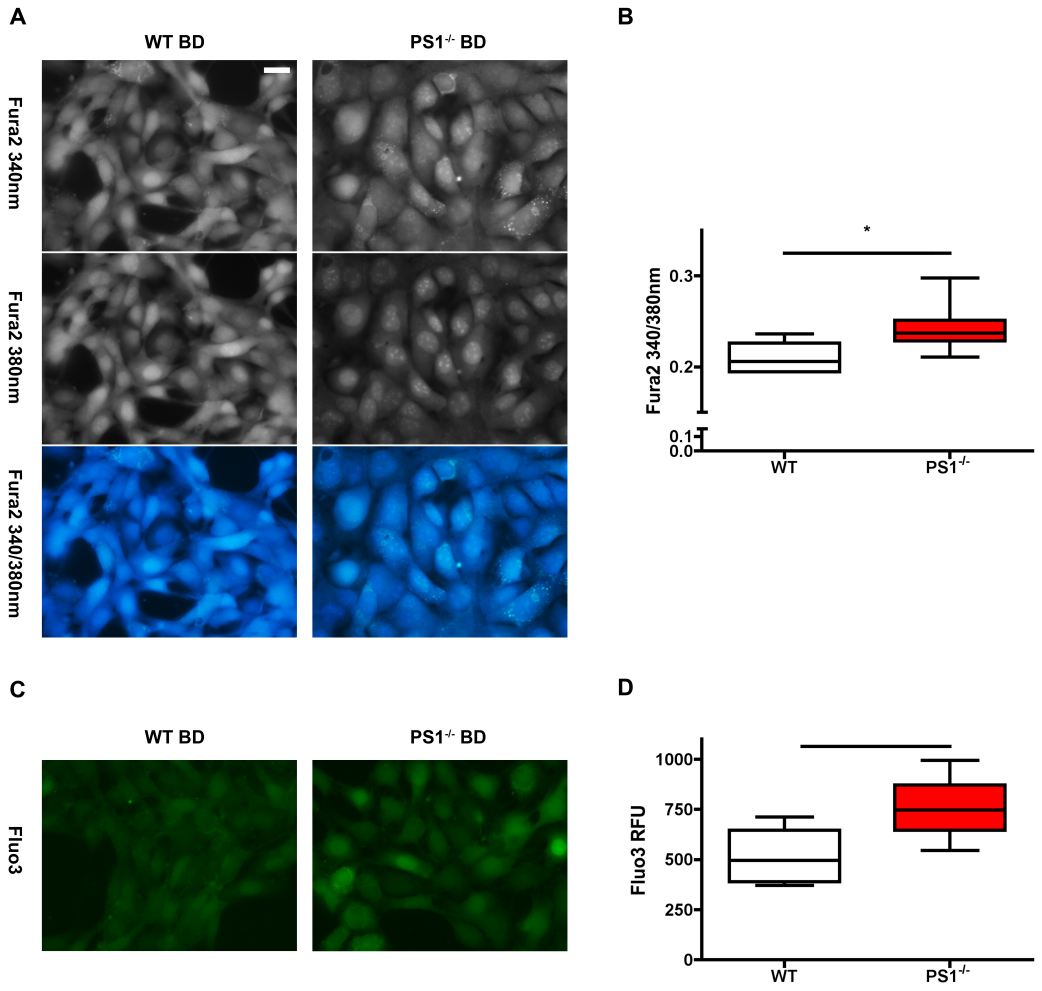

Figure 3.3.11. – Basal cytosolic Ca^{2+} in $PS1^{-/-}$ BD cells. A - *Representative images of the Ca^{2+} probe Fura2 at both 340nm and 380nm followed by a ratiometric representation of Fura2 340/380nm.* ***B –*** *Quantification of resting cytosolic Ca^{2+} measured by ratiometric quantification of Fura2 fluorescence. Error bars = range. n = 6 for WT cells and n = 8 for $PS1^{-/-}$ cells. * = P < 0.05 calculated by T test.* ***C -*** *Representative images of the Ca^{2+} probe Fluo3.* ***D –*** *Quantification of resting cytosolic Ca^{2+} measured by quantification of Fluo3 fluorescence. Error bars = range. n = 4. No significant difference observed by T test. Scale bar = 7.5μm.*

We began to investigate Ca^{2+} dyshomeostasis by determining the basal cytoplasmic Ca^{2+} levels in $PS1^{-/-}$ cells in relation to controls. This was significantly elevated ($P < 0.05$, $t = 2.798$, $df = 12$, $F_{7,5} = 2.655$) in $PS1^{-/-}$ cells, as previously reported, measured by Fura2 which provides ratiometric measurement of Ca^{2+} levels. This shows that the differences in Ca^{2+} probe fluorescence is not a result of differences in probe uptake between cell lines. In turn this validates the measurement of basal cytosolic Ca^{2+} elevation with the non-ratiometric Ca^{2+} probe Fluo3. Although the difference between cell lines is not significant in this instance a similar trend has been observed and this phenotype has been confirmed using multiple probes in Lee et al. (2015). Importantly, the images also show that there is not significant compartmentalisation of either of these probes. This is often problematic when cells with endolysosomal

dysfunction are being studied. The use of two different Ca^{2+} probes is also beneficial as some agonists can cause changes in pH of the cell which in turn alters the kD of these Ca^{2+} probes, a process which changes Ca^{2+} binding properties of the probe and as a result the fluorescence signal. This can confound results. For example this has previously been observed when Fura2 is used as the Ca^{2+} probe in experiments utilising GPN to burst lysosomes (Lloyd-Evans, Unpublished). Accordingly, we have used Fluo3 for the majority of experiments in which we utilise this agonist. If pH changes are not of concern we use Fura2 for the experiments as the ratiometric properties of this dye reduce problems such as photobleaching and extrusion of the probe from the cytosol.

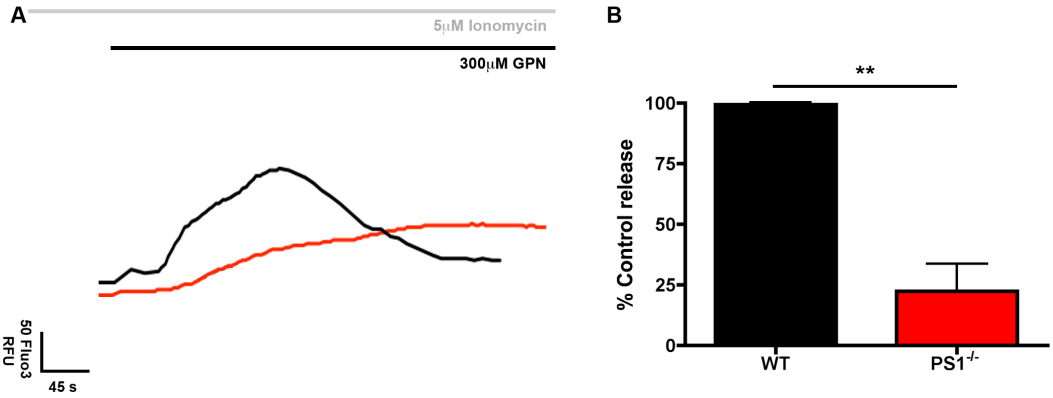

Figure 3.3.12. – Lysosomal Ca^{2+} release in $PS1^{-/-}$ BD cells after GPN induced lysosomal rupture in the presence of 5μM ionomycin. A - *Representative traces of Ca^{2+} release in Fluo3 loaded cells induced by 300μM GPN. Grey bar indicates the presence of ionomycin, black bar indicates the presence of GPN. U18666a treated WT cells are used as a positive control for depletion of lysosomal Ca^{2+}.* ***B –*** *Quantification of Ca^{2+} release measured by change in Fluo3 fluorescence. Error bars = SEM. n = 3. ** = P < 0.01 calculated by T test.*

After assessing the basal cytosolic Ca^{2+} levels in cells we attempted to validate the findings of Coen et al. (2012) who observed reduced lysosomal Ca^{2+} in the lysosomes of $PS1^{-/-}$ cells. In order to ensure that we only measured release from the lysosomes of cells, we used the Ca^{2+} ionophore, ionomycin, to permeabilise all the other cellular Ca^{2+} stores, lysosomes remain intact as a result of the inability of ionomycin to cross the glycocalyx. As such, when we induce osmotic swelling and subsequent lysis of the lysosome by GPN, we can be sure that any changes in fluorescence of the Ca^{2+} probe situated in the cytosol are the result of Ca^{2+} release from the lysosome. It is important to note that GPN is cleaved in lysosomes by cathepsin C, an enzyme which has a broad pH optima between pH 5-6 (Vanha-Perttula et al., 1965), accordingly lysosomal alkalisation is not likely to inactivate this enzyme and prevent its use in any cell lines which do exhibit this phenotype. Upon

stimulation of Ca^{2+} release with GPN we were able to observe an approximately 75% reduction in lysosomal Ca^{2+} in presenilin deficient cells compared to controls ($P < 0.01$, $t = 6.847$, $df = 4$, $F_{2,2} = 1321x10^{10}$, figure 3.3.12.). The importance of using ionomycin before GPN in this experiment is highlighted in figure 3.3.13.

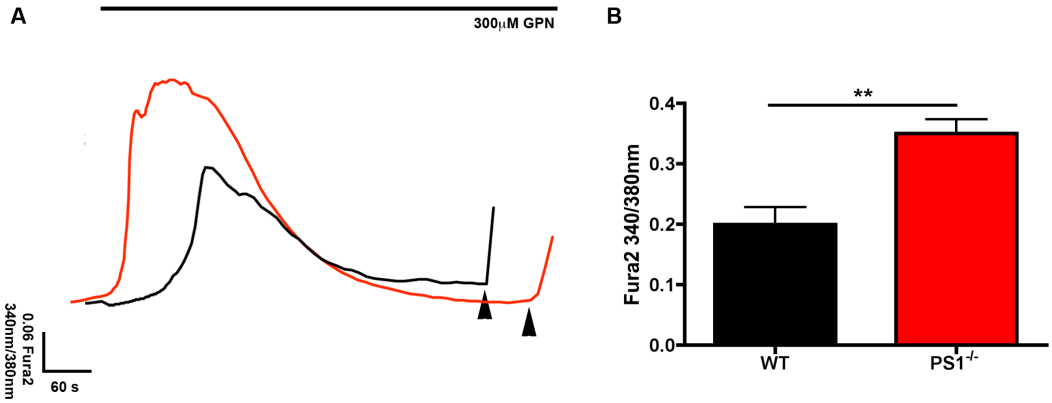

Figure 3.3.13. – Ca^{2+} release in $PS1^{-/-}$ BD cells after GPN induced lysosomal rupture. A - *Representative traces of Ca^{2+} release in Fura2 loaded cells induced by 300μM GPN. Black bar indicates the presence of GPN.* ***B –*** *Quantification of Ca^{2+} release measured by change in Fura2 fluorescence ratio. Error bars = SEM. n = 5 for WT and n = 6 for $PS1^{-/-}$. ** = $P < 0.01$ calculated by T test.*

Under conditions where only GPN is added to cells it can be seen that the Ca^{2+} released from $PS1^{-/-}$ cells is significantly elevated when compared to control cells ($P < 0.01$, $t = 4.112$, $df = 9$, $F_{4,5} = 1.198$. In this situation Ca^{2+} induced Ca^{2+} release (CICR) from the ER is a major contributor to this Ca^{2+} response as the close contact between lysosomes and the ER concentrate Ca^{2+} transients in this area and potentiate Ca^{2+} release from a store which is more concentrated than the lysosome and also much larger in volume (Kilpatrick et al., 2012). This is particularly problematic in cells where the ER levels of Ca^{2+} are altered, as has been reported in $PS1^{-/-}$ cells.

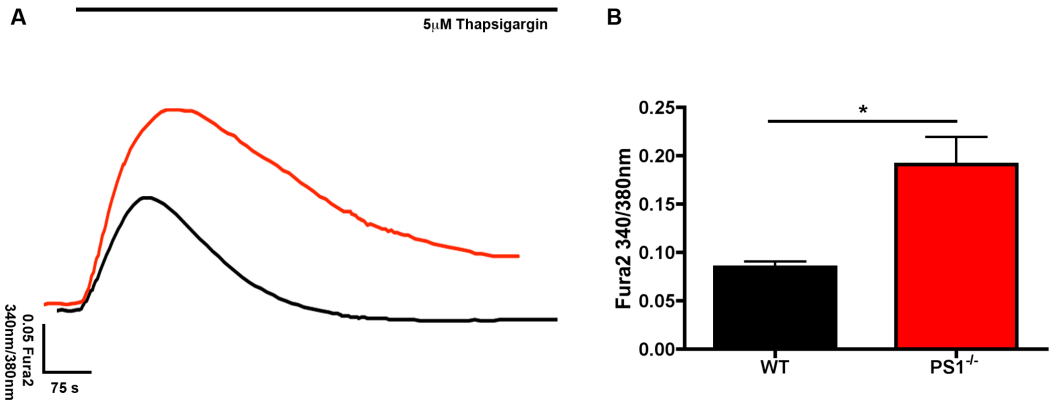

Figure 3.3.14. – Ca^{2+} release from the ER in $PS1^{-/-}$ BD cells after thapsigargin stimulation. A - *Representative traces of Ca^{2+} release in Fura2 loaded cells induced by 5μM thapsigargin. Black bar indicates the presence of thapsigargin.* ***B –*** *Quantification of Ca^{2+} release measured by change in Fura2 fluorescence ratio. Error bars = SEM. n = 3. * = P<0.05 calculated by T test.*

We were also able to reproduce this data in $PS1^{-/-}$ cells when we induced Ca^{2+} release from the ER using thapsigargin and observed almost double the release (P = < 0.05, t = 3.655, df = 4, $F_{2,2}$ = 24.72, figure 3.3.14.). The impact of ER Ca^{2+} release accounts for the higher Ca^{2+} release when GPN alone is used (figure 3.3.13.). Importantly, the proportional difference between thapsigargin stimulated release is higher than with GPN stimulated release suggesting that the higher lysosomal Ca^{2+} in control cells reduces the difference between these cells and presenilin deficient cells.

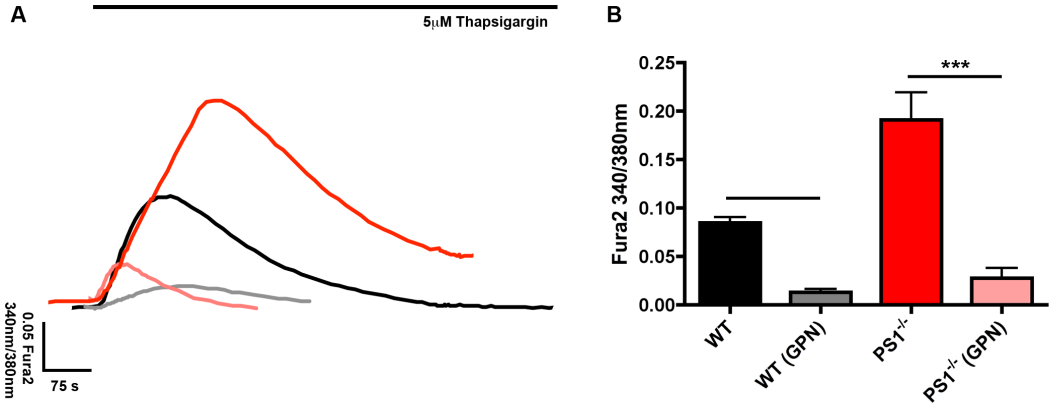

Figure 3.3.15. – Lysosomal rupture and Ca^{2+} release causes subsequent reduction in thapsigargin stimulated ER Ca^{2+} release. A - *Representative traces of Ca^{2+} release in Fura2 loaded cells induced by 5μM thapsigargin in the presence and absence of 300μM GPN. Black bar indicates the presence of thapsigargin.* ***B –*** *Quantification of Ca^{2+} release measured by change in Fura2 fluorescence ratio. Error bars = SEM. n = 3. *** = P < 0.001 calculated by one way ANOVA with Bonferroni post test. .*

The interaction between lysosomal and ER Ca^{2+} release in these cells is further evidenced by the observation that inducing lysosomal Ca^{2+} release reduced the release of Ca^{2+} from the ER induced by thapsigargin. Although this only reached significance in $PS1^{-/-}$ cells ($P < 0.001$, $t = 7.443$, $df = 4$) there was also a trend towards reduction in WT cells. This experiment demonstrates depletion of the ER store following lysosomal Ca^{2+} release and a similar protocol can be utilised in order to investigate the effects of more physiologically relevant lysosomal Ca^{2+} agonists upon the ER.

As osmotic lysis of the lysosome is not a physiological process we were interested to see what the effects of a physiologically relevant Ca^{2+} agonist upon lysosomes from Presenilin deficient cells was. NAADP is one of the most potent Ca^{2+} releasing second messengers within cells. The target of this ligand is believed to be the lysosomal TPC2 channel which releases Ca^{2+} from the lysosome in order to potentiate vesicular binding events (Luzio et al., 2007; Ruas et al., 2015).

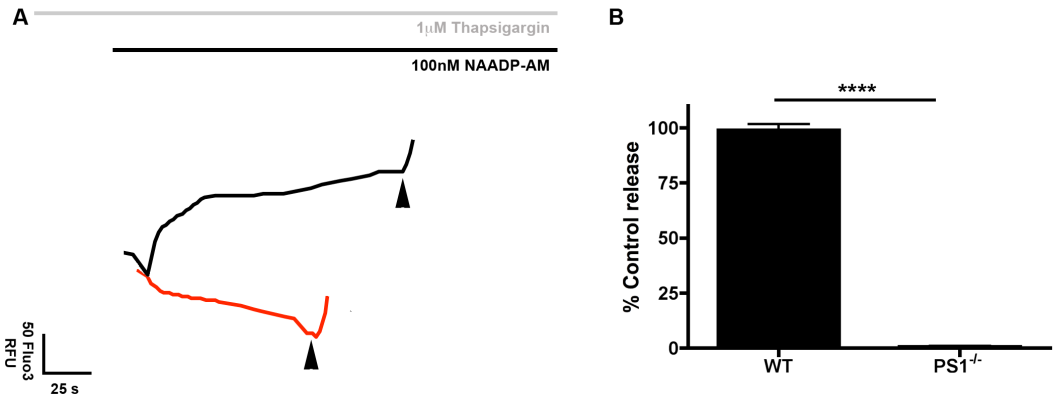

Figure 3.3.16. – No Ca^{2+} release in $PS1^{-/-}$ BD cells after stimulation of TPC2 with NAADP-AM. A - *Representative traces of Ca^{2+} release in Fluo3 loaded cells induced by 100nM NAADP-AM. Grey bar indicates the presence of thapsigargin, black bar indicates the presence of NAADP-AM, black arrowheads show the addition of 2μM ionomycin to confirm cell viability. U18666a treated WT cells are used as a positive control for depletion of lysosomal Ca^{2+}.* ***B –*** *Quantification of Ca^{2+} release measured by change in Fluo3 fluorescence. Error bars = SEM..n = 3 for WT cells and n = 3 for $PS1^{-/-}$ cells. **** = P<0.0001.*

Using NAADP which has had its charge masked by the addition of an AM group we are able to investigate the response of TPC2 in live, unpermeabilised $PS1^{-/-}$ cells. When we added this second messenger to cells, in which we have prevented ER Ca^{2+} release with thapsigargin, we were surprised to see almost no Ca^{2+} release from $PS1^{-/-}$ cells ($P < 0.0001$, $t = 34.83$, $df = 4$, $F_{2,3} = 34.95$, figure 3.3.16.). As the

TPC2 channel is expressed normally in PS1$^{-/-}$ cells, it is most likely changes in lysosomal physiology are responsible for the lack of Ca^{2+} release (Neely-Kayala et al., 2012).

The observation of ablated Ca^{2+} release from lysosomes in PS1$^{-/-}$ cells may be explained by the fact TPC2 is a dual sensor of Ca^{2+} and pH in the lumen of lysosomes. When lysosomes are maintaining correct pH, at around 4.5, NAADP in the cytosol can transiently bind to the channel or, perhaps, a binding protein in order to trigger lysosomal Ca^{2+} release. If the pH of the lysosomal lumen has become more alkaline, then TPC2 channels are blocked as NAADP no longer dissociates from the channel (Pitt et al.,2010). This may explain why PS1$^{-/-}$ cells do not release any Ca^{2+} in response to NAADP-AM.

It is important to note that when NAADP-AM was added to PS1$^{-/-}$ cell in the absence of thapsigargin robust Ca^{2+} releases were observed (data not shown). This observation demonstrates the potency of CICR on the ER where even the small amount of Ca^{2+} release from the lysosome can potentiate this process. It is also interesting that during preliminary calibration experiments for this experiment, higher concentrations of NAADP-AM (500nM) were able to induce Ca^{2+} releases from thapsigargin treated PS1$^{-/-}$ cells (data not shown). The activation of TPC2 by NAADP is subject to a bell-shaped curve with respect to NAADP (Pitt et al., 2010) concentration and as such an optimal concentration must be determined for experimentation. As higher concentrations seemed to potentiate release in PS1$^{-/-}$ cells, but not controls, it may be that this activation curve has been shifted by a change in pH in the lysosomal lumen, this remains to be investigated.

Interestingly, this almost complete ablation of NAADP-AM induced Ca^{2+} release observed in PS1$^{-/-}$ cells may explain the severe endolysosomal sphingolipid trafficking phenotype (figure 3.3.8) also observed in these cells. Lack of Ca^{2+} release from the TPC2 channel would lead to a profound defect in endolysosomal vesicle fusion, and therefore, the trafficking of substrates through this system. This process requires localized Ca^{2+} fluxes to activate the protein machinery required for fusion (Luzio et al., 2007). This observation also provides a potential mechanism for the annexin A2 mislocalisation shown in figure 3.3.9.

As a number of the results we have achieved so far have suggested that lysosomal alkalisation may be occurring in PS1$^{-/-}$ cells we were interested to see if we could

demonstrate increased sensitivity of these cells to Ca^{2+} release in response to further lysosomal alkalisation.

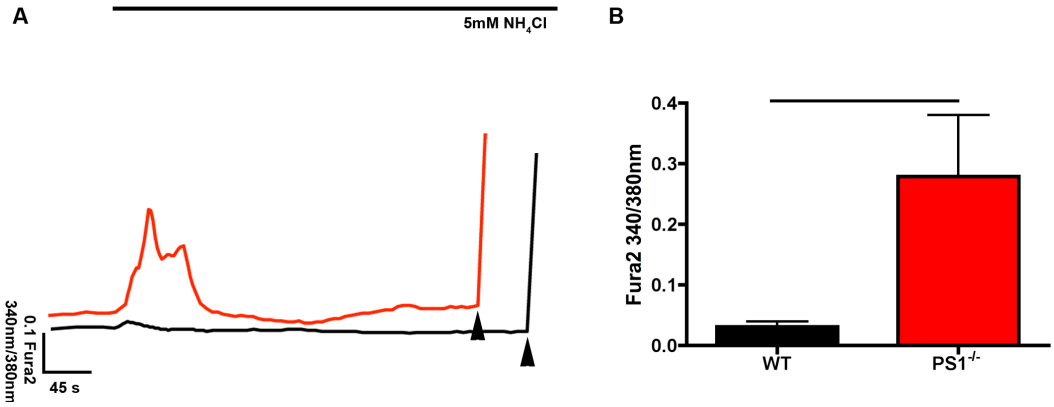

Figure 3.3.17. – Ca^{2+} release from $PS1^{-/-}$ BD cells in response to alkalisation with sub-inhibitory concentrations of NH_4Cl. A - *Representative traces of Ca^{2+} release in Fura2 loaded cells induced by 5mM NH_4Cl. Black bar indicates the presence of NH_4Cl, black arrowheads show the addition of 5μM ionomycin to confirm cell viability.* ***B –*** *Quantification of Ca^{2+} release measured by ratiometric change in Fura2 fluorescence. Error bars = SEM. n = 2. No significance calculated by T test.*

The first alkalising agent we used to investigate if $PS1^{-/-}$ cells were more susceptible to Ca^{2+} release was NH_4Cl as NH^{4+} has previously been shown to empty lysosomal Ca^{2+} stores by inducing Ca^{2+} leak after chelation of H^+ ions (Christensen et al., 2002). Using a lower concentration of NH_4Cl than that normally used to induce leak in control cells in control cells we were able to induce substantive Ca^{2+} release from $PS1^{-/-}$ cells (figure 3.3.17.). Although this difference was non significant there is a clearly evident trend towards more Ca^{2+} release from $PS1^{-/-}$ cells. When considered alongside the lower overall levels of Ca^{2+} in these compartments it is indicative of lysosomal alkalisation in $PS1^{-/-}$ cells leading to increased leak of Ca^{2+} from the endolysosomal system. Subsequent experiments have supported these data. Preliminary calibration experiments also revealed a similar pattern of increased Ca^{2+} release in $PS1^{-/-}$ cells at comparable concentrations (data not shown).

As chelation of lysosomal H^+ ions in order to induce alkalisation resulted in more Ca^{2+} leak from the endolysosomal system we were interested to see if inducing lysosomal alkalisation by vATPase inhibition was capable of doing the same. This is particularly interesting as lack of vATPase function in proposed to be the initiating factor for lysosomal alkalisation in $PS1^{-/-}$ cells (Lee et al., 2010).

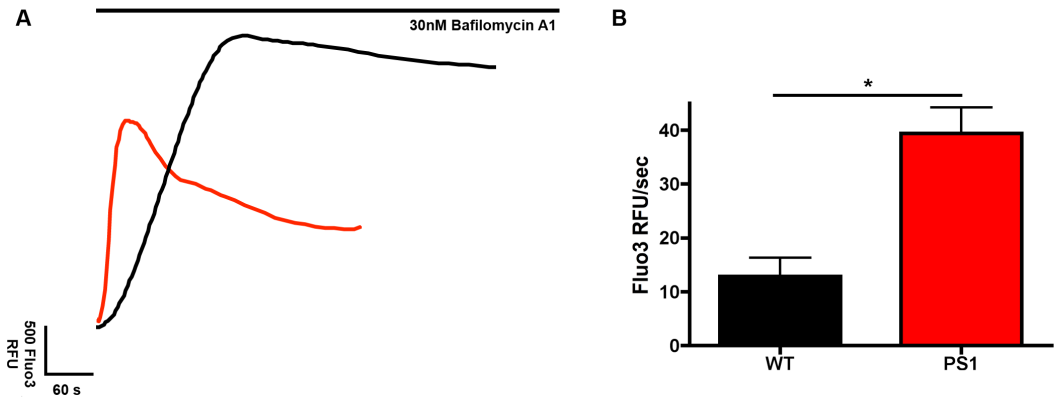

Figure 3.3.18. – Sensitivity of PS1$^{-/-}$ BD cells to alkalisation and subsequent Ca^{2+} release in response to sub-inhibitory concentrations of Bafilomycin A1. A - *Representative traces of Ca^{2+} release in Fluo3 loaded cells induced by 30nM Bafilomycin A1. Black bar indicates the presence of Bafilomycin A1.* ***B –*** *Quantification of Ca^{2+} release rate measured by change in Fluo3 fluorescence over time in seconds. Error bars = SEM. n = 3. * = P<0.05.*

When vATPase in PS1$^{-/-}$ cells is partially inhibited by the selective inhibitor Bafilomycin A1 (Harada et al., 1997) we can see that Ca^{2+} is released from these cells at a 3 fold greater initial rate ($P < 0.05$, $t = 4.494$, $df = 4$, $F_{2,2} = 2.002$, figure 3.3.18.), measured in the change of fluorescence units per second. This is further evidence of increased lysosomal alkalisation in these cells and a greater sensitivity of the vATPase to inhibition leading to a greater degree of Ca^{2+} leaking out of this system upon inhibition. Importantly, we were able to observe a 60 -70% greater release in control cells with high completely inhibitor concentrations of Bafilomycin (500nM) after thapsigargin pretreatment further demonstrating the lysosomes in control cells have a greater Ca^{2+} content (data not shown).

The experiments shown in figure 3.3.17. – 3.3.18 demonstrate that lysosomes from PS1$^{-/-}$ cells show increased Ca^{2+} leak in response to alkalisation. However, the channel that facilitates this is unknown. An attractive potential candidate for this channel is TRPML1. This is thought to be a pH sensitive Ca^{2+} efflux channel which exhibits peak activity within a more alkaline pH range than that observed in lysosomes. This suggests that it is most active in an earlier compartment within the endolysosomal system (Raychowdhury et al., 2004; Waller-Evans et al., 2015).

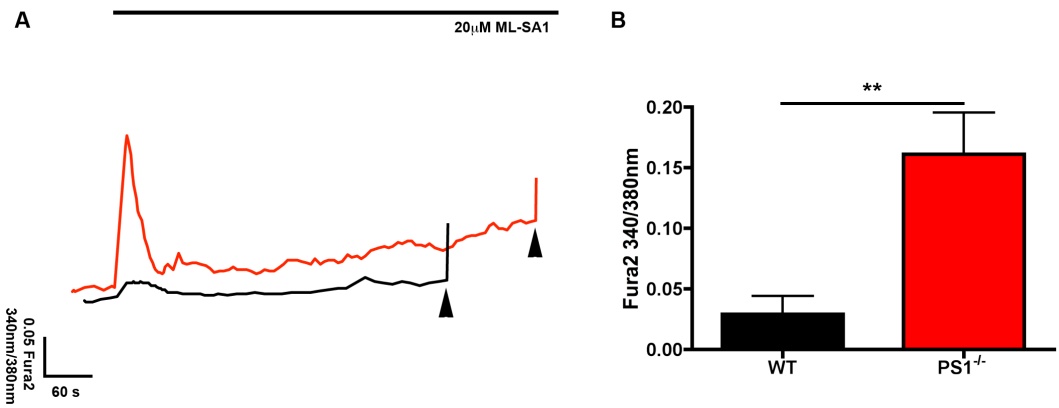

Figure 3.3.19. – Ca^{2+} release from $PS1^{-/-}$ BD cells in response to the synthetic TRMPL1 agonist ML-SA1. A - *Representative traces of Ca^{2+} release in Fura2 loaded cells induced by 20μM ML-SA1. Black bar indicates the presence of ML-SA1, black arrowheads show the addition of 5μM ionomycin to confirm cell viability.* ***B –*** *Quantification of Ca^{2+} release measured by ratiometric change in Fura2 fluorescence. Error bars = SEM. n = 12. ** = P < 0.01.*

In order to study the TRPML1 channel we utilised the synthetic TRPML1 agonist ML-SA1 (Shen et al., 2012). When we treated $PS1^{-/-}$ cells with this agonist we observed a vastly increased release compared to control cells ($P < 0.01$, $t = 3.540$, $df = 22$, $F_{11,11} = 5.344$, figure 3.3.19.). This suggests that TRPML1 is hyperactive in $PS1^{-/-}$ cells and is it is likely that this channel mediates efflux of Ca^{2+} from the endolysosomal system into the cytoplasm. Accordingly, we consider the activity of this channel as central to the Ca^{2+} dyshomeostasis observed in $PS1^{-/-}$ cells and that excessive Ca^{2+} leak from TRPML1 may be responsible for the low levels of endolysosomal Ca^{2+}, and, contributes to increased levels of cytosolic Ca^{2+}.

In order to confirm this role of TRPML1 we first needed to confirm the specificity of ML-SA1 for this channel. Firstly, we wanted to see if ML-SA1 induced Ca^{2+} release resulted in CICR from the ER.

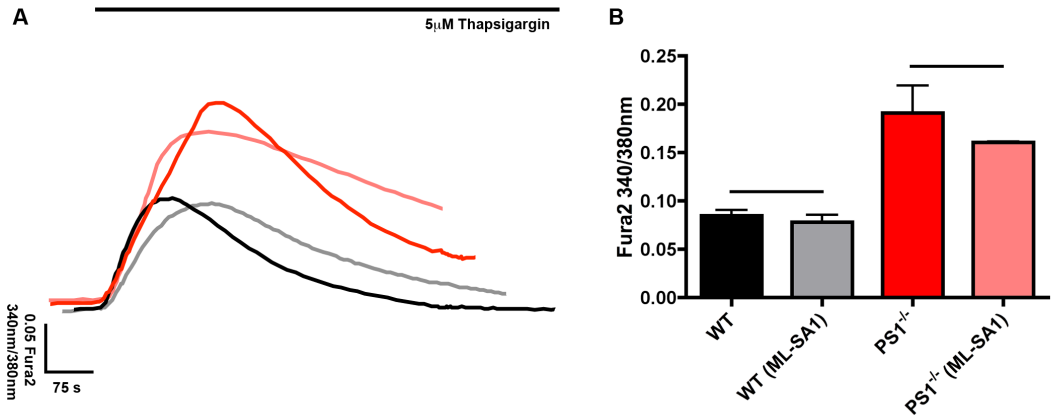

Figure 3.3.20. –Thapsigargin mediated ER Ca^{2+} release in cells after the addition of ML-SA1. A - *Representative traces of Ca^{2+} release in Fura2 loaded cells induced by 20μM ML-SA1 in the presence and absence of ML-SA1. Black bar indicates the presence of thapsigargin.* ***B –*** *Quantification of Ca^{2+} release from all cellular populations measured by ratiometric change in Fura2 fluorescence. ML-SA1 presence indicated by brackets. Error bars = SEM. n = 3 for WT and $PS1^{-/-}$, n= 2 for WT and $PS1^{-/-}$ in the presence of ML-SA1. No significant differences calculated by one way ANOVA with Bonferroni post test.*

Accordingly, we replicated the experiment described in 3.3.15. but changed GPN for ML-SA1 prior to the addition of thapsigargin in both control and $PS1^{-/-}$ cells. The results obtained after ML-SA1 stimulation show only a minimal non-significant reduction in both cell lines. In $PS1^{-/-}$ there is a trend towards a reduction in thapsigargin mediated Ca^{2+} release, however, this is much smaller than the significant reduction observed with GPN treatment (figure 3.3.15). This indicates that, unlike in experiments utilising GPN, the addition of ML-SA1 to cells does not result in significant CICR from the ER. As such the differences seen in 3.3.19. are not due to the increased levels of ER Ca^{2+} present in $PS1^{-/-}$ cells. Accordingly, we do not need to pre-treat cells with either ionomycin or thapsigargin prior to ML-SA1. Subsequently, we decided to clarify that ML-SA1 was specific for TRPML1 and did not potentiate Ca^{2+} release from related channels.

To begin this we utilised mucolipidosis type IV (MLIV) patient fibroblasts which carry a mutation leading to no functional expression of the TRPML1 channel. In these cells we would expect no Ca^{2+} release in response to ML-SA1 if the agonist specifically induces Ca^{2+} release from this channel.

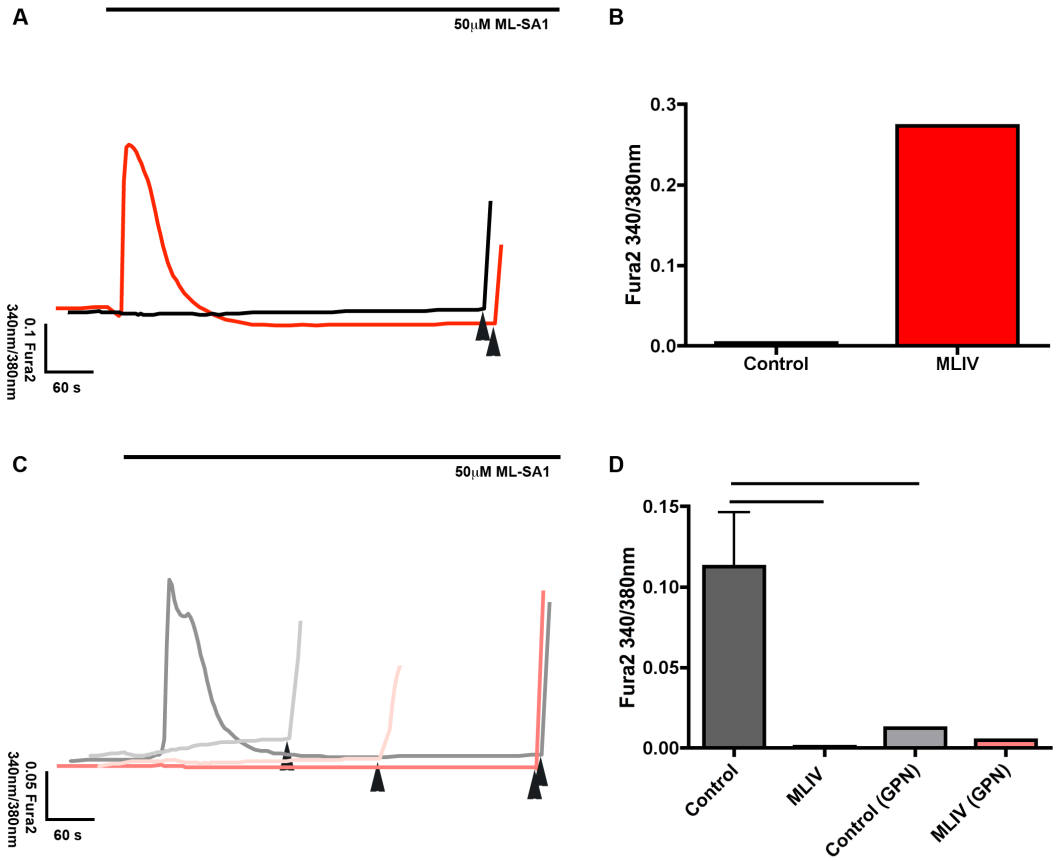

Figure 3.3.21. – Analysis of MLSA1 release events in MLIV cells. *Confirmation of ML-SA1 specificity for the TRPML1 channel in the presence of lysosomal alkalization using MLIV patient fibroblasts which do not express functional TRPML.* ***A -*** *Representative traces of Ca^{2+} release in Fura2 loaded cells induced by 50μM ML-SA1. Black bar indicates the presence of ML-SA1, black arrowheads show the addition of 5μM ionomycin to confirm cell viability. In this experiment the imaging buffer contained 1mM Ca^{2+}.* ***B –*** *Quantification of Ca^{2+} release measured by ratiometric change in Fura2 fluorescence. Error bars = SEM. n = 1.* ***C*** *– Representative traces of Ca^{2+} release in Fura2 loaded cells induced by 50μM ML-SA1 after 12 hr treatment with 50nM Concanamycin A in the presence and absence of 300μM GPN. Black bar indicates the presence of ML-SA1, black arrowheads show the addition of 5μM ionomycin to confirm cell viability. Control cells are shown in grey, control cells post GPN are shown in light grey. MLIV cells are shown in red, with MLIV cells post GPN shown in light red.* ***D*** *– Quantification of Ca^{2+} release from cell treated with 50nM Concanamycin A for 12 hours in the presence and absence of GPN measured by ratiometric change in Fura2 fluorescence. GPN presence is indicated in brackets. Error bars = SEM. n = 2 for Control and MLIV cells, n = 1 for Control and MLIV cells in the presence of GPN.*

Upon performing this experiment we observed Ca^{2+} release from MLIV patient fibroblasts treated with ML-SA1, despite the presence of no functional TRPML1 in these cells (Wakabayashi et al., 2012). In the initial experiment this was far in excess of the Ca^{2+} release observed in control patient fibroblasts which have active TRPML1 (figure 3.3.21. A and B). Interestingly, this release was reduced when extracellular Ca^{2+} was not present. This suggests ML-SA1 could result in Ca^{2+} influx into the cytoplasm as a result of interaction with TRPM type channels such as TRPM8 in the

plasma membrane (Zhu et al., 2014). Accordingly we performed all experiments with ML-SA1 in Ca^{2+} free imaging buffer.

In order to investigate this in a similar situation to that observed in PS1 cells we induced lysosomal alkalisation with concanamycin A. When we did this the response from control fibroblasts was significantly increased and that from MLIV fibroblasts was ablated. We showed that the Ca^{2+} released in response to ML-SA1 was lysosomal in origin as we were able to prevent this response by using GPN pretreatment to remove lysosomes (3.3.21. C and D). Although these preliminary experiments do not have sufficient repeats to confirm these observations the results obtained suggest that under conditions of lysosomal alkalisation in the absence of extracellular Ca^{2+} ML-SA1 is specific for the TRPML1 channel.

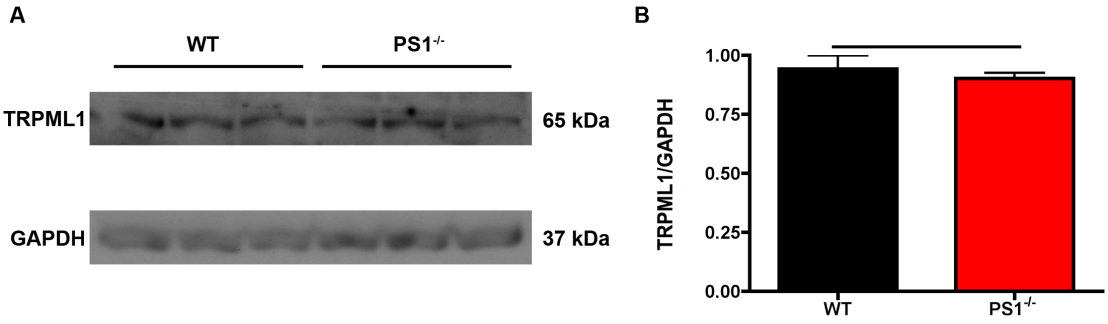

Figure 3.3.22. – Western blot analysis of TRPML1 levels in PS1$^{-/-}$ cells. *No change in TRPML1 levels is observed in PS1$^{-/-}$ BD cells.* ***A –*** *Western blotting of TRPML1 in WT and PS1$^{-/-}$ BD blastocysts.* ***B –*** *Densiometric quantification of protein levels from all cellular populations. Error bars = SD, from three independent cell cultures.*

We also confirmed that TRPML1 levels remain unchanged in PS1$^{-/-}$ cells by western blotting for the protein (figure 3.3.22.). The band identified as TRPML1 in these experiments has been validated as it is reduced by siRNA against TRPML1 in other experiments (Waller-Evans *et al.* Unpublished).

The experiments described in 3.3.20 – 3.3.22. indicate that the increased response of PS1$^{-/-}$ cells to ML-SA1 results from the hyperactivity of the TRPML1 channel. Accordingly, we began to investigate whether we could modulate the activity of TRPML1 in an attempt to re-establish Ca^{2+} homeostasis within the endolysosomal system.

Interestingly, our collaborators had observed that intra-luminal endolysosomal Ca^{2+} levels could be restored by treating $PS1^{-/-}$ cells with Ned-19 (Lee et al., 2015). This molecule is a NAADP analogue which prevents the activation of NAADP dependent lysosomal Ca^{2+} channels preventing Ca^{2+} efflux (Naylor et a., 2009). As TPC2 is well defined as an NAADP-activated lysosomal Ca^{2+} efflux channel, Ned-19 is considered to be an antagonist of this channel. However, as this channel is essentially inactivated in $PS1^{-/-}$ cells further inhibition of this channel would not cause the recovery of intra-luminal Ca^{2+} levels. As TRPML1 is hyperactive in these cells we were interested to see if Ned-19 pretreatment had any effect on ML-SA1 induced Ca^{2+} release.

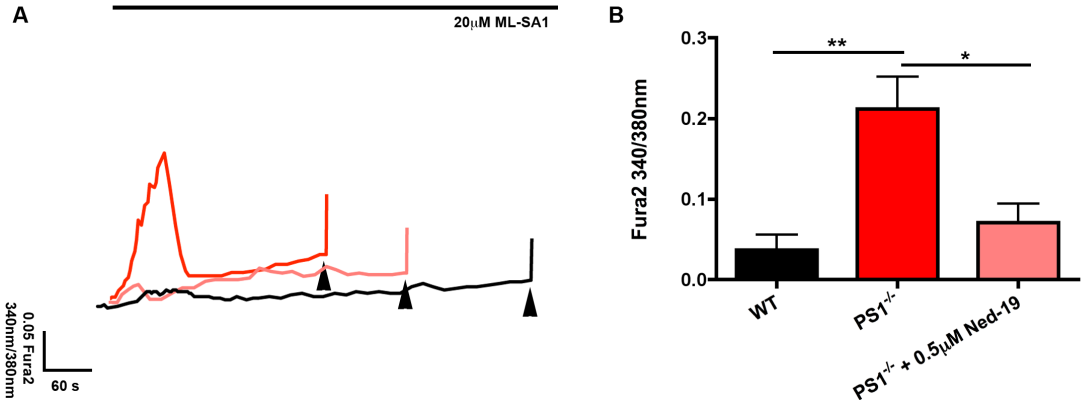

Figure 3.3.23 – Effect of Ned-19 pretreatment on Ca^{2+} release from $PS1^{-/-}$ BD cells in response to the synthetic TRMPL1 agonist ML-SA1. *$PS1^{-/-}$ cells were treated with 0.5μM Ned-19 for 24 hours.* ***A -*** *Representative traces of Ca^{2+} release in Fura2 loaded cells induced by 20μM ML-SA1. Black bar indicates the presence of ML-SA1, black arrowheads show the addition of 2μM ionomycin to confirm cell viability.* ***B –*** *Quantification of Ca^{2+} release measured by ratiometric change in Fura2 fluorescence. Error bars = SEM. n = 9 for WT, n = 8 for $P1^{-/-}$ and n = 4 for $PS1^{-/-}$ +Ned-19. * = P < 0.05, ** = P < 0.01 calculated by one way ANOVA with Bonferroni post test.*

As can be seen in figure 3.3.23. Ned-19 pretreatment is able to reduce the pathogenically elevated Ca^{2+} release ($P < 0.01$, $t = 4.337$, $df = 14$) in response to ML-SA1 to almost control levels in $PS1^{-/-}$ cells ($P < 0.05$, $t = 2.769$, $df = 6$). Although this finding was unanticipated as TPC2 and TRPML1 are functionally distinct channels, both are activated by phosphoinositiols (Waller-Evans and Lloyd-Evans, 2015; Jentsch, et al., 2015). This suggests that they are able to interact with similar lipids. It is also interesting that knockout of TPC2 does not abolish Ca^{2+} signaling events initiated by NAADP (Ruas et al, 2015). It may be that that a binding partner to the TPC2 channel may be present in cells and this is the site of NAADP binding. If this is the case NAADP could interact with multiple channels via this binding partner, as

Ned-19 is a functional analogue of NAADP it would be expected that it would also interact with this protein and, accordingly, could affect both TPC2 and other channels, potentially TRPML1.

The interaction of TRPML1 with the phosphoinisitol-3,5-bisphosphate ($PI(3,5)P_2$) results in increased open probability of the channel, resulting in increased conductance of Ca^{2+}. The enzyme responsible for production of this phosphoinisitol is PIKfyve and this can be inhibited by YM201636 (Jefferies et al., 2008). When cells are treated with this inhibitor vacuolation has been reported and this provides a measure of the susceptibility of different cell lines to PIKfyve inhibition. The vacuolation phenotype observed in $PS1^{-/-}$ cells is markedly more severe to that observed in control cells (data not shown). The presence of a significantly greater number of vacuoles in $PS1^{-/-}$ cells suggests the they are much more susceptible to PIKfyve inhibition and the subsequent reduction in PI(3,5)P2. This is unsurprising, as it is known that $PS1^{-/-}$ cells have lower levels of this phosphoinositol. Interestingly, the effects of the endolysosomal Ca^{2+} release agonists upon these vacuoles reveals that they are likely lysosomal in origin. Firstly, GPN treatment removes these vacuoles showing they contain Cathepsin C and maintain a pH which is at least marginally acidic. When the numbers of vacuoles were analysed after ML-SA1 treatment it can be observed that, as expected from a channel agonist, it did not remove these structures although slight fluctuations in the number of vacuoles observed are likely the result of fusion between vacuoles as observed in videos of these cell populations (data not shown). Accordingly this data shows that although YM201636 may be used to study the effects of PI(3,5)P2 on certain channels it creates a non-physiological phenotype within cells and, accordingly, results must be interpreted as such. YM201636 treatment does, however, remain the most direct way of modulating the activity of PI(3,5)P2 stimulated channels within cells.

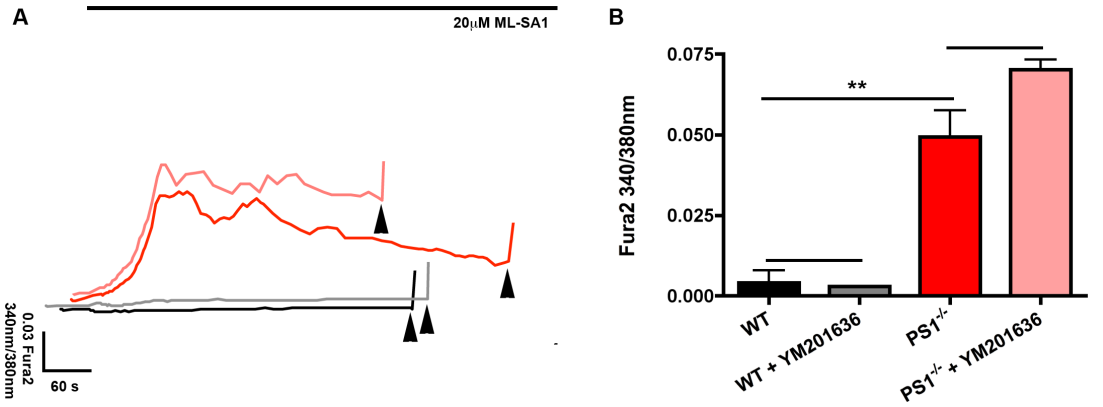

Figure 3.3.24. – Effect of YM201636 pretreatment on Ca^{2+} release from TRPML1 in $PS1^{-/-}$ BD cells stimulated with ML-SA1. *Cells were treated with 10μM YM201636 for 1 hour.* ***A -*** *Representative traces of Ca^{2+} release in Fura2 loaded cells induced by 20μM ML-SA1. Black bar indicates the presence of ML-SA1, black arrowheads show the addition of 2μM ionomycin to confirm cell viability.* ***B –*** *Quantification of Ca^{2+} release measured by ratiometric change in Fura2 fluorescence. Error bars = SEM. n = 2 for WT, n = 2 for WT + YM201636, n = 2 for $PS1^{-/-}$ and n = 3 for $PS1^{-/-}$ + YM201636. ** = P<0.01.*

When we looked at the effect of YM201636 treatment on Ca^{2+} release after stimulation of TRPML1 in preliminary experiments we observed a trend towards increase in Ca^{2+} release in $PS1^{-/-}$ cells. Initially this finding was surprising as PIKfyve inhibition leads to a reduction in PI(3,5)P2 which is expected to reduce the open probability of the channel and as such reduce Ca^{2+} release from this channel. However, when we consider this more carefully it stands to reason that luminal Ca^{2+} levels should increase if the channel is less likely to be open as less Ca^{2+} is released from the store. If confirmed, these data may suggest that TRPML1 is more active in presenilin deficient cells as a larger increase in Ca^{2+} release is observed in these cells and only a slight trend towards increase is observed in control cells. Whether this drives the vacuolation process remains to be determined as this was also significantly more severe in Presenilin deficient cells. This potentially shows that ML-SA1 can potentiate TRPML1 Ca^{2+} release in the absence of PI(3,5)P2 in mice as previously published by Feng et al. (2014). Whether this is due to similarities in the structure of ML-SA1 and PI(3,5)P2 remains to be investigated. In addition to further repeats at this concentration of YM201636 it would also be useful to optimize YM201636 treatment for the induction of vacuolation phenotypes in control cells as this would allow us to study further the role of TRPML1 in healthy cells. As these data suggest that YM201636 treatment induced the filling of lysosomal Ca^{2+} stores we were interested to see if this was occurring in cells.

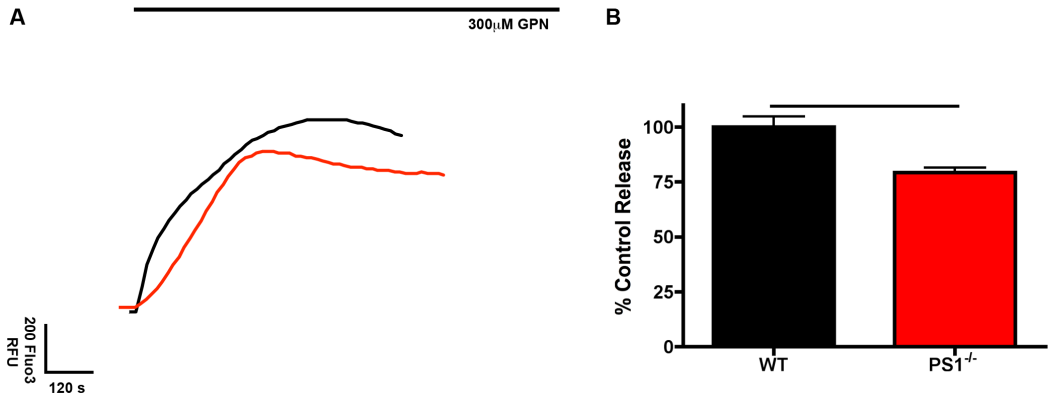

Figure 3.3.25. – Effect of YM201636 pretreatment on GPN-induced lysosomal Ca^{2+} release in $PS1^{-/-}$ cells in relation to WT cells in the presence of ionomycin. *Cells were treated with 10μM YM201636 for 1 hour.* ***A -*** *Representative traces of Ca^{2+} release in Fluo3 loaded cells induced by 20μM ML-SA1. Black bar indicates the presence of ML-SA1.* ***B –*** *Quantification of Ca^{2+} release measured by change in Fluo3 fluorescence. Error bars = SEM. n = 2. No significance calculated by T test.*

By using the ionomycin GPN method described in figure 3.3.12. we are able to do this. As previously described the lysosomal system has been significantly altered by YM201636 treatment. Due to this and as we were interested in inhibiting the hyperactivity of TRPML1 we decided that it would be most relevant to compare the two cell lines after PIKfyve inhibition. Upon doing this, the difference in endolysosomal Ca^{2+} content was reduced from a 75% reduction in $PS1^{-/-}$ cells to a reduction of approximately 25%. This difference did not reach significance although in future repeats it may due to there still being a trend towards reduced Ca^{2+} in the $PS1^{-/-}$ cells. These data suggest that the increase in Ca^{2+} release in response to ML-SA1 was a result of an increased releasable pool of Ca^{2+}.

Taken together the data shown if figures 3.3.24. and 3.3.25. are suggestive that a potentiation in the activity of the TRPML1 channel is responsible for the increased efflux of Ca^{2+} from lysosomes which, in turn, leads to reduced levels of endolysosomal Ca^{2+}. As there is evidence of lysosomal alkalisation in these cells this increased efflux is most likely a result of an increased number of compartments of the endolysosomal system at an appropriate pH for TRPML1 to remain active when in healthy cells it has become inactive due to acidification (Raychowdhury et al., 2004).

However, as YM201636 represents a non-physiological situation we were interested to look at other method with which we could inhibit Ca^{2+} release from TRPML1 and see if this corrected Ca^{2+} homeostasis. A recent publication had used an antibody

raised against TRPML1 as a means of inhibiting this channel (Zhang et al., 2012) so we decided to see if we could use this method in PS1$^{-/-}$ cells.

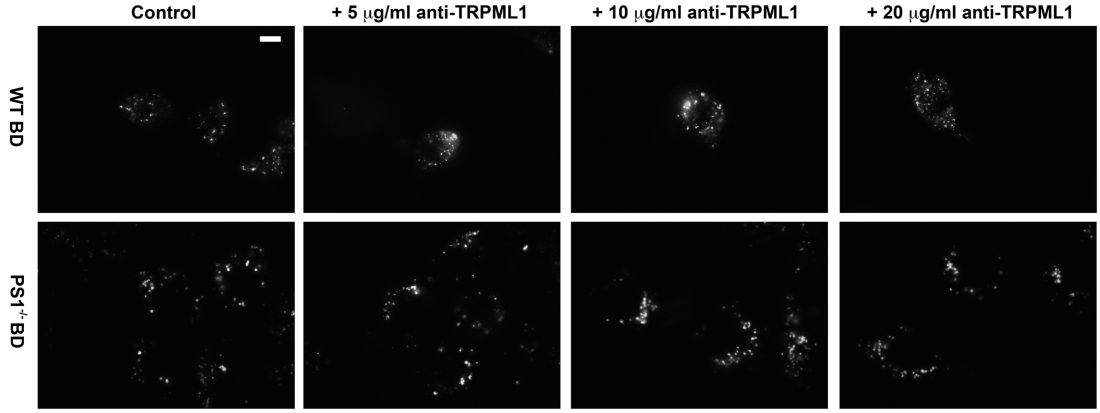

Figure 3.3.26. – Treatment of WT and PS1$^{-/-}$ BD blastocyst cells with an antibody against TRPML1*. Enlargement of acidic vesicles within cells a phenotype observed upon inactivation of TRPML1. Cells were treated with different titrations of anti-TRPML1 for 16hours before loading with the acidotrophic dye lysotracker green. Representative images for each cell population are shown, n = 1. Scale bar = 7.5 μm.*

Initially, we used increased levels of lysotracker fluorescence within cells as a marker of TRPML1 inhibition as this is one of the most robust phenotypes observed in MLIV patient cells which, as discussed previously, have inactive TRPML1. This was observed to increase in both control and PS1$^{-/-}$ cells from low antibody concentrations of 5 μg/ml, this increase became more evident at 10 μg/ml. Interestingly, although an increase was observed at 20 μg/ml this did not seem to have increased compared to 10 μg/ml and the interaction appeared to reach saturation. As these changes seemed potent at 5 μg/ml we decided to continue experiments using that inhibitory concentration of antibody. Accordingly, the Ca^{2+} responses of cells treated with 5 μg/ml anti-TRPML1 antibody were investigated after stimulation of TRPML1 with ML-SA1.

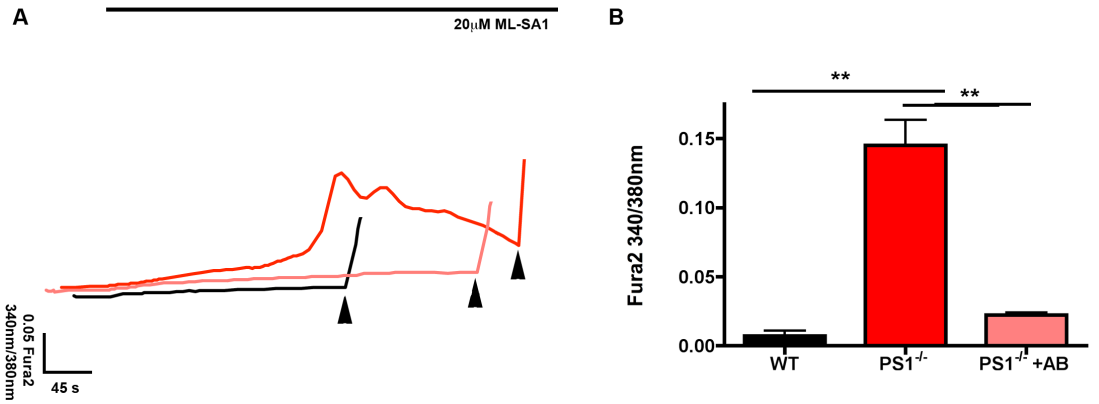

Figure 3.3.27. – Effect of anti-TRPML1 antibody pretreatment on ML-SA1 induced Ca^{2+} release. *Cells were treated with 5 μg/ml anti-TRPML1 for 16 hours.* ***A -*** *Representative traces of Ca^{2+} release in Fura2 loaded cells induced by 20μM ML-SA1. Black bar indicates the presence of ML-SA1,black arrowheads show the addition of 2μM ionomycin to confirm cell viability.* ***B –*** *Quantification of Ca^{2+} release measured by ratiometric change in Fura2 fluorescence. Error bars = SEM. n = 3 for WT and $PS1^{-/-}$ cells, n = 2 for $PS1^{-/-}$ cells + AB. ** = P<0.01.*

Following incubation with the antibody a significant decrease ($P < 0.01$, $t = 6.543$, $df = 2$) was observed in Ca^{2+} releases in $PS1^{-/-}$ cells (Figure 3.3.27). This was so potent it almost returned the cells to the same levels of release as control cells. This provides further evidence that the lysosomal Ca^{2+} channel sensitive to ML-SA1 is TRPML1

We were also interested to see if the TRPML1 channel in these cells would be amenable to patch clamping to look more closely at channel open and closed states. In order to do this the endolysosomal system is expanded by treating cells with Vacuolin so that the swollen organelle can be clamped (Wang et al., 2012). Initially, we examined the effects of Vacuolin treatment on $PS1^{-/-}$ cells.

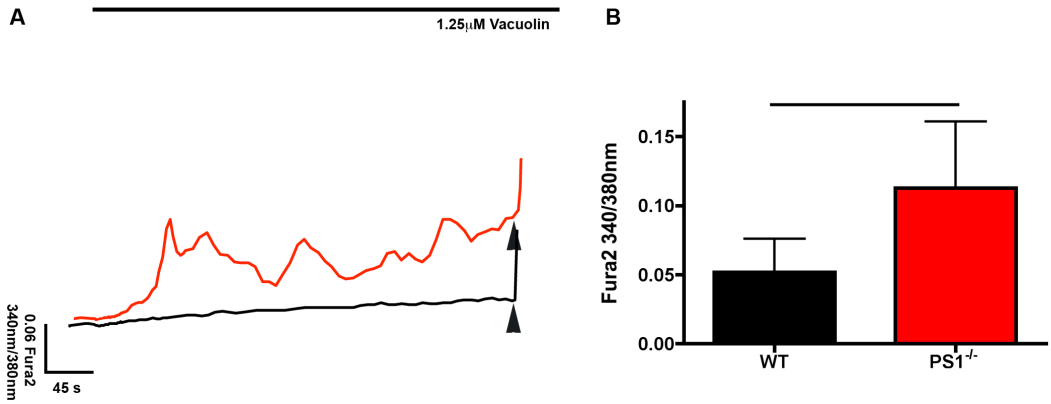

Figure 3.3.28. – Effect of vacuolin treatment on Ca^{2+} release in $PS1^{-/-}$ cells. A - *Representative traces of Ca^{2+} release in Fura2 loaded cells induced by 1.25μM vacuolin. Black bar indicates the presence of vacuolin, black arrowheads show the addition of 5μM ionomycin to confirm cell viability.* ***B –*** *Quantification of Ca^{2+} release measured by ratiometric change in Fura2 fluorescence. Error bars = SEM. n = 2. No significance calculated by T test.*

When cells were treated with vacuolin Ca^{2+} release was observed in both cell lines, although there is a trend towards elevation of this Ca^{2+} release in $PS1^{-/-}$ cells ($P = 0.0604$, $t = 3.883$, $df = 2$, $F_{1,1} = 1,790$). Firstly, this is problematic as Ca^{2+} release at this stage would mean that the lumenal levels of Ca^{2+} in the endolysosomal system have been altered prior to any experiments; if the flow of ions is then to be analysed the changes in this would affect the subsequent results. This is especially true if both cell lines respond differently to vacuolin during the pretreatment, although the impact of this that has been observed so far is slight this may be amplified in subsequent experiements where Ca^{2+} release is measured at the lysosomal membrane. Interestingly, vacuolin treatment has been shown to change Ca^{2+} before and it has also been reported that the majority of the membrane constraining vacuolin expanded vesicles contains markers for early endosomes (Cerny et al., 2004). As such, if we were to investigate TRPML1 by this method it would be under non-physiological conditions and would not contribute to the careful analysis of TRPML1 function and the modulators of this in $PS1^{-/-}$ cells.

Our experiments in 3.3.1 – 3.3.3 have shown that Presenilin deficient cells have a number of interesting phenotypes which could be important to disease processes and the further examination of Presenilin deficiency as a means of causing familial Alzheimer's. However, the cells used for these experiments were from mice and have complete genetic knockout of PS1 (and in some cases PS2). As patients with familial Alzheimer's have mutations in presenilin proteins rather than knockout of those proteins these cells may not be wholly representative of the disease processes

occurring in patients. As such, we were interested to investigate the phenotypes we have observed in a more relevant cell line.

3.3.4. – Preliminary examination of Lysosomal Pathology in Down's Syndrome is indicative of lipid homeostasis and Ca^{2+} homeostasis defects

As patient fibroblasts are a well used tool for such experiments and they also closely model Ca^{2+} dyshomeostasis and endocytosis defects observed in many other cell lines (Lloyd-Evans et al., 2008) we decided to investigate some of the phenotypes observed in 3.3.1 – 3.3.3 in these cells.

Initially, we have used Down's Syndrome (DS) patient fibroblasts in order to examine some of these phenotypes. Patients with DS almost universally exhibit early neurodegeneration and post-mortem analysis reveals hallmarks of Alzheimer's disease in the brains of these patients. The cause of DS is trisomy of all or part of the 21st chromosome and on this chromosome the *APP* gene is located (Masters et al., 1985). As such patients with DS have increased levels of this protein leading to Alzheimer's phenotypes, similarly genetic duplication of the APP locus has been wobserved in some cases of familial Alzheimer's (Delebar et al., 1987).

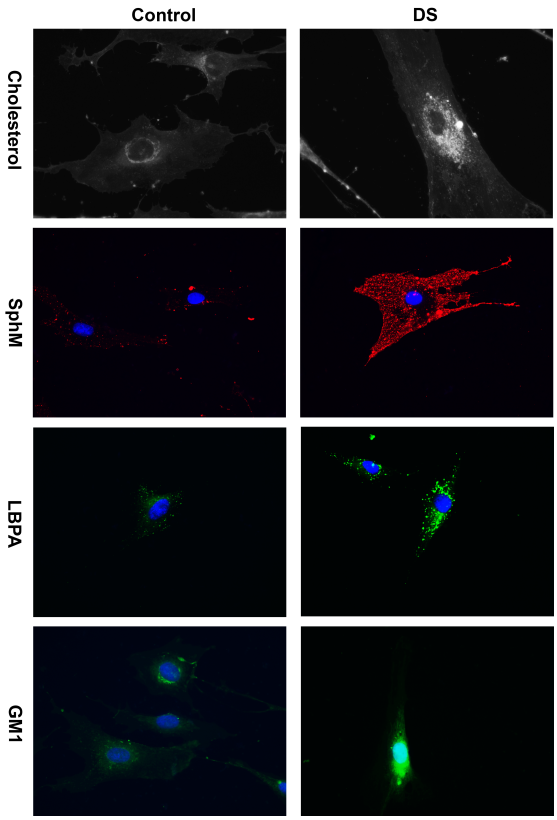

Figure 3.3.29. – Sphingolipid, phospholipid and cholesterol distribution in PS1$^{-/-}$ cell lines. *Representative microscopy images of control and Down's syndrome patient fibroblasts showing levels of cholesterol (white) visualised by filipin, sphingomyelin (SphM, red) visualised by IHC against the lysenin toxin, LBPA (green) visualised by IHC and ganglioside GM1 (GM1, green) visualised by FITC-tagged CtxB. Hoechst stained nuclei are shown in blue. n = 3. Scale bar = 15μm.*

We examined the lipid phenotypes described in section 3.3.1. and found that there are some similarities in lipid storage; including the increase in cholesterol and LBPA levels as has been previously reported in these cells (Cataldo et al., 2008). Interestingly, however, the levels of sphingomyelin and ganglioside GM1 which we have shown are decreased in PS deficient cells are elevated in the DS cells. These phenotypes are more similar to those observed in NPC and this appears to be complemented by the localisation of cholesterol accumulation which, in this initial analysis, is in the perinuclear region (figure 3.3.29.). As such it may be interesting to subject these cells to the analysis performed in section 3.3.2. As distinct differences were also observed by biochemical analysis of lipid levels in PS1$^{-/-}$ cells we subjected DS patient cell lines to this.

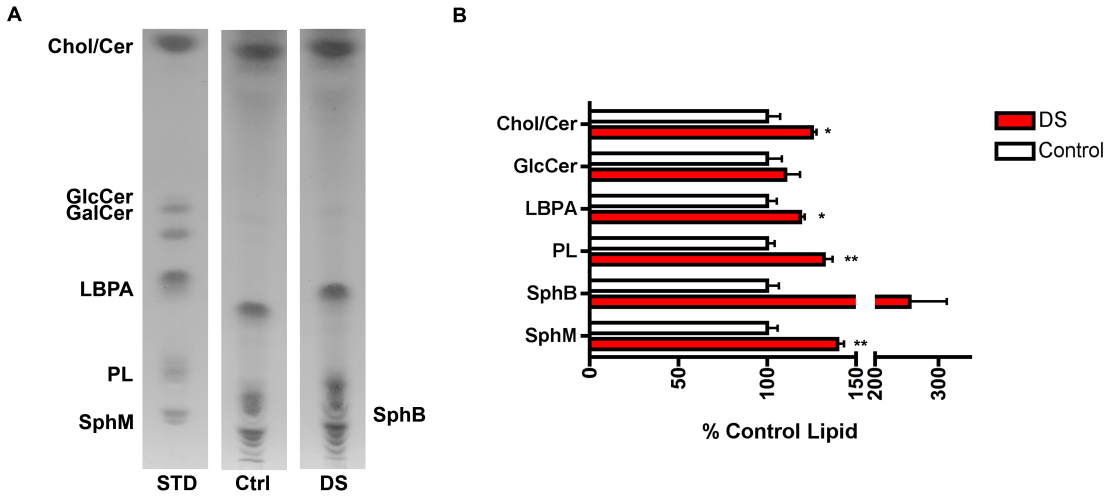

Figure 3.3.30. – Biochemical quantification of sphingolipids, sterols and phospholipids in Down's syndrome patient fibroblasts. A – *Representative images of thin-layer chromatography analysis of various lipids in control (Ctrl) and Down's syndrome patient fibroblasts (DS) ran alongside identified lipid standards (STD). Chol/Cer = combined levels of cholesterol and ceramide, GlcCer = glucosylceramide, GalCer = galactosylceramide, LBPA = lysobisphosphatidic acid, PL = phospholipids, SphB = sphingoid bases and SphM = sphingomyelin.* ***B –*** *Densiometric quantification of lipid levels in Down's syndrome patient fibroblasts (DS) as a percentage of the lipid levels in control fibroblasts. Lipid species are labeled as in A. Error bars = SD. n = 3. ** = P<0.01, * = P<0.05 calculated by T test.*

Upon doing so we, again, observed elevations in lipids which were more similar to the differences observed in NPC1 disease (Lloyd-Evans et al., 2008) than in the PS deficient cell lines examined in section 3.3.1. This analysis confirms elevations in cholesterol (P = < 0.05, t = 3.187, df = 4, F2,2 = 7.671) (although the contribution of ceramide to this remains to be observed by running the TLC with the different mobile phase) alongside elevations in sphingomyelin (P = < 0.01, t = 5.580, df = 4, $F_{2,2}$ = 2.730) and LBPA (P = < 0.05, t = 3.018, df = 4, $F_{2,2}$ = 4.003). There is also a trend

towards elevation in sphingoid bases in these cells (P = 0.058, t = 2.634, df = 4, $F_{2,2}$ = 76.97) and a trend towards elevation of the simple glycosphingolipid GlcCer. Considering these data the lipid storage phenotypes observed in DS cells is much more reminiscent of NPC disease than the lipid phenotypes observed in PS deficient cells.

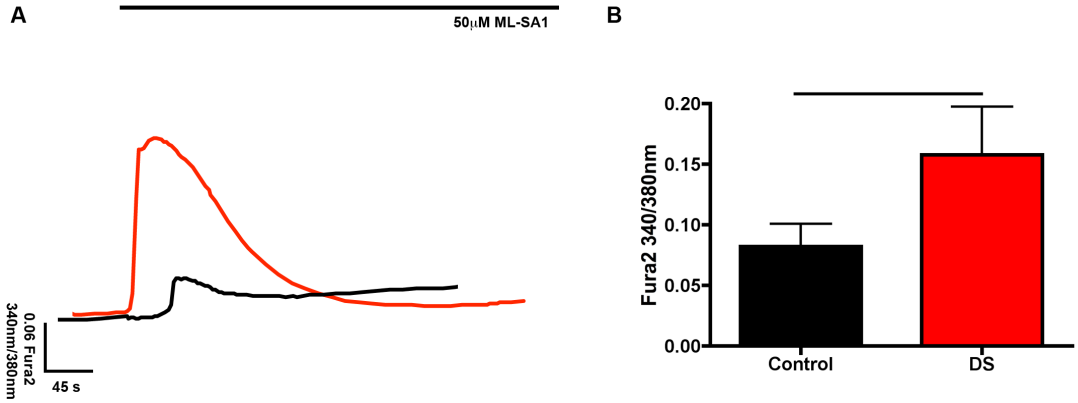

Figure 3.3.31. – Ca^{2+} release in response to ML-SA1 in Down's Syndrome patient fibroblasts*. A - Representative traces of Ca^{2+} release in Fura2 loaded cells induced by 50μM ML-SA1. Black bar indicates the presence of ML-SA1.* ***B –*** *Quantification of Ca^{2+} release measured by ratiometric change in Fura2 fluorescence. Error bars = SEM. n = 4. No significance calculated by T test.*

Accordingly, we were interested to see if our novel reports of TRPML1 hyperactivity, observed in $PS1^{-/-}$ cells, were present in DS fibroblasts as this is not a phenotype seen in cell models of NPC1 disease (Waller-Evans *et al.* Manuscript in preparation). Interestingly, although the lipid accumulation phenotypes we have observed in DS cells is much more reminiscent of NPC1 a trend towards increased Ca^{2+} release in response to ML-SA1 was observed in these cells although the differences between these cell lines were not as distinct as in $PS1^{-/-}$ cells (figure 3.3.19.). This trend would likely become significant if ML-SA1 concentration was titrated until the maximum differences between these cell lines occurred.

Although these preliminary studies do suggest some conservation of phenotypes to other models of Alzheimer's, it is clearly shown that there are some differences. It would be interesting to see what phenotypes patient relevant mutations in PS1 elicit and the subsequent comparison of these to DS patient fibroblasts could provide further insights into conserved and divergent mechanisms of disease.

3.4. – Summary of Results and Discussion

The results presented in section 3.3. clearly show that PS deficient cells have a different phenotype from NPC1 cells in relation to lipid and Ca^{2+} homeostasis (Lloyd-Evans et al., 2008). In addition it is shown that the changes in both these systems in $PS1^{-/-}$ cells are suggestive of changes to lysosomal pH as an underlying cause.

3.4.1. – Lysosomal alkalization in $PS1^{-/-}$ cells

A number of publications show that it has been difficult to confirm that lysosomal pH has been changed in these cells resulting in contrasting views on the subject (Avrahami et al., 2013; Coen et al., 2012; Wolfe et al., 2013). Differences in the cell lines utilised in these studies may be responsible for some of these differences however the probes used to assay lysosomal pH also vary in these studies meaning that they are not always directly comparable. Wolfe et al. (2013) have profiled a number of these pH probes in a number of different cell lines and found that lysosensor yellow/blue dextran has the optimal profile for the assessment of lysosomal pH before using it to measure lysosomal pH in a variety of cellular models of familial Alzheimer's including patient fibroblasts and mouse models; in all these models lysosomal alkalization was reported. The degree of this elevation in pH was a ~0.5 pH units in $PS1^{-/-}$ cells.

An additional study by (Coffey et al., 2014) noted that a number of the autophagy phenotypes present in PS deficient cells were reminiscent of other conditions in which lysosomal pH becomes more alkaline, such as macular degeneration. They utilised familial Alzheimer's patient fibroblasts with the A246E mutation in PS1 and observed a modest elevation of 0.2 – 0.3 pH units in these cells. This suggests that although we have conducted our experiments in $PS1^{-/-}$ and $PS1/2^{-/-}$ cells that have lysosomal alkalisation at the extreme end of the biological spectrum there is still significant lysosomal alkalisation in more disease relevant cell lines.

In a recent publication, Lee et al. (2015), our Ca^{2+} data is presented alongside further studies on lysosomal alkalisation and the underlying mechanism leading to this. Firstly, inhibition of the vATPase using concanamycin A1 lead to a similar defective autophagy phenotype with defects in lysosomal proteolytic enzymes as that observed in $PS1^{-/-}$ cells. Our collaborators were also able to correct these defects by

re-acidifying the lysosomes of PS1$^{-/-}$ cells. They achieved this by treating cells with acidifying nanoparticles which have previously been shown to correct alkalisation defects in the endolysosomal system (Balatazar et al., 2012). Importantly, the Ned-19 treatment which re-filled lysosomal Ca^{2+} stores by inhibiting the excessive release from TRPML1 in PS1$^{-/-}$ cells did not lead to a correction of autophagic defects in the same way. Additionally, the application of acidic nanoparticles to cells resulted in the re-filling of lysosomal Ca^{2+} stores and reduction of cytosolic Ca^{2+} levels in the absence of Ned-19.

Lysosomes from control and PS1$^{-/-}$ cells were purified using a method developed in our lab (Walker and Lloyd-Evans, 2015). These lysosomal preparations were shown to be enriched in lysosomal markers and without markers of other organelles. Compared to lysosomes prepared from control cells those prepared from PS1$^{-/-}$ had significantly decreased levels of the Voa1 and V1E1 subunits of the vATPase whilst the levels of lysosome marker LAMP-1 remained constant. These purified organelles were then used to show that the quenching of the proton sensitive dye 9-amino-6-chloro-2-methoxyacridine (ACMA) was decreased in lysosomes prepared from PS1$^{-/-}$ cells showing that they were less able to translocate protons.

Specific siRNA knockdown of Voa1 was also used to induce the same pH, autophagic and proteolytic defects in cells demonstrating that this was essential for lysosomal acidification and autophagy. Glycosylation of this subunit was also investigated utilising Voa1 protein which contained a mutation known to cause glycosylation defects in related proteins. This process was found to be critical for both its stability and function. Finally, PS1$^{-/-}$ primary neurons were investigated and they were found to have the pH, autophagy and proteolysis defects reported in other cells alongside decreased lysosomal Ca^{2+} and increased cytosolic Ca^{2+} (Lee et al., 2015).

3.4.2. – Lysosomal Ca^{2+} homeostasis in PS1$^{-/-}$ cell lines is a result of lysosomal alkalisation

Considering the experiments discussed above, and the data shown in section 3.3.3., there is evidence that the elevated pH in PS1$^{-/-}$ cells is the primary cause of the reduced levels of lysosomal Ca^{2+} and, as such, is a more primary event in the pathological cascade which leads to autophagic dysfunction in PS deficient cells.

Nevertheless, Ca^{2+} dyshomeostasis in the lysosome will contribute this as fusion between lysosomes and autophagosomes and their subsequent clearance is dependent upon properly regulated lysosomal Ca^{2+} release (Luzio et al., 2007). The changes in Ca^{2+} homeostasis within the lysosomes are represented diagrammatically in figure 3.4.1.

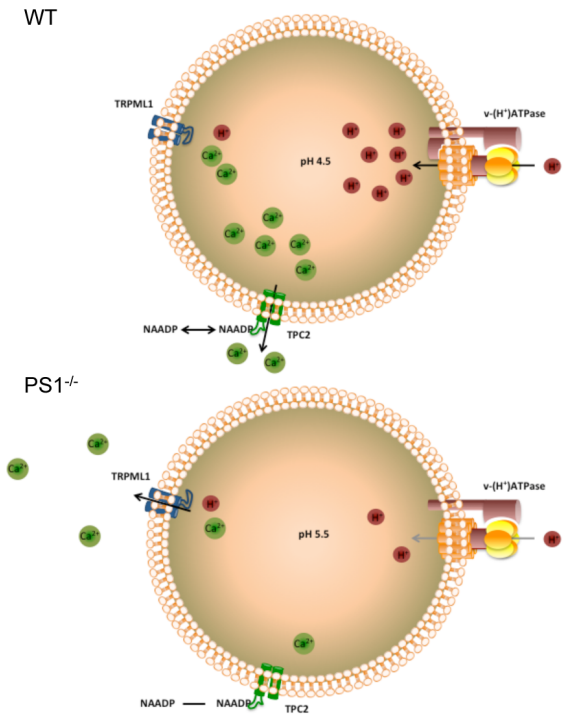

Figure 3.4.1. – Lysosomal Ca^{2+} dyshomeostasis in lysosomes of $PS1^{-/-}$ cells is a result of lysosomal alkalisation. *Reduction in vATPase activity is indicated by a grey arrow showing reduced translocation of protons. Note the removal of the Voa1 subunit from vATPase on the lumenal side of the protein complex.*

The loss of vATPase function due to mistrafficking of the Voa1 subunit of this protein complex elevates pH in the lysosomes of $PS1^{-/-}$ cells as proton translocation is less efficient. Whilst this could potentially also reduce the activity of the proteins responsible for filling the lysosomes with Ca^{2+} these have not yet been identified, as such it is difficult to study this aspect of the problem. $PS1^{-/-}$ cell lines may help validate any candidates we discover for these proteins however, as we would expect their activities to be reduced in these cells.

Lysosomal Ca^{2+} release channels have been investigated in much more detail and a number described in studies which included single channel recordings of their activities at different pH (Raychowdhury et ., 2004; Pitt et al., 2010). Of these channels, we are selectively able to activate Ca^{2+} release from TPC2 with NAADP-AM although we could not do the same in $PS1^{-/-}$ cells. As discussed, this is due to the inability of NAADP to dissociate from the receptor when the pH is above pH 5.0 and no Ca^{2+} release can be induced (Pitt et al., 2010). As Ca^{2+} release from TPC2 is

known to be extremely important for providing the localised Ca^{2+} elevations near to the endolysosomal membranes required for the interaction of proteins such as VAMP7 (Luzio et al., 2007) this phenotype is highly likely to contribute to the inability of autophagosomes and lysosomes to fuse, resulting in the build up of autophagic vacuoles. This has been shown to occur in cellular and animal models of NAADP signaling inhibition we have developed following treatment with Ned-19 (Waller-Evans *et al.* Manuscript in preparation) which inhibits TPC2 mediated Ca^{2+} release in the absence of pH defects.

We were also able to selectively activate the TRPML1 channel, under the conditions discussed in section 4.3.3., with the synthetic agonist ML-SA1. As discussed this is a endolysosomal Ca^{2+} efflux channel which is active at a higher pH than channels such as TPC2 (Raychowdhury et al., 2004) and the hyperactivity we have observed in this channel is expected in cells which have undergone lysosomal alkalisation. Our inhibition of this channel with Ned-19 though initially unexpected may reveal novel information with respect to the activation of TRPML1 by different agonists. The fact that both channels can be regulated by phosphoinositols may support this observation (Waller–Evans and Lloyd-Evans; Jentsch et al., 2015). Further study of how these channels act in co-ordination is required to understand this. To do so $PS1^{-/-}$ cells may provide a suitable experimental system.

It is interesting that the only other report linking TRPML1 channel activity to the pathogenesis of Alzheimer's disease like pathology implicates the inactivation of this channel as an important pathogenic event (Bae et al., 2014). In this publication activation of the channel was shown to initiate clearance of interneuronal Aβ, although the lysosomal pathology of the model seems very different to what we have observed in $PS1^{-/-}$ cells as sphingomyelin levels are elevated in cells and lysosomal Ca^{2+} levels are increased. This data was collected using a genetically encoded Ca^{2+} sensor conjugated to TRPML1 in which a non-naturally occurring, constitutively activating mutation has been added (Bae et al., 2014). As such this represents a non-naturally occurring system which may have altered Ca^{2+} homeostasis within these cells.

When our findings in relation to the TPC2 and TRPML1 channels are taken together it implicated TRPML1 in increased 'leak' of Ca^{2+} from lysosomes and this may contribute to increased cytosolic Ca^{2+} levels alongside the decrease in intraluminal endolysosomal Ca^{2+} levels. As such, hyperactivated TRPML1 may contribute the

Ca^{2+} dyshomeostasis that is observed in many model of Alzheimer's disease. This would be interesting to further investigate by inhibition of TRPML1 Ca^{2+} release. Unfortunately, loss of function in this channel quickly leads to MLIV disease phenotypes so there would only be a small window in which these studies would be relevant (Waller-Evans et al., Unpublished). As for inhibitor studies the only currently known TRPML1 inhibitor is Ned-19 after the discovery in this study that it could reduce ML-SA1 mediated Ca^{2+} release. It also seems that this inhibition will only occur in the presence of lysosomal alkalisation. It would be interesting to see if any more inhibitors of TRPML1 could be discovered by *In silico* screening as this method has been successful in finding TRPML1 agonists such as ML-SA1 (Shen et al., 2012).

Another potential way of studying this would be either expressing a constitutively active TRPML1 mutant in control cells to see if any of the autophagy and lipidology phenotypes observe in $PS1^{-/-}$ cells can be induced. This could be potentially achieved by longer term incubation with ML-SA1 although the feasibility of this with respect to cell viability has not yet been assessed. Finally overexpression of wild-type TRPML1 in healthy cells may help recapitulate the phenotype of hyperactivity observed in $PS1^{-/-}$ cells.

The studies described above may help us to tease apart which aspects of pathology are a result of endolysosomal Ca^{2+} dyshomeostasis and which are due to lysosomal alkalisation. Particularly relevant to this is the recent finding that Ca^{2+} release from TRPML1 stimulates autophagy through activation of the phosphatase calcineurin, which binds an dephosphorylates the regulator of lysosomal biogenesis, TFEB (Medina et al., 2015). This has the potential to create a detrimental feedback loop in PS deficient cells as autophagy stimulation would lead to the generation of more autophagic vacuoles which could still not be cleared due to the alkalisation of the lysosome. Interestingly, inhibition of calcineurin signaling in neurons carrying a PS1 mutation rescued signaling defects. It would be particularly interesting to test this inhibitor in Presenilin deficient cells.

Although much remains to be done to study the impact of Ca^{2+} signaling dyshomeostasis as a result of lysosomal alkalisation, we now have a basic understanding of this process in a simple model of familial Alzheimer's; PS deficient cell lines. This is summarised in figure 3.4.2. which also highlights that the mechanism proposed to cause reductions in the lysosomal Ca^{2+} store by

Bezprozvanny (2012) is unlikely to be correct. This is due to the fact that in the cell lines we utilised for this study cytosolic Ca^{2+} is increased so the Ca^{2+} loading protein, or proteins, of the lysosome would have available ions to transport. Lysosomal alkalisation however may cause a different defect in the function of these proteins.

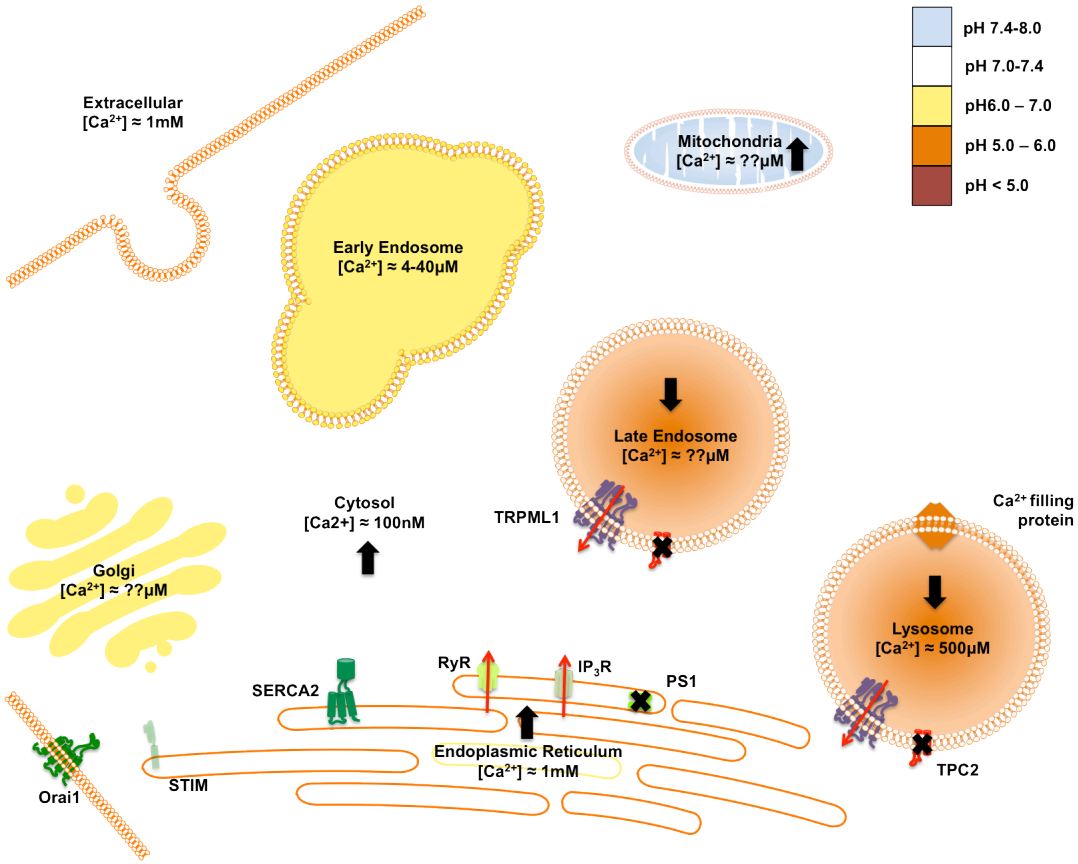

Figure 3.4.2. – An updated picture of Ca^{2+} dyshomeostasis in $PS1^{-/-}$ cells. *Changes to Ca^{2+} stores are shown by black arrows, pathogenically changes to Ca^{2+} releases are shown by thin arrows, red arrows indicate elevated release, grey arrows indicate reduced release. Protein loss of function is indicated by black crosses. Protein loss of function is indicated by black crosses. Adapted from Popugaeva et al., 2013 and Lloyd-Evans et al., 2010.*

Interestingly, this diagram highlights another Ca^{2+} containing compartment which may be interesting to study in models of familial Alzheimer's; the early endosome. Correct acidification of this store is required for Ca^{2+} efflux, if acidification does not take place, then channels such as TRPML3 are not activated (Martina et al., 2009). This would suggest there may be increased Ca^{2+} in early endosomes in $PS1^{-/-}$ cells. This observation is an example of how, from this starting point, we can look at the myriad of cellular processes Ca^{2+} can impact and begin to understand the role this has in familial Alzheimer's.

3.4.3. Changes to lipid homeostasis in Presenilin Deficient cells are also suggestive of lysosomal alkalisation.

Initially we looked at the lipidology of Presenilin deficient cell in order to see that if NPC-like phenotypes were present in these cells. The numerous experiments conducted in sections 4.3.1. supported by observations of endolysosomal lipid trafficking in section 4.3.2. indicate that this is not the case and another complex lipid pathology broadly summarised by: decreases in glycosphingolipids accompanied by increases in simple sphingolipids, cholesterol and phospholipids is present. Lipid dyshomeostasis has been implicated with multiple forms of Alzheimer's disease and were one of the first pathogenic changes reported in post-mortem brain samples from patients by Alois Alzheimer (Grimm et al., 2013). Accordingly, I will just discuss the changes observed within lipids in relation to changes in the endolysosomal system.

The redistribution of cholesterol within $PS1^{-/-}$ cell remains intriguing. The pattern of cholesterol accumulation observed in Presenilin deficient cells was predominantly in diffuse punctate structures away from the nucleus of cells. This is clearly in contrast to the NPC-like accumulation of cholesterol in punctate structures in the perinuclear region – these represent cholesterol storage in the late-endosomes and lysosomes (Lloyd-Evans et al., 2008). Although the compartment in which cholesterol predominantly accumulates in has not yet been confirmed, by co-localisation studies, an attractive proposition would be that there is some buildup of cholesterol within early endosomes as they are spread throughout cells more towards the plasma membrane in a similar pattern to the cholesterol rich punctae. In relation to this it is particularly interesting that the early endosomes should appear affected in these cells as defects in vATPase activity are also likely to impact upon this compartment, as discussed above. It would be interesting to see if the decrease in proton translocation observed in $PS1^{-/-}$ cells prevents the efficient extrusion of Ca^{2+} from these compartments which accompanies their acidification (Gerasimenko et al., 2007). This may provide an explanation for the proposed early endosomal pathology, although this must be further investigated by co-localisation studies as previously mentioned.

The presence of cholesterol accumulation in other compartments, such as the endocytic recycling compartment, was also observed in $PS1^{-/-}$ cells which may suggest that cholesterol flux throughout the endolysosomal pathway is reduced. This

could be further studied with fluorescently tagged cholesterol and low-density lipoprotein. These studies may prove particularly interesting as cholesterol is strongly implicated in the pathogenesis of Alzheimer's by numerous genetic studies, implicating genes such as Apoε as Alzheimer's risk factors (Grimm et al.,2013). Accordingly, novel phenotypes concerning the handling of cholesterol in cells from Alzheimer's models may further explain the role of this vital structural lipid.

Reduction of the GSL GlcCer has previously been reported in Presenilin deficient cells (Mutoh et al., 2012), and differential levels of gangliosides have been observed in numerous models of Alzheimer's; with some gangliosides elevated and others decreased (Yang et al., 2013). Whilst the explanation for this currently involves the reduced activity of glucosylceramide synthase (the enzyme responsible for producing GlcCer) it must also be noted that up to 90% of glycosphingolipid synthesis proceeds by utilising the products of endolysosomal lipid degradation (Sandhoff and Schulze, 2011). As we observed a reduction in GlCer after inhibition of lysosomal vATPase with concanamycin A this may contribute to the reduction in GSLs. This remains to be further investigated.

There was some evidence of elevation in phospholipids in PS deficient cells, as expected in cells which have lysosomal alkalisation. Phospholipidosis is a major consequence of this process (Nujic et al., 2012). Whilst we did observe a trend towards the accumulation of phsopholipids by biochemical assay we were unable to see the same process by using *in situ* fluorescent probes. We ascribed this fact to the fact this probe was itself a fluorescently tagged phospholipid which must be trafficked into cells through the endolysosomal system, The fundamental defects we observed in trafficking in this system, likely due to TPC2 inactivation, may have been responsible for decreased uptake of this probe and delivery to the correct compartments. Accordingly, development of this technique to use a loading probe or measurement of the phospholipids produced would be needed to develop this technique.

One particularly interesting consequence of PS1 inactivation was the increased levels of ceramide observed alongside decreased sphingomyelin. Ceramide has been extensively studied in relation to Alzheimer's and has been found to be elevated in cells, animal models and post mortem brain tissue from Alzheimer's patients (Haughey et al., 2010). As ceramide can be produced by degradation of sphingomyelin by sphingomyelinases, the interplay between these two lipids may be

particularly important, this is particularly evident as they seem to be differentially affected by changes in pH as observed by the differences in sphingomyelin and ceramide in PS1$^{-/-}$ and PS1/2$^{-/-}$ MEF cells. This is suggestive of a phenotype that can be subtly altered by changes in pH to result in larger changes to lipid levels. Further interest has been added by the recent observation that inhibition of acid sphingomyelinase (ASM) is protective in some mouse models of Alzheimer's (Lee et al., 2014). As a primary consequence of this would be decreased ceramide, the localisation and activity of ASM may be interesting to compare in PS1$^{-/-}$ and PS1/2$^{-/-}$ cell lines.

As with the alterations in Ca^{2+} homeostasis we have described much remains to be understood about the changes in lipid homeostasis, but, we have again established a baseline for this analysis and highlighted some interesting avenues of interest to pursue.

3.4.4. – What do these findings mean with respect to Familial and Sporadic forms of Alzheimer's disease?

The overwhelming majority of this research has been conducted in cells in which PS1 or even both PS1 and PS2 have been removed. Accordingly, they do not represent the reality of familial Alzheimer's disease in which the Presenilin protein may have loss of function mutations as opposed to complete removal (Roeber et al., 2015). However, we began research in knockout cells so that our studies were directly comparable to recent research conducted in this area. Accordingly, we plan to develop this study to test for the phenotypes we have described in patient fibroblast cell lines. There are some advantages of starting studies with such cell lines as they do represent a clarified background against which we can identify targets. With the clarification that lysosomal alkalisation occurs in familial Alzheimer's patient fibroblasts (Coffey et al., 2014) it will be exciting to see which of the phenotypes identified in PS1$^{-/-}$ cells with respect to Ca^{2+} and lipids are present in patient fibroblasts.

Whether these phenotypes extend to other form of Alzheimer's either those caused by genetic changes or even sporadic forms of Alzheimer's also remains to be studied. As we have seen from the preliminary study of a small subset of these phenotypes in fibroblasts from patients with Down's syndrome this will not be

straightforward as the contrasting findings when comparing lipid and Ca^{2+} phenotypes to PS deficient cell illustrate. Nevertheless, the careful characterisation of dysfunction in $PS1^{-/-}$ cells leaves us with a solid base to begin these analyses from.

Chapter 4

Lysosomal dysfunction in Huntington's disease implicates the Niemann-Pick type C1 protein in Pathogenesis

4.1. – Introduction

4.1.1. – Huntington's Disease

Huntington's disease is a rare neurodegenerative disorder which is predicted to affect around 6,000 people in the UK (Evans et al., 2013). It is a progressive neurodegenerative disorder which manifests with motor, cognitive and psychiatric disturbances. Symptoms of these disturbances tend to onset around the ages of 35-44 with a median survival time of 15-18 years after onset. (Warby et al., 1998) Common findings during the onset of disease include clumsiness, subtle changes to eye movements including defects in saccades (Turner et al., 2011), involuntary movements and mood disturbances. Around one third of patients also present with psychiatric changes. Subsequently chorea becomes more prominent, dysarthia and dysphagia worsen and voluntary activity becomes increasingly difficult. This may also be accompanied by aggressive outbursts or other symptoms of worsening psychiatric changes. In the final stages of disease motor disability becomes increasingly severe and patients are often rendered totally dependent, mute and incontinent. The average age of death is around 55 years (Warby et al., 1998).

Approximately 25% of patients are diagnosed after the age of 50 years with some patients as old as 70 years; these patients tend to present with a chorea, gait disturbances and dysphagia. Disease progression follows a more prolonged benign course. (Warby et al., 1998)

Within the brains of Huntington's patients, degeneration localizes to neurons of the caudate and putamen (Cowan and Raymond, 2006), particularly the enkephlin and dopamine receptor D2 positive medium spiny neurons. These are GABAergic inhibitory neurons which are active in the indirect pathway of movement control and, as such, this neuronal loss provides the physiological basis for chorea (Mitchell et al., 1999). Degeneration within the striatum can be observed by MRI prior to disease onset and progression of this feature can be a useful for clinical study of Huntington's (Aylward et al, 2004). Glutamate excitotoxicity and subsequent Ca^{2+} dyshomeostasis are proposed to be important in the process of neuronal loss (HD iPSC consortium study., 2012). Other regions of the brain affected in Huntington's are the cerebellum, substantia nigra, hippocampus and various regions of the cortex (Vonsattel et al., 1985; Rub et al., 2013)

A prominent feature observed in post-mortem analysis is intraneuronal inclusions which contain the protein Huntingtin (Warby et al., 1998); these are, however, not considered to be important early on within the pathogenic cascade of Huntington's as they are not present in the areas of selective degeneration within the brain and may be the result of a protective mechanism (Kuemmerle et al., 1999; Arrasate et al., 2004). In addition to pathology within the CNS there is widespread peripheral pathology in Huntington's patients and animal models much of which is proposed to occur independently from neurological defects or the result of general malaise (van der Burg et al., 2009).

4.1.2. – Inheritance of Huntington's Disease

Huntington's is a monogenic disease with an autosomal dominant mode of inheritance, accordingly genetic testing is used to confirm diagnosis and genetic counselling is vital for patients with families. The gene associated with Huntington's is *HTT* (cytogenetically located at 4p16.3) which encodes the protein Huntingtin (HTT) and is situated on chromosome 4 (Huntington's Disease collaborative research group, 1993). In this gene expansion of a CAG repeat region in exon 1 is the only pathogenic variant resulting in an expanded poly-glutamine tract in the translated HTT protein. The degree of expansion in the CAG repeat region is used to classify each *HTT* allele as normal, intermediate or Huntington's causing with a single Huntington's causing allele sufficient for disease pathogenesis (Burugunder, 2014).

Alleles with a CAG repeat region below 26 are considered normal, those between 27 and 35 CAG repeats are considered intermediate. Although an individual with this allele was originally not considered to be at risk of developing Huntington's recent evidence suggests that psychiatric symptoms may be prevalent in these populations and some patients may show late onset Huntington's phenotypes. Any children these patients have will also be at an increased risk of developing Huntington's as the expanded CAG repeat is more unstable and, therefore, more susceptible to expansion (Warby et al., 1998).

Disease causing repeat lengths begin at CAG repeats over 36 trinucleotides long. These can be further subdivided into reduced penetrance alleles (between 36 and 39

CAG repeats), an individual with which may not develop Huntington's symptoms but is considered at risk, and full penetrance alleles (over 40 CAG repeats) individuals with which will almost certainly develop disease (Warby et al., 1998). There is a well defined inverse correlation between the number of CAG repeats and the age of disease onset (Langbehn et al., 2010), with greater CAG expansion linked with more severe disease progression in terms of motor, cognitive and functional measures and less disease modification by other heritable factors (Gusella and Macdonald, 2009). Interestingly, psychiatric symptoms associated with Huntington's do not appear to be dependent upon the size of CAG expansion (Ravina et al., 2008). When CAG repeats expand beyond 60 individuals are increasingly likely to have juvenile onset of symptoms, these occur before 20 years of age and account for 5-10% of Huntington's cases (Warby et al., 1998). In such cases the presentation of symptoms can be quite different with markedly more severe disease progression and cerebellar involvement (Rodda., 1981; Ruocco et al., 2006).

4.1.3. – Huntingtin

The protein product of the *HTT* gene huntingtin (HTT) is a large protein with a mass of around 350kDa which is essential for development. Although it is expressed throughout the body the highest levels are observed in the brain (Zeitlin et al., 1995; Cattaneo et al., 2005). The trinucleotide CAG repeat, which determines if a *HTT* allele is pathogenic, codes for a poly-glutamine tract near the N-terminus of the protein. When this tract expands beyond 36 residues the protein is considered pathogenic and is often referred to as mutant HTT (mHTT). It is unclear how this expansion causes pathogenesis as the endogenous function of HTT has not been defined (Labbadia and Morimoto, 2013). However, increases in polyglutamine tracts (and the accompanying trinucleotide expansion) are a common feature of a group of diseases known as polyglutamine (polyQ) diseases and include several forms of spinocerebellar ataxia (Shao and Diamond, 2007).

It is proposed that such proteins become pathogenic after enzymatic cleavage generates a protein fragment which becomes misfolded due to the disruption caused by the expanded polyQ tract. These misfolded peptides may exert toxicity as a monomer or may oligomerise to form micro-aggregates. Toxicity may result from transcriptional alteration, metabolic dysfunction, proteolytic impairment and stress response abnormalities (Ross, 2002). Ultimately polyQ proteins may form larger

aggregated species and ultimately inclusions; these are thought to exert a protective influence by reducing the levels of misfolded peptide and micro-aggregates (Arresate et al., 2004). mHTT exerts a number of these effects, including transcriptional repression of brain-derived neurotrophic factor (BDNF) through a lack of cytoplasmic interaction with RE1-silencing transcription factor (REST) (Zuccato et al., 2003; Schiffer et al., 2014),

4.1.4. – Huntingtin and the endolysosomal system

A recent study has shown that HTT positively modulates selective autophagy by acting as a scaffold by facilitating the binding of p62 (a key protein in this pathway) and the autophagosome component LC3, to promote substrate recognition and autophagy regulation (Rui., 2015). Loss of this function as a result of polyQ expansion in mHTT may explain the autophagy defects observed in Huntington's particularly the observation of 'empty autophagosomes' suggestive of a failure in sequestration of substrates (Martinez-Vicente et al., 2010). The requirement of autophagy for the degradation of aggregated proteins and the fact that mHTT can inhibit this process results in a 'Catch 22' situation within neurons that are situated at the crossroads between the autophagic process and apoptosis. Accordingly, the presence of reduced autophagic function in Huntington's has been extensively researched as aggregation prone proteins such as HTT are preferentially degraded by this process (Sarkar et al., 2008). As the lysosome is the terminus of the autophagic system, dysfunction in this organelle could also contribute to reduced autophagic flux.

Increased endolysosomal volume has been observed in iPS derived neurons from Huntington's disease mouse models and iPS derived neurons from homozygous and heterozygous Huntington's patients (Castiglioni et al., 2012; Camniaso et al., 2012). In these cells alterations in genes encoding lysosomal proteins were shown to be dependent upon the polyQ repeat length of mHTT and result in an increase in vesicles positive for the acidotrophic dye lysotracker, a commonly utilised method for examination of endolysosomal expansion. In this study the authors concluded that increased lysosomal activity was present in these cell lines and this was the reason for increased endolysosomal volume (Castiglioni et al., 2012) as opposed to substrate storage which is the reason for an expanded endolysosomal system in LSDs (Platt et al.,2012). Lysosomes have also been reported to become increasingly

concentrated in the perinuclear regions of fibroblasts from Huntington's patients (Erie et al., 2015).

Further studies have also suggested that HTT and interacting proteins are capable of stimulating the endolysosomal system. Huntingin interacting protein 1 (HIP1) is a protein which is known to be involved in the assembly of endocytic protein complexes (Metzler et al., 2001). It interacts with the N-terminus of HTT and this process is disrupted in mHTT (Hackam et al., 2000). Changes in the expression of HIP1 and modulation of its ability to interact with binding partners can result in varied changes to endocytosis including the formation of expanded perinuclear vesicles which contain HTT alongside proteins such as clathrin. (Waelter et al., 2001). Accordingly HIP1 is an important protein to consider when looking at changes to endocytosis in Huntington's.

There have also been reports of elevated levels of a number of lipids which can accumulate in lysosomes in the brains of Huntington's animal models and a variety of cell lines with expanded polyQ repeats in HTT. Cholesterol accumulation has been observed in striatal neurons from the HD72 mouse model of Huntington's, both *In vitro* and *In vivo* (Trushina et al., 2006). In both experimental models the cholesterol accumulation was age related increasing with the time in culture for primary striatal neurons extracted from this mouse model and the age of mice for the accumulation of this lipid within the brain. Interestingly cells from this mouse model also exhibited defects in the internalisation and subsequent transport of the fluorescently tagged sphingolipid BODIPY-lactosylceramide (BOD-LacCer) (Trushina et al., 2006). This internalisation and transport occurs along the same Caveolin-1 dependent pathway as CtxB bound to ganglioside GM1 (Singh et al., 2007). This caveolin-1 dependent pathway was found to be required for mHTT dependent cholesterol accumulation (Trushina et al., 2006). Despite these initial data there is some debate about the levels of cholesterol in animal and cell models of Huntington's. There are numerous reports of polyQ length dependent defects in cholesterol biosynthesis in rodent models of Huntington's with total cholesterol levels reduced in a number of such models Valenza et al., 2005; Valenza et al., 2007; Marullo et al., 2012). Nevertheless, there have been other reports where although levels of precursors were affected total levels of brain cholesterol did not change (Valenza et al., 2007a) other groups have reported polyQ length dependent increases in cholesterol in different rodent models (Trushina et al., 2014) and it has been reported that down-regulation of cholesterol biosynthetic genes in *D.melanogaster* and *C.elegans*

models of Huntington's is beneficial (Luthi-Carter et al., 2009). The sheer number of different animal models of Huntington's make it difficult to draw any sure conclusions from such data.

Further studies have shown increases of cholesterol evident as punctae in cell lines and neurons expressing expanded mHTT alongside increased cholesterol levels in post-mortem brain samples from the caudate of Huntington's patients (del Toro et al., 2010). Recently another study reported increased levels of cholesterol in the caudate alongside changes in cholesterol precursors (Kreilaus et al., 2015) Accumulation of ganglioside GM1 was also observed in mHTT expressing neurons in the study of del Toro *et al.* (2010).

Conversely, in other studies, the levels of ganglioside GM1 have been shown to be reduced in Huntington's mouse models (Maglione et al., 2010; Di Pardo et al., 2012). As the total levels of ganglioside are to some extent governed by lipid catabolism and recycling in the endolysosomal system (Schulze and Sandhoff, 2010) defects in these compartments may impact upon this phenotype, particularly the plasma membrane availability of this lipid. A recent publication has detailed striatal lipid accumulation in a mouse model of Huntington's carrying Q111 mHTT. In this brain region sphingomyelin, phosphatidylcholine, cholesterol esters and triglyceride species all accumulated and similar results were observed in cellular models with the same mHTT (Carroll et al., 2015).

These data all suggest that a thorough examination of lysosomal phenotypes is warranted in models of HD with a particular emphasis on storage and trafficking manifestations which have been observed in LSDs to see if these processes could be contributing to the expansion of the endolysosomal system in the presence of HTT with expanded polyQ repeats.

As a variety of lysosomal dysfunction has been reported in cell and animal models of Huntington's we were interested to apply the assays performed in the lab to cellular models of this disease in order to assess whether lysosomal dysfunction was prevalent in a wide array of cells with an expanded polyQ repeat in huntingtin (mHTT) and, if observed, was it reminiscent of any of the phenotypes observed in cells with known causes of lysosomal dysfunction.

4.2. – Procedures

In section 4.3.1. we will investigate iPSC derived neural stem cells generated from a juvenile Huntington's patient cell line with a polyQ repeat length of 180, these cells are described in section 2.1.4.. Firstly, we will investigate these cell for lysosomal expansion using LAMP2 as a marker before subsequent investigations into what may cause this. As lipids are stored in a variety of LSDs we will utilise cell biology to examine these.

In order to try and see if lysosomal phenotypes are present in multiple Huntington's models we will also examine these phenotypes in ST14A cells (section 4.3.2.). These cell are described in 2.1.5. As these cells are more easily grown in larger numbers they will also be examined by TLC. In addition we will examine another cellular model of Huntington's disease in which polyQ HTT is inducibly expressed in PC12 cells (section 2.1.6) to supplement the data obtained.

In both of the NSC and ST14A cells discussed above we will also look at lysosomal proteins which may be dysfunctional in order to try and identify the mechanism of lysosomal dysfunction. Subsequently, we will study if the ST14A cells have specific lysosomal dysfunction such as sphingosine trafficking and lysosomal Ca^{2+} homeostasis defects in order to verify this mechanism. The final cell model which we will utilise in this study are iPSC derived mature striatal medium spiny neurons (section 4.3.3.) with a range of PolyQ repeats. These will be subject to the maximum number of analyses possible.

As we are interested in finding new therapeutic targets for neurodegenerative disease we will apply therapies known to be of benefit to LSDs to our models of Huntington's disease. Initially, we will preform a preliminary analysis of whether these can reduce the lysosomal phenotypes observed in ST14A cells (section 4.3.4.). If we observe benefit we will apply these therapeutics to a functional assay of neuronal Ca^{2+} homeostasis in response to glutamate excitotoxicity. This is a well defined assay which will demonstrate if we have been able to cause a functional benefit to neuronal models of Huntington's disease.

Where possible 3 or more independent plating replicates will be used in these experiments and appropriate statistical analysis will be performed as detailed in

individual figure legends. In instances where 3 independent plating replicates were not performed due to unavailability of cells this will be shown in the figure legend. This has not been possible for all cell lines due to the technical difficulties of preparing these cell lines and their availability, this has impacted most upon the studies described in section 4.3.1. and 4.3.3.

Statistical analyses as described in section 2.7 have been performed on all these experiments as appropriate, details of these are given in individual figure legends.

4.3. – Results

4.3.1. – Preliminary Evidence of Specific Lysosomal Dysfunction in iPSC neuronal stem cells from Huntington's Disease Patients

In order to initially analyse if the reported lysosomal dysfunction was prevalent in cells which express mHTT we utilised a line of iPSC derived neuronal stem cells (NSCs, often referred to as neuronal precursor cells (NPCs) but referred to by the alternative name NSCs for clarity) which have 180 glutamine residues in their polyQ repeat (HD iPSC consortium study., 2012). Although this is an extreme expansion in polyQ repeats compared to the average for Huntington's patients (Warby et al., 1998) it was ideal for initial experiments to see if we could observe robust differences. Firstly we looked for instances of endolysosomal expansion in these cells.

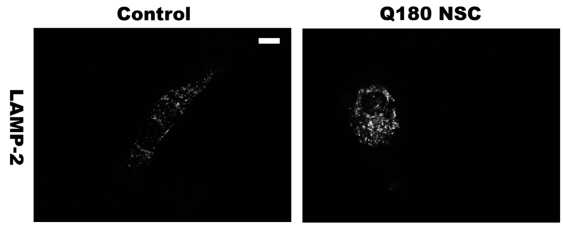

Figure 4.3.1. – Lysosomal markers in iPS derived neural stem cells. *NSCs from a control and a juvenile Huntington's Patient (Q180). Representative immunofluorescence images of the lysosomal marker Lysosomal-Associated Membrane Protein 2 (LAMP-2, white) shows changes in lysosome and late-endosome number, size and localisation within cells. n = 1. Scale bar = 10μm. Data collected with assistance from Naomi Killick, Cardiff University.*

In preliminary experiments expansion of the lysosomal system was observed in the endolysosomal system of Q180 NSCs when the levels of the lysosomal and late-endosomal protein LAMP-2 were analysed in cells. It is also interesting to note that the recently reported phenotype of perinuclear lysosomal clustering was evident in these cells (Erie et al., 2015). As we were able to observe lysosomal expansion we were interested to see if we could characterise storage substrates which may be responsible for this expansion. Due to multiple reports of lipid accumulation in models of Huntington's (Trushina et al., 2006; del Toro et a., 2010; Carroll et al., 2015) and the prevalence of lipid storage in the LSDs in general we began by probing cells with the various lipid probes commonly employed in our studies.

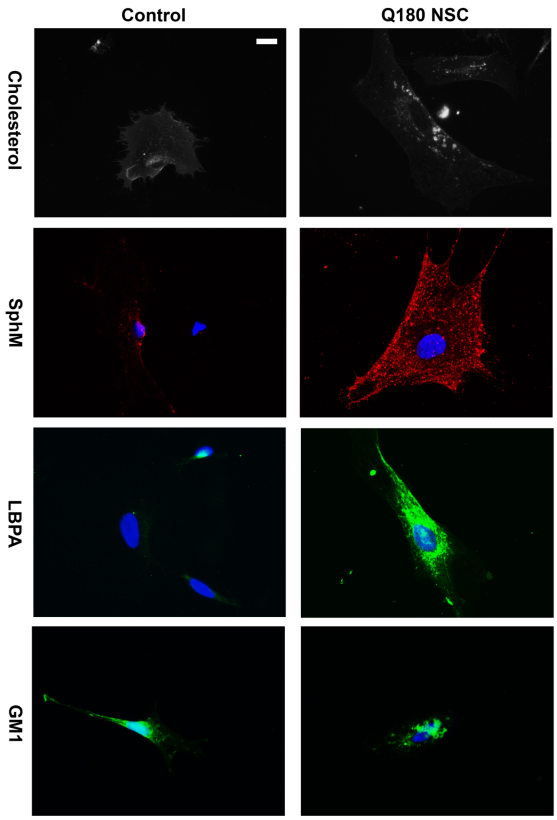

Figure 4.3.2. – Lipid storage phenotypes in iPS derived neural stem cells. *NSCs from a control and a juvenile Huntington's Patient (Q180). Representative fluorescence microscopy of filipin stained cells (white) show endo-lysosomal cholesterol accumulation and lysenin stained cells (SphM, red) show increases in sphingomyelin levels. Representative immunofluorescence images of lysobisphosphatidic acid (LBPA, green) show increased levels of this lyso-phospholipid. FITC-tagged cholera toxin B subunit is used to visualise the redistribution of ganglioside GM1 (green) within Q180 cells. Hoechst stained nuclei are shown in blue in the Lysenin, LBPA and CtxB images. n = 1 - 2. Scale bar = 10μm. Data prepared with assistance from Naomi Killick, Cardiff University.*

As shown in figure 4.3.2. a number of lipids were observed to be increased in Q180 NSCs. Firstly, in line with multiple reports in the literature we observed cholesterol elevation. This was particularly evident as punctae in the perinuclear regions of cells in which the expanded endolysosomal system was situated suggestive of endolysosomal cholesterol accumulation. This punctate accumulation was accompanied by less evident plasma membrane staining of cells which may be evidence of a defect in recycling this lipid. We next looked at sphingomyelin levels in cells and observed clear elevations in this lipid, although the distribution of this was throughout the cells as opposed to in clustered punctae. Interestingly, we have observed this in LSDs where sphingomyelin accumulates in the lysosome so does not exclude lysosomal storage (Halsett et al., Unpublished). This lipid has also been reported to accumulate in the brains of Huntington's mouse models (Carroll et al., 2015). LBPA levels are also elevated throughout the cell, as has been observed in models of NPC (Chevallier et al., 2008). The accumulation of this lipid is also in the perinuclear region of cells. Finally we can see relatively constant levels of the ganglioside GM1 accompanied by a redistribution from plasma membranes to a distinct perinuclear punctate localisation, further indications of lysosomal lipid accumulation alongside defective recycling of lipids.

As recycling of ganglioside GM1 appeared to be dysfunctional in these cells we were interested to use the well characterised CtxB trafficking assay as a means of determining whether this was due to an endolysosomal trafficking defects in cells with mHTT.

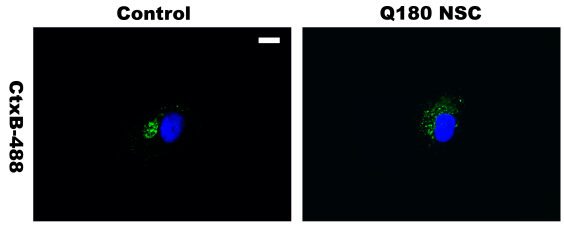

Figure 4.3.3. – Endolysosomal sphingolipid trafficking in iPS derived neural stem cells. *NSCs from a control and a juvenile Huntington's Patient (Q180). Representative fluorescence microscopy images of pulse-chased FITC-tagged Cholera toxin B-subunit (CtxB-488, green) to assay trafficking of ganglioside GM1 through the endolysosomal system. Hoechst stained nuclei are shown in blue. n = 1. Scale bar = 10μm. Data collected with assistance from Naomi Killick, Cardiff University.*

In initial analyses we observed a clear trafficking defect of CtxB-bound GM1 to the Golgi in Q180 NSCs represented by increased presence of punctae in these cells as opposed to a clear Golgi localisation in control cells. This phenotype has been previously reported in primary neurons from the HD72 mouse model (Trushina et al., 2006).

The presence of lysosomal lipid storage and endolysosomal trafficking defects in these cells suggests lysosomal disease phenotypes may be present. Accordingly we began to investigate more specific phenotypes previously observed in LSD cells. An example of such a phenotype is ER expansion (Wang et al., 2011) which can be observed by immunohistochemistry against the ER protein SERCA2.

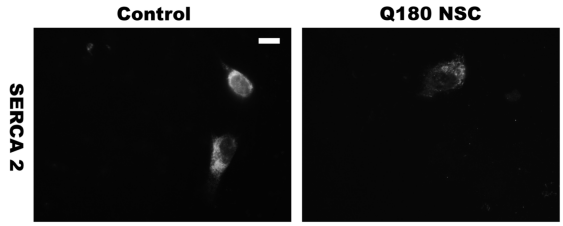

Figure 4.3.4. – Endoplasmic reticulum structure in iPS derived neural stem cells*. NSCs from a control and a juvenile Huntington's Patient (Q180). Representative immunofluorescence images of Sarcoplasmic/Endoplasmic Reticulum Ca^{2+} ATPase isoform 2 (SERCA2, white) is used as a marker to examine endoplasmic reticulum morphology. n = 1. Scale bar = 10μm. Data collected with assistance from Naomi Killick, Cardiff University.*

No expansion of the ER was evident after preliminary examination of the ER marker SERCA2. Although it was observed that levels of SERCA2 were reduced, which may be evidence of other changes in the ER of these cells. This remains to be further investigated in Huntington's cell lines utilising other markers of the ER, and western blotting for accurate levels of protein expression. Interestingly, reduced SERCA2 in peripheral B-cells has also been suggested as a disease biomarker (Cesca et al., 2015).

The array of cellular phenotypes which have been observed so far alongside reports of cholesterol and sphingomyelin dyshomeostasis and sphingolipid mistrafficking in other cellular models of Huntington's we were interested to see if the distribution or levels of the NPC1 protein was affected in Q180 NSCs.

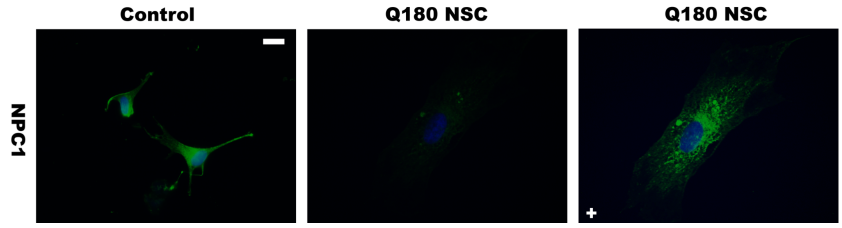

Figure 4.3.5. – Levels of the NPC1 protein in iPS derived neural stem cells. *NSCs from a control and a juvenile Huntington's Patient (Q180). Representative immunofluorescence images of Niemann-Pick type C1 protein (NPC1, green) show the distribution of this late-endosomal and lysosomal transmembrane protein within cells. Q180 panel marked + has had the brightness enhanced to allow visualisation of NPC1 distribution. Hoechst stained nuclei are shown in blue. n = 1. Scale bar = 10μm. Data collected with assistance from Naomi Killick, Cardiff University.*

As seen in figure 4.2.5. there is preliminary evidence of a reduction in NPC1 protein levels in Q180 cells. Interestingly, when the images had their brightness increased, in order to observe the localisation of NPC1 (image marked with +), large aggregates were observed rather than fine diffuse staining. This phenotype has been observed before in cells which have had an NPC1 phenotype induced (Lloyd-Evans., Unpublished); as such it is indicative of NPC1 dysfunction in these cells. These observations are being further studied by western blotting.

Taken together these preliminary data are suggestive of endolysosomal system expansion linked to dysfunction of the NPC1 protein. In addition to the fact that these datasets were only preliminary, this cell line was also relatively novel with respect to the study of Huntington's; accordingly we were keen to see if these phenotypes were replicated in other more thoroughly researched models of the disease.

4.3.2. – Confirmation of lysosomal phenotypes in rat striatal neuronal precursor cells overexpressing HTT

One cell line which has been extensively used for such analysis is the ST14A *R.novegicus* neuronal precursor cell line which overexpresses a fragment corresponding to amino acids 1-548 of huntingtin with 120 polyQ repeats (HTT Q120 ST14A) (Ehrlich et al., 2001; Valenza et al., 2005; Maglione et al., 2010). As such, these were subjected to the same cell analyses described in 4.3.1.

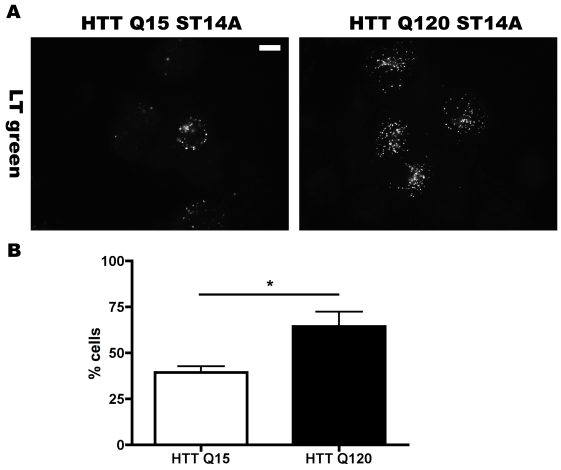

Figure 4.3.6. – Lysosomal markers in ST14A cells expressing mHTT. *ST14A cells expressing fragment 1-548 of the human huntingtin protein with different polyQ repeat lengths.* ***A*** *– Representative immunofluorescence images of lysotracker green loaded cells (LT green, white) shows changes in lysosome and late-endosome number, size and localisation within cells.* ***B*** *– Threshold analysis of LT green fluorescence. n = 3. * = P < 0.05 by T-test. Scale bar = 10μm.*

Q120 expressing ST14A cells showed a significant increase ($P < 0.05$, $t = 2.910$, $df = 4$, $F_{2,2} = 6.068$) in lysotracker fluorescence indicative of expansion in the endolysosomal system of these cells. This was expected from the prevalence of this phenotype in a variety of cell lines (Castiglioni et al., 2012; Camnasio et al., 2012; Erie et al., 2015). Increased perinuclear clustering of lysosomes was not as obvious in the cells, although this may be due to comparison between the lysosomal populations in different parts of the cell being difficult due to divergent fluorescence levels. Unfortunately, the same analyses of LAMP-2 by immunohistochemistry (4.3.1.) cannot be conducted in these cells as antibodies against LAMP proteins are highly species specific and those raised against mouse and human LAMP proteins do not bind to the proteins present in ST14A cells. Nevertheless, the general increase in endolysosomal compartment size remains a robust phenotype that can be analysed quantitatively by threshold counting.

Due to the increased size of the endolysosomal store we would like to see if the lipid storage phenotypes observed in NSCs were replicated in these cells.

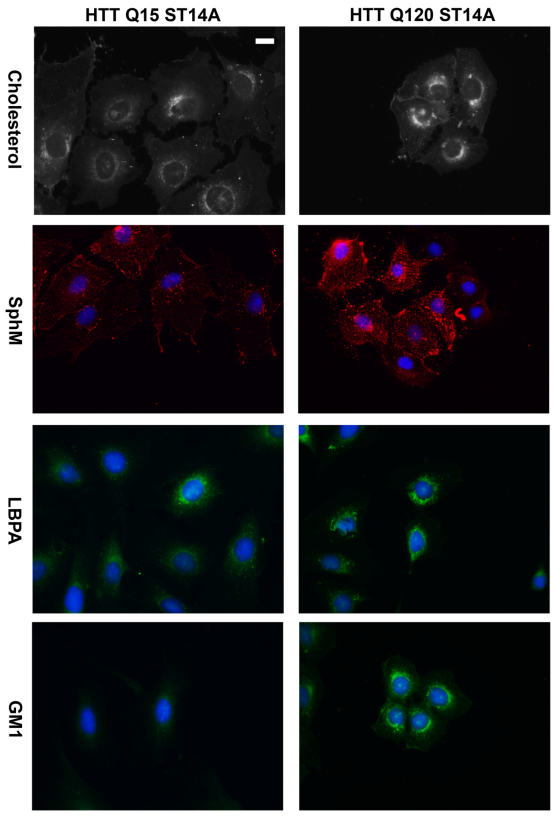

Figure 4.3.7. – Lipid storage phenotypes in ST14A cells. *ST14A cells expressing fragment 1-548 of the human huntingtin protein with different polyQ repeat lengths. Representative fluorescence microscopy images of filipin stained cells (white) show endo-lysosomal cholesterol accumulation and lysenin stained cells (red, SphM) show increases in sphingomyelin levels. Representative immunofluorescence images of lysobisphosphatidic acid (LBPA, green) show increased levels and altered localization of this lyso-phospholipid . FITC-tagged cholera toxin B subunit (CtxB, green) is used to visualise the increase of ganglioside GM1 within cells. Hoechst stained nuclei are shown in blue in the Lysenin, LBPA and CtxB images. n = 3 for cholesterol, LBPA and GM1, n = 1 for SphM. Scale bar = 10μm.*

As can be seen in figure 4.3.7. lipid accumulation is observed in Q120 ST14A cells with a broadly similar pattern to the lipid phenotypes previously demonstrated (figure 4.3.2.). These lipid accumulations seem to be less severe than the lipid differences between control and Q180 NSCs which may be due to less difference between the severity of the cell lines; Q180 is an extremely high repeat length for a Huntington's patient (Warby et al., 1998), whereas, much higher repeat lengths are used to generate phenotypes in rodent models of Huntington's compared to those which cause human disease (Zuccato et al., 2010; Carroll et al., 2015). The least elevated lipid appears to be cholesterol although this may be explained by differential levels of cholesterol synthesis reported in Huntington's cell and mouse models (Valenza et al., 2005; Valenza et al., 2007; Marullo et al., 2012). Accordingly, cholesterol phenotypes are currently under detailed investigation (Clark *et al.*). Nevertheless, there is still a defined accumulation of cholesterol in small punctae in the perinuclear region of cells expressing Q120 HTT suggesting a milder cholesterol accumulation than that previously observed may be taking place. Sphingomyelin is, similarly, elevated to a

lesser degree than in Q180 NSCs although it is clearly elevated throughout the cell. LBPA and ganglioside GM1 both increase in Q120 ST14A cells and are redistributed to the perinuclear regions of the cell, suggestive of lysosomal lipid accumulation. As this is conserved across human and rat cell lines it is strongly suggestive of a lipid storage phenotype in cells with expanded polyQ repeats.

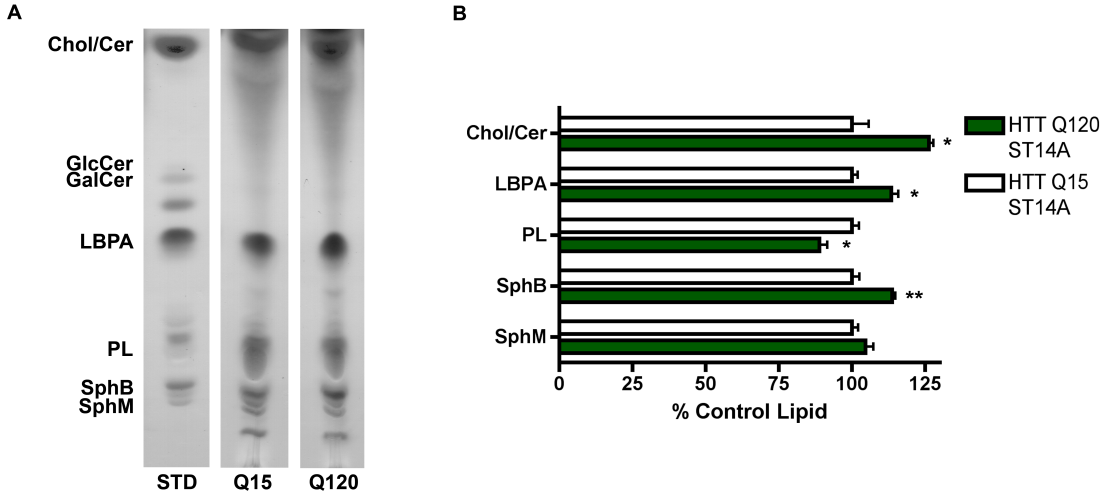

Figure 4.3.8. – Biochemical analysis of lipid levels in ST14A cells. *ST14A cells expressing fragment 1-548 of the human huntingtin protein with different polyQ repeat lengths.* ***A –*** *Representative images of thin-layer chromatography analysis of various lipids in Q15 and Q120 ST14A cells ran alongside identified lipid standards (STD). Chol/Cer = combined levels of cholesterol and ceramide, GlcCer = glucosylceramide, GalCer = galactosylceramide, LBPA = lysobisphosphatidic acid, PL = phospholipids, SphB = sphingoid bases and SphM = sphingomyelin.* ***B –*** *Densiometric quantification of lipid levels in Q120 ST14A cells as a percentage of the lipid levels in Q15 ST14A cells. Lipid species are labelled as in A. Error bars = SD. n = 2 - 3. * = P < 0.05, ** = P < 0.01 calculated by T test.*

As it was possible to culture greater numbers of ST14A cell lines than the NSCs previously examined it was possible to perform a preliminary analysis of lipid levels in Q120 cells by biochemical analysis using thin-layer chromatography. Cholesterol was elevated by around 25% ($P < 0.05$, $t = 4.422$ $df = 2$, $F1,1 = 12.69$, in this analysis the cholesterol bands for 1 repeat from each cell line were removed due to uneven spray distribution). No significant change was observed in sphingomyelin levels but LBPA levels were significantly increased ($P < 0.05$, $t = 4.210$, $df = 3$, $F_{1,2} = 1.080$, a LBPA band frm the Q15 cells was removed from this analysis due to uneven spraying). We were also able to demonstrate increases in sphingoid bases ($P < 0.01$, $t = 4,812$, $df=4$, $F_{2,2} = 5.263$) and a decrease in phospholipid levels ($P < 0.05$, $t = 3.038$, $df = 4$, $F_{2,2} = 1.217$). Interestingly, sphingoid bases would be expected to increase in cells in which the NPC1 protein was dysfunctional (Lloyd-Evans et al., 2008). Another lipid which would be expected to increase is GlcCer, however, lipid levels were not sufficiently high for accurate analysis by this method. No evidence of

increased phospholipids suggests that the pH of lysosomes is not affected by increased levels of mHTT. The levels of phospholipid were, in fact, slightly reduced ($P < 0.05$, $t = 3.038$, $df = 4$, $F_{2,2} = 1.217$). Due to some imperfections in the development of this plate this analysis will be repeated in future.

It was also possible to examine the lipidology of another widely used Huntington's disease cell line in order to further confirm the presence of lipid storage across various models of Huntington's. We were able to culture a PC12 cell line inducibly expressing full length human mHTT with a 145 amino acid polyQ expansion and compare these to a cell line expressing Q23 huntingtin.

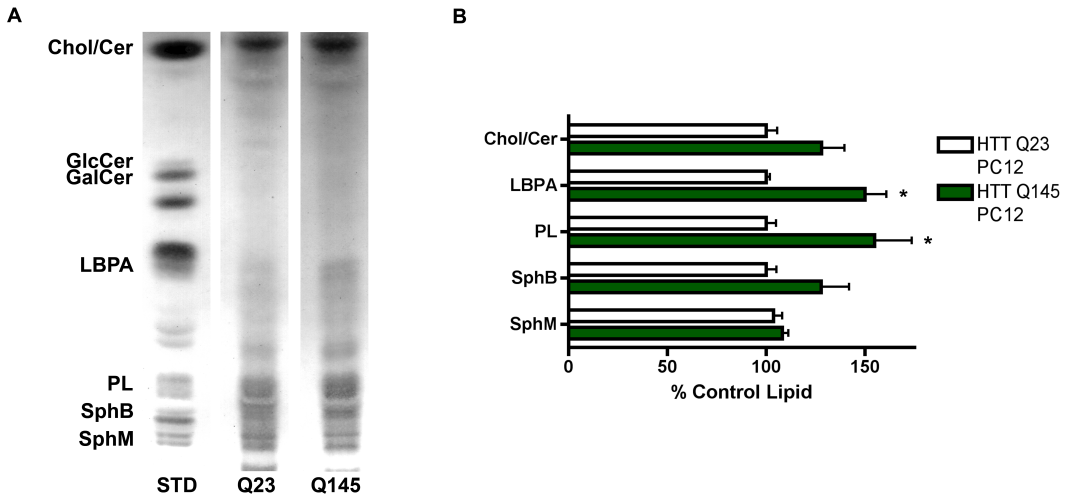

Figure 4.3.9. – Biochemical analysis of lipid levels in PC12 cells. *PC12 cells expressing full length human huntingtin protein with different polyQ repeat lengths.* ***A –*** *Representative images of thin-layer chromatography analysis of various lipids in Q23 and Q145 PC12 cells ran alongside identified lipid standards (STD). Chol/Cer = combined levels of cholesterol and ceramide, GlcCer = glucosylceramide, GalCer = galactosylceramide, LBPA = lysobisphosphatidic acid, PL = phospholipids, SphB = sphingoid bases and SphM = sphingomyelin.* ***B –*** *Densiometric quantification of lipid levels in Q145 PC12 cells as a percentage of the lipid levels in Q23 PC12 cells. Lipid species are labeled as in A. Error bars = SD. n = 3. * = P < 0.05 calculated by T test.*

In initial analysis of these cells a similar trend of increased cholesterol and sphingoid bases occurred. There was also significant elevation in LBPA ($P < 0.05$, $t = 4.488$, $df = 4$, $F_{2,2} = 33.87$), sphingomyelin was again not elevated. The TLC loaded at these protein levels did not provide visible bands of either GlcCer or GalCer so it was not possible to quantify these lipids. The levels of phospholipid were also observed to increase in these cells ($P < 0.05$, $t = 2.812$, $df = 4$, $F_{2,2} = 14.64$). While this may be suggestive of a phospholipidosis phenotype indicating lysosomal alkalisation we did not observe any of the other phenotypes observed in the study of PS deficient cells

in the different Huntington's cell lines examined. Accordingly, it may be a process specific to these cells causing elevations in phospholipid.

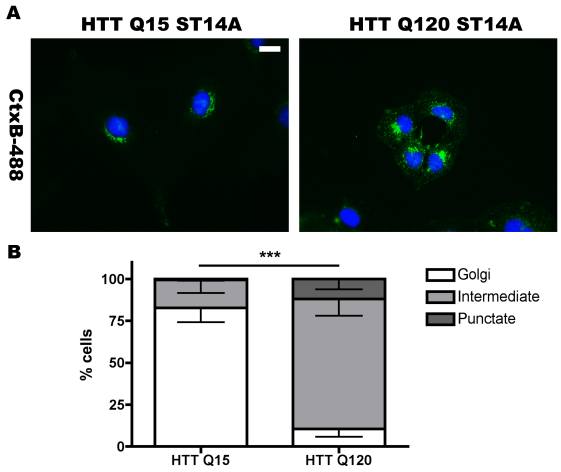

Figure 4.3.10. – Endolysosomal sphingolipid trafficking in ST14A cells. *ST14A cells expressing fragment 1-548 of the human huntingtin protein with different polyQ repeat lengths.* ***A*** *– Representative fluorescence microscopy images of pulse, chased FITC-tagged Cholera toxin B-subunit (CtxB-488, green) to assay trafficking of ganglioside GM1 through the endo-lysosomal system. Hoechst stained nuclei are shown in blue.* ***B –*** *Qualitative quantification of CtxB-488 localisation as Golgi, punctate or intermediate between the two states in ST14A cells as a percentage of the total cell population. Error bars = SD. n = 3. Scale bar = 10μm. *** = P < 0.001 calculated by X^2 test.*

As discussed in 4.3.7., the prevalence of perinuclear lipid accumulation is strongly indicative of endolysosomal lipid trafficking defects. These trafficking defects were robustly observed in ST14A cells expressing Q120 huntingtin when this process was investigated using the CtxB transport assay to study endolysosomal trafficking of ganglioside GM1, figure 4.3.10 ($P < 0.001$, $X^2 = 492.87$ for run 1, 430.51 for run 2 and 742.70 for run 3, df = 4). This analysis was performed by comparing the values obtained from the three HTT Q120 repeats of this experiment to expected values calculated from the mean of each population in HTT Q15 cells. As variation between the three repeats was minimal (SEM = < 6% in all populations) this approach was applicable.

A useful tool to examine the activity of the cathepsin enzymes B and L are *In situ* probes which localise to lysosomes and are specifically cleaved by these enzymes to yield a fluorescent product. As both these enzymes have been shown to be involved in the degradation of Huntingtin (Kim et al., 2006) we thought it would be interesting to see if any changes in their activity were observed in cells expressing mHTT.

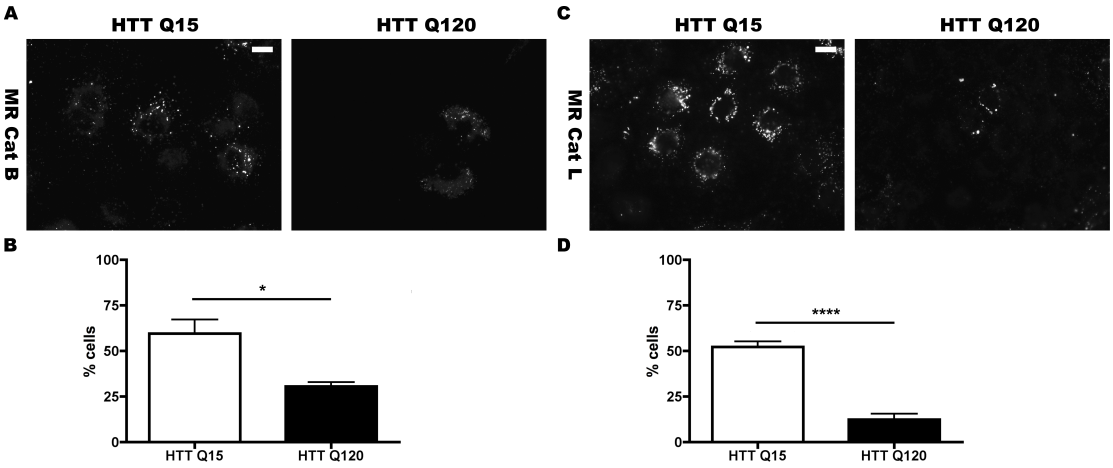

Figure 4.3.11. –Lysosomal proteolysis defects in ST14A cells. *ST14A cells expressing fragment 1-548 of the human huntingtin protein with different polyQ repeat lengths.* ***A*** *– Representative fluorescence microscopy images of cells loaded with the magic-red cathepsin B substrate (MR Cat B, white) shows the in situ activity of cathepsin B within cells.* ***B*** *– Threshold analysis of magic-red cathepsin B fluorescence. n = 4. * = P < 0.05 by T-test. .* ***C*** *– Representative fluorescence microscopy images of cells loaded with the magic-red cathepsin L substrate (MR Cat L, white) shows the in situ activity of cathepsin L within cells.* ***D*** *– Threshold analysis of magic-red cathepsin L fluorescence. n = 4. **** = P < 0.0001 calculated by unpaired T-test. Scale bar = 10μm.*

The activities of both Cathepsin B ($P < 0.05$, $t = 3.614$, $df = 6$, $F_{3,3} = 9.714$) and Cathepsin L ($P < 0.0001$, $t = 9.202$, $df = 6$, $F_{3,3} = 1.151$) were significantly reduced in Q120 ST14A cells although the degree of reduction in Cathepsin L activity was greater. As these enzymes are known to interact with HTT (Kim et al., 2006), which was overexpressed in the pathogenic cell line, this is to be expected as the protein and fluorescent substrate may act as competitive inhibitors of each other. The fact that Cathepsin L activity is more obviously reduced in these cells is supportive of this enzyme being more critical for this process than Cathepsin B (Bhutani *et al.,* 2012). Of course, the activities of these enzymes could also be an indication of lysosomal alkalisation reducing their activity due to divergence from their acid pH optima. This is however unlikely, as the lipid changes and other phenotypes observed are not similar to those observed in PS deficient cells where lysosomal alkalisation has been confirmed (Coffey et al., 2014; Lee et al., 2015).

As the accumulation of autofluorescent material termed lipofuscin is a lysosomal storage phenotype which is observed in cells with lysosomal alkalisation and loss of Cathepsin activity (although it can be caused by other lysosomal dysfunction), cells were subsequently investigated for increased levels of autofluorescence after visible excitation at 470 nm.

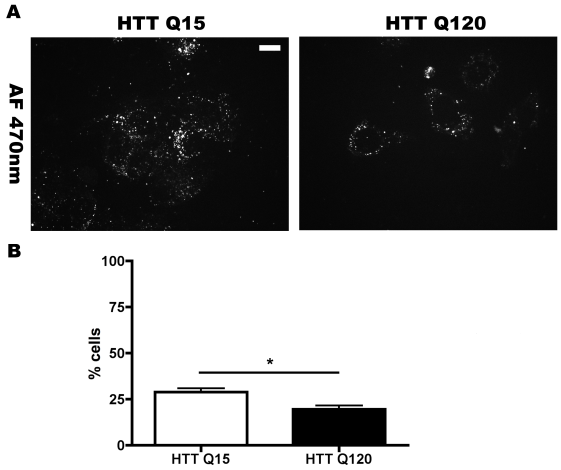

Figure 4.3.12. – Autofluorescent material in ST14A cells. *ST14A cells expressing fragment 1-548 of the human huntingtin protein with different polyQ repeat lengths.* ***A*** *– Representative fluorescence microscopy images of unstained cells at 470nm excitation wavelength (AF 470nm, white) shows the distribution of any autofluorescent pigment within cells.* ***B*** *– Threshold analysis of autofluorescence at 470nm excitation wavelength. n = 4. * = P < 0.05 by T test. Scale bar = 10μm.*

Autofluorescence was, in fact, slightly reduced in Q120 mHTT cells ($P < 0.05$, $t = 3.191$, $df = 6$, $F_{3,3} = 1.020$, 4.3.12.) although it was difficult to observe any autofluorescence in either cell line. This further confirms that lysosomal alkalisation was not present in these cells. Lysosomal alkalisation and subsequent autofluorescence are not phenotypes associated with NPC1 dysfunction (Lloyd-Evans et al., 2008; Waller-Evans., manuscript in preparation) so this further suggests that lysosomal storage phenotypes in these cells may be due to dysfunction in NPC1. In order to confirm that no changes in lysosomal pH are present in these cell lysosensor yellow/blue dextran could be used (Wolfe *et al.,* 2013) although in the absence of any evidence of lysosomal alkalisation this does not seem necessary.

In the NSCs we also examined the ER for expansion, as this is specifically associated with some lipidoses but not NPC1 disease. The slight reductions observed by SERCA2 immunohistochemistry may also be present in Q120 ST14A cells in initial experiments (data not shown) and we further examined these cells using ER tracker blue white which is a specific fluorescent marker for the ER.

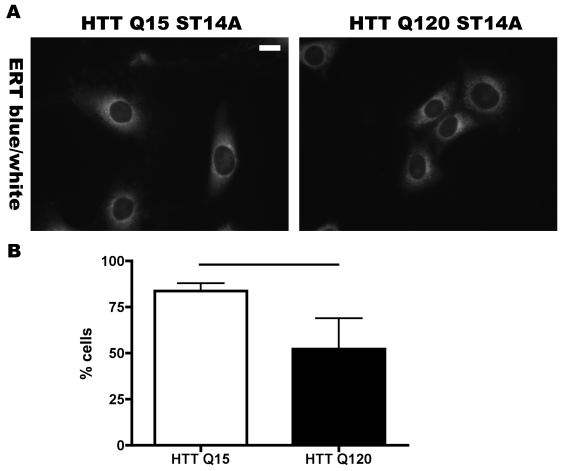

Figure 4.3.13. – Endoplasmic reticulum structure in ST14A cells. *ST14A cells expressing fragment 1-548 of the human huntingtin protein with different polyQ repeat lengths.* ***A*** *– Representative fluorescence images of ER tracker blue/white loaded (ERT b/w), white) is used as a marker to examine endoplasmic reticulum morphology and density.* ***B*** *– Threshold analysis of ER tracker blue/white fluorescence. n = 4. No significant difference observed by T test. Scale bar = 10μm.*

Figure 4.3.13. suggests a trend towards a minor reduction in ER density, as Q120 cells had lower levels of fluorescence indicative of reduced ER size. Interestingly, this reduction in fluorescence was not significantly different due to highly evident variability in the ER of Q120 HTT cells. ER tracker variability has been observed before in cells known to be undergoing ER stress and is supported by preliminary observations of increased extra-Golgi localised transmembrane emp24 protein domain containing (TMED4) which is a protein marker of ER stress (data not shown) (Walker et al., Unpublished).

The combined finding of figures 4.3.6. – 4.3.13. alongside the phenotypes observed in Q180 NSCs are suggestive of NPC1 protein dysfunction in cells which express mHTT. Accordingly we decided to examine the levels of this protein alongside the protein active in the same pathway and a cause of comparable cellular lysosomal storage phenotypes Niemann-Pick type C2 (NPC2) (Iouannou, 2005).

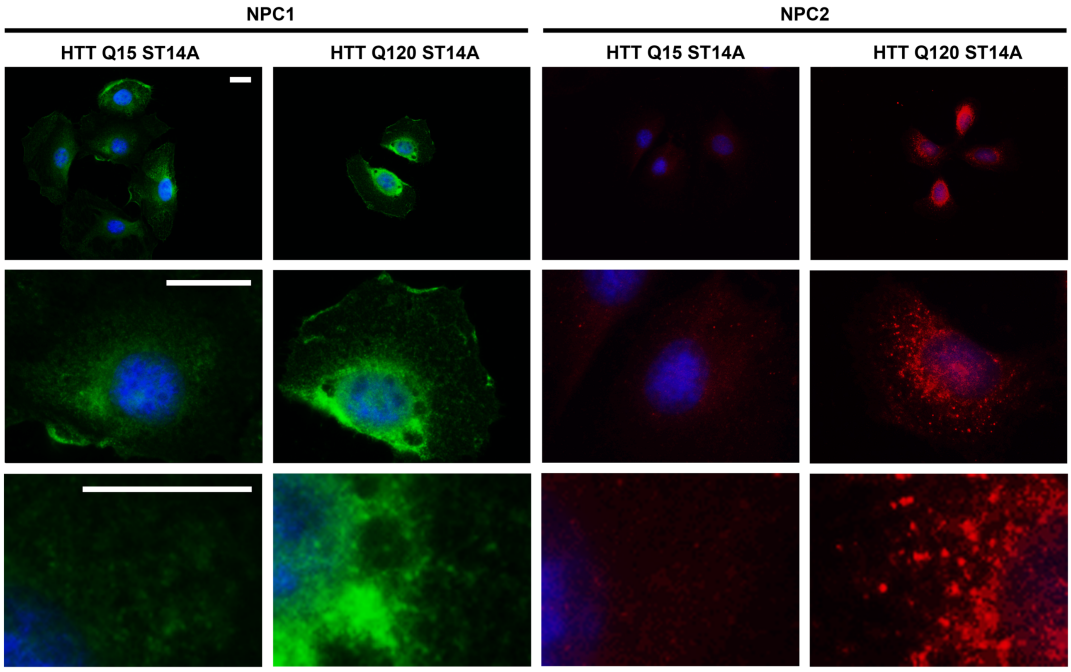

Figure 4.3.14. – Localisation of NPC proteins in ST14A cells. *ST14A cells expressing fragment 1-548 of the human huntingtin protein with different polyQ repeat lengths. Representative immunofluorescence images of Niemann-Pick type C1 protein (NPC1, green) show the distribution of this late-endosomal and lysosomal transmembrane protein within cells. Representative immunofluorescence images of Niemann-Pick type C2 protein (NPC2, red) show the distribution of this soluble lysosomal protein within cells. Hoechst stained nuclei are shown in blue. n = 4. Scale bar = 10μm for the upper two images and 5μm for the lower images.*

In contrast to the reduced levels of protein observed in Q180 cells we observed increases in NPC1 in Q120 ST14A cells. It was however, similarly mislocalised with dense perinuclear accumulation of the protein, as opposed to fine punctate staining expanding throughout the cell (figure 4.3.14.). Interestingly, NPC1 was also excluded from large areas of the cell when expanded polyQ huntingtin was present. Although the compartments within the cell which NPC1 becomes localised to are yet to be defined it is clearly not in the same location as in healthy cells and this could potentially be the underlying cause of the specific lysosomal dysfunction observed in cellular models of Huntington's.

There also appears to be an increase in NPC2 in Q120 cells (figure 4.3.14.) and the increasingly obvious punctae observed may be the result of cells attempting to compensate for reduced levels of NPC1 in the lysosome, as both proteins interact in a non-redundant functional co-operativity (Sleat et al., 2004). These data are being confirmed by western blotting (Clark et al.).

If NPC1 is not functioning correctly in these cells then a phenotype we would expect to see in these cells is reduced lysosomal Ca^{2+}, as this has been observed in all cells deficient in NPC1 and in cell lines in which NPC1 has been inactivated (Lloyd-Evans et al., 2008).

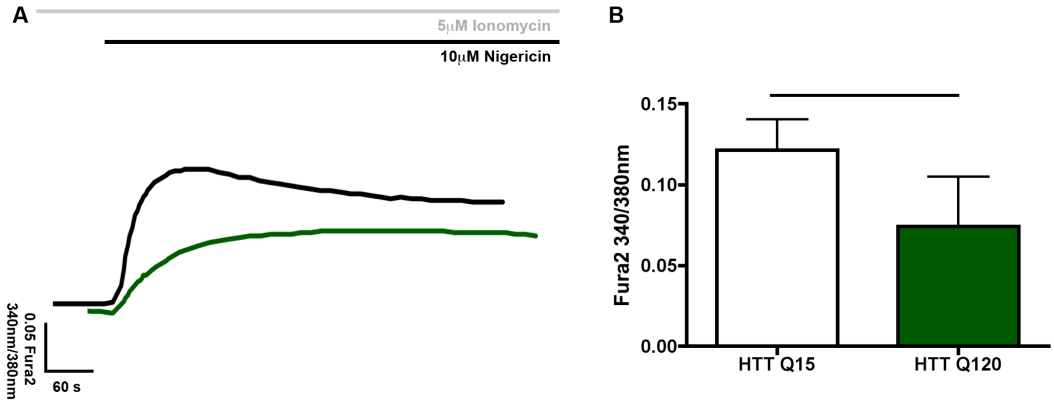

Figure 4.3.15. – Lysosomal Ca^{2+} release induced by nigericin in ST14A cells. *ST14A cells expressing fragment 1-548 of the human huntingtin protein with 120 polyQ repeats after nigericin induced lysosomal Ca^{2+} release in the presence of 5μM ionomycin.* ***A -*** *Representative traces of Ca^{2+} release in Fura2 loaded cells induced by 10μM nigericin. Grey bar indicates the presence of ionomycin, black bar indicates the presence of nigericin. U18666a treated WT cells are used as a positive control for depletion of lysosomal Ca^{2+}.* ***B –*** *Quantification of Ca^{2+} release measured by ratiometric change in Fura2 fluorescence. Error bars = SEM. n = 3. No significance calculated by T test.*

Figure 4.3.15. shows a trend towards reduced lysosomal Ca^{2+} release of around 40% in Q120 ST14A cells when it is induced by Nigericin after pre-treatment of cells with ionomycin to remove all other cellular Ca^{2+} stores. This remains to be confirmed by subsequent repeats. Importantly preliminary experiments and published data both show that ER Ca^{2+} content is changed in cellular models of Huntington's, as expected from reports in the literature (Suzuki et al., 2012), and as such in order to accurately determine levels of lysosomal Ca^{2+} the other cellular stores must be prevented from signalling first; accordingly pre-treatment with ionomycin is vital in this experiment.

Another assay which is useful for determining if cells have defective NPC1 function is the trafficking of FITC-tagged sphingosine (FITC-SphO) which can be loaded into cells and the location of fluorescence checked after various incubation times. FITC-SphO loaded cells were examined after 10 minutes of incubation and these clearly show that in both cell lines the probe initially localises to the lysosome where it requires an active transport process to exit. This process does not occur in cells which do not have active NPC1 protein and punctate distribution of FITC-SphO persists (Lloyd-Evans et al., Unpublished).

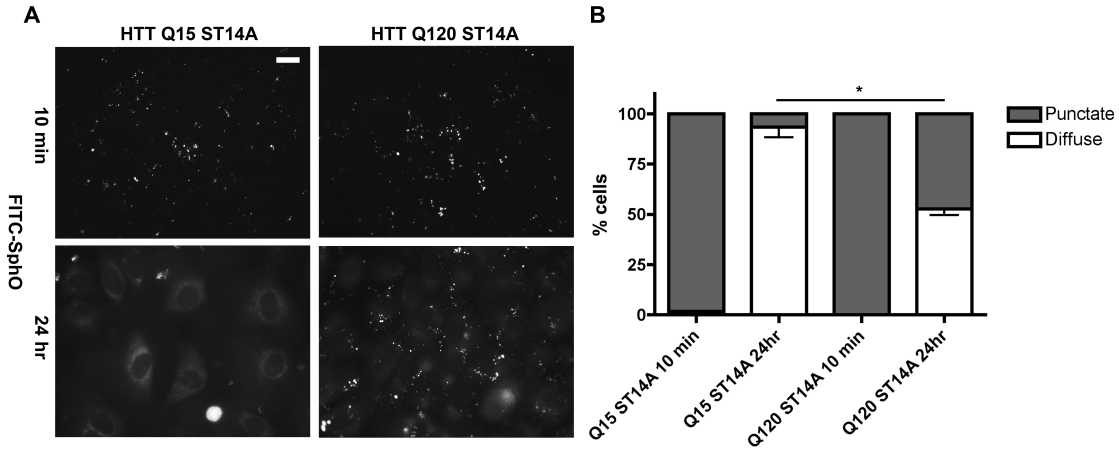

Figure 4.3.16. – Altered FITC-tagged Sphingosine trafficking after 24 hours in ST14A cells. *ST14A cells expressing fragment 1-548 of the human huntingtin protein with different polyQ repeat lengths.* ***A*** *– Representative fluorescence images of FITC-tagged sphingosine loaded cells (FITC-SphO, white) after incubation for 10minutes and 24 hours within cells. This probe is used to assay the ability of lysosomes to efflux the simple sphingolipid sphingosine.* ***B*** *– Localisation analysis of FITC-Sphingosine fluorescence. n = 2. * = P < 0.05 by T test. Scale bar = 10μm.*

This retention of FITC-SphO in the endolysosomal system observed by persistence of punctate staining is present in around 50% of HTT Q120 cells after 24 hours of incubation with the probe as opposed to an almost uniform diffuse distribution in

HTTQ15 cells (figure 4.3.16. A.). This difference is statistically significant ($P < 0.05$, $t = 9.537$, $df = 2$, $F_{1,1} = 2.582$). These data are suggestive of NPC1 dysfunction in these cells.

Taken together the data presented in sections 4.3.1. – 4.3.2. indicate that endolysosomal expansion takes place alongside lipid homeostasis changes which are reminiscent of those seen in NPC disease are observed in cellular models of Huntington's. The alterations to the levels and localisation of the NPC1 protein which also takes place in these cells and the subsequent analysis of cellular phenotypes increasingly specific to NPC1 disease suggest that the NPC1 protein is dysfunctional in Huntington's disease. As these studies were conducted in precursor cell line we were interested to see of we could make our study more relevant to the actual processes which are ongoing in the brains of Huntington's patients (Warby et al., 1998; HD iPSC Consortium, 2012). Accordingly we expanded our studies to iPSC derived striatal medium spiny neurons.

4.3.3. – Preliminary examination of lysosomal phenotypes in iPSC derived mature Neurons from Huntington's Disease Patients

In Huntington's disease the predominant cell type affected are DARRP-32 positive medium spiny neurons of the striatum. As NPC1 dysfunction has been observed in a variety of cell models of Huntington's we were extremely interested to see if the phenotypes of NPC1 dysfunction were replicated in neuronal cultures representative of the lateral ganglionic eminence, shown to be positive for DARPP-32, with expanded polyQ repeats differentiated from iPSC derived NSCs (HD iPSC Consortium, 2012).

An extra consideration we needed to be aware of for the study of these neurons was the number of days post initiation of differentiation from NSCs that we conducted our experiments. Differentiation of neurons for 14 days post NSC plating has previously been shown to generate mature, electrophysiologically active neurons susceptible to glutamate toxicity (HD iPSC Consortium, 2012). However, as the levels of various lipids including cholesterol and sphingolipids had not been investigated in these neurons it was important to investigate these lipid changes and determine whether any particular time post initiation of differentiation exhibited substantial lipid changes. Initially, we examined these phenotypes in control neurons with a polyQ repeat

number of 33 (Q33) and examined how lipid levels changed with number of days post differentiation. Examining these neurons at days 1, 4, 7, 11, 14 and 21 days post initiation of differentiation for the levels of cholesterol, sphingomyelin, ganglioside GM1 and LBPA (data not shown). Both cholesterol and ganglioside GM1 levels were elevated with a relatively linear progression in both the cell body and in axons. Variations in the levels of sphingomyelin and LBPA were more difficult to observe, as these lipids were not strongly stained by the probes utilised in this study. Accordingly, we discounted these lipids from initial analysis until staining protocols could be improved. Due to the levels of cholesterol and ganglioside GM1 being sufficient for clear visualisation after 14 days and the convenience of being able to refer to published phenotypes in these cells at this timepoint (HD iPSC Consortium, 2012) we decided that this was the most suitable stage to examine these cells for lysosomal phenotypes.

As with the other cell lines examined in this chapter we began by assaying the endolysosomal system for expansion and as the neurons were of human origin we were able to utilise both lysotracker and LAMP-2 staining.

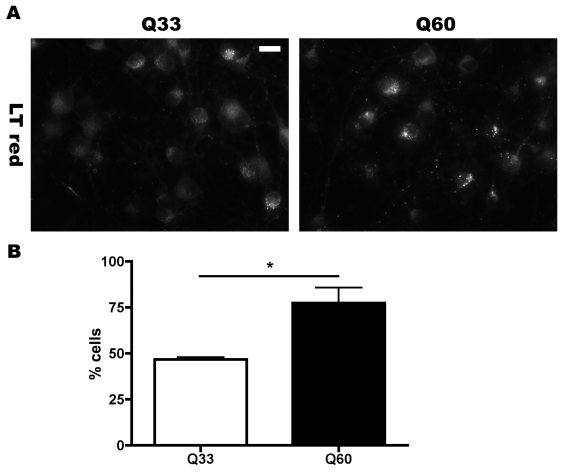

Figure 4.3.17. – Endolysosomal expansion in iPSC derived neurons. *iPSC derived neurons with different polyQ repeat lengths in HTT differentiated for 14 days from NSC cells obtained from human subjects.* ***A*** *– Representative fluorescence microscopy images of lysotracker red loaded cells (LT red, white) shows changes in lysosome and late-endosome number, size and localisation within cells.* ***B*** *– Threshold analysis of LT red fluorescence. n = 2 * = P< 0.05 by T test. Scale bar = 5µm. Cells prepared by Sun Yung, Cardiff University.*

Initially, we examined the difference in lysotracker staining between the two most similar neuronal cell lines, with respect to polyQ repeat length, Q33 and Q60 which are either side of the divide between unaffected and suffering from Huntington's. Upon doing so it was possible to measure a statistically significant difference between lysotracker fluorescence levels and, as such, the difference in the endolysosomal volume between these two cell lines ($P = < 0.05$, $t = 5.099$, $df = 2$, $F_{1,1} = 51.19$). Although a polyQ repeat length of 60 is higher than the repeat length

that is average for HD patients these cells remain strongly suited for direct comparison. Firstly, 33 polyQ repeats is very high for an unaffected patient (Warby et al., 1998) reducing the difference in severity between the two cell lines and, secondly, the patient and control that these cells were generated from were siblings meaning that they are likely to have very similar genetic backgrounds (HD iPSC Consortium, 2012).

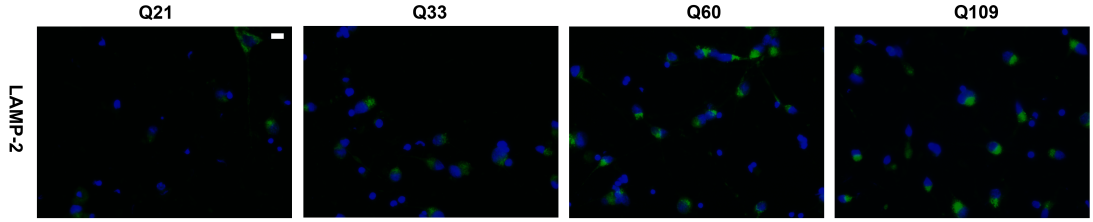

Figure 4.3.18. – LAMP-2 immunofluorescence in iPSC derived neurons. *iPSC derived neurons with different polyQ repeat lengths in HTT differentiated for 14 days from NSC cells obtained from human subjects. LAMP-2 increase is indicative of increased endolysosomal compartment size. Representative immunofluorescence images of LAMP-2 protein (LAMP-2, green) show the distribution of this late-endosomal and lysosomal transmembrane protein within cells. n = 1. Scale bar = 5μm. Cells prepared by Sun Yung, Cardiff University.*

As discussed above we were further able to assay for endolysosomal expansion in these cells by LAMP-2 immunofluorescence (figure 4.3.18.). We performed this in the full range of iPS derived neurons available with polyQ repeat lengths of 21 (Q21), 33 (Q33), 60 (Q60) and 109 (Q109). In this initial study there is an evident expansion in the endolysosomal system which is increased in a polyQ-dependent manner. LAMP-2 immunofluorescence also helps to confirm the location of the endolysosomal system in these cells as almost entirely in the cell body, no significant fluorescence from either probe was observed in axonal regions of these cells. As we have been able to observed endolysosomal expansion in these cells we were interested to determine if lipid accumulation could be a causative factor for this as observed in human NSCs and rat-derived ST14A cells.

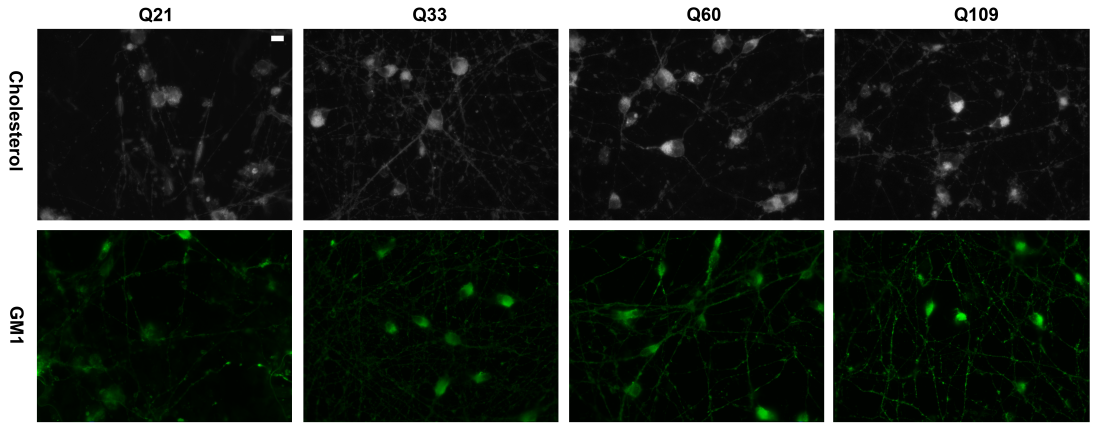

Figure 4.3.19. – Lipid storage phenotypes in iPSC derived neurons. *iPSC derived neurons with different polyQ repeat lengths in HTT differentiated for 14 days from NSC cells obtained from human subjects. Representative fluorescence microscopy images of filipin stained cells (white) show perninuclear cholesterol accumulation and FITC-tagged cholera toxin B subunit (CtxB, green) is used to visualise the increase of ganglioside GM1 within cells. n = 1. Scale bar = 5μm. Cells prepared by Sun Yung, Cardiff University.*

In all of the neuronal populations assayed the levels of both cholesterol and ganglioside GM1 levels increased with increases in polyQ repeat length (figure 4.3.19.), importantly, all of these cell lines have been shown to reach maturity at 14 days after the intiation of differentiation (HD iPSC Consortium, 2012). The cholesterol accumulation was most evident in the cell bodies of these neurons and may have been accompanied by a decrease in axonal cholesterol levels, a phenotype very similar to that observed in neuronal models of NPC disease. These phenotypes will be examined closely in the subsequent repeats of this study.

Increased ganglioside GM1 was more prevalent throughout the cells with both the cell body and axons more strongly stained by CtxB. This increase in axonal ganglioside GM1 clearly shows that the cell lines with high polyQ repeat lengths have comparable levels of axonal outgrowth to other cell lines.

As lipid storage phenotypes were present in neurons with increased polyQ repeat lengths, we have begun to utilise the assays described throughout this thesis in order to determine if lipid accumulation is likely to be the major cause of lysosomal expansion, or, whether there may be accumulation of other substrates. Subsequently, we will also perform assays for the more specific NPC1 dysfunction phenotypes of reduced lysosomal Ca^{2+} and increased lysosomal retention of sphingosine. Interestingly, in intial experiments with FITC-SphO the probe did not immediately localise to punctate structures and many cells had brightly fluorescent

nuclei (data not shown). Accordingly, the protcol for investigating the localisation of FITC-SphO in neurons may need to be developed.

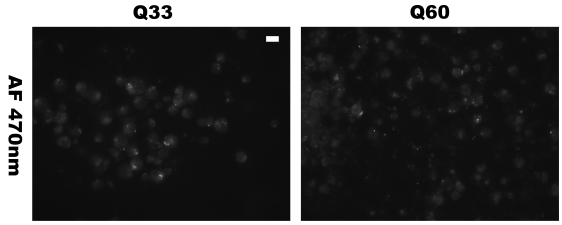

Figure 4.3.20. – Autofluorescence in iPSC derived neurons. *iPSC derived neurons with different polyQ repeat lengths in HTT differentiated for 14 days from NSC cells obtained from human subjects. Representative fluorescence microscopy images of autofluorescence after stimulation of cell with light at 470nm (AF470nm, white) show the distribution autofluorescent material within cells. n = 1. Scale bar = 5μm. Cells prepared by Sun Yung, Cardiff University.*

In terms of other lysosomal storage phenotypes we have examined the levels of autofluorescence in the closely related Q33 and Q60 cell lines. In a preliminary experiment we found no evidence of the accumulation of autofluorescent material visible at 470nm excitation in these neurons (4.3.20.). This suggests no lipofuscin accumulation in these cells. During the live assay of autofluorescence observable levels of fluorescence from all cell lines investigated was observed after cells were stimulated by 380nm light. As the levels of the fluorescence was consistent across all of the neuronal lines investigated (Q21 – Q109) it was attributed to a constituent of the growth medium – PD0332991 which is as an inducer of G_1 phase arrest in these cell lines (Toogood et al., 2005). Fortunately, after PFA fixation this appeared to have been washed out of cells so it does not affect experiments conducted at these wavelengths such as filipin staining for cholesterol.

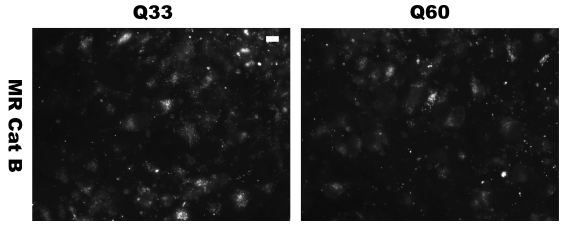

Figure 4.3.21 – Lysosomal proteolysis by cathepsin B in iPSC derived neurons. *iPSC derived neurons with different polyQ repeat lengths in HTT differentiated for 14 days from NSC cells obtained from human subjects. Representative fluorescence microscopy images of cells loaded with the magic-red cathepsin B substrate (MR Cat B, white) shows the in situ activity of cathepsin B within cells. n = 1. Scale bar = 5μm. Cells prepared by Sun Yung, Cardiff University.*

We were also able to perform an initial examination for the activity of the lysosomal enzyme cathepsin B in Q33 and Q60 neurons and observed a similar pattern to that observed in ST14A cells expressing different polyQ lengths of HTT. A small decrease has been observed in this activity, however, this remains to be quantified in subsequent repeats (figure 4.3.21.). Cathepsin L remains to be assayed in these cells and as this was more clearly divergent in the ST14A cells (figure 4.3.11.) it may be a better assay for changes in the proteolytic capacity of neurons to be examined.

Finally, we investigated the levels and localisation of the NPC1 protein in these neurons. Interestingly, isobaric tag for relative and absolute quantification (iTRAQ) data has suggested that the levels of this protein are elevated in Q60 cells compared to control cell lines (data courtesy of Akimov *et al*. 2014)(Rauniyar et al., 2014). This was the only protein to have increased levels from a list of investigated proteins which includes the related protein NPC2, the lysosomal transport protein LIMP-2 (recently implicated in cholesterol transport), and the cholesterol efflux regulatory protein ABCA1. This is further evidence of pathogenic changes in cells related to the NPC1 protein which are dependent upon increases in polyQ length.

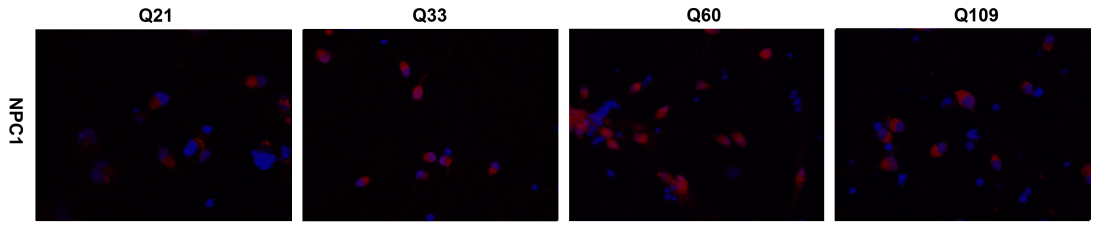

Figure 4.3.22. –NPC1 protein distribution in iPSC derived neurons. *iPSC derived neurons with different polyQ repeat lengths in HTT differentiated for 14 days from NSC cells obtained from human subjects. Representative immunofluorescence images of Niemann-Pick type C1 protein (NPC1, red) show the distribution of this late-endosomal and lysosomal transmembrane protein within cells. n = 1. Scale bar = 5μm. Cells prepared by Sun Yung, Cardiff University.*

Initial immunohistochemical analysis of NPC1 in Q21 – Q109 neurons is confirmatory of increased levels in neurons with increased lengths of polyQ repeat (figure 4.3.22.). This is particularly evident between Q60 cells and controls although it may be more variable in higher repeat length neurons. This remains to be further investigated.

These data presented in 4.3.3. show preliminary evidence for the conservation of lysosomal storage phenotypes in neurons and potentially implicate the NPC1 protein dysfunction as a initiating factor in this. Although NPC disease remains a devastating condition there are disease modifying and experimental therapies which have been

used to treat patients with the disorder. We were interested to test the disease modifying treatment, miglustat, and experimental therapy, hydroxyl-propyl-β-cyclodextrin (HPβCD) (section 1.5.2.), in our cellular models of Huntington's to see if they may be of benefit to lysosomal storage phenotypes in this disease.

4.3.4. – Preliminary investigation of the impact of therapies beneficial in NPC upon lysosomal storage phenotypes in Huntington's disease cell models

Initially, we investigated the effects of the experimental therapy HPβCD on lysosomal storage phenotypes in our cellular models of Huntington's. Although the mechanism of action has not been fully defined for the benefits provided by HPβCD in cellular and animal models of NPC1 disease (Davidson et al., 2009; Vite et al., 2015), it is well characterised as a cholesterol reducing agent in cellular models of NPC (Chen et al., 2010). Initially we tested HPβCD in the NSC cells from a juvenile Huntington's patient.

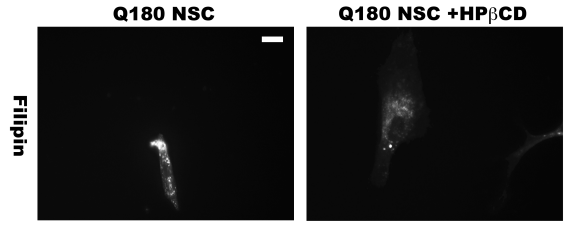

Figure 4.3.23. – Effects of hydroxyl-propyl-β-cyclodextrin on cholesterol storage in iPS derived neural stem cells. *iPS derived neural stem cells from a control and a juvenile Huntington's Patient (Q180). Representative fluorescence microscopy of filipin stained cells (white) show endo-lysosomal cholesterol accumulation. Cells are treated with 0.04mg/ml hydroxyl-propyl-β-cyclodextrin (HPβCD) for 16 hours. n = 1. Data prepared with assistance from Naomi Killick, Cardiff University. Scale bar = 10μm.*

As expected a reduction in punctate filipin staining, suggesting a reduction endolysosomal lipid storage, was evident in cells treated with HPβCD (Figure 4.3.23.). HPβCD induced benefits seem to be specific for diseases in which NPC1 dysfunction is present as it has been shown to improve phenotypes in animal models of NPC1 and NPC2 but not in a models of GM1 gangliosidosis and MPS IIIA (Davidson et al., 2009). Accordingly, it may provide further evidence of NPC1 dysfunction in these cells. Due to the observation that HPβCD was of benefit in these cells we have begun to expand our study to the other cellular models of Huntington's we have investigated so far.

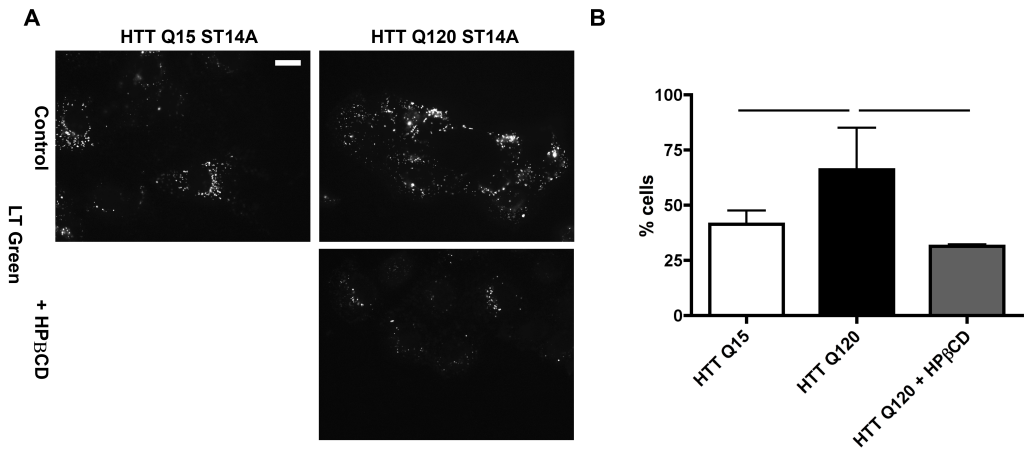

Figure 4.3.24. – Effect of hydroxyl-propyl-β-cyclodextrin on increased endolysosomal volume in ST14A cells. *ST14A cells expressing fragment 1-548 of the human huntingtin protein with different polyQ repeat lengths.* ***A*** *– Representative fluorescence microscopy images of lysotracker green (LT Green, white) loaded cells.* ***B –*** *Threshold analysis of LT green fluorescence. Cells are treated with 0.04mg/ml hydroxyl-propyl-β-cyclodextrin (HPβCD) for 24 hours. Error bars = SD. n = 2. Scale bar = 10μm. No significant difference observed one-way ANOVA with Bonferroni post-test.*

As differences in lysotracker fluorescence was observed to be a sensitive way of studying changes in endolysosomal volume in ST14A cells with different polyQ repeat lengths (figure 4.3.6.) this assay was used to see if HPβCD was capable of reducing this lysosomal storage phenotype. We utilised an established protocol of 0.04mg/ml HPβCD for 24 hours in order to do so (Chen et al., 2010). In preliminary experiments this was observed as Q120 cells showed a trend towards reduction in the number of cells with lysotracker fluorescence above threshold levels (figure 4.3.24. B.). Surprisingly the number of cell above threshold in the treated cell population was lower than in Q15 cells although further repeats are needed to confirm these observations.

Nevertheless, this result showed evidence of reductions in lysosomal storage so we progressed to examine lipid storage in these cells, in this preliminary analysis the levels of cholesterol in Q120 ST14A cells was examined after treatment with HPβCD. Upon doing a reduction in cholesterol levels was observed in treated cells. This seemed most evident in the perinuclear region of Q120 cells where cholesterol punctae were observed indicative of a reduction in endolysosomal cholesterol accumulation being specifically affected in these cells.

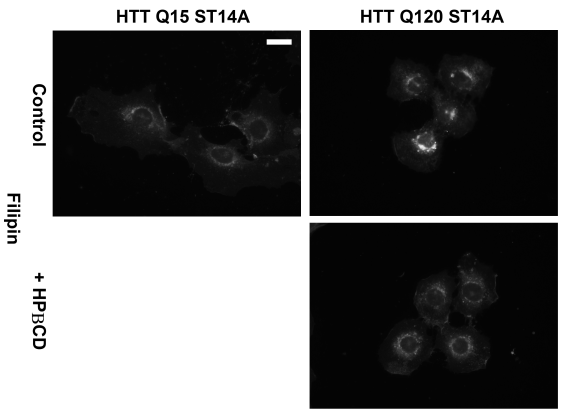

Figure 4.3.25. – Effect of hydroxyl-propyl-β-cyclodextrin on cholesterol storage in ST14A cells. *ST14A cells expressing fragment 1-548 of the human huntingtin protein with different polyQ repeat lengths. Representative fluorescence microscopy of filipin stained cells (white) show endo-lysosomal cholesterol accumulation. Cells are treated with 0.04mg/ml hydroxyl-propyl-β-cyclodextrin (HPβCD) for 24 hours. n = 2. Scale bar = 10μm.*

These initial data are promising although the effect of HPβCD upon other lipids shown to increase in these cells (sphingomyelin, LBPA and ganglioside GM1) remains to be examined. The observations of cholesterol reduction should also be confirmed by biochemical analysis.

The final phenotype studied in this preliminary examination of benefit mediated by HPβCD on ST14A cells expressing extended polyQ HTT was endolysosomal mistrafficking of ganglioside GM1. This provides a sensitive assay with which we can examine phenotypic improvement.

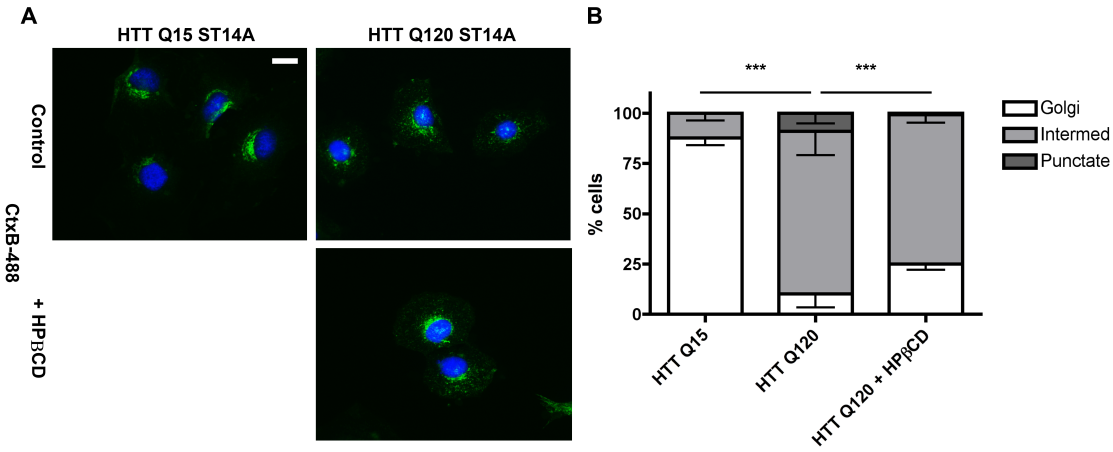

Figure 4.3.26. – Effect of hydroxyl-propyl-β-cyclodextrin on disrupted endolysosomal sphingolipid trafficking in ST14A cells. *ST14A cells expressing fragment 1-548 of the human huntingtin protein with different polyQ repeat lengths.* ***A*** *– Representative fluorescence microscopy images of pulse, chased FITC-tagged Cholera toxin B-subunit (CtxB-488, green) to assay trafficking of ganglioside GM1 through the endo-lysosomal system. Hoechst stained nuclei are shown in blue.* ***B –*** *Qualitative quantification of CtxB-488 localisation as Golgi, punctate or intermediate between the two states in ST14A cells as a percentage of the total cell population. Cells are treated with 0.04mg/ml hydroxyl-propyl-β-cyclodextrin (HPβCD) for 24 hours. Error bars = SD. n = 2 . Scale bar = 10μm.*

A marginal improvement was observed in trafficking post treatment with HPβCD (figure 4.3.26.). Trafficking defects between control and ST14A cells expressing Q120 huntingtin were confirmed to be different ($P < 0.001$, $X^2 = 539.44$ for run 1, 585.63 for run 2, df = 2). This analysis was performed by comparing the values obtained from the three HTT Q120 repeats of this experiment to expected values calculated from the mean of each population in HTT Q15 cells. A similar analysis was conducted to confirm variation between HTT Q120 cells and HTT Q120 cells treated with HPβCD. Although the change in the populations was much more marginal the changes were still significant ($P < 0.001$, $X^2 = 25.42$ for run 1, 35.19 for run 2, df = 2). As variation between the three repeats was minimal (SEM = < 5% in all populations) this approach was applicable.

As this phenotype has not been examined in NPC cells treated with HPβCD this may not be due to correction of NPC phenotypes, however, as HPβCD has been observed to cause cytoplasmic Ca^{2+} elevation in cells (Maguire *et al*., Unpublished) it may act in a similar way to curcumin inhibition of SERCA2. Curcumin treatment also causes transient elevations in cytosolic Ca^{2+} and this compensates for the reduced intraluminal Ca^{2+}, allowing for endolysosomal trafficking improvements in cells. Interestingly, curcumin has been shown to be beneficial to Huntington's disease models. The mechanism underlying this benefit is unclear, however, and curcumin can interact with a myriad of pathways within cells although it has been shown to mediate benefits via Ca^{2+} in NPC (Goike et al. Unpublished).

Taken together these data suggest that HPβCD has the potential to be therapeutically beneficial in Huntington's disease as it can reduce lysosomal storage phenotypes which we have shown to occur within cells. Accordingly, it would be interesting to see if this molecule can be used to reduced neuronal loss in models of Huntington's disease.

As previously mentioned Miglustat is an approved therapy in the EU for the neurological manifestations of NPC disease (Patterson et al., 2015). Accordingly we were interested to test Miglustat to see if it was of benefit to cellular models of Huntington's. To do this we utilised the cell model most thoroughly characterised in this study, ST14A cells expressing HTT with different polyQ lengths.

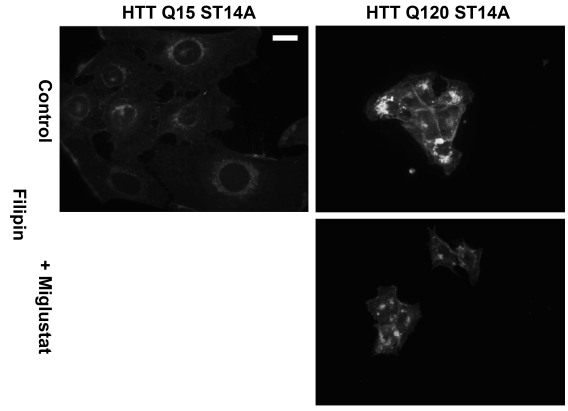

Figure 4.3.27. – Effect of miglustat on cholesterol storage in ST14A. *ST14A cells expressing fragment 1-548 of the human huntingtin protein with different polyQ repeat lengths. Representative fluorescence microscopy of filipin stained cells (white) show endo-lysosomal cholesterol accumulation Cells are treated with 50 μM Miglustat for 5 days. n = 1. Scale bar = 10 μm.*

In a preliminary experiment, reduction in cholesterol levels was observed in these cells after miglustat treatment. It also appears that some redistribution of cholesterol has taken place in these cells, leading to increased plasma membrane staining. This is interesting, as in NPC1 deficient cells miglustat does not reduce cholesterol storage (Haslett et al., Unpublished). One phenotype clearly shown to be improved by miglustat treatment of NPC cellular models and patient samples is the endolysosomal trafficking of sphingolipids (Lachmann et al., 2004). Accordingly, this was investigated in miglustat treated Q120 cells utilising the CtxB transport assay.

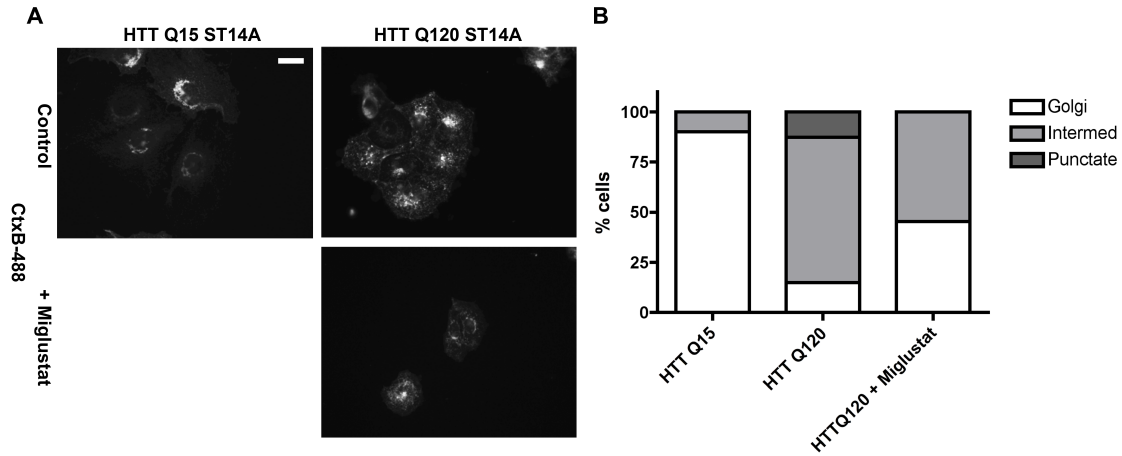

Figure 4.3.28. – Effect of miglustat on disrupted endolysosomal sphingolipid trafficking in ST14A cells. *ST14A cells expressing fragment 1-548 of the human huntingtin protein with different polyQ repeat lengths.* ***A*** *– Representative fluorescence microscopy images of pulse, chased FITC-tagged Cholera toxin B-subunit (CtxB-488, white) to assay trafficking of ganglioside GM1 through the endo-lysosomal system.* ***B –*** *Qualitative quantification of CtxB-488 localisation as Golgi, punctate or intermediate between the two states in ST14A cells as a percentage of the total cell population. Cells are treated with 50 μM Miglustat for 5 days. n = 1. Scale bar = 10 μm.*

In the preliminary experiment, conducted after miglustat treatment, there was an improvement in endolysosomal ganglioside GM1 trafficking with no punctate staining observed in the treated cells and almost half of these cells showing a Golgi distribution of CtxB. Potentially, this is an extremely important phenotype as endolysosomal lipid trafficking could potentially be at the root of many of the lipid disturbances observed in various model of Huntington's (Trushina et al., 2006; Di Pardo et al., 2012).

Taking these data into consideration we have preliminary evidence that therapies that have been shown to be beneficial in NPC disease, are able to reduce the lysosomal storage phenotypes we observe in cellular model of Huntington's. We have not however shown that these lysosomal phenotypes are involved in the pathogenesis of Huntington's, although, the prevalence of neurodegeneration in LSDs including NPC (Vanier, 2009) would suggest that these phenotypes could contribute to neuronal loss. Accordingly, to determine if therapies that are capable of reducing these phenotypes are protective to neurons, it would be good to investigate if they could prevent neuronal loss. This would be strongly suggestive of LSD phenotypes being involved in pathogenesis and would also suggest that these therapies could be of benefit to Huntington's patients.

4.3.5. – Prevention of excitotoxic cell death by NPC therapies

Due to the above observations we expanded our study to a neuronal model of glutamate induced excitotoxic Ca^{2+} dyshomeostasis, which has been shown to increase in neurons with extended polyQ forms of HTT. In this study the increase in Ca^{2+} dyshomeostasis correlated with increases in markers of cellular death, and, did not alter HTT aggregation (HD iPSC consortium study., 2012). Accordingly, it is considered a robust way of measuring the levels of cellular death in Huntington's neurons, particularly as we are using the same cell lines utilised in this study, initiated by the pathophysiological process of Glutamate excitotoxicity. Due to these considerations it is an extremely well suited assay with which to determine if LSD therapies were beneficial to neuronal loss it Huntington's.

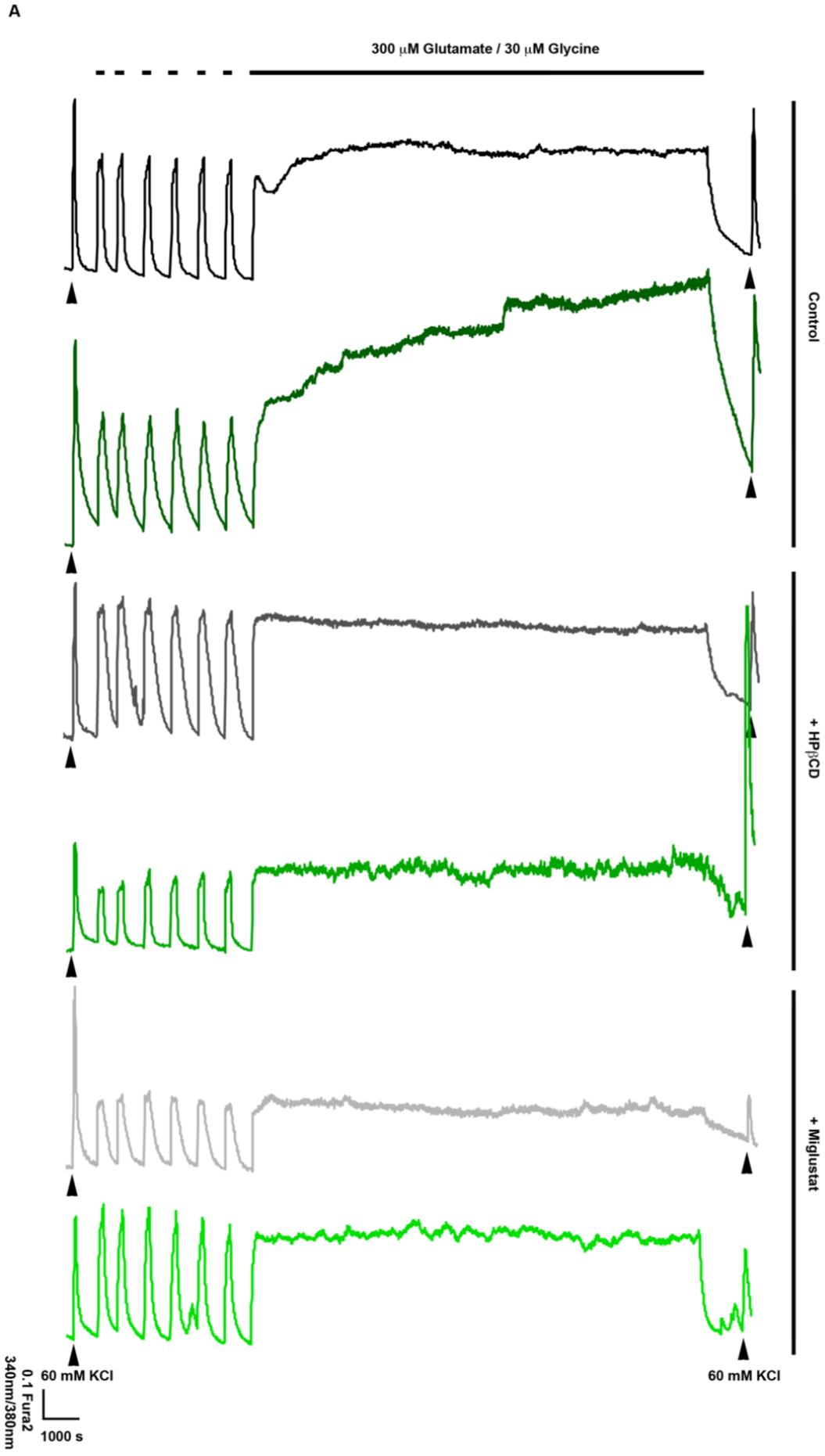
A
300 μM Glutamate / 30 μM Glycine
Control
+ HPβCD
+ Miglustat
60 mM KCl
60 mM KCl
0.1 Fura2
340nm/380nm
1000 s

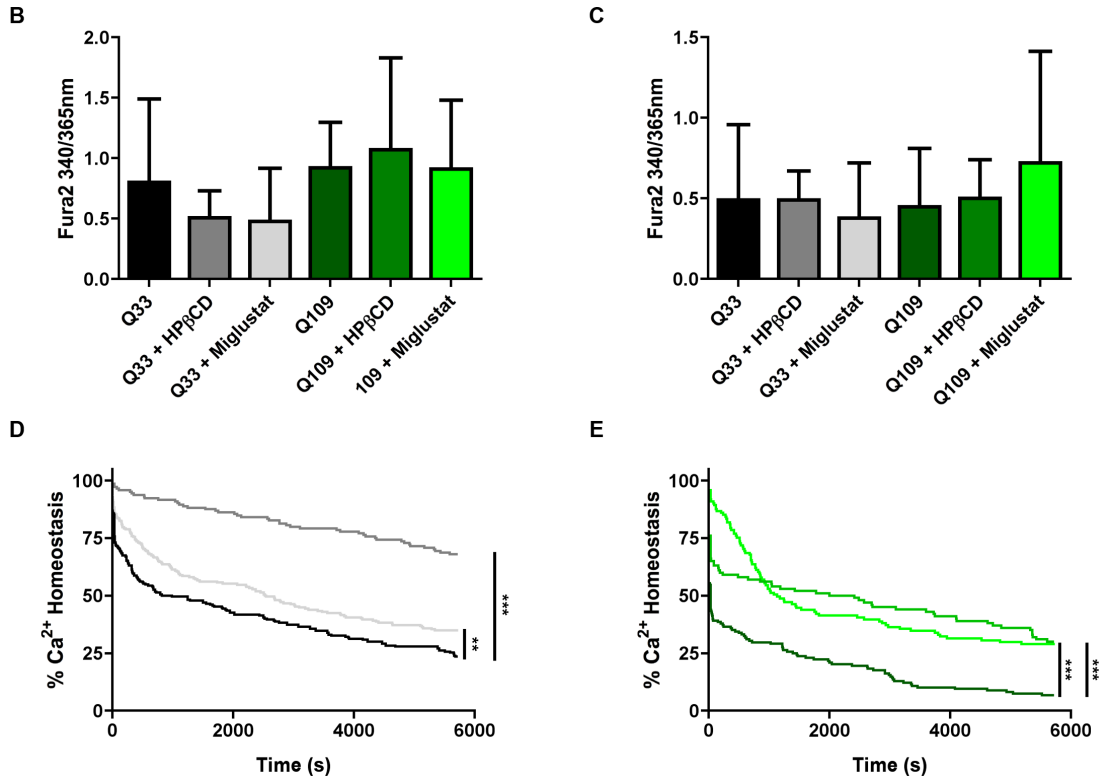

Figure 4.3.29. – Effect of therapies beneficial in NPC disease upon Ca^{2+} dyshomeostasis in iPSC derived neurons. A *– Representative traces of Ca^{2+} responses from neuronal populations subjected to 60 second pulses of 60mM KCl (black arrowheads) or 300μM glutamate and 30μM glycine (black bar) followed by prolonged treatment with 300μM glutamate and 30μM glycine (black bar). All cell populations were subjected to BDNF withdrawal for 24 hours prior to the experiment, control cells were untreated, + HPβCD cells were treated with 0.04mg/ml +HPβCD for 24 hours prior to the experiment, + Miglustat cells were treated with 50μM Miglustat for 5 days prior to the experiment.* ***B –*** *Quantification of Ca^{2+} response measured by change in Fura2 fluorescence during glutamate plateau phase. No significant difference in responses was observed by one way ANOVA. Error bars = SD.* ***C*** *– Quantification of Ca^{2+} response measured by change in Fura2 fluorescence ratio after addition of 300μM glutamate and 30μM glycine. No significant difference in responses was observed by one way ANOVA. Error bars = SD.* ***D*** *– Analysis of the percentage of Q33 neurons which lose Ca^{2+} homeostasis during long term application of 300μM glutamate and 30μM glycine. Cells are considered dyshomeostatic when the Fura2 fluorescence ratio exceeds the baseline set at 5 min of prolonged application and does not return to below this point. The percentage of cells which maintain Ca^{2+} homeostasis is plotted against time. ** = $P < 0.01$ and *** = $P < 0.0001$ calculated by Logrank test.* ***E*** *– Analysis of the percentage of Q109 neurons which lose Ca^{2+} homeostasis during long term application of 300μM glutamate and 30μM glycine. Cells are analysed as in D. *** = $P < 0.0001$ calculated by Logrank test. n = 3 – 5 from 3 independent differentiations. Cells prepared by Sun Yung, Cardiff University. Experiments performed by or with assistance from Polina Yarova, data analysed by Polina Yarova, Cardiff University.*

In order to observe Ca^{2+} dyshomeostasis we removed BDNF from the medium of neuronal cultures 24 hours prior to the initiation of experiments. This withdrawal has been shown to be necessary to observe Ca^{2+} dyshomeostasis, and, as BDNF depletion in the striatum is a process known to occur in Huntington's it is physiologically relevant (HD iPSC consortium study., 2012). For this study we

employed the Q109 cell line as a more severe model of this cell death process was likely to provide more stringent examination of any potential therapeutic benefit from LSD therapies.

The survival curves shown in 4.3.29. D and E show that Q109 neurons were less able to maintain Ca^{2+} homeostasis after long term glutamate treatment with a quicker loss of Ca^{2+} homeostasis observed and more cells becoming dyshomeostatic by the end of glutamate exposure. Loss of Ca^{2+} homeostasis is observed when the Ca^{2+} levels, shown by ratiometric Fura2 fluorescence, exceed the baseline fluorescence calculated from the first minute of prolonged glutamate exposure. This process can be observed by escalation in the representative Ca^{2+} trace from Q109 cells (4.3.29. A, dark green) where baseline Ca^{2+} is quickly lost. As can be seen in the black trace from this figure this escalation is much less rapid and severe in Q33 cells.

It is important to note that, although, the individual peak heights elicited in response to glutamate do vary between cell lines and treatment conditions (as shown by the representative traces in A and the graphs B and C, glutamate plateau height glutamate responses from initial pulses and respectively), these responses are also variable within cell lines and as such are not significantly different ($P > 0.05$ in both instances, $F = 0.7367$ for glutamate plateau, $F = 0.2695$ for glutamate peak). Representative traces were chosen which show the relative onset of dyshomeostasis in different cell types and treatments.

When we observe cell survival in Q109 cells post treatment with both miglustat and HPβCD it is shown that these treatments allow a greater number of neurons to maintain Ca^{2+} homeostasis, which is strongly suggestive of increased survival in these neuronal populations. Both miglustat and HPβCD lead to a greater number of Q109 neurons maintaining homeostasis ($P < 0.001$, $df = 1$, $X^2 = 39.08$ for miglustat and $P < 0.0001$, $df = 1$, $X^2 = 30.96$ for HPβCD). These levels were similar to those observed in Q33 neurons. Miglustat also showed a clear benefit in the rate of neuronal loss during prolonged glutamate exposure, as evidenced by the slower decrease in cells maintaining Ca^{2+} homeostasis (bright green line, 4.3.29. E). It is interesting that both treatments also produced a survival benefit in Q33 cells ($P < 0.01$, $df = 1$, $X^2 = 8.597$ for miglustat and $P < 0.0001$, $df = 1$, $X^2 = 81.83$ for HPβCD). This survival benefit was much more pronounced after HPβCD treatment and was

accompanied by a obvious reduction in rate of Ca^{2+} homeostasis loss – this remains to be further investigated.

These data provide evidence for increased neuronal survival in an *in vitro* model of Huntington's disease after treatment with therapies shown to be beneficial in NPC disease. Not only does this reveal new therapeutic options for Huntington's, but, it provides strong evidence to link the LSD phenotypes we have observed in a variety of models of Huntington's disease contributes to neuronal loss.

4.4. – Summary of Results and Discussion

Due to multiple reports of increased lysosomal volume (Catiglioni et al., 2012; Camnasio et al., 2012) and alterations in lysosomal localisation in models of Huntington's disease (Erie et al., 2015) we were interested to see if they bore any relation to the phenotypes observed in LSDs. In doing so, we observed a number of phenotypes which were reminiscent of NPC disease or dysfunction in the NPC1 pathway (Lloyd-Evans et al., 2008).

4.4.1. – Niemann-Pick type C phenotypes in Huntington's Disease

In addition to increases in lysosomal volume in cellular models of Huntington's, we have also been able to observe accumulation of the lipids cholesterol, LBPA, sphingomyelin and ganglioside GM1 in regions of the cell which are suggestive of lysosomal storage of these substrates. This finding has been replicated by other studies in the lab by co-localisation of the lysosomal marker LAMP-2 with stored lipids (Clark *et al.* Unpublished.). Cholesterol and LBPA were also shown to be elevated biochemically, alongside evidence of sphingoid base accumulation, in cell lines which were amenable to this form of study. These studies are currently being repeated with the inclusion of further cell lines and tissue from animal models.

Additional phenotypes such as endolysosomal lipid mistrafficking were also observed and Huntington's cells did not appear to be accumulating autofluorescent material or have an expanded ER. Taken together, these phenotypes are suggestive of a LSD in which the major accumulating molecules are lipids. The particular profile of storage lipids observed in this disease is similar to those observed in NPC1 (Chevallier et al., 2008; Lloyd-Evans et al., 2008). Interestingly, there is also evidence of lysosomal proteolytic defects but lack of autofluorescence showed these are unlikely to be a result of defective lysosomal pH homeostasis (Guha et al., 2014). As proteolytic defects were present in both of the cell lines investigated for this phenotype, it may be worth studying further. It may also be worth studying similar phenotypes in cellular models of NPC1 as it is unknown if there is any difference between these *in situ* probes in NPC1 deficient cells compared to control cells.

Upon studying the subcellular distribution of this protein we found that it was differentially localised in all cell lines studied and, although, initial results from NSCs suggested decreased levels of the protein subsequent studies have shown that it is increased in other cellular model of Huntington's. This may have been a result of the H9 control cell line used alongside NSCs not being ideally suited as it was not iPSC derived. The observation of increased NPC1 protein has been validated by iTRAQ analysis showing elevated protein levels. Alongside elevation of NPC1 there was a clear re-distribution of this protein. Although we have not identified the compartment to which NPC1 becomes redistributed lysosomal lipid accumulation is strongly indicative of a loss of lysosomal function so it is probable that it has not reached the endolysosomal system. The observation of NPC1 mislocalisation and elevation has been confirmed in another cellular model of Huntington's disease prepared from Q111 Huntington's mice. In addition to this western blotting is also being undertaken to study protein levels (Clark et al., Unpublished.)

The evidence presented in this chapter includes cells from patients (section 4.3.1.), including the population of neurons most susceptible to loss in Huntington's (4.3.3.), and cell lines established from rodent models of polyQ expansion (4.3.2.). NPC1 phenotypes have been observed in all the cell lines investigated suggesting that it is a prevalent phenomenon, although this remains to be further confirmed by repeating our studies in neurons. Further evidence is provided by the identification of these phenotypes in an additional cellular model of Huntington's prepared from the striatum of the Q111 mouse model (Clark *et al.,* Unpublished)(Carroll et al., 2015). Lipid storage has also been observed in the brains of mice with expanded polyQ repeats (Carrol et al., 2015) and a full allelic sequence of Huntington's mouse tissue is currently under analysis.

Changes in lipid levels are well studied in Huntington's and there are varying reports of increases in lipids such as cholesterol and ganglioside GM1 (Trushina et al., 2006; del Toro etal., 2010; Trushina et al., 2014). It is interesting that, in some of the studies in which reductions in lipid levels are observed, a more punctate distribution of lipids is also present within cells (Marullo et al., 2012). This may be indicative of a lipid trafficking defect which is one of the primary pathogenic events in NPC1 (Lloyd-Evans et al., 2008). It is also interesting to note, that the changes in lipids observed in LSDs are not always simply accumulation but can be more influenced by lipid mislocalisation in cells. For example, the levels of cholesterol in NPC brains is not elevated but it is redistributed from the plasma membranes of cells to the

endolysosomal system (Zervas et al., 2001; Lloyd-Evans et al., 2010) – this may be particularly problematic in cells with large extensions such as neurons. Interestingly, there are reports of similar processes in human brain samples from Huntington's patients. It has also been reported that dysregulation of cholesterol precursors can cause endolysosomal lipid accumulation (Kreilaus et al., 2015); in some cases, such as Smith-Lemli-Opitz Syndrome (SLOS), these phenotypes are reminiscent of NPC (Platt, 2014).

With respect to the reduction in the levels of certain gangliosides, it is interesting that ganglioside biosynthetic defects can also cause the increase of other types of ganglioside from different parts of the pathway. For example in GM3 synthase deficiency, which causes a childhood epilepsy syndrome, patients do not produce ganglioside GM3 or any of its metabolites but do accumulate lactosylceramide and the derivative gangliosides Gb3 and Gb4 (Simpson et al., 2004). Interestingly, increases in ganglioside GD3 in the R6/2 mouse model of Huntington's could be suggestive of a similar synthetic pathway imbalance occurring in the presence of expanded mHTT (Desplats, 2007).

Combined with the observations of lipid dyshomeostasis and endolysosomal trafficking defects in the literature, there is an increasing case for an involvement of NPC1 in the pathogenesis of Huntington's. Upon initial examination, there are some overlaps in the pathological changes observed in patients including eye movement defects, and, movement abnormalities such as dysphagia (Patterson et al., 2007, Warby et al., 1998). It is, however, extremely difficult to compare such phenotypes in neurodegenerative diseases with complex aetiology. To aid this it may be interesting to look at the presentation of Huntington's in juvenile cases and compare these patients with classical NPC patients. Similarly, the recent discovery that there may be more adult-onset NPC patients than recently thought (Wassif et al., 2015) may allow comparison of NPC and Huntington's patients of a more similar age.

A similar study could be conducted to look at striatal pathology in NPC, to supplement the observations that striatal neurons from NPC mouse models could not initiate neurite outgrowth in response to BDNF treatment (Henderson et al., 2000). Further study of cerebellar pathology in Huntington's may also be of interest. There is some evidence of the latter, with patients presenting with cerebellar symptoms (Rodda et al., 1981; Rub et al., 2013, Sakai et al., 2015) and mouse model of polyQ expansions in HTT causing cerebellar dysfunction (Denny et al., 2010). To this end,

we performed a preliminary study on the cerebellar regions of mouse brains from the Q150 mouse model of Huntington's and observed some disorder in the purkinje neurons populations of which are devastated in NPC1 disease.
Accordingly, there is clear evidence of NPC phenotypes in Huntington's disease cell models and we are beginning to observe NPC phenotypes in animal models. As a result it is interesting to discuss the potential mechanism leading to NPC1 dysfunction in Huntington's.

4.4.2. – Proposed mechanism for NPC1 dysfunction in Huntington's disease

The data in 4.3.2 and 4.3.3 show that relative levels of NPC1 are elevated in Huntington's cells and this has been biochemically confirmed in other Huntington's cell lines, as are levels of NPC2 (Clark *et al.,* Unpublished). There was clearly evident mislocalisation of the NPC1 protein in the cells in which this could be examined whereas NPC2 maintained a punctate distribution; although this was an expected compensatory mechanism. Unfortunately, it was not possible to examine the distribution of NPC1 in iPSC derived neurons from Huntington's patients as the cell bodies were too small to see differences in localisation, although, the increase in protein levels was recapitulated. Accordingly, mislocalisation of NPC would, currently, appear to be the most obvious reason for lipid accumulation similar to that observed in NPC disease, this is shown in figures 4.3.5. and 4.3.14.

Reduced levels of NPC1 in the lysosome would lead to reduced sphingosine efflux leading to increased levels within the lysosome. (Lloyd-Evans et al., 2008) Although sphingosine has not been specifically shown to be elevated in this study the levels of sphingoid base were increased and a fluorescently tagged version of this lipid constituent was also observed not to leave the lysosome so dysfunction in sphingosine handling is evident. Nevertheless, it will be important to biochemically characterise the level of sphingosine in Huntington's model using a more specific technique. In NPC, increased levels of sphingosine are proposed to cause a lysosomal Ca^{2+} defect (Lloyd-Evans et al., 2008) a trend towards which has been observed in Q120 ST14A cells, and, a significant Ca^{2+} defect has been observed in Q111 murine striatal cells (Clark *et al.* Unpublished). This Ca^{2+} defect leads to defective endocytosis and subsequently lipid storage – both phenotypes clearly evident in this study. Lower levels of lysosomal Ca^{2+} may also cause autophagy defects due to lack of vesicle fusion (Luzio et al., 2007) – we have not yet studied

this with relation to NPC1 in these cells although proteolytic defects may be indicative of this process occurring. Potential implications for processes within the cell as a result of NPC1 mislocalisation are expanded upon in figure 4.4.1.

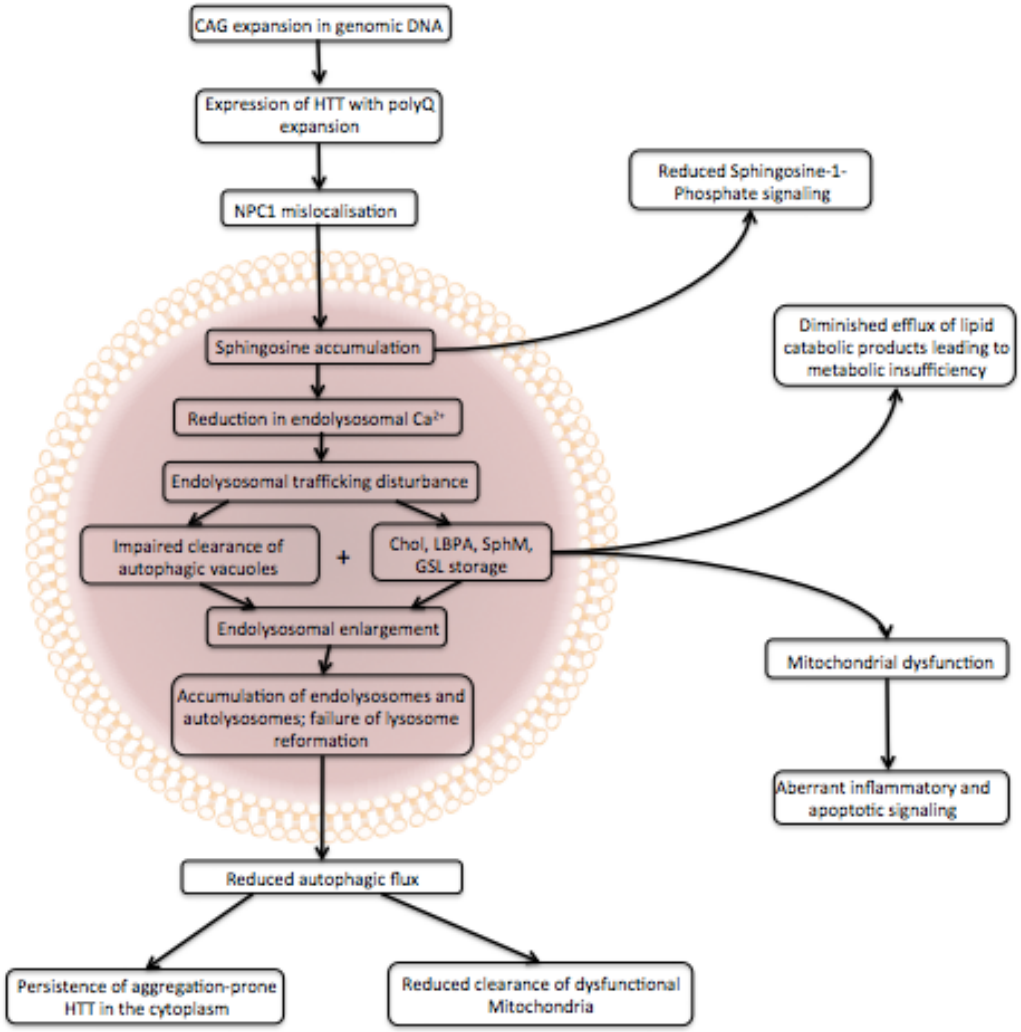

Figure 4.4.1. – Proposed mechanism of pathological changes to the lysosomal system in cells expressing mHTT. *Detailed discussion of the resultant impact upon lysosomal processes in cells with expression of HTT with pathogenically expanded polyQ repeats. Adapted from Platt et al., 2012*

Further research also needs to be conducted as to why NPC1 does not reach the late endosome and lysosome. As HTT is proposed to be a scaffold protein important during selective autophagy processes by interacting with the proteins important to this process (Rui et al., 2015). To this end it has been shown that NPC1 can interact with HTT which does not have expanded polyQ repeats in co-immunoprecipitation (co-IP) studies (Williams *et al*. Personal communication). The reverse of this experiment is being conducted in our lab where a colleague is attempting to show the

interaction of HTT and mHTT with NPC1 by co-IP. This would suggest that the aggregation of HTT with expanded polyQ repeats prevents interaction with NPC1 although this does not exclude aggregate prone HTT trapping NPC1. Other cell lines modelling diseases with polyQ repeat expansions are also being tested in this study to see if this process is specific to Huntington's, or, is more prevalent. HTT knockdown studies are also being conducted to see if NPC1 phenotypes are induced. As mentioned in section 4.1.4. HIP1 is an important protein to consider when looking at endocytosis defects in models of Huntington's (Waelter et al., 2001; Metzler et al., 2001). Potential for the interaction of this protein with NPC1 should also be considered when investigating the mislocalisation of NPC1.

4.4.3. – Are NPC1 therapies potential treatments for Huntington's disease.

As shown in section 4.3.5., Ca^{2+} dyshomeostasis in the well established model of glutamate excitotoxicity in iPSC derived neurons from Huntington's patients showed an improved outcome, after the cells were treated with therapies which are of benefit in NPC disease. This was evident in terms of both numbers of cells maintaining Ca^{2+} homeostasis, and, increasing the time until Ca^{2+} dyshomeostasis occurred. Whilst this has not yet been proven to be linked to reduced cell death in these neurons by direct assay, these processes are very closely linked in mechanisms of neuronal cell death and have been shown to take place in the same neurons this study was conducted in (HD iPSC Consortium, 2012). Accordingly, this method provides good *in vitro* evidence of potential therapies for Huntington's which could provide the basis for further study. This evidence also supports the data showing lysosomal storage in neurons by reducing the pathology in cells using compounds known to reduce lysosomal storage. Further, it implicates these storage phenotypes contribute to pathogenic processes, as, their reduction leads to improved resistance to glutamate excitotoxicity. Although the reduction of the NPC phenotypes observed in neurons in response to miglustat or HPβCD has yet to be confirmed, the observation of this in different cell lines which share the same phenotype suggests that it will be effective in doing so.

It is arguable that miglustat provided the most obvious benefit in Huntington's neurons, as it provided greater delay in the onset of Ca^{2+} dyshomeostasis. This is perhaps fortuitous as miglustat has a number of advantages over HPβCD as a therapy. Firstly, miglustat is an approved treatment that has been used to treat two

diseases (Gaucher and NPC1) (Platt et al., 2012), accordingly, there is extensive safety data on miglustat as a drug and it has been shown to be safe for long term administration (Patterson et al., 2015). Miglustat has also been shown to be relatively free of side effects with gastrointestinal disturbances; the most commonly reported complication (Belmatoug et al., 2011). Contrastingly, HPβCD has only been used in cases of compassionate use and initial clinical trials (Ottinger et al., 2014). HPβCD is also associated with hearing loss (Crumling et al., 2012). In addition to this, miglustat is an orally available therapy so administration to patients is convenient and relatively risk free. Again, HPβCD, presents difficulty in this respect. Studies in murine and feline animal models have shown that in order to be most beneficial HPβCD should be administered by either intrathecal or intercerebroventricular injection (Davidson et al., 2009; Vite et al., 2015). Due to this, there are significant complications in the administration of HPβCD (Ottinger et al., 2014) making it a less suitable therapy.

In longitudinal studies of NPC patients treated with miglustat it has been observed to improve disturbances is saccadic eye movements, reduce dysphagia, stabilise auditory acuity and improve the ambulatory index of some patients (Patterson., 2015). Importantly, with miglustat and other types of substrate reduction therapy (SRT) early treatment has been shown to improve patient outcomes. Whilst diagnosis remains a challenge for most cases of NPC, Huntington's patients can be more easily identified due to the mechanism of disease inheritance (Warby et al., 1998). Accordingly, patients could be treated with miglustat in pre-symptomatic phases which may lead to increased effectiveness. An example of this is the dietary supplementation of erucic acid which acts as a SRT for X-linked adrenoleukodystrophy. This shows little benefit in symptomatic patients treated but can be useful for the treatment of mildly affected patients (Rizzo et al., 1989). It is also worth noting that miglustat has been shown to be amenable to administration in combination with other therapies. This has been demonstrated in a recent study where it was administered, alongside ibuprofen and curcumin, in an animal model of NPC disease to generate increased benefit (Williams et al.,2014).

It is currently unknown how miglustat provides benefit in NPC. Originally, it was postulated that reduction of glycosphingolipids such as gangliosides which accumulate in NPC provided benefit – this was the expected mechanism of action as miglustat inhibits glucosylceramide synthase (Platt et al., 1994). However, a knockout mouse model of NPC which also had the ability to synthesise gangliosides genetically ablated did not show improvements in pathology (Gondre-Lewis et al.,

2003). Subsequently, it was realised that miglustat was capable of reducing sphingosine in cells (Haslett et al., Unpublished); this has also been observed in the CSF of patients treated with miglustat (Wassif et al., Unpublished) and cat models of NPC1 (Stein et al., 2012). Interestingly however, miglustat does not reduce the storage of lipids such as cholesterol and LBPA and, even, increases sphingomyelin storage. This is proposed to involve a secondary defect in the enzyme which catabolises sphingomyelin in lysosomes, acid sphingomyelinase (ASM). This enzyme is not located in the same compartments as storage lipids and therefore cannot catabolise them. Miglustat does not correct this mislocalisation and as such sphingomyelin cannot be broken down and accumulates, trapping cholesterol in molecular interaction (Haslett *et al.*, Unpublished). Without this secondary defect in ASM localisation it is proposed that Miglustat reduces sphingosine resulting in increases in lysosomal Ca^{2+} and endolysosomal trafficking (improvements that are present in NPC patient cells treated with miglustat (Lachmann et al., 2004)) resulting in reduced lipid storage. This may explain why cholesterol accumulation in Q120 HTT ST14A cells was reduced after miglustat treatment. A similar correction to this has also been shown in cellular models of SLOS where the accumulation of endocytosed cholesterol in the endolysosomal system can be reduced by miglustat treatment (Lloyd-Evans *et al.*, Unpublished.)

In addition to an, as yet, undefined mechanism of action there are other problems with miglustat therapy such as poor blood-brain barrier (BBB) permeability. This is demonstrated in a case report of an NPC patient treated with miglustat where the concentration in the CSF was far below that in the serum (Lachmann et al., 2004). Nevertheless, benefit was observed when NPC deficient cells were treated with CSF relevant concentrations of miglustat (0.15μM), as opposed to the normal experimental concentration of 50μM; the improvement simply took longer to manifest (Haslett et al., Unpublished). This is further evidence that the potential for earlier intervention with miglustat in Huntington's patients may be beneficial.

It is also important to consider that as a form of SRT acting upon glycosphingolipids miglustat will reduce the synthesis of gangliosides. These may already be reduced in Huntington's. As previously discussed the potential for other species of ganglioside to be elevated in Huntington's and the possibility that they may accumulate in the endolysosomal system could potentially mean that the improvements in endocytic trafficking may benefit this aspect of lipid dyshomeostasis. Nevertheless, this phenotype of reduction in certain species of ganglioside and the impact miglustat will

have upon this must be carefully considered in any instance of miglustat therapy for Huntington's.

Taken into consideration all the points raised above still suggest that miglustat may be a useful therapy for the treatment of patients with Huntington's disease; a disease which does not currently have a disease modifying treatment.

Chapter 5

Investigation of Ca^{2+} dyshomeostasis in Genetically Influenced forms of Parkinson's Disease

5.1. – Introduction

5.1.1. – Parkinson's Disease

Parkinson's disease is progressive neurological disorder characterised by motor phenotypes first described by James Parkinson in 1817 in "An essay on the shaking palsy (Kempster et al., 2007). Although the cardinal features of Parkinson's: resting tremor, bradykinesia, rigidity, postural instability all describe motor phenotypes, a large number of non-motor phenotypes have been described in patients with the disease in addition to a diverse array of additional motor phenotypes. Non-motor phenotypes may include behavioural disorders, autonomic dysfunction and sleep and sensory disturbances (Farlow et al., 2004). A sixfold increase in the risk of dementia has been reported in Parkinson's patients (Aarsland et al., 2005) and similar neuropathology has been found in patients with other forms of dementia (McKeith et al., 1996). In many cases non-motor phenotypes can be as disabling as motor phenotypes.

Parkinson's affects 1-2% of the population over the age of 65 and is the second most prevalent form of neurodegeneration (Nuytemans et al., 2010); the incidence is predicted to double by 2030 (Dorsety et al., 2007). Parkinson's onset is usually around the age of 60 years. In a generalised scheme patients presenting before age 20 years are considered juvenile onset, those before 50 years early onset and those after this age late onset (Farlow *et al.,* 2004). Parkinson's disease is considered to be of multifactorial aetiology, with environmental exposure to substances such as pesticides and metals implicated in increased disease risk (Goldman, 2014). However, cases of familial Parkinson's have been described and, more recently, genes which predispose patients to Parkinson's have been identified (De Rosa et al., 2015), these will be discussed in section 5.1.2.

The neuropathology of Parkinson's disease is primarily characterised by the loss of dopaminergic neurons which project to the putamen from the substantia nigra pars compacta (SNpc). These neurons form the dopaminergic nigrostriatal pathway which is particularly involved with the production and regulation of movement. In addition to this neuron loss remaining neurons contain filamenteous, proteinaceous inclusions in the perikarya. These inclusions are known as Lewy bodies and smaller inclusions in neuronal processes are known as Lewy neurites, both are primarily composed of the

protein α-synuclein (Dickson, 2012). More recently, smaller inclusions of α-synuclein have been reported in the synaptic compartments of neurons raising the question of smaller aggregates causing pathogenic processes (Kramer and Schulz-Schaeffer, 2007). This may support observations made in relation to Alzheimer's and Huntington's diseases suggesting that larger aggregates of protein are protective to neurons by reducing the amount of smaller, more pathogenically active, aggregates or toxic soluble protein present (Nilsberth et al., 2004; Arrasante et al., 2004). Lewy bodies have been identified throughout the central, and in some cases, peripheral nervous systems in patients with Parkinson's (Braak and Del Tredici, 2009) and in a number of other neurodegenerative diseases such as Dementia with Lewy Bodies, a disease which has both Parkinson's and Alzheimer's phenotypes (McKeith et al., 2004).

Parkinson's is characterised by neuronal loss in selective populations of vulnerable neurons. Specifically these are the Dopaminergic neurons of the substantia Nigra pars compacta (SNpc) which project into the putamen as part of the nigrostriatal pathway. (Dickson, 2012) The result is loss of striatal dopamine and dysregulation of this pathway which is important for movement (Dauer and Prezdborski, 2006). Due to this Parkinson's patients are often treated with L-DOPA a blood-brain barrier (BBB) permeable precursor of dopamine which can be converted within the CNS into dopamine. To prevent the excessive peripheral production of noradrenaline from L-DOPA this drug is commonly co-administered with compounds that inhibit this process in the periphery. Unfortunately, a number of motor and non-motor side effects are caused by long term administration of L-DOPA. As such research for new therapies for Parkinson's remains an active field (Bastide et al., 2015).

Interestingly protoplasmic astrocytes of the SNpc are shown to have numerous interactions with DA neurons (Halliday and Stevens 2011). In Parkinson's astrocyte-neuronal crosstalk has been described as a 'double-edged sword' with astrogliosis providing both protection and damage to neuronal populations (Cabezas et al., 2013). Increases in Ca^{2+} excitability of astrocytes has been shown to be a consequence of pharmacological disruption of dopamine transmission in a model of Parkinson's. These remain to be investigated in genetic models of Parkinson's disease (Vaarman et al., 2012).

5.1.2. – Inherited forms of Parkinson's disease

Although there have long been indications that some forms of Parkinson's were familial it is only with the advent of new genetic technologies that inherited forms of Parkinson's have been clearly defined. Of these genes mutations in both SNCA and LRRK2 lead to autosomal dominant Parkinson's. *SNCA* codes for the major constituent of Lewy bodies, α synuclein, and *LRRK2* which codes for leucine rich repeat kinase 2 (LRRK2). There are also autosomal recessive forms of PD caused by inherited mutations in *PARKIN*, *PINK1*, *DJ-1* and *ATP13A2*. Subsequently each of these genetic loci were designated PARK along with a number defining their chronological identification (De Rosa et al., 2015). The identification of genes for all these loci remain incomplete and only the six loci mentioned above have been confirmed to cause monogenic Parkinson's. For clarity I will continue to use the original gene names. Collectively these genes are though to only account for 3-10% of Parkinson's cases (De Rosa et al., 2012) and this, perhaps, illustrates that Parkinson's is a disease of multifactorial aetiology resulting from a complex interplay of multiple factors. In most patients the majority of these remain unknown. Considering this, polymorphisms which increase the risk of Parkinson's may also be present in many patients. Accordingly genome wide association studies (GWAS) are beginning to reveal these associations (Mullin and Schapira 2015). The most prominent of these risk factors to be identified so far is within the *GBA1* gene (Sidransky et al., 2009) which is the genetic cause of Gaucher disease (section 1.5.1.).

5.1.2.1. – *GBA1* and Parkinson's

Polymorphisms at the *GBA1* locus increase the risk of Parkinson's 5 fold (Sidransky et al., 2009). Although this risk was confirmed by GWAS studies the initial observation of type 1 Gaucher patients suffering from the symptoms of Parkinson's disease was published in 1996 (Neudorfer et al., 1996). This was likely to inform the suggestion in 2003 that mutations in the glucocerebrosidase (GCase) gene *GBA1* could cause susceptibility to Parkinson's made by the Sidransky group (Lwin et al., 2004). In this study Parkinson's patients were found to have the N370S mutation, which causes type 1 Gaucher, and Parkinson's phenotypes were observed in the absence of brain storage of glucosylceramide (Lwin et al., 2004). Subsequent studies

showed the prevalence of Parkinson's in 10 unrelated families of patients with Gaucher disease partitioned into carriers of *GBA1* mutations, and, that the most common genetic cause of Parkinson's (G2019S causing mutations in *LRRK2*) was not present in these patients (Eblan et al., 2006). While these observations were compelling it was suggested that this incidence may be associated with Jewish ancestry (Clark et al., 2005). In 2009 (Sidransky et al., 2009) performed a multicentre analysis of *GBA1* mutations in 5691 Parkinson's patients alongside 4898 healthy individuals which confirmed polymorphisms in *GBA1* to be a pan-ethnic risk factor for Parkinson's, a finding confirmed by subsequent GWAS studies. It is interesting to note that Parkinson's patients who carried *GBA1* mutations presented, on average 4 years earlier, with less severe bradykinesia and resting tremor but more severe cognitive changes (Sidransky et al., 2009). Considering this, it is perhaps not surprising that a subsequent multicentre analysis also found *GBA1* to be a risk factor for dementia with Lewy bodies (Nalls et al., 2013).

Although mutations in *GBA1* are now well defined as a risk factor for Parkinson's disease and, perhaps, α-synucleinopathy in general (Sardi., 2015) the mechanism causing this risk has not been delineated. Of particular interest in this regard is whether or not the substrate of glucocerebrosidase (GCase), the protein product of *GBA1*, is accumulating. As it has been reported that only 11-15% of normal enzyme activity is required in order to prevent the accumulation of glucosylceramide (GlcCer) (Schueler et al., 2004) it can be proposed that lipid accumulation cannot occur in carriers of GBA1 mutations where enzyme activity is > 50%. A number of hypotheses have been mooted to explain this with many focussing on impairment of lysosomal function slowing down the clearance of aggregate prone proteins (Bendikov-Bar et al., 2014). Other explanations propose disturbed Ca^{2+} homeostasis within cells may be responsible (Schondorf et al., 2014) or that GCase and α-synuclein interact and a bidirectional pathogenic feedback loop is caused by increases in α-synuclein oligomerisation and accumulation of GlcCer (Mazzulli et al., 2011). One feature of these hypotheses is that they do not necessarily point specifically to *GBA1* mutations as the sole cause; even if loss of GCase function is occurring this could be the result in mutation within other lysosomal proteins. An example of this is mutations in *SCARB2,* which codes for LIMP-2, the protein responsible for trafficking GCase to the lysosome; this has also been implicated as a risk factor for Parkinson's (Hopfner et al., 2013).

5.1.2.2. – An expanding role for the lysosome in Parkinson's disease

The role of lysosomal proteins other than GCase in Parkinson's was thoroughly examined by Shachar et al. (2011) in a comprehensive literature review. In this study literature related to individual LSDs was studied to determine if there was a prevalence of Parkinson's in the patients and carriers of this LSD (or their extended families), documented evidence of SN pathology or the presence of synucleinopathy, ubiquitin carboxyl-terminal esterase L1 (UCH-L1) downregulation, increased presence of ubiquitinated protein aggregates and, finally, evidence of decreases in the activity of the lysosomal protein in question in Parkinson's patients. After undertaking this analysis the authors concluded that the biochemical and cellular pathways linking Parkinson's to LSDs should not be solely restricted to Gaucher (Shachar et al., 2011). Recent genetic analyses have supported this conclusion with genes such as *SMPD1* which causes the LSD Niemann-Pick type A also being implicated as a genetic risk factor for Parkinson's (Gan-Or et al., 2015). Accordingly, the broader implications of lysosomal dysfunction are becoming an area of intense research in relation to Parkinson's pathogenesis. It is interesting that in their recent review De Rosa et al. (2015) highlighted five different pathways that were implicated in Parkinson's pathogenesis by the array of genes known to cause the disease. Of these impairment of cellular clearance pathways is clearly linked to the lysosome, and the other pathways (mitochondrial homeostasis, ER stress, ER Ca^{2+} homeostasis, inflammation)(De Rosa et al., 2015) are all affected in various lysosomal diseases (Platt et al., 2012). As with the other neurodegenerative diseases discussed so far the lysosome, as an important hub for many cellular processes lying at the centre of the greater lysosomal network, may be important to a number of pathological processes in Parkinson's.

Recently, studies have begun to highlight lysosomal Ca^{2+} dyshomeostasis in genetic models of Parkinson's and investigated the links between changes to this cellular store of Ca^{2+} and ER Ca^{2+} stores. In this regard, the role of LRRK2 as a modulator of lysosomal Ca^{2+} homeostasis with downstream effects on autophagy has been determined (Gomez-Suaga et al., 2012). As LRRK2 has also been observed within the endolysosomal system (Gomez-Suaga et al., 2014), can act as a modulator of both endocytic trafficking (Gomez-Suaga et al., 2014) and lysosomal positioning (Dodson et al., 2012) it is likely to play a role in the normal functioning of this system.

Recent studies have implicated the TPC2 channel pathogenesis resulting from *LRRK2* mutation as Ca^{2+} release from lysosomes stimulated by NAADP-AM was increased in patient fibroblasts carrying the most common *LRRK2* mutation G2019S. In these cells endolysosomal system enlargement was observed alongside increased perinuclear clustering, a phenotype also observed in a *D.melanogaster* model of LRRK2 induced Parkinson's (Dodson et al., 2012). These defects were corrected by inhibition with of TPC2 with Ned-19 and localised buffering of exaggerated Ca^{2+} release (Hockey et al., 2015). The close interaction between lysosomes and the ER suggest that any potentiation of signals from TPC2 will induce ER Ca^{2+} release events, and thus, they impact upon ER Ca^{2+} homeostasis (Penny et al., 2015).

Interestingly, the two LSD proteins most strongly linked to Parkinson's are GCase and ASM which cause the LSDs Gaucher and Niemann-Pick type A/B respectively. Both these LSDs have been shown to cause elevated Ca^{2+} release from the ER and subsequently elevated cytosolic Ca^{2+} (Platt et al., 2012). The other two LSDs most strongly associated with ER Ca^{2+} phenotypes are the GM1 and GM2 gangliosidoses and in the case of both of these diseases LSD patients and carriers with Parkinson's have been observed (Shachar et al., 2011).

Considering the implication of ER Ca^{2+} in a number of models of genetic susceptibility to Parkinson's, it is worth investigating Ca^{2+} homeostasis in the ER. Also, due to the close relationship and interaction with the ER (Penny et al., 2015), it would be interesting to investigate the lysosome in any novel models of Parkinson's disease caused by proteins which interact with this compartment.

5.1.3. – Kufor-Rakeb Syndrome

Inherited mutations in *ATP13A2* (a 26kb gene with 29 exons located at 1p36.13) are the cause of Kufor-Rakeb syndrome (KRS). This is a rare form of juvenile Parkinson's disease (Ramirez et al., 2006). The protein product of the gene, also called ATP13A2, is a P-type transport ATPase, which localises to the lysosomal membrane. It was first reported in five siblings of unaffected consanguineous parents from a Jordanian community known as Kufor-Rakeb (Hampshire et al., 2001). The *ATP13A2* gene was subsequently identified by Ramirez *et al*. in 2006 after they found compound heterozygous mutations in the gene in patients with similar phenotypes from another consanguineous family. After this finding they also found

ATP13A2 mutations in the Jordanian community for which the disease is named (Ramirez et al., 2006). Since this time around 30 additional patients have been identified with KRS (Yang and Xu, 2014) and the gene was given the moniker *PARK9,* due to the universal presence of Parkinson's in these patients (Park et al., 2015).

Due to the fact that KRS has only been recently identified and genetically characterised it is unknown what the carrier frequency and disease incidence is. It is also currently unclear whether or not carriers of *ATP13A2* are more at risk of suffering from Parkinson's as in some populations no increase in *ATP13A2* mutations within patients has been reported (Pan et al., 2015). Other studies have found such an increase and consider *ATP13A2* to be a risk gene and age of onset modifier in Parkinson's (Di Fonzo et al., 2007; Chen et al., 2011). The majority of these studies were performed in relatively small patient datasets from single countries analysing a single variant and, perhaps, the situation will not be clarified until it is investigated in a multicenter analysis similar to that which has shown *GBA1* to be a Parkinson's risk gene (Sidransky et al., 2009).

The major clinical observations in KRS patients: parkinsonism, supranuclear gaze palsy and cognitive impairment usually present before the age of 20 years with the oldest age of onset currently reported to be 30 years (Malakouti-Nejad et al., 2014; Park et al., 2015). Progression subsequent to disease onset varies widely with a generalised divide between slowly progressing disease over the course of years-decades, in patients with missense mutations, to rapid progression over the course of months in patients with frameshift mutations (Park et al., 2015). Parkinson's phenotypes suffered by KRS patients predominantly involve bradykinesia and ridgity and the prevalence of resting tremor is generally lower. Although patients initially respond well to L-DOPA therapy, it is common for side effects such as dyskinesia and hallucinations to develop soon after treatment begins (Park et al., 2015). Supranuclear gaze palsy has been reported almost universally in patients and is accompanied by slowness in saccadic eye movements (Hampshire et al., 2001; Malakouti Nejad et al., 2014). Cognitive impairment has also been reported in the majority of patients however it is not universal (Park et al., 2015). Histopathological examination of KRS patients has not been conducted to date due to the lack of availability of post-mortem tissue (Park et al., 2015). Recently there have, however, been observations of reduced ATP13A2 levels in the post mortem tissue biopsies from patients with sporadic Parkinson’s disease, compared to control brain tissue. In

this study it was also reported that the levels of ATP13A2 were elevated in surviving dopaminergic neurons, in these neurons ATP13A2 was found to be a constituent of Lewy bodies (Murphy et al., 2013).

5.1.3.1. – The ATP13A2 protein

As previously mentioned wild-type ATP13A2 localises to the lysosomal membrane, whereas, mutated forms associated with PD remain in the ER in all cases examined so far (Ramirez et al., 2006; Ugolino et al., 2011). Subsequent ER stress phenotypes are reported in these cells. When ATP13A2 is defective in cells a myriad of lysosomal phenotypes have been reported including lysosomal expansion, lipofuscin accumulation, lysosomal alkalinisation, reduced autophagic flux and changes to heavy metal ion homeostasis and proteolytic defects (Schneider et al., 2010; Dehay et al., 2012; Tsunemi et al., 2014).

Studies into heavy metal ion dyshomeostasis are commonly initiated by the likelihood that ATP13A2 is thought to be a divalent cation transporter, due to similarities to other proteins of the P5 ATPase family which transport these ions (van Veen et al., 2014). Thus far, ATP13A2 has been implicated in the transport of Mn^{2+}, Zn^{2+}, Fe^{2+} and Cd^{2+} (Schmidt et al., 2009; Schneider at al., 2012; Tsunemi et al., 2014) and it is thought that loss of function in this protein results in abnormal cation transfer between the cytosol and lysosomal lumen. Subsequently, lysosomal dysfunction occurs and deposition of cations in the brain is thought to trigger damaging metal-induced oxidative stress (Ramonet et al., 2012; Park et al., 2014). The changes in heavy metal ion homeostasis have also been linked to proteolytic defects which result in less efficient degradation of protein such as α-synuclein leading to the accumulation of this protein in neurons (Usenovic et al., 2012; Tsunemi et al., 2014). In this situation resultant changes in the lysosomal system, the induction of lysosomal storage phenotypes, and resultant defects in autophagy, are thought to occur (Usenovic et al., 2012; Tsunemi et al., 2014).

Unsurprisingly, mitochondria are affected by these processes and decreased ATP synthesis, increased lesioning of mitochondrial DNA, higher oxygen consumption rates and an increasingly fragmented mitochondrial network have been reported in patient fibroblasts (Grunewald et al., 2012; Park et al., 2014). Importantly, all these defects were corrected by re-expression of wild-type ATP13A2. Subsequent studies

showed that increase in intracellular Zn^{2+} could compound these phenotypes although they did not rule out changes to levels of other ions.

Recently, after review of the literature on ATP13A2 and other more well studied P-type ATPases, (van Veen et al., 2014) contended the view that ATP13A2 is a transporter for metal cations. They suggested instead that the protein may, instead, act as a flippase likely involved in lipid dynamics during membrane fusion and fission events. In a subsequent publication this research group proposed a 10 transmembrane domain membrane structure for ATP13A2 which included an extended hydrophobic N-terminus which interacts with the cytosolic side of the lysosomal membrane. Here the lipid can interact with the signalling lipids phosphatidic acid (PA) and phosphatidylinositol-3,5- bisphosphate (PI(3,5)P2). Upon interaction with these lipid autophosphorylation regulates the activity of ATP13A2, and, overexpression of catalytically active protein is protective against toxic insults to the mitochondria (Holemans et al., 2015).

It is interesting that Ca^{2+} homeostasis remains to be investigated in these cells as ATPases are prevalent in Ca^{2+} transport pathways and dyshomeostasis in these pathways is prevalent in genetic models of Parkinson's.

5.2. – Procedures

In section 5.3.1. of this chapter well will investigate Ca^{2+} homeostasis using the KRS patient fibroblasts described in section 2.1.8. These cells will be studied against a control fibroblast cell line which has been extensively characterised in the Lloyd-Evans lab with respect to cellular Ca^{2+} levels.

Cellular Ca^{2+} stores will be interrogated using the techniques described in section 2.5. Where possible 3 independent plating replicates will be used in these experiments and appropriate statistical analysis will be performed as detailed in individual figure legends. In instances where 3 independent plating replicates were not performed due to unavailability of cells this will be shown in the figure legend. In most cases this relates to the second patient cell line.

Subsequently, section 5.3.2., we will investigate the impact of intralysosomal heavy metal ion chelation on the most severe Ca^{2+} dyshomeostasis phenotypes observed in KRS cells using the chelator phytic acid as described in section 2.2.8. These will be subject to the same analyses as described for section 5.3.1.

Section 5.3.3. of this chapter will begin to investigate whether primary astrocytes have abnormal spontaneous Ca^{2+} signalling events in models of Gaucher disease. This analysis will utilise astrocytes prepared from both genetic Gaucher models (section 2.1.9.) and astrocytes independently prepared from control mice which have then had Gaucher phenotypes induced by a well characterised inhibitor of GCase (section 2.1.10.). As this analysis has so far been preliminary 3 independent replicates has not been achieved, repeat numbers are detailed in individual figure legends.

Statistical analyses as described in section 2.7 have been performed on all these experiments as appropriate, details of these are given in individual figure legends.

5.3. – Results

5.3.1. – Ca^{2+} dyshomeostasis is prevalent in multiple cellular Ca^{2+} stores in KRS patient fibroblasts

Recently, numerous publications have implicated lysosomal Ca^{2+} homeostasis in the pathogenesis of Parkinson's (Gomez-Suaga et al., 2014; Hockey et al., 2015). Due to the cellular location (Ramirez et al., 2006), proposed role in divalent cation homeostasis (Ramonet et al., 2012; Park et al., 2014) and implication of phosphoinisitols as regulators of the ATP13A2 protein (Holemans et al., 2015) we are interested to see if the lysosome or any other cellular Ca^{2+} stores were altered in KRS patient fibroblasts.

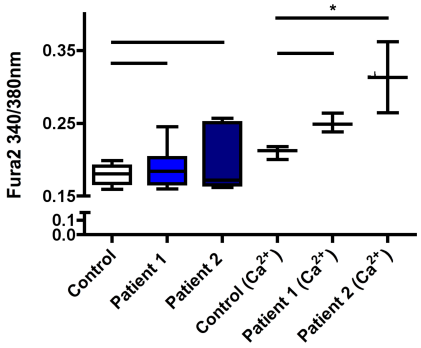

Figure 5.3.1. – Resting cytosolic Ca^{2+} in KRS patient fibroblasts in the presence and absence of extracellular Ca^{2+}. *Quantification of resting cytosolic Ca^{2+} measured by ratiometric quantification of Fura2 fluorescence in the absence of extracellular Ca^{2+} and presence of 1mM extracellular Ca^{2+} (Ca^{2+}). Error bars = range. Data shown is from individual cellular values in each experimental repeat. n = 8 for WT and Patient 1 cells in the absence of Ca^{2+}, n = 5 for Patient 2 cells in the ansence of Ca^{2+}, n = 3 for WT and Patient 1 cells in the presence of Ca^{2+} and n = 2 for patient 2 cell lines in the presence of Ca^{2+}. * = P < 0.05, calculated by one way ANOVA with Bonferroni post test.*

Initially, we observed the basal cytosolic Ca^{2+} levels in two KRS patient cell lines used in multiple publications on ATP13A2 (Dehay et al., 2012; Grunewald et al., 2012; Park et al., 2014) and are known to have inactivating mutations in ATP13A2 which result in the retention of misfolded protein in the ER (Ramirez et al., 2006). The mean basal Ca^{2+} level of both patient cell lines was comparable to the Ca^{2+} levels in a control fibroblast cell line (extensively characterised in studies of cellular Ca^{2+}) in the absence of extracellular Ca^{2+} in the imaging buffer. It can be observed, however, that there was a trend towards an increased range of Ca^{2+} levels in both patient cell lines.

Interestingly, in a preliminary investigation this range further increased when extracellular Ca^{2+} was present in the imaging buffer and a statistically significant change ($P < 0.05$, $t = 3.783$, $df = 2$) in the mean baseline between patient 2 cell lines and control fibroblasts were observed. This wil be investigated more thoroughly in future experiments.

Due to these observations, we began to investigate the content and signalling of the cellular Ca^{2+} stores. We began with the lysosome, as this organelle is implicated in KRS by the location of the ATP13A2 protein, and the prevalence of dysfunction in signalling from this store in other genetic cases of Parkinson's.

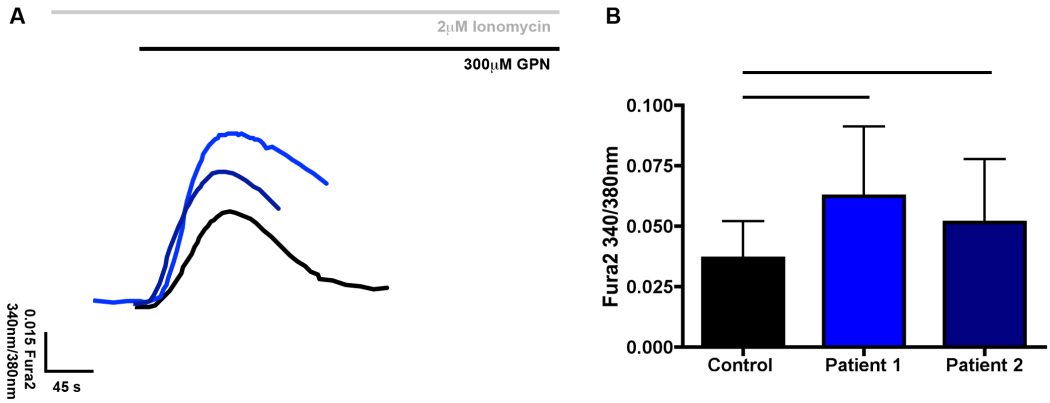

Figure 5.3.2. – Lysosomal Ca^{2+} release in response to GPN in KRS patient fibroblasts. *KRS patient fibroblasts after GPN induced lysosomal rupture in the presence of 2μM ionomycin.* ***A -*** *Representative traces of Ca^{2+} release in Fura2 loaded cells induced by 300μM GPN. Grey bar indicates the presence of ionomycin, black bar indicates the presence of GPN.* ***B –*** *Quantification of Ca^{2+} release measured by ratiometric change in Fura2 fluorescence. Error bars = SEM. n = 4 for control and patient 1 cells, n = 2 for patient 2 cells. No significant differences were observed as calculated by one way ANOVA with Bonferroni post test.*

In order to study total levels of Ca^{2+} in the lysosomes of KRS patient fibroblasts we used the well established method of GPN induced lysosomal lysis after removal of the other cellular Ca^{2+} stores by ionomycin treatment (Lloyd-Evans et al., 2008). Figure 5.3.2. shows that no statistically significant change in total lysosomal Ca^{2+} was observed by this method although, there was a trend for increased Ca^{2+} in both patient fibroblast cell lines accompanied by more variable levels of Ca^{2+} in the endolysosomal system. These observations are potentially interesting as an increase in lysosomal Ca^{2+} levels has been implicated in lysosomal diseases which have increased storage of autofluorescent material within lysosomes, MLIV (Waller-Evans

et al., In preparation) and CLN3 (Walker *et al.,* Unpublished), a phenotype which has been reported in cellular and animal models of KRS (Dehay et al., 2012; Schultheis et al., 2013; Wohlke et al., 2011). Accordingly, further study of the endolysosomal Ca^{2+} signalling in this disease is warranted.

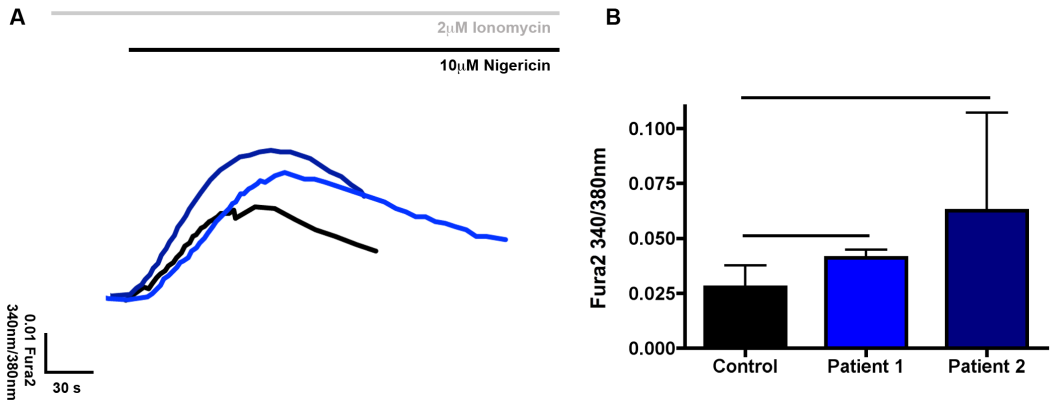

Figure 5.3.3. – Lysosomal Ca^{2+} release in KRS patient fibroblasts in response to nigericin. *KRS patient fibroblasts after nigericin induced lysosomal Ca^{2+} release in the presence of 2μM ionomycin.* ***A -*** *Representative traces of Ca^{2+} release in Fura2 loaded cells induced by 10μM Nigericin. Grey bar indicates the presence of ionomycin, black bar indicates the presence of GPN.* ***B –*** *Quantification of Ca^{2+} release measured by ratiometric change in Fura2 fluorescence. Error bars = SEM. n = 7 for control cells, n = 6 for patient 1 cells and n = 2 for patient 2 cells. No significant differences were observed as calculated by one way ANOVA with Bonferroni post test.*

A similar trend towards increased lysosomal Ca^{2+} was observed when nigericin was used to induce lysosomal Ca^{2+} release. Although this was again non-significant showing that there is no change in Ca^{2+} levels within this store this remains useful data as it shows an NPC-like phenotype does not occur in these cells.

As previously discussed although Ca^{2+} release after lysosomal lysis (GPN) or ionophore disruption (Nigericin) provides an accurate estimation of total Ca^{2+} levels it does not represent physiological lysosomal Ca^{2+} release. In order to do this we can use the lysosomal Ca^{2+} channel agonists NAADP-AM which stimulates the TPC2 channel on lysosomes (Ruas et al., 2015) and ML-SA1 which causes Ca^{2+} release from the endolysosomal TRPML1 channel (Shen et al., 2012).

In initial experiments after thapsigargin treatment to prevent subsequent CICR from the ER we observed Ca^{2+} release from TPC2 which reflected the Ca^{2+} levels observed in response to GPN (data not shown). This data suggests that any pH defect present in these cells is not as robust as that in PS1 deficient cells, as discussed in chapter 3, although further experimentation is required to confirm this as

very low Ca^{2+} release was observed from all cells at all NAADP-AM concentrations tested. NAADP-AM concentrations may need to be further optimised, as stimulation of the TPC2 channel by NAADP is subject to a bell-shaped curve meaning non-optimal concentrations may inhibit rather than stimulate release (Pitt et al., 2010). To investigate TPC2 response in a physiological setting, in which lysosomal Ca^{2+} release is intrinsically linked to ER Ca^{2+} release, we added NAADP-AM to cells without any pre-treatment to remove other cellular Ca^{2+} stores. This situation also mimics the conditions of recent experiments which implicate exaggerated NAADP evoked Ca^{2+} release in the pathogenic cascade which leads to Parkinson's as a result of LRRK2 mutations (Hockey et al., 2015).

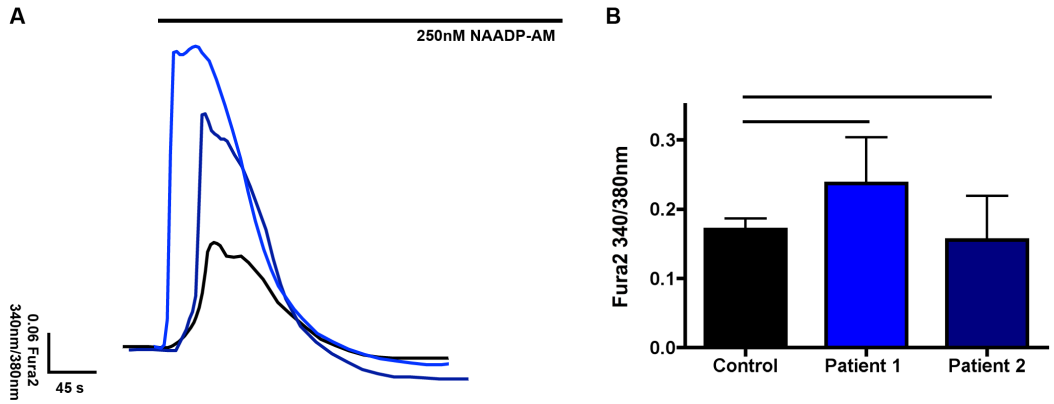

Figure 5.3.4. – Ca^{2+} response to NAADP-AM in KRS patient fibroblasts. A - *Representative traces of Ca^{2+} release in Fura2 loaded cells induced by 250nM NAADP-AM. Black bar indicates the presence of NAADP-AM.* ***B –*** *Quantification of Ca^{2+} release measured by ratiometric change in Fura2 fluorescence. Error bars = SEM. n = 3 for control and patient 1 cells, n = 2 for patient 2 cells. No significant differences were observed as calculated by one way ANOVA with Bonferroni post test.*

From this experiment it can be observed that no significant increase in Ca^{2+} release in response to NAADP-AM occurred in either of the patient cell lines. However, in a similar pattern to that observed in the other studies of lysosomal Ca^{2+}, a trend towards increased NAADP-mediated Ca^{2+} release was observed in patient 1 cells. This was not, however, replicated in cells from patient 2 although increased variability and a lower number of repeats conducted on these cells may account for this. The differences observed in these data are non-significant, however, the recurring pattern observed is suggestive of increased signalling from the lysosome which may impact upon other cellular Ca^{2+} stores. Importantly, robust Ca^{2+} release in response to NAADP-AM does not exclude a lysosomal pH defect in these cells. NAADP-AM is capable of evoking Ca^{2+} release in $PS1^{-/-}$ cells which have not been pre-treated with thapsigargin as even the minimal amount of Ca^{2+} released from

lysosomes in this situation causes CICR from the ER; this results in robust Ca^{2+} responses. Accordingly, to further study changes in NAADP-induced responses in these cells the size of the ER Ca^{2+} store must be compared. This may demonstrate if the potential increases seen after NAADP stimulation are caused by subsequent CICR.

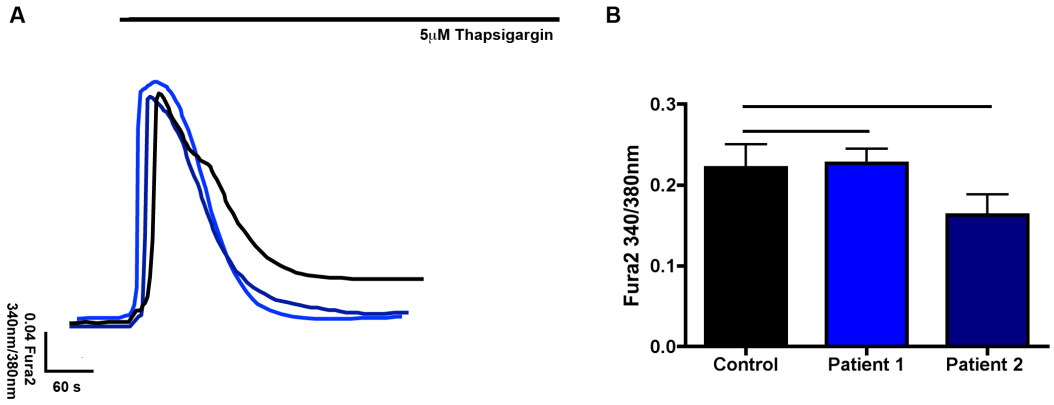

Figure 5.3.5. – Thapsigargin mediated ER Ca^{2+} release in KRS patient fibroblasts. A - *Representative traces of Ca^{2+} release in Fura2 loaded cells induced by 5μM thapsigargin. Black bar indicates the presence of thapsigargin.* ***B –*** *Quantification of Ca^{2+} release measured by ratiometric change in Fura2 fluorescence. Error bars = SEM. n = 4 for control cells, n = 6 for patient 1 cells and n = 4 for patient 2 cells. * = P<0.01, calculated by one way ANOVA with Bonferroni post test. No significant differences were observed as calculated by one way ANOVA with Bonferroni post test.*

As shown in figure 5.3.5. stimulation of Ca^{2+} release from the ER in KRS patient fibroblasts and controls reveals that CICR is unlikely to cause changes in NAADP-induced Ca^{2+} signalling. The overall size of Ca^{2+} release from the ER in response to completely inhibitory concentrations of thapsigargin (5μM) show no statistically significant differences. The trend towards increased Ca^{2+} release from patient 1 cells (figure 5.3.4.) is also not observed which suggests that any trends towards increases in Ca^{2+} signalling are initiated from the lysosomal Ca^{2+} store as the responses are more closely mimicked in experiments where only that store is being measured (figures 5.3.2. and 5.3.3.). It may also explain why there is a trend for lower Ca^{2+} release from patient 2 cells in response to NAADP (figure 5.3.4.) as there is also a trend for lower Ca^{2+} release from the ER. This would result in less potentiation of the signal as a result of CICR. In order to study the effects of TPC2 induced Ca^{2+} signalling in response to NAADP-AM upon CICR thapsigargin was used to induce Ca^{2+} release after cells had been treated with NAADP-AM.

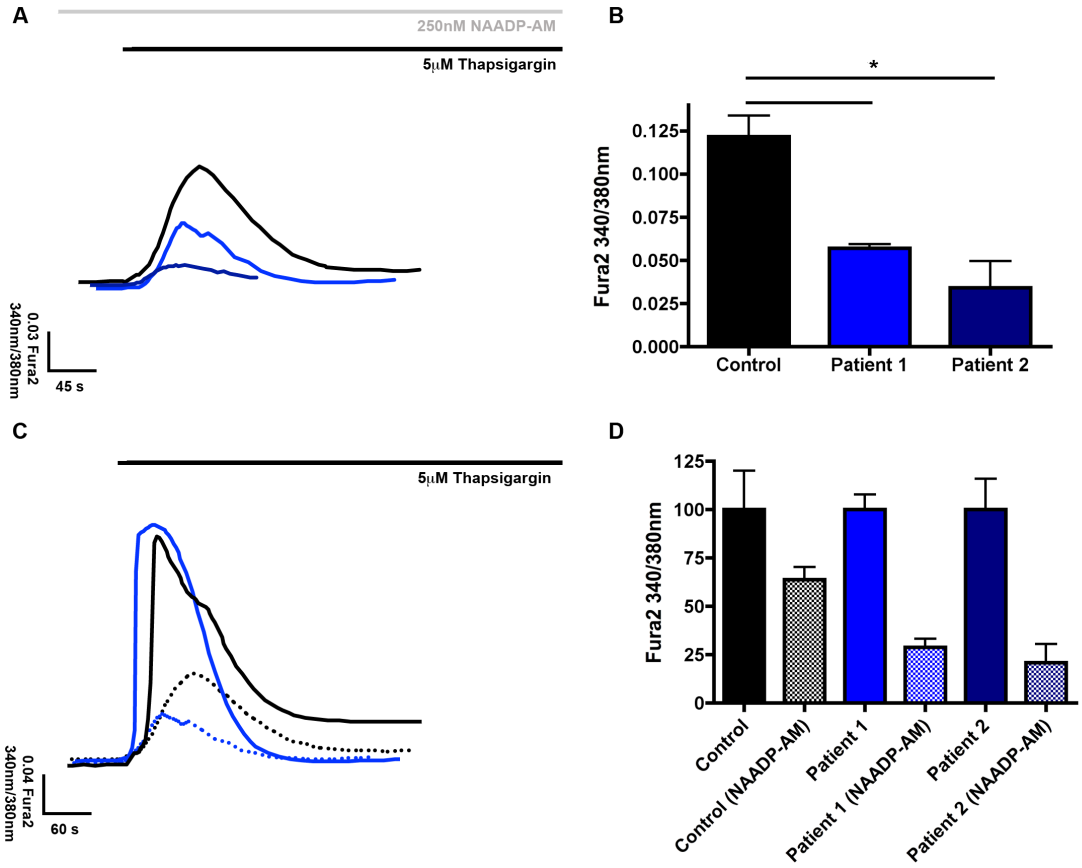

Figure 5.3.6. – Thapsigargin mediated ER Ca^{2+} release after NAADP-AM treatment of KRS patient fibroblasts. A - *Representative traces of Ca^{2+} release in Fura2 loaded cells induced by 5μM thapsigargin after pretreatment with 250nM NAADP-AM. Black bar indicates the presence of thapsigargin, grey bar indicates the presence of NAADP-AM.* ***B –*** *Quantification of Ca^{2+} release measured by ratiometric change in Fura2 fluorescence. Error bars = SEM. n = 3 for control cells, n = 2 for patient cell lines. * = P < 0.05, calculated by one way ANOVA with Bonferroni post test.* ***C –*** *Comparative representative traces of Ca^{2+} release in Fura2 loaded cells induced by 5μM thapsigargin in the absence (solid bar) and presence (dashed bar) of NAADP-AM.* ***D –*** *Quantification of the percentage of Ca^{2+} release measured by ratiometric change in Fura2 fluorescence in the presence and absence of NAADP-AM. Error bars = SEM. n = 3 for control cells, n = 2 for patient cell lines.*

As expected the ER Ca^{2+} release was reduced in all cells following NAADP-AM treatment compared to untreated cells, this is most clearly shown in figure 5.3.6. D. A clear trend of a larger reduction was observed in patient cell lines, this became significant in cells from patient 2 ($P < 0.05$, $t = 3.820$, $df = 2$). The increased impact of NAADP induced Ca^{2+} release on patient cell lines is strongly suggestive of increased CICR induced from lysosomal Ca^{2+} release. Representation of this data as a percentage of thapsigargin release prior to NAADP-AM induced release reveals subsequent Ca^{2+} release to be 25% or less as opposed to greater than 50%. A combination of these observations show that KRS cells may to have pathogenically hyperactive responses as a result of NAADP signals. These observations may underlie the greater variability in baseline Ca^{2+} observed in KRS patient fibroblasts.

The analysis of other Ca^{2+} channels may help elucidate if excessive signalling from the endolysosomal system or ER is the initiating factor in the Ca^{2+} hyper reactivity observed in KRS patient cells.

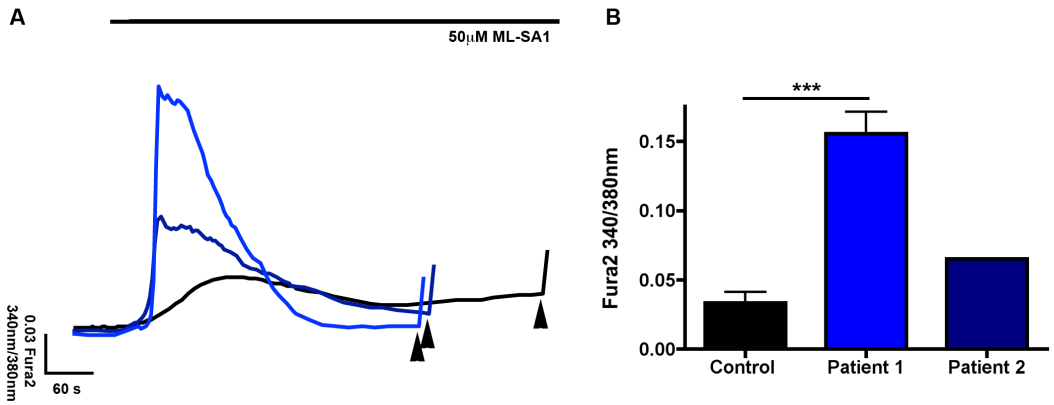

Figure 5.3.7. – ML-SA1 potentiated Ca^{2+} release in KRS patient fibroblasts. A - *Representative traces of Ca^{2+} release in Fura2 loaded cells induced by 50μM ML-SA1. Black bar indicates the presence of ML-SA1, black arrowheads indicate the addition of 5μM ionomycin to confirm cell viability.* ***B –*** *Quantification of Ca^{2+} release measured by ratiometric change in Fura2 fluorescence. Error bars = SEM. n = 4 for control cells, n = 8 for patient 1 cells and n = 1 for patient 2 cells. *** = P<0.001 calculated by T test.*

Utilising the synthetic agonist ML-SA1 we were able to observe increased Ca^{2+} release from the TRPML1 channel of over 2 fold in patient 1 cells. This increase was also evident in a preliminary experiment with patient 2 cells (5.3.7.). As previously discussed (chapter 3) this channel does not potentiate CICR from the ER to the same degree as that observed after NAADP-AM treatment (5.3.6). From our observations in $PS1^{-/-}$ cells it could be suggested that this potentiation of TRPML1 signalling supports the observation of lysosomal alkalisation by (Dehay et al., 2012), however, the trend towards increased lysosomal Ca^{2+} would suggest that a different mechanism underlies endolysosomal Ca^{2+} dyshomeostasis. It must also be noted that the control experiments we conducted to clarify that elevated response in $PS1^{-/-}$ cells was from the TRPML1 channel remain to be performed in these cells. Consequently other TRPM type Ca^{2+} channels cannot be excluded as the source of elevated Ca^{2+} signals. Interestingly, the presence of elevated lysosomal Ca^{2+} may be indicative of an MLIV like Ca^{2+} pathology in KRS patient cells. MLIV Ca^{2+} pathology is primarily characterised by an increase in endolysosomal Ca^{2+}. This is accompanied by increased variability in the store due to the presence of a small number of large Ca^{2+} rich vesicles thought to be persistent homotypic organelles which result from disruptions in the separation of lysosomes and late endosomes (Waller-Evans *et al.* In preparation). Other hallmarks of cellular pathology in this disease is the

accumulation of autofluorescent material in the endolysosomal system (Jennings et al., 2006) – a phenotype observed in KRS cells (Dehay et al., 2012). In order to determine if phenotypes are present in KRS cells intraluminal Ca^{2+} measurements should be performed to determine if any large Ca^{2+} rich vesicles are present.

Another disease in which lysosomal Ca^{2+} is elevated and elevated release from this store has been implicated in cellular pathology is CLN3 disease. It has recently been reported in our lab that cells expressing a mutant form of the CLN3 protein which leads to ER retention are more susceptible to Ca^{2+} release in response to low concentrations of thapsigargin (Chandrachud et al., 2015).

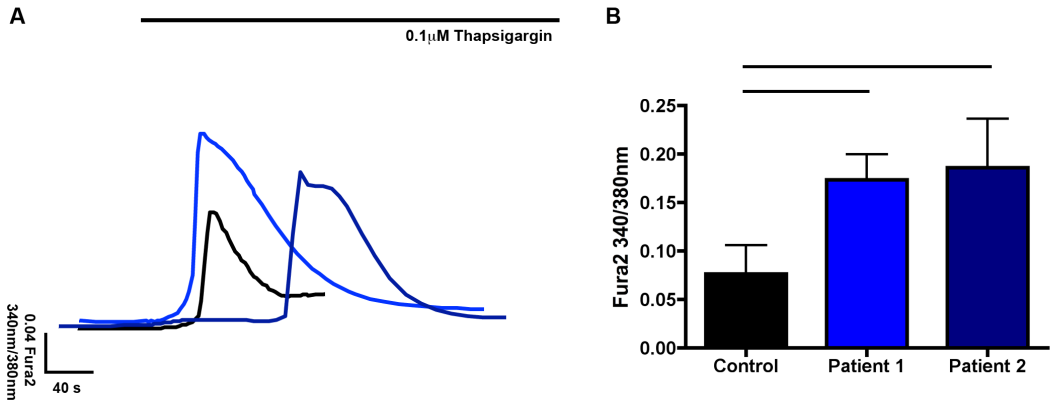

Figure 5.3.8. – Effect of low concentrations of thapsigargin in KRS patient fibroblasts. ***A -*** *Representative traces of Ca^{2+} release in Fura2 loaded cells induced by 0.1μM thapsigargin. Black bar indicates the presence of thapsigargin.* ***B –*** *Quantification of Ca^{2+} release measured by ratiometric change in Fura2 fluorescence. Error bars = SEM. n = 5 for control cells, n = 5 for patient 1 cells and n = 3 for patient 2 cells. No significant differences were observed as calculated by one way ANOVA with Bonferroni post test.*

As can be seen in figure 5.3.8. a trend towards more substantive Ca^{2+} release was observed from patient fibroblasts in relation to control cells. Interestingly, once Ca^{2+} release was initiated in these cells the subsequent release proceeded at comparable rates; there was, however, observable variability in the time after thapsigargin addition that release occurred, this has not yet been analysed. As increased Ca^{2+} release may be indicative of ER stress in response to misfolded ATP13A2 protein retained within this organelle (Ugolino et al., 2011) this phenotype should be further studied by subsequent experimental repeats. This phenotype could also be further investigated using IHC against targets such as TMED4 as this protein can be used as a marker of ER stress in CLN3 mutant cells (Walker et al., unpublished). Increased sensitivity to ER Ca^{2+} release observed in fig 5.3.8. may also be indicative of the ability of the ER to more readily potentiate Ca^{2+} transients originating from

other sources in KRS patient fibroblasts and, as such, contribute to Ca^{2+} dyshomeostasis. As this dyshomeostasis seems to also be potentiated by the addition of Ca^{2+} to the extracellular milieu an interesting phenotype to investigate would be store-operated Ca^{2+} entry (SOCE) which is governed by the interaction of the STIM protein with the ORAI channel; this is stimulated by the emptying of ER Ca^{2+} stores.

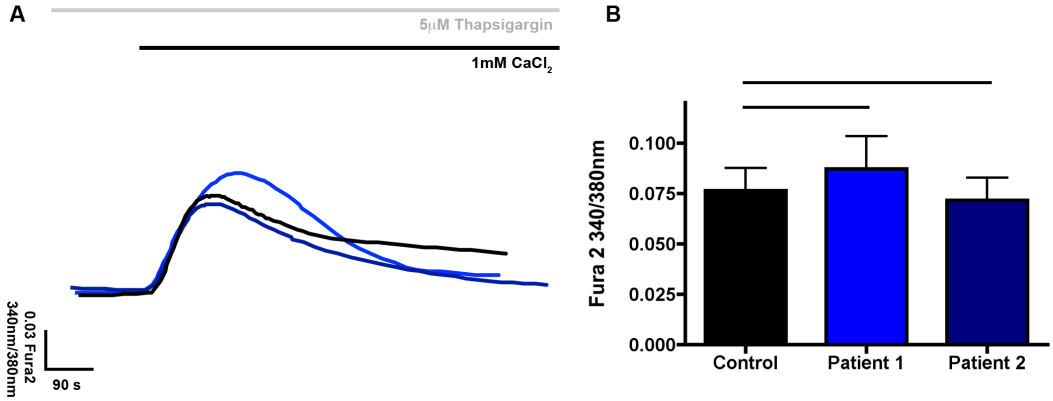

Figure 5.3.9. – SOCE in KRS patient fibroblasts. A - *Representative traces of Ca^{2+} influx in Fura2 loaded cells after the addition of 1mM Ca^{2+} after ER Ca^{2+} release had been induced by 5μM thapsigargin. Black bar indicates the presence of $CaCl_2$, grey bar indicates the presence of thapsigargin.* ***B –*** *Quantification of Ca^{2+} release measured by ratiometric change in Fura2 fluorescence. Error bars = SEM. n = 5 for control cells, n = 5 for patient 1 cells and n = 4 for patient 2 cells. No significant differences were observed as calculated by one way ANOVA with Bonferroni post test.*

Analysis of the levels of SOCE in patient and control cell lines reveals a similar pattern between cells to that observed when total ER Ca^{2+} levels were analysed (figure 5.3.9.), similarly, none of the differences observed are statistically significant. This indicates that this process is proceeding normally within cells as the changes observed are likely to be related to the size of the initial store. Accordingly, it suggests that STIM and ORAI interact normally to facilitate SOCE, and, ER stimulated Ca^{2+} influx is not responsible for the changes in basal Ca^{2+} levels in KRS patient fibroblasts observed when extracellular Ca^{2+} is present. Another, as yet, undefined mechanism may underlie this phenotype.

Further investigation of ER Ca^{2+} homeostasis in KRS cells may also be achieved by direct stimulation of ER Ca^{2+} channels. For example, stimulation of the ryanodine receptor by its eponymous agonist ryanodine. This channel is of particular interest as it has been shown to be dysregulated in cell lines and tissue samples obtained from LSD patients (Lloyd-Evans et al., 2003; Pelled et al., 2005).

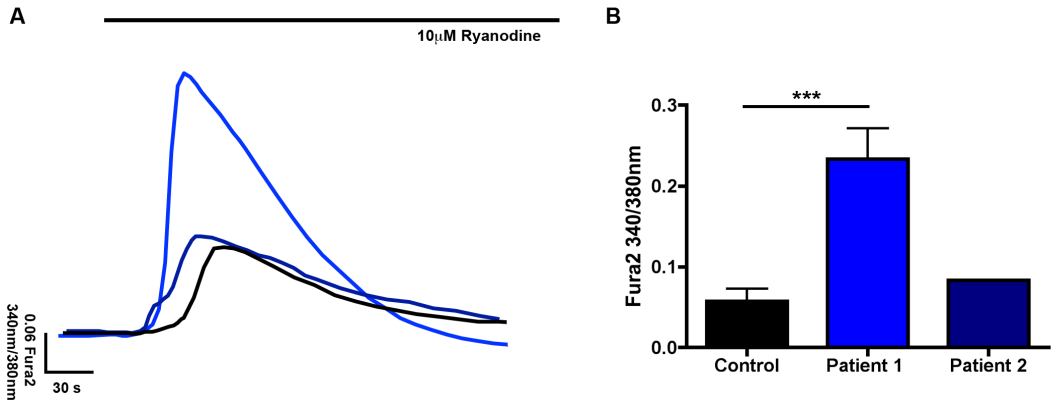

Figure 5.3.10. – Ca^{2+} release from the ryanodine receptor in KRS patient fibroblasts. A - *Representative traces of Ca^{2+} response in Fura2 loaded cells after the addition of 1mM Ca^{2+} after ER Ca^{2+} release had been induced by 5μM thapsigargin. Black bar indicates the presence of $CaCl_2$, grey bar indicates the presence of thapsigargin.* ***B –*** *Quantification of Ca^{2+} release measured by ratiometric change in Fura2 fluorescence. n = 9 for control cells, n = 8 for patient 1 cells and n = 1 for patient 2 cells. *** = P<0.001, calculated by T test.*

Figure 5.3.10. clearly shows that Ca^{2+} release from the ryanodine receptor is significantly higher in fibroblasts from KRS patient 1 ($P < 0.001$, $t = 4.467$, $df = 15$) with a trend for increased response in patient 2 from a single repeat. As the total levels of Ca^{2+} in the ER are relatively similar to control levels in both patient cell lines it appears that release from the ryanodine receptor is potentiated by an, as yet, undefined mechanism. An attractive proposition is that this mechanism of potentiation may involve low levels of glucosylceramide in the ER, as has been observed in Gaucher disease, perhaps providing links between the protein defective in this disease (GCase) and ATP13A2 – this remains to be investigated.

The final cellular Ca^{2+} store which we are currently able to analyse are the mitochondria. As these organelles are known to buffer cytosolic Ca^{2+} levels by Ca^{2+} influx. This store is particularly interesting in KRS, as numerous publications have reported mitochondrial defects in cell deficient in ATP13A2 (Grunewald et al., 2012; Park et al., 2014). One way to induce mitochondrial Ca^{2+} release is depolarisation of mitochondria with rotenone, which leads to Ca^{2+} efflux. Recently, it has been reported that expression of catalytically active ATP13A2 is protective against rotenone induced toxicity (Holemans et al., 2015) so it is of particular interest to look at the Ca^{2+} release induced by rotenone in cells which do not have functional ATP13A2.

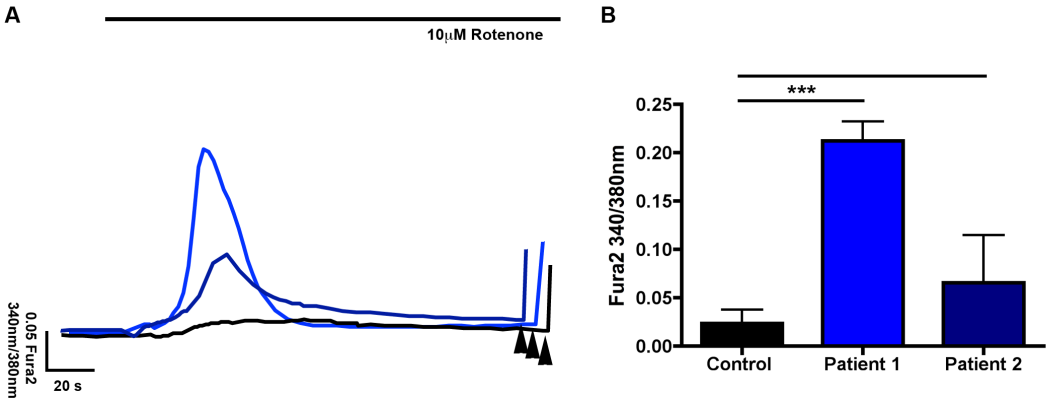

Figure 5.3.11 – Ca^{2+} release from mitochondria in response to rotenone induced depolarisation in KRS patient fibroblasts. A - *Representative traces of Ca^{2+} responses in Fura2 loaded cells after the addition of 10μM rotenone. Black bar indicates the presence of rotenone. Arrowheads indicate the addition of 5μM ionomycin to confirm cell viability.* ***B –*** *Quantification of Ca^{2+} release measured by ratiometric change in Fura2 fluorescence. Error bars = SEM. n = 6 for control cells, n = 8 for patient 1 cells and n = 3 for patient 2 cells. *** = P<0.001, calculated by one way ANOVA with Bonferroni post test.*

As can be seen in figure 5.3.11. Ca^{2+} release induced by rotenone in cells was significantly elevated in the cell line from patient 1 ($P < 0.001$, $t = 5.926$, $df = 12$) and there was a trend towards elevation in the preliminary experiment conducted in patient 2 cells. Over a four fold elevation was observed in cells from patient 1. As mitochondrial Ca^{2+} overload and subsequent signalling events is a pro-apoptotic event, and functional ATP13A2 is protective against this, the substantial elevations in Ca^{2+} response may represent a contributing factor to the proposed dopaminergic neuron loss in ATP13A2. This may be important as mitochondrial dysfunction is pre-eminent in pathogenic cascades associated with Parkinson's, and, can be caused by elevated cytosolic Ca^{2+}. Nevertheless, this phenotype should be confirmed by In situ measurement of mitochondrial Ca^{2+} in KRS patient fibroblasts especially as subsequent experiments in which ER Ca^{2+} agonists were added after rotenone stimulated Ca^{2+} release resulted in substantially reduced Ca^{2+} release (data not shown). These levels were in excess of that shown after NAADP-AM, this suggests that some of this Ca^{2+} release originated from the ER. It is important to note, however, that the most likely method to potentiate ER Ca^{2+} release after rotenone depolarisation of mitochondria is by CICR, suggesting that Ca^{2+} efflux from mitochondria is increased in patient cells as they are initially overloaded with Ca^{2+}. Unfortunately, it is difficult to isolate Ca^{2+} signalling events after mitochondrial depolarisation, as we are able to do for the lysosome, ionophores such as ionomycin cause release from mitochondria and agonists which release Ca^{2+} from the ER result in increased mitochondrial Ca^{2+} due to their activity as a cytosolic Ca^{2+} buffer.

When this buffering capacity of mitochondria is considered, alongside the propensity for KRS patient cells to have higher levels of cytosolic Ca^{2+} , it would suggest that this phenotype may be pathogenically important. This will be further discussed in section 5.4.2. It may be of interest to study cytochrome C release and assay for caspase activation in these cells as both caspase 3 and 7 activity has been shown to increase in cells from KRS patients (Radi et al., 2012); it would be interesting to see if these differences were exacerbated by increased Ca^{2+} from any of the sources discussed above.

Taken together the above data clearly indicates Ca^{2+} dyshomeostasis in multiple cellular stores, many of which have been implicated in KRS pathogenesis in different cellular models. Although further work remains to temporally resolve these dyshomeostatic events we thought it would be interesting to see if lysosomal heavy metal ion homeostasis could play a role in any of these phenotypes.

5.3.2. – Preliminary observations of chelation of lysosomal heavy metals reducing excessive Ca^{2+} signalling events from the ER and mitochondria in KRS patient fibroblasts.

Heavy-metal homeostasis has been implicated in KRS since the discovery of ATP13A2 as the molecular cause of the disease (Ramirez et al., 2006). Numerous publications have further implicated divalent metal ions in the pathogenic cascade of events which lead to KRS (Schneider et al., 2010; Ramonet et al., 2012; Tsunemi et al., 2014; Park et al., 2014). It is, however, very difficult to accurately determine the identities of many ions using fluorescent probes as they generally display a high degree of promiscuity with respect to the species of ion they interact with. In preliminary experiments we were able to observe quenching of Fura2 loaded specifically into the endolysosomal system. This has previously been used as an assay for Mn^{2+} accumulation, although it is not specific for this ion (Kwakye et al., 2011; Kress et al., 2012).

Whilst chelators can be added to cells loaded with these probes to improve specificity, many of these do not function properly in the lysosome due to the highly acidic environment. One chelator which has been shown to be effective in the lysosome is phytic acid (Maguire *et al.* unpublished). Although this chelator is non-

specific it does chelate a number of ions implicated in KRS pathology, and, will do so preferentially within the lysosome. Accordingly, we can use it in order to see if heavy metal ion accumulation within the lysosomal lumen is important to disease phenotypes reported in KRS. We are particularly interested to see if we can reduce any of the Ca^{2+} dyshomeostasis events described above. As such, we have used the two assays above which provided us with the most striking differences between KRS patient and control fibroblasts. These are ryanodine mediated ER Ca^{2+} release and Ca^{2+} release from the mitochondria as a result of depolarization by rotenone.

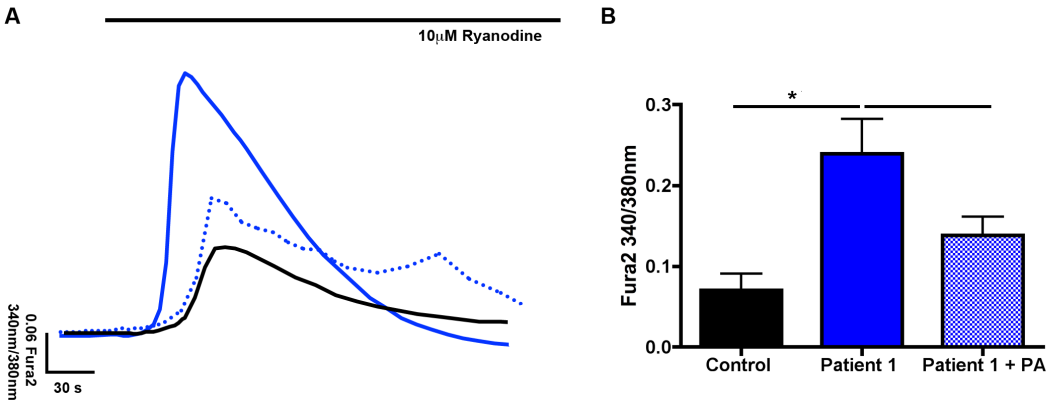

Figure 5.3.12. – Effect of phytic acid treatment on Ca^{2+} release from the ryanodine receptor in KRS patient fibroblasts*. Cells were treated with 1mM phytic acid for 14days.* ***A -*** *Representative traces of Ca^{2+} response in Fura2 loaded cells after the addition of 10μM ryanodine.* ***B –*** *Quantification of Ca^{2+} release measured by ratiometric change in Fura2 fluorescence. Error bars = SEM. n = 6 for control cells, n = 7 for patient 1 cells and n = 3 for phytic acid treated cells. * = P<0.05, calculated by one way ANOVA with Bonferroni post test.*

In order to chelate heavy metal ions cells were treated with 1 mM phytic acid for 14 days prior to Ca^{2+} assay in order to effectively chelate heavy metals within the lysosome, and, allow cells to adjust to these new conditions. It can be seen from figure 5.3.12. that the excessive Ca^{2+} release from the ryanodine receptor proposed to be caused by hyperactivity of this channel is reduced by around 40% by phytic acid treatment, although this reduction is not significant the trend indicates that more repeats of this experiment would prove beneficial. It remains to be confirmed whether the total ER Ca^{2+} levels have been affected by phytic acid treatment with higher concentrations of thapsigargin, it is anticipated that phytic acid will not affect the total levels of this Ca^{2+} store and it is more likely that the effects lysosomal heavy metal ion content will lead to the reduction in ryanodine receptor hyperactivity.

With reduction in the hyperactivity of Ca^{2+} release from the ryanodine receptor we would anticipate that there would be a concomitant reduction in the levels of cytosolic Ca^{2+} which would need to be buffered by the mitochondria in order to maintain the

comparable levels between control and patient fibroblasts observed in the absence of extracellular Ca^{2+}. Accordingly, this was the second Ca^{2+} phenotype investigated in phytic acid treated cells.

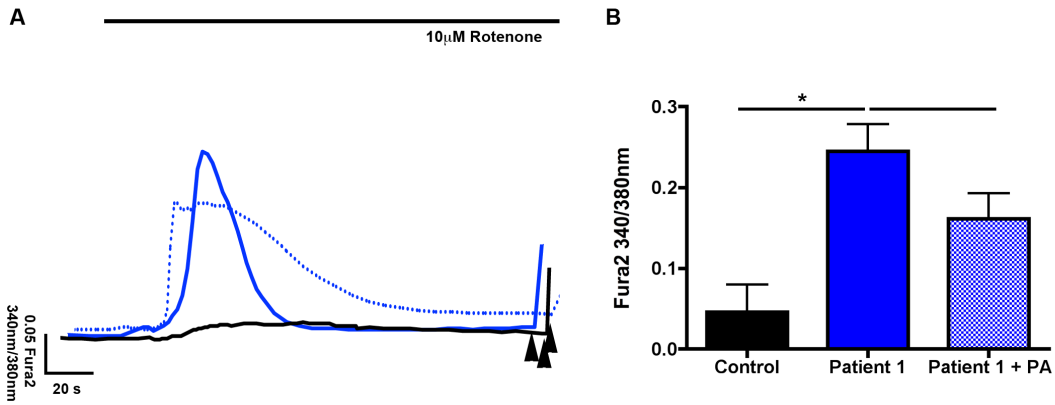

Figure 5.3.13– Effect of phytic acid treatment on Ca^{2+} release after rotenone induced mitochondrial depolarisation in KRS patient fibroblasts. *Cells were treated with 1mM phytic acid for 14 days (+PA).* ***A -*** *Representative traces of Ca^{2+} responses in Fura2 loaded cells after the addition of 10μM rotenone. Black bar indicates the presence of rotenone. Arrowheads indicate the addition of 5μM ionomycin to confirm cell viability.* ***B –*** *Quantification of Ca^{2+} release measured by ratiometric change in Fura2 fluorescence. Error bars = SEM. n = 3 for control cells, n = 3 for patient 1 cells and n = 3 for phytic acid treated cells. * = P<0.5, calculated by one way ANOVA with Bonferroni post test.*

The trend towards reduction of the Ca^{2+} response after rotenone was not as great as that shown after ryanodine stimulated Ca^{2+} release, around 25% reduction as opposed to 40%. Again, this trend suggest further repeats of this experiment should be performed. As the temporal progression of Ca^{2+} phenotypes in KRS cells is currently unclear this may be due to this phenotype being downstream of excessive Ca^{2+} release from the ER. As such, a longer treatment time may be needed to correct this phenotype. As cells are grown in the presence of Ca^{2+} until imaging excessive Ca^{2+} influx from the extracellular milieu may still be occurring until shortly before the experiment in conducted; as such, the mitochondria may still contain excessive Ca^{2+} as a result of this. The reduction observed may be due to reduced ryanodine receptor activity not contributing further to this.

As described the onset of these phenotypes remains to be delineated. Phytic acid may be beneficial in this regard as if the lysosome is the initiating compartment for Ca^{2+} hyper-reactivity it may be reduced by chelation of heavy metal ions. Accordingly, signalling events following the stimulation of lysosomal Ca^{2+} channels TRPML1 and TPC2 by ML-SA1 and NAADP-AM respectively should be investigated

in phytic acid treated cells. It is, however, encouraging that phytic acid reduces Ca^{2+} hyper-reactivity in these cells and this therapeutic action should be further investigated.

5.3.3. – Preliminary investigation of astrocytic Ca^{2+} abnormalities in models of Gaucher disease reveal potentiation by ER Ca^{2+} dyshomeostasis

In Gaucher disease astrocytes have been shown to be important in brain pathology (Farfel-Becker et al., 2011). These cells have not been examined for Ca^{2+}dysregulation; shown to be an early event in this pathogenesis of other neurodegenerative diseases. We were interested to see if the Ca^{2+} dysregulation in other cellular models of Gaucher could be extended to primary astrocytes which have GCase defects.

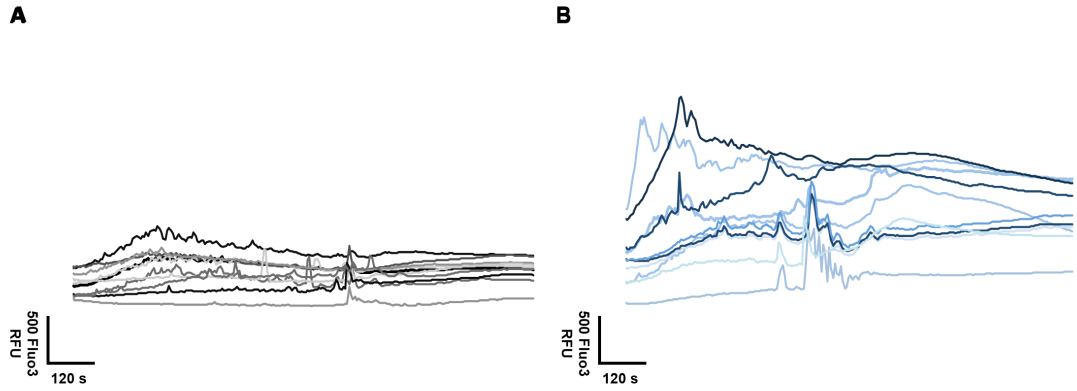

Figure 5.3.14. – Spontaneous Ca^{2+} signalling events in primary mouse astrocytes from a mouse model of Gaucher disease. A - *Representative traces of Ca^{2+} response in Fluo3 loaded wild-type astrocytes.* ***B –*** *Representative traces of Ca^{2+} response in Fluo3 loaded Gaucher astrocytes. n = 1.*

In order to do this we prepared a culture of astrocytes from a mouse model of Gaucher in which GCase expression has been specifically ablated in neurons and astrocytes (Farfel-Becker et al., 2011). Upon loading with a cellular Ca^{2+} fluorophore we observed that spontaneous Ca^{2+} signalling events occurred in these cell lines as expected from primary astrocyte preparations (5.3.14. A and B). In this preliminary experiment when we compared these responses in cells prepared from WT animals to those in which GCase was deficient we observed a striking variability in spontaneous Ca^{2+} signalling events in cells prepared from Gaucher mice. The amplitude of this response was appeared to be increased in the Gaucher astrocytes. There also may be an increase in Ca^{2+} signalling events, where cells deviated more

than 10% from the current baseline signal. This experiment remains to be repeated so that the number of spontaneous signalling events and their amplitude can be analysed.

In order to further study these phenotypes and investigate if loss of activity in GCase could cause an increase in astrocyte Ca^{2+} signalling we treated independently prepared wild-type astrocyte cultures with a specific, irreversible inhibitor of GCase. Conduritol β epoxide (CβE) has been extensively used to model Gaucher in both cells and animals and is becoming increasingly utilised as a way to study the pathogenic changes accompanying CGase activation, which may lead to Parkinson's disease (Manning-Bog et al., 2009).

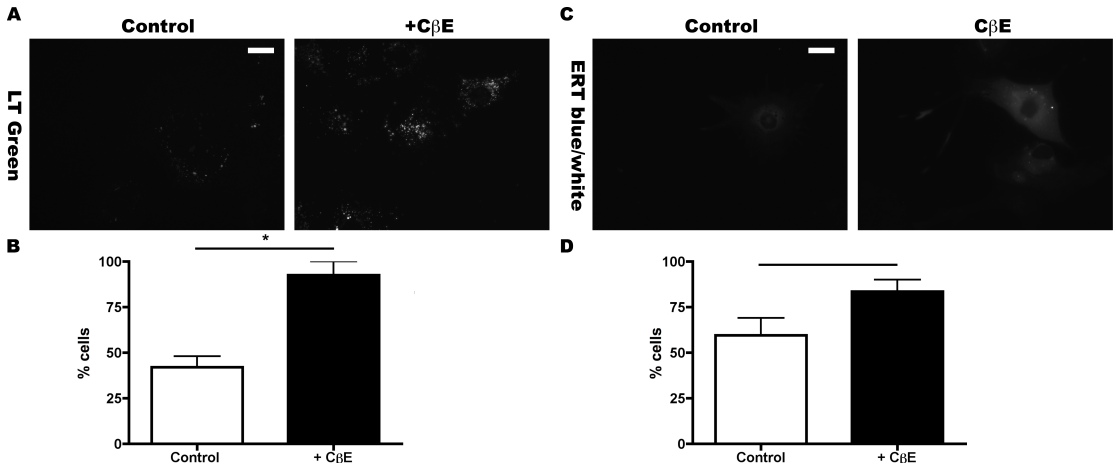

Figure 5.3.15. – Cellular phenotypes in murine astrocytes treated with CβE. A - *Representative lysotracker green images of control cells and those treated with 200μM CβE for six days.* ***B –*** *Threshold analysis of lysotracker green images from both astrocyte populations.* ***C*** *– Representative ER tracker blue/white images of control cells and those treated with 200μM CβE for six days.* ***D*** *– Threshold analysis of ER tracker blue/white images from both astrocyte populations. Error bars = SD. * = P<0.05 calculated by T test. n = 2. Cells were prepared by Jenny Lange, KCL.*

After 200μM treatment of astrocytes for six days we were able to see significant increases in lysotracker signal ($P < 0.05$, $t = 5.258$, $df = 2$, $F_{1,1} = 1.563$) indicative of increased acidic compartment size due to storage of the glycosphingolipid GlcCer. We also observed a trend towards increases to ER density (5.3.15. B), measured by increased lysotracker signal. Both these phenotypes can be used as a marker of Gaucher phenotypes and provide preliminary evidence that CβE treatment is having the desired effect on a novel cell line for Gaucher research although this remains to be confirmed by enzyme assay.

As we were able to show CβE treatment was able to induce phenotypes indicative of GlcCer storage we proceeded to investigate if this resulted in any changes to spontaneous Ca^{2+} signalling in these astrocyte populations.

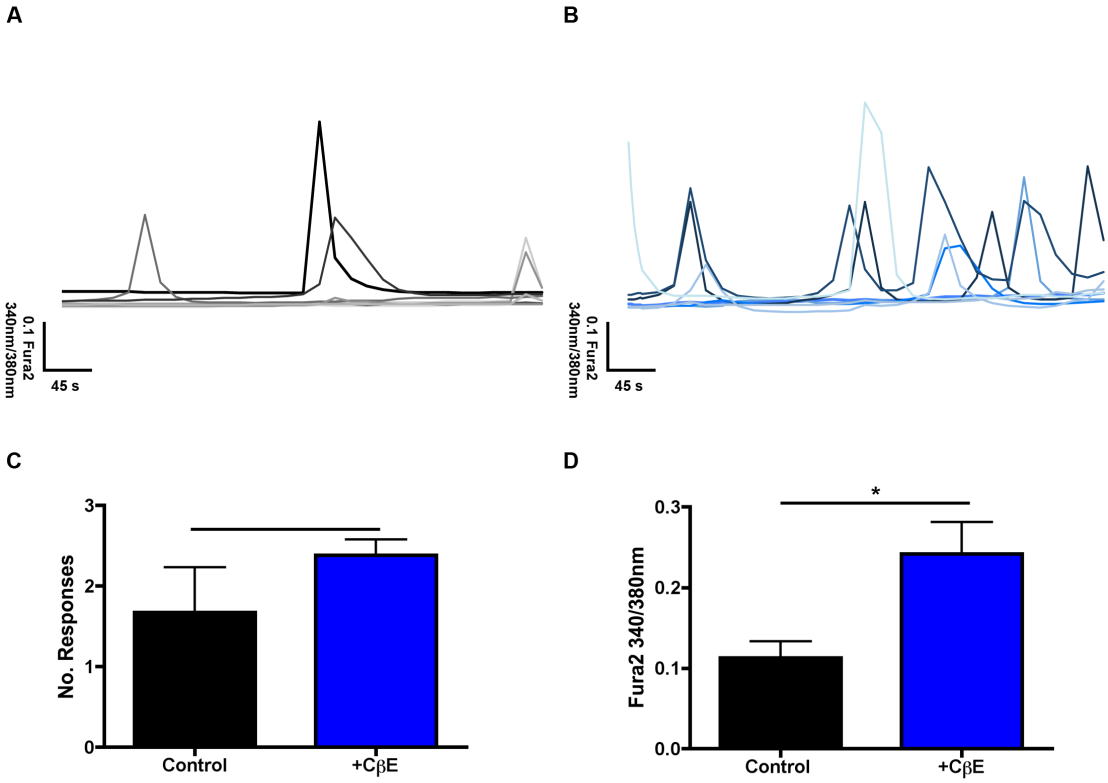

Figure 5.3.16. – Spontaneous Ca^{2+} signalling events in primary mouse astrocytes with pharmacologically induced Gaucher phenotypes. A - *Representative traces of Ca^{2+} response in Fura2 loaded wild-type astrocytes.* ***B –*** *Representative traces of Ca^{2+} response in Fura2 loaded astrocytes after treatment with 200μM CβE for six days.* ***C*** *– The number of Ca^{2+} signalling events counted over the course of 5 minutes in both control astrocytes and astrocytes treated with with 200μM CβE for six days (+CβE).* ***D*** *– Quantification of the amplitude of Ca^{2+} release events in both control astrocytes and astrocytes treated with 200 μM CβE for six days (+CβE). Error bars = SEM. * = P < 0.05 calculated by T test. n = 3. Cells were prepared by Jenny Lange, KCL.*

It can be observed in figure 5.3.16 that similar phenotypes were observed in CβE treated astrocytes and those prepared from Gaucher mice. Although the increased number of experiments performed on CβE treated astrocytes did not show a statistically significant increase in the frequency of Ca^{2+} signalling events there was a also a trend towards an increase (5.3.16. C). When the amplitude of signalling events was measured (5.3.16. D) these had increased two-fold ($P < 0.05$, $t = 2.907$, $df = 4$, $F_{2,2} = 3.707$). It is notable that the overall response profiles shown by cell prepared from the Gaucher mouse models and the wild-type astrocytes prepared by our collaborator (Jenny Lange, King's College London) did differ but this is most likely a result of reduce time between culturing and experiments in the wild-type astrocytic

preparations. Nevertheless, as each of the Gaucher models cells is independently controlled by identically prepared cells within the same experiment these results remain robust.

As Ca^{2+} signalling events are exaggerated in CβE treated cells we were interested to see if intracellular Ca^{2+} stores were responsible for this. As it is known that Ca^{2+} signals in astrocytes are primarily induced by ER Ca^{2+} release, and, this store is known to be more responsive in Gaucher disease (Lloyd-Evans et al., 2003) we were interested to investigate whether dyshomeostasis in this store could potentiate astrocyte Ca^{2+} signalling. We were able to significantly impact subsequent Ca^{2+} release events using ER Ca^{2+} agonists in both control and CβE treated as described in figure 5.3.17.

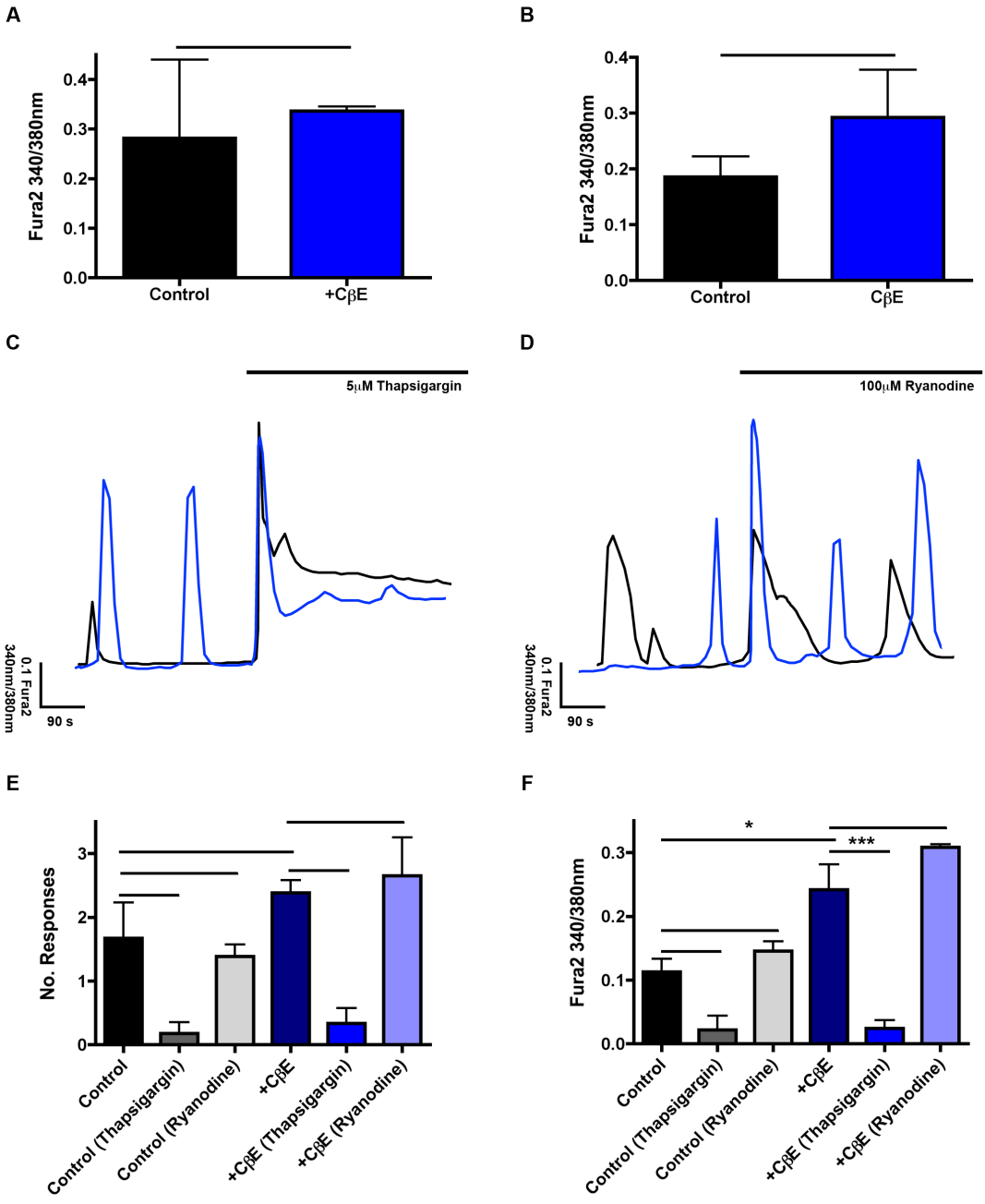

Figure 5.3.17. – Modulation of spontaneous Ca^{2+} signalling events by ER Ca^{2+} agonists. ***A*** *– Quantification of instantaneous Ca^{2+} release in response to thapsigargin by ratiometric change in Fura2 fluorescence from control astrocytes and astrocytes treated with with 200 μM CβE for six days (+CβE).* ***B*** *– Quantification of instantaneous Ca^{2+} release in response to ryanodine by ratiometric change in Fura2 fluorescence from control astrocytes and astrocytes treated with with 200 μM CβE for six days (+CβE).* ***C*** *– Representative traces of Ca^{2+} response in Fura2 loaded control and CβE treated astrocytes before and after addition of 5 μM thapsigargin.* ***D*** *– Representative traces of Ca^{2+} response in Fura2 loaded control and CβE treated astrocytes before and after addition of 100 μM ryanodine.* ***E*** *– Quantification of the amplitude of Ca^{2+} release events in both control and CβE treated astrocytes before and after the administration of thapsigargin.* ***F*** *– Quantification of the amplitude of Ca^{2+} release events in both control and CβE treated astrocytes before and after the administration of ryanodine. Error bars = SEM. In A and B no significant difference was observed by unpaired T test. In E and F * = P<0.05, *** = P<0.001, calculated by one way ANOVA with Bonferroni post test. n = 3 for control and thapsigargin experiments, n = 2 for ryanodine experiments. Cells were prepared by Jenny Lange, KCL.*

Initial releases from both cell lines after stimulation with thapsigargin were comparable within both cell lines suggesting that the overall Ca^{2+} store in the ER was unchanged and elevation of this store was not responsible for the exaggerated Ca^{2+} signalling events observed in Gaucher and CβE treated astrocytes. Interestingly, there was a trend towards increased response to ryanodine in treated cells suggesting that the ryanodine receptor was more responsive in these cells as has previously been described in Gaucher disease (Lloyd-Evans et al., 2003). This remains to be investigated in subsequent repeats. Supplementary to this we investigated the spontaneous astrocytic Ca^{2+} responses before and after addition of Ca^{2+} agonists. As we observed in cell from CLN1 disease mouse models (Lange *et al*., unpublished) thapsigargin treatment had a strong trend towards a suppressive effect on signalling events; as expected from previous observations that the ER is central to astrocytic Ca^{2+} signalling. This was accompanied by a trend towards reduced numbers of signalling events and a significant reduction in amplitude of signal ($P < 0.001$, $t = 6.604$, $df = 4$). These observations may implicate the ER in exaggeration of these signals.

Converse trends were observed after ryanodine treatment of both astrocyte populations as a potentially stimulatory effect on spontaneous Ca^{2+} signals was observed. Although the number of responses remained consistent after ryanodine addition there was a trend towards an increase in the amplitude of these responses in CβE treated astrocytes. This implicates hyperactivity of the ryanodine receptor as previously reported in Gaucher disease (Lloyd-Evans et al., 2003) as a potential underlying cause of increased astrocytic Ca^{2+} responses in these cells. In addition to further repeats of these experiments, to confirm the trends observed, it may also be interesting to study the effects of inhibition of the ryanodine receptor on these responses. This could potentially further implicate this Ca^{2+} release channel in the potentiation of spontaneous Ca^{2+} signalling events in astrocytes.

If confirmed, the identification of ryanodine receptors as the initiating factor in increases in the excitability of astrocytic Ca^{2+} signalling events may provide an early pathogenic change prior to astrogliosis in Gaucher disease which has been shown to contribute to neuronal loss and dysfunction in other neurodegenerative diseases (Farfel-Becker et al., 2011). As astrocytic excitability has also been implicated in Parkinson's disease (Vaarman et al., 2010) it may be an important pathogenic event linking dysfunction in GCase to loss of SNpc dopaminergic neurons – a population of neurons shown to be vulnerable to Ca^{2+} dyshomeostasis (Surmeier et al., 2011).

5.4. – Summary of Results and Discussion

The study of various Ca^{2+} stores in cells lines which model genetic causes of, and susceptibility to, Parkinson's with lysosomal defects clearly reveals that Ca^{2+} is not correctly maintained by these cells. KRS patient cell lines which have mutations in ATP13A2 are hyper responsive to Ca^{2+} agonists with respect to multiple stores and astrocytic models of Gaucher disease appear to have pathogenic elevations seen in spontaneous astrocytic Ca^{2+} responses. Both cell lines are however not SNpc Dopaminergic (DA) neurons so in order to understand how the Ca^{2+} pathology observed may lead to the death of these neurons, and the subsequent onset of Parkinson's phenotypes, we have to consider why Ca^{2+} is particularly important in this type of neuron.

5.4.1. – The role of Ca^{2+} in SNpc Dopaminergic neurons

The DA neurons which are lost in Parkinson's disease are dependant upon Ca^{2+} channels for autonomous pacemaking. In this process, Ca^{2+} is used to mediate the broad and slow action potentials generated in these neurons. These are generated in the absence of synaptic input and instead rely on ambient dopamine levels in the regions of the brain they innervate (Surmeier et al., 2011). A consequence of this is that Ca^{2+} homeostasis in DA neurons is distinct from most other cell types as they utilise L-type Ca^{2+} channels with a specific catalytic core in order to allow extracellular Ca^{2+} to enter the cytoplasm (Striessnig., et al 2006). This core allows the channel to remain permeable to Ca^{2+} at more hyperpolarized levels than most other channels, thus, predisposes these neurons to autonomous pacemaking (Surmeier et al., 2011).

Autonomous pacemaking comes at a substantial metabolic cost to these neurons, as cytosolic Ca^{2+} must be maintained at around 100nM. Accordingly, channels such as SERCA2 must pump Ca^{2+} against the steep concentration gradient in order to achieve this. In most neurons the brief spikes of Ca^{2+} excitability result in influxes of Ca^{2+} that can quickly be sequestered; the prolonged open state of Ca^{2+} channels in DA neurons means that this process has to be constantly functioning. This also puts increased stress on mitochondria as they act to buffer increased cytosolic Ca^{2+}, a process which puts them under increased basal levels of stress. This process appears to be more prevalent in populations of neurones sensitive to cell death

during Parkinson's pathogenesis (Surmeier et al., 2011). Interestingly, genetic forms of Parkinson's, which affect genes expressed in mitochondria, also have this affect on DA neurons (Surmeier et al., 2011).

Importantly, other types of neurons which are vulnerable to loss in Parkinson's also undergo autonomous Ca^{2+} pacemaking and utilise L-type Ca^{2+} channels whereas VTA DA neurons, the population of which remains relatively intact in Parkinson's patients and animal models, do not. As Ca^{2+} also stimulates Dopamine biosynthesis regulation of this key signalling ion is evidently at the heart of many aspects of Parkinson's pathogenesis (Surmeier et al., 2011).

5.4.2. – Ca^{2+} hyper reactivity in ATP13A2 deficient cells

In our study of KRS patient fibroblasts we were able to observe multiple forms of Ca^{2+} hyperactivity in cells which do not have functional ATP13A2. A benefit of these cells is that they have been extensively characterised in numerous publications and in many of these publications specific defects in lysosomes (Dehay et al., 2012), and mitochondria (Grunewald et al., 2012), have been corrected by re-expression of functional ATP13A2 in order to confirm that these defects were due to loss of function, as opposed to toxic gain of function. Nevertheless, our study of ER phenotypes may benefit from either re-expression of functional ATP13A2 or further study in ATP13A2$^{-/-}$ cells as the mutant protein expressed in these cells may be responsible for or contributing to the ER Ca^{2+} dyshomeostasis we observe. Additionally, the control human fibroblast cell line utilised in this study is extremely well characterised with respect to the lysosomal Ca^{2+} store, and well characterised with respect to the content of other stores (Lloyd-Evans et al., 2008).

The evidence presented in section 5.3.1. shows that the Ca^{2+} stores in KRS cells are dysfunctional leading to increased Ca^{2+} release in numerous situations (summarised in 5.4.1.). The observation that cytosolic Ca^{2+} may be elevated compared to the level in control human fibroblasts by the addition of extracellular Ca^{2+} is likely to have severe effects on DA neurons which are constantly in high states of Ca^{2+} influx during autonomous pacemaking (Surmeier et al., 2011). Reduced ability of cells to lower cytosolic Ca^{2+} would increase the mitochondrial stress phenotypes to which DA neurons are susceptible whilst upregulating dopamine biosynthesis, potentially initiating a detrimental cycle.

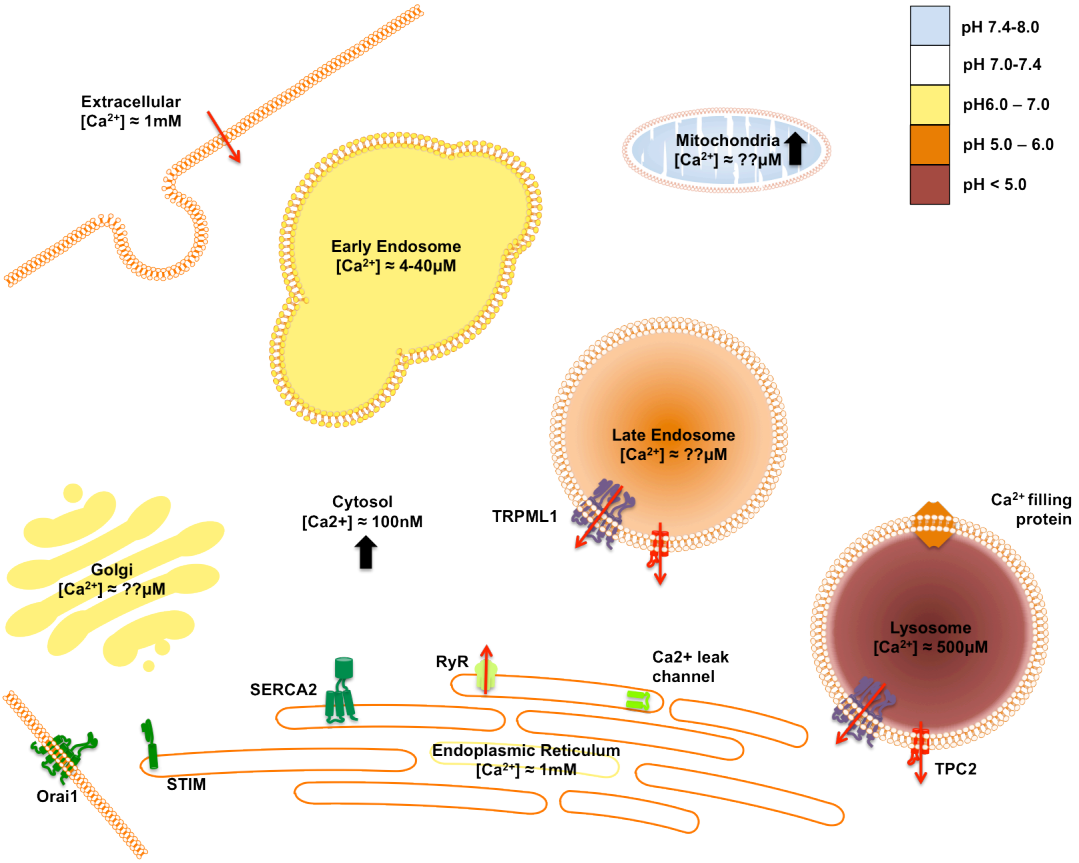

Figure 5.4.1. – Ca^{2+} hyper reactivity in KRS patient fibroblasts. *Potentially elevated Ca^{2+} stores are shown by black arrows and channels which are more active in KRS cell are labelled with red arrows. Adapted from Lloyd-Evans et al., 2008.*

Increased Ca^{2+} release from the cellular stores assayed would obviously contribute to this and dysfunction within mitochondria in these cells. This has been shown by increased sensitivity to mitochondrial toxins by Holemans et al., (2015). The next step in this study would be to find the initiating factor which underlies this Ca^{2+} dyshomeostasis. siRNA inactivation of ATP13A2 followed by assay of Ca^{2+} stores at different time points would be able to temporally resolve the onset of Ca^{2+} dyshomeostasis in intracellular stores although this may not be necessary due to the observations present in the literature in addition to our findings.

As ATP13A2 is a protein which localises to the lysosome (Ramirez et al., 2006) it is most likely that initial defects would begin here, however, with respect to ER Ca^{2+} phenotypes these may be caused by the presence of misfolded ATP13A2 protein (Ramirez et al., 2006). These stores are also closely linked functionally as discussed throughout this thesis. Interestingly, however the reduction of heavy metal ion accumulation in the lysosomes of KRS cells reduced the ER signalling defect of increased ryanodine receptor Ca^{2+} release. This is suggestive of dysfunctional

lysosomal processes initiated by heavy metal ion accumulation contributing to the ER hyper-reactivity, possibly due to Ca^{2+} signalling from the TPC2 channel having an exaggerated impact upon the ER. As this phenotype has been recently shown to be present in patient fibroblast carrying dominant *LRRK2* mutations (Hockey et al., 2015) it could be further investigated by the inhibition of TPC2 channels with Ned-19 – an intervention which may be doubly beneficial in cells which also have increased ML-SA1 signalling. Interestingly, LRRK2 and ATP13A2 have recently been linked with inhibition of the kinase activity of mutated LRRK2 helping to rescue lysosomal defects by a mechanism involving upregulated expression of ATP13A2 (Henry et al., 2015). It would be interesting to see if LRRK2 kinase inhibition corrected any of the defects observed in KRS patient cells.

As previously mentioned increased signalling from the TRPML1 channel can activate calcineurin and de-phosphorylate and bind TFEB initiating lysosomal biogenesis (Medina et al., 2015). In these cells this may well lead to accumulation of autophagic vacuoles as endolysosomal fusion and fission defects are expected in cells which have Ca^{2+} dyshomeostasis in this system. This may be particularly relevant in terms of fission defects as observed in cells deficient in TRPML1 (Waller-Evans et al., manuscript in preparation), which also have higher endolysosomal Ca^{2+} levels and exhibit trafficking defects. We do not however expect increased release from TRPML1 to lead to increased release of Ca^{2+} from the ER in the same way that TPC2 does.

Another way in which the lysosome could affect Ca^{2+} release from the ER and subsequently the mitochondria is by lysosomal lipid accumulation and escape to the ER as hypothesised to occur in multiple LSDs (Platt et al., 2012). Interestingly, in preliminary biochemical analysis the only lipid significantly elevated in both KRS patient cell lines was GlcCer. In Gaucher disease GlcCer accumulation has been shown to potentiate the pathogenic release of Ca^{2+} from ryanodine receptors (Lloyd-Evans et al., 2003). As this lipid is elevated and Ca^{2+} release from the ryanodine receptor is exaggerated in KRS cells it is an attractive proposal for this GlcCer accumulation to be the cause of this; especially as the enzyme responsible for the degradation of GlcCer GCase is a genetic risk factor for Parkinson's (Sidransky et al., 2009). *In situ* enzyme assays of GCase may provide the evidence for this process in KRS cells – it may be particularly relevant to see if heavy metal ion chelation could modulate any changes in GCase activity observed in KRS cells as

this would further indicate that GlcCer accumulation may lead to increased activation of the ryanodine receptor.

It is also important to note that increased release of Ca^{2+} from the ER of cells and other methods of increasing cytosolic Ca^{2+} is proposed to lead to lead to elevations in endolysosomal Ca^{2+} (Lloyd-Evans et al., 2008) and it cannot be absolutely ruled out that the ER is the initiating factor in intracellular Ca^{2+} stress. Nevertheless, evidence from this study and others into Ca^{2+} dyshomeostasis in genetic forms of Parkinson's suggest that lysosomal involvement may be primary.

Whilst these observations remain interesting it will be important to corroborate them in different cellular models of KRS. We plan to do this in ATP13A2$^{-/-}$ cells, these would provide a potential model in which phenotypes could be assayed in a similar way to that detailed in chapter 3. It cannot be ruled out that unrecognised genetic variation in KRS patient fibroblast may confound the results we have obtained. Accordingly, although they are closer to the reality of KRS they present their own challenges and studies utilising them would be strengthened by the addition of knockout cell lines. This is why we are planning to perform this study in relation to KRS and the converse of this study in relation to familial Alzheimer's.

5.3.3. – KRS as a neuronal ceroid lipofuscinosis

A variety of the Ca^{2+} phenotypes we have reported are supportive of the links between ATP13A2 and NCLs (Bras et al., 2012). A number of the Ca^{2+} phenotypes present in these cells suggest that there is some overlap with this class of lysosomal storage disease. Firstly, the potential for elevated endolysosomal Ca^{2+} signalling has been observed in cellular models of CLN3. Although there are differences here as cellular models of CLN3 have been shown to have significant increases in lysosomal Ca^{2+}, whereas this was not clearly observed in KRS cells, both have been shown to respond excessively to agonists of lysosomal Ca^{2+} release channels (Walker et al., Unpublished). CLN3 cells also exhibited an increased sensitivity towards thapsigargin (Chandrachud et al., 2015), another trend exhibited in KRS patient fibroblasts. Interestingly, the increased Ca^{2+} release which resulted from this phenotype caused the accumulation of autophagic vacuoles in a Ca^{2+} dependant manner in CLN3 (Chandrachud et al., 2015). This may partially explain the

autophagic defects observed in KRS cells and accumulation of autofluorescent storage material.

Another condition which causes the accumulation of autofluorescent material is MLIV caused by inactivation of the TRPML1 channel (Jennings et al., 2006). Interestingly increased levels of endolysosomal Ca^{2+} have also been measured in this disease (Waller-Evans et al., manuscript in preparation). Although MLIV is not considered an NCL lysosomal diseases in which endolysosomal Ca^{2+} is elevated may share a number of defects and could possibly form a novel disease grouping which would inform us about conserved pathogenesis in LSDs which have previously been considered disparate. It would be interesting to see which other LSDs could be added to this group which would so far include CLN3, MLIV and KRS. The most obvious potential source of other members is the broader family of NCLs as some of the causative genes such as CLN5 are proposed to interact with CLN3 (Carcel-Trullols et al., 2015). Accordingly, it may be interesting to look for phenotypic overlap in cells and patients; for example recent findings of synucleinopathy in CLN10 (Cullen et al., 2009) and clinical observations that movement disorders in diseases such as CLN3 and CLN1 are considered to forms of parkinsonism (Schulz et al., 2013)

5.4.4. – Preliminary evidence of alterations in astrocytic Ca^{2+} signalling in Gaucher disease

As we were interested in extending our study of Ca^{2+} dyshomeostasis in models of genetic susceptibility to Parkinson's we utilised primary astrocyte models of Gaucher disease. We were able to utilise cells from both Gaucher knockout mouse models (Farfel-Becker et al., 2011) and a well-characterised pharmacological model of Gaucher (Manning-Bog et al., 2009). This was able to add strength to our study as we could show that specific inhibition of GCase and the subsequent accumulation of GlcCer lead to similar phenotypes of astrocytic Ca^{2+} signalling hyperactivity.

In the CBE model we were also able to observe the expected phenotype of lysosomal expansion and although ER expansion was not highly evident we were able to link the increased Ca^{2+} signalling to the ER by modulating this store using thapsigargin and may have implicated the ryanodine receptor in this process. It is currently unknown how GlcCer escapes to the ER although lysosome;ER membrane

contact sites (Penny et al., 2015) would seem to be a natural location for this. Interestingly, this increased astrocytic Ca^{2+} signalling is highly likely to impact upon other Ca^{2+} stores such as the mitochondria were the need for increased absorbance of Ca^{2+} could lead to increases in the basal levels of mitochondrial stress and subsequently make these organelles more susceptible to other insults (Surmeier et al., 2011).

As with the study we conducted in KRS cells it is important to consider how these phenotypes could affect SNpc DA neurons. As discussed in section 5.4.1. these neurons take in large amounts of Ca^{2+} over prolonged periods of time when compared to other neurons so increased Ca^{2+} activity in surrounding cells may well increase the chances of cytosolic Ca^{2+} overload, mitochondrial stress and increased dopamine synthesis (Surmeier et al., 2011). This could further increase astrocytic Ca^{2+} signals (Vaarman et al., 2010). When we consider that the same hyper activation of the ryanodine receptors in the DA neurons themselves may also be prevalent it can be seen that an increase requirement for Ca^{2+} homeostasis has been added to a system which is already stressed in this regard.

In this study we have provided the first example of increased Ca^{2+} excitability in astrocytes from a genetic model of Parkinson's disease. It would be particularly interesting to examine this phenotype in other genetic forms of Parkinson's to see if the increased astrocytic signalling was also present; KRS and G2019S LRRK2 may provide particularly good models for this as Ca^{2+} the have already been reported to exhibit hyper reactivity with regard to Ca^{2+} signalling (Hockey et al., 2015). It may also provide a link to sporadic forms of Parkinson's as disruption of dopamine transmission has also been shown to result in increased astrocytic Ca^{2+} signalling (Vaarman et al., 2011).

5.4.5 – Observations of Ca^{2+} dyshomeostasis in other forms of PD and the potential role in sporadic Parkinson's

As with our study of Alzheimer's disease taking observation from cellular models and applying them to human disease is never an easy task. We are, however, closer to the disease in this study then we were using knockout cell models of Alzheimer's disease as this study has been based on patient mutations and astrocytes models which are more closely linked to pathogenesis in Parkinson's.

In these studies we have again, however, been able to provide a good baseline for further examination of Ca^{2+} dyshomeostasis in genetic models of Parkinson's disease. The use of KRS patient fibroblasts was extremely important in this regard as these patients represent an extremely severe example of Parkinson's disease (Park et al., 2015). Accordingly, we would expect the important phenotypes to be prevalent in this disease model. The observation of clear Ca^{2+} signalling hyper reactivity was encouraging as the very early onset of Parkinson's phenotypes would suggest that the underlying pathology would be very evident. It would be interesting to examine similar phenotypes in less severe genetic models of Parkinson's disease.

To some extent we have initiated this in our examination of astrocytic Ca^{2+} signalling in models of Gaucher. These were clearly evident Ca^{2+} signalling changes in cells that have completely ablated function of GCase and provides an interesting starting point for our observations. This phenotype would be much more subtle if only a small amount of GlcCer was stored and escaped to the ER. Nevertheless over the course of the approximately 50 years Parkinson's commonly takes to onset these subtle changes may be sufficient to increase Ca^{2+} stress in DA neurons eventually leading to cell loss (Surmeier et al., 2011). With numerous other reports of increased Ca^{2+} signalling in genetic models of Parkinson's this may well be an interesting avenue of investigation.

In order to apply these finding to sporadic Parkinson's disease much more work will need to be performed although the Ca^{2+} phenotypes discussed in this chapter may provide a basis for these studies.

Chapter 6

General Discussion and Concluding Remarks

The studies contained in this thesis have applied techniques developed in the study of LSDs and utilised them in the study of more commonly occurring neurodegenerative diseases associated with ageing. In doing so we have implicated the lysosomal ion channel TRPML1 in the pathogenesis of familial Alzheimer's disease, identified a potential new therapeutic target for Huntington's disease and provided further implicated Ca^{2+} dyshomeostasis in genetic models of, and models of genetic predisposition to, Parkinson's. The diverse pathologies which are present in the different models we have examined clearly show that the lysosome is a multifunctional organelle and its location at the centre of the greater lysosomal system allows it to influence all aspects of cellular function.

The prevalence of neurodegenerative phenotypes in the majority of lysosomal storage diseases clearly implicates these organelles as vital for neuronal survival (Cox and Chacon Gonzalez, 2011). Interestingly, a large number of mutations known to lead to the onset of various neurodegenerative diseases further implicate lysosomes as vital in this process. The lysosome can be considered a 'hot spot' for neurodegenerative disease.

6.1. – The endolysosomal system as a hot spot for neurodegenerative disease

It has already been discussed how mutations in various genes which affect the endolysosomal system can result in Alzheimer's and Parkinson's disease, however, a number of other genes known to cause other neurodegenerative diseases can also impact the vital cellular pathway. Some of these genes are highlighted in figure 6.1.

Charged multi-vesicular body protein 2B (CHMP2B) is an ESCRT complex component important in the delivery of a variety of endocytosed cargoes to the correct cellular compartments. Truncated forms of this protein, expressed as a result of mutations in *CHMP2B,* have been shown to be the molecular cause of rare forms of autosomal dominant frontotemporal dementia (FTD). The impact of these proteins on vesicular fusion events in the endolysosomal system is though to be important to pathogenesis (Isaccs et al., 2011).

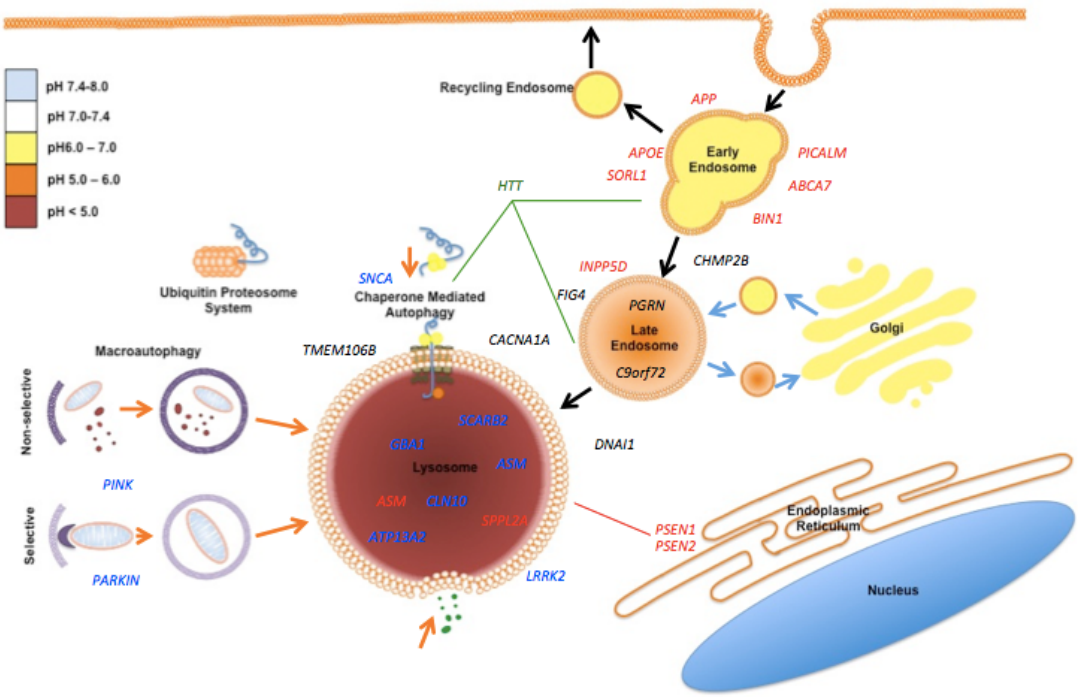

Figure 6.1. – Genes associated with neurodegenerative diseases which express proteins which localise to, or impact upon, the endolysosomal system. *Genes associated with Alzheimer's disease are shown in red, genes associated with Parkinson's disease are shown in blue, HTT is shown in green. Key on the left indicates compartment pH. Adapted form Nixon, 2013.*

A number of other genes coding for proteins which are expressed in the endolysosomal system have also been linked to FTD. These include *PGRN* (progranulin) (Petkau and Leavitt, 2014), and *C9ORF72* (c9orf72). Hexanucleotide repeat expansion in *C9ORF72* have been shown to cause both FTD and amyotrophic lateral sclerosis (ALS) and the protein product is known to co-localise with markers of the endocytic system in neurons (Farg et al., 2014).

Interestingly, a genetic modifier of the severity of neurodegenerative phenotypes caused by both of these genes is *TMEM106B* the protein product of which, transmembrane protein 106B is localised in the endolysosomal system where it can regulate lysosomal morphology and function (Gallagher et al., 20134). Accordingly, it would be potentially interesting to look at the impact of this protein on LSDs as much of the phenotypic variability in patients with these diseases remain unexplained.

Particularly relevant to this thesis is *FIG4,* this produces a 5' phosphoinositide phosphatase, which regulates levels of PI(3,5)P2. When his protein is deficient lysosomal storage phenotypes are observed and patients suffer from a form of

Charcot-Marie-Tooth disease (CMT). Recently lysosomal storage phenotypes in cells deficient in FIG4 were rescued by ML-SA1 stimulated Ca^{2+} efflux from ML-SA1. Incidentally, this is supportive of our finding that ML-SA1 does not require PI(3,5)P2 to facilitate Ca^{2+} release from ML-SA1 (Zou et al., 2015).

As can be observed in figure 7.1.1. there are a myriad of established and newly emerging genetic causes of neurodegenerative disease which interact with the greater lysosomal system, it is likely that the number of these will continue to grow.

6.2. – Changes in the lysosome with ageing

A key risk factor in virtually all neurodegenerative disease is ageing, with only rare diseases causing neurodegenerative phenotypes in juvenile and adolescent patients. As LSDs are one of the more common causes of juvenile neurodegenerative disease (Cox and Chacon Gonzalez, 2011) they may in some respects be considered diseases of early, or accelerated, ageing. The NCLs are a particularly good example of this as the characteristic storage substrate lipofuscin (Pearce 2015) is a hallmark of aged cells and tissues (Ottis et al., 2012).

An excellent model for the study of cellular ageing processes are retinal pigment epithelium (RPE) cells, in particular for the study of age related macular degeneration (AMD) (Guha et al., 2014). These cells are particularly vulnerable to lipofuscin accumulation, as they phagocytose large amounts of photoreceptor outer segment tips subjecting these cells to a high proteolytic load. Interestingly, these cells have been shown to be extremely sensitive to alkalisation whether by pharmacological means (such as the well characterised phenomenon of chloroquine induced retinopathy) (Ben-Zvi et al., 2012); genetic disruption of proteins important for lysosomal pH maintenance (such as ClC-7) (Kasper et al., 2005); or, by the amount of time for which they have been cultured (Sparrow and Boulton, 2005). Autophagy is known to play a key role in the health of these cells and the elevation of pH has been shown to impair the fusion of autophagosomes and lysosomes (Kawai et al., 2007). These cells have also been used for the study of techniques which can re-acidify lysosomes such as the acidic nanoparticles described in chapter 3 (Baltazar et al., 2012). Interestingly the derivative of artemisinin, artesunate, has also been shown to be capable of re-acidifying lysosomes (Yang et al., 2014). If this is successful in RPE

cells then it could potentially be used to treat $PS1^{-/-}$ cells and other diseases in which lysosomal alkalisation is present.

Another model of cellular ageing processes is *S.cerevisiae,* in which the vacuole is considered to be the equivalent of the mammalian lysosome. Hughes and Gottschling, (2012). showed that mitochondrial dysfunction in replicatively aged yeast arises from vacuolar alkalisation. In a mutational screen the authors identified that ovexpression of two subunits of the yeast vATPase, VMA1 and VPH2, reduced mitochondrial dysfunction in aged yeast cells; a process which could be blocked by concanamycin A. Subsequently, they were able to show that alkalisation was evident in mother cells, but not daughter cells, and was increased in mother cells which had had greater numbers of daughter cells budding from them – the cells which were considered to have aged. Interestingly, lysosomal alkalisation was reduced in yeast subjected to caloric restriction, and, modulated by differential expression of amino acid transporters. Amino acid starvation has recently been shown to govern the formation of the vATPase complex, in a mammalian target of rapamycin (mTORC1) dependant manner, with lysosomes from amino acid starved cells more able to translocate protons into the lysosome (Hughes and Gottschling, 2012; Henderson et al., 2013).

Such studies are providing links between lysosomal alkalisation in ageing and dysfunctional autophagy. This process has been shown to regulate lifespan in simple organisms like *C.elegans* (Hars et al., 2007), and, is recognised as a pathway which is decreased in ageing (Cuervo, 2008). It will be interesting to see if in future the pathway we have identified in $PS1^{-/-}$ cells, increased TRPML1 activity due to lysosomal alkalisation, will play any role in the modulation of autophagic process as Ca^{2+} signalling from the TRPML1 channel has been proposed to stimulate autophagy (Medina et al., 2015). However, as discussed in chapter 3, without the correct maintenance of lysosomal pH lysosomes fusion of autophagic vacuoles and substrate degradation can not proceed which may cause a pathological accumulation of autophagic vacuoles (Lee et al., 2010; Lee et al., 2015).

The *INPP5D* gene, recently implicated in Alzheimer's (Rosenthal and Kamboh, 2014), and the *FIG4* gene (Zou et al., 2015) may be interesting to study in this regard. Both can modulate phosphoinositol biosynthesis and as such affect the levels of the endogenous ligand of TRPML1, $PI(3,5)P_2$. This would modulate the activity of TRPML1 in cells in which FIG4 or SHIP-1 (the protein coded for by *INPP5D*) are

deficient. This has the potential to be used as a model of perturbed TRPML1 signalling in the absence of lysosomal alkalisation. This could also be achieved using pharmacological inhibition (Jefferies et al., 2008;Viernes et al., 2014).

6.3. – Ca^{2+} signalling and neurodegenerative disease.

Studies such as those mentioned above may be able to provide further links between the lysosome and dysfunctional Ca^{2+} signalling in neurodegenerative disease. In chapter 6 it was detailed how the SNpc DA neurons lost in Parkinson's are susceptible to increased levels of Ca^{2+} within neurons and in the surrounding brain (Surmeier et al., 2011) and how mutations in ATP13A2 or loss of GCase activity could potentially contribute to this. The process of Ca^{2+} dyshomeostasis induced by glutamate excitotoxicity, resulting in the loss of the medium spiny neurons of the striatum in Huntington's disease, has also been demonstrated in chapter 4. We are also beginning to understand the dysregulation of lysosomal Ca^{2+} homeostasis in familial models of Alzheimer's, chapter 3. In addition to these Ca^{2+} dysregulation has been observed in amyotrophic lateral sclerosis (ALS), various spinocerebellar ataxias, multiple LSDs and in more moderate forms as part of the normal ageing process (Bezprozvanny, 2009).

The majority of work on this subject has focussed on extracellular Ca^{2+} channels and the ER and mitochondria with respect to intracellular stores. The impact of these channels and stores on processes such as synaptic plasticity, synaptic vesicle fusion, phosphorylation, and changes to gene expression means that even subtle changes to Ca^{2+} signalling within the brain can have devastating consequences in the long term (Bezprozvanny, 2009).

The role of the lysosome as a Ca^{2+} store and component of Ca^{2+} signalling pathways is beginning to emerge. There has long been evidence from neuronal models of LSDs showing that Ca^{2+} signalling is dysregulated in these diseases (Platt et al., 2012); particularly primary sphingolipidoses. Recently there has been a renaissance of such studies particularly in relation to Gaucher disease due to the appreciation of *GBA1* as a risk factor for Parkinson's (Sidransky et al., 2009, Schondorf et al., 2014).

LSDs will play an important role in respect to the future study of the impact the lysosome can have on Ca^{2+} signalling pathways as we can utilise cellular and animal models of diseases such as NPC to model the effects of reductions in endolysosomal Ca^{2+} on Ca^{2+} signalling pathways in the brain. Conversely, we can utilise models of disease such as CLN3 to inform us of the impact of increased lysosomal Ca^{2+} on Ca^{2+} signalling in the brain (Chandrachud et al., 2015). This may be particularly informative with respect to the increasing evidence of exaggerated Ca^{2+} release from TPC2 in response to NAADP acting as a trigger for pathogenic Ca^{2+} elevation in Parkinson's (Hockey et al., 2015). To this end, we have recently been able to reduce spontaneous Ca^{2+} signalling in the forebrains of embryonic zebrafish using Ned-19 – interestingly we also observed lysosomal storage phenotypes identical to NPC is doing so. Finally, diseases such as Gaucher can be used to model the impact that accumulating lipids can have upon Ca^{2+} signalling – a process which is also of potential importance to Parkinson's.

6.4. – How has the study of lysosomal storage disorders helped facilitate research into neurodegenerative disease?

The lysosomal proteins which are at the centre of each chapter of this thesis were discovered as a result of research into LSDs. This identification of proteins as a result of disease models is particularly evident with respect to lysosomal transmembrane proteins, as many more are thought to be present in the limiting membrane of the lysosome but remain to be identified (Saftig and Klumpermann, 2009; Schwake et al., 2013).

If more overlapping pathology with LSDs is discovered in neurodegenerative diseases associated with ageing then we may be able to identify therapies from LSDs which can be applied to neurodegenerative diseases.

The discovery and application of therapies in the field of LSD research is highly dynamic, and, is potentially accelerated by the severity of disease. As previously described, primary enzymatic defects of the endolysosomal system can be treated by enzyme replacement therapy (ERT) (Brady, 2006). Although this has proven an excellent treatment for peripheral pathology in many LSDs it can not be used to treat neurodegenerative disease, as enzymes are not BBB permeable so are unable to

treat pathology in the CNS (Platt et al., 2012). Accordingly, if an insufficiency of enzyme activity was shown to be the cause of pathology in neurodegenerative diseases new approaches would be needed to circumvent this problem.

Although bone marrow (BM) transplantation has shown promise in some LSDs, such as NPC disease caused by NPC2, this approach is not suitable for age-related neurodegenerative diseases as it as require microglia of BM origin to enter the CNS and provide local sites of protein production. Accordingly therapy must be conducted early in life. The risks involved in this procedure and difficulty in locating tissue matched donors also present difficulties with this approach (Platt et al., 2012).

Gene therapy clearly has the potential to address the problem of enzyme delivery to the brain in neurodegenerative disease and is the subject of intense research for the treatment of LSDs (Sands and Davidson, 2006). Recent results have been promising, with clear benefits observed in patients with metachromatic leukodystrophy (Biffi et al., 2014). The treatment of neurodegenerative LSDs is likely to yield many important lessons for the potential treatment of neurodegenerative diseases by such approaches.

The major other therapeutic avenue for the treatment of LSDs is substrate reduction therapy (SRT). This treatment has the benefit of utilising small molecules which can be made orally available for ease of administration, and, can be BBB permeable (Platt et al., 2012). Evidently, these are much more suited to the treatment of age-related neurodegenerative disease than ERT; importantly they can also be used to treat LSDs caused by transmembrane proteins (Patterson et al., 2015). These are not corrected by ERT and it is unlikely that gene therapy will be able to correct these diseases, due to a lack of scope for cross-correction of cells. This means that extremely high levels of gene transduction would be needed in order for disease processes to be reduced.

The most well characterised SRT is miglustat, used in the treatment of Gaucher and NPC as previously discussed. Another example of SRT is the use of the soy isoflavanone Genistein (Piotrowska et al., 2011) to treat mucopolysaccharidoses. This is currently being investigated for the treatment of Mucopolysaccharidosis type III (Arfi et al., 2010). As with all small molecule drugs, their chemistry can induce side effects and these must be managed in patients. For example gastrointestinal disturbances in patients treated with miglustat, due to disaccharidase inhibition

(Belmatoug et al., 2011). Nevertheless, SRT still remains an attractive therapeutic option for LSDs and potentially neurodegenerative diseases as the potential for BBB permeable, orally available drugs is very desirable. A particular clinical challenge in relation to SRT is early enough treatment of patients, as it stands to reason that this would improve benefit. Accordingly it would be best to treat patients in early symprtomatic stages – the advent of new screening technologies, biomarkers and diagnostic procedures is helping to rectify this. As discussed in chapter 4, some of these considerations may mean that SRT has the potential to be utilised in neurodegenerative diseases which share lysosomal storage profiles with LSDs.

Recently, other therapeutic directions have been applied to LSDs reflecting their complex pathology. These may often target different organelles in an attempt to upregulate functions which may be able to reduce lysosomal pathology. An example of such a therapy is the neutraceutical curcumin, as a Ca^{2+} homoestasis modulator for the treatment of NPC discussed in section 1.5.2. The efficacy of treatments such as curcumin is difficult to evaluate due to a lack of a defined pharmaceutical formulation and the availability of a wide variety of supplements with different formulations, preventing defined clinical study. Further therapies (such as HPβCD for NPC, section 1.5.2.) have no defined mechanism of action and while they may be beneficial it is important that the mechanism behind their action is studied so they can be either improved by rational alterations or used at the optimal therapeutic intervention point. Clearly, more development of such therapies would be needed before they could be utilised for the treatment of more common neurodegenerative diseases.

The complex pathological cascades present in LSDs may be a limiting factor of efficacy with many of these therapeutic options in isolation. This may be compounded in neurogenerative diseases of complex, multifactorial aetiology such as Parkinson's and Alzheimer's.

Considering pathogeneic cascades, it is desirable to try and address an aspect of which that is the most fundamental – the primary defect. This explains why ERT is so successful; when a limiting factor such as BBB permeability or the primary defect occurring in a transmembrane protein are not present. However, most LSDs have these limiting factors and the primary defect in these diseases may not be a viable therapeutic target or early pathological steps may not be clearly defined. Clearly this is also the case in the majority of neurodegenerative diseases of ageing. In such

cases combination therapy may be the best therapeutic option. This has recently been demonstrated in animal models of NPC in which increased therapeutic benefit when mice were treated with miglustat (SRT), curcumin (Ca^{2+} homeostasis modulator) and ibuprofen (non-steroidal anti-inflammatory) to address multiple stages of the pathogenic cascade (Williams et al., 2014).

Considering the issues above the lessons learned from LSDs, and, future advances in therapy which may be achieved in this area of clinical research have great potential to inform the development of novel therapies for other neurodegenerative diseases.

References

Aarsland, D., J. Zaccai, and C. Brayne. "A Systematic Review of Prevalence Studies of Dementia in Parkinson's Disease." *Mov Disord* 20, no. 10 (Oct 2005): 1255-63.

Aerts, J. M., W. W. Kallemeijn, W. Wegdam, M. Joao Ferraz, M. J. van Breemen, N. Dekker, G. Kramer*, et al.* "Biomarkers in the Diagnosis of Lysosomal Storage Disorders: Proteins, Lipids, and Inhibodies." *J Inherit Metab Dis* 34, no. 3 (Jun 2011): 605-19.

Andrews, N. W., P. E. Almeida, and M. Corrotte. "Damage Control: Cellular Mechanisms of Plasma Membrane Repair." *Trends Cell Biol* 24, no. 12 (Dec 2014): 734-42.

Appelmans, F., and C. De Duve. "Tissue Fractionation Studies. 3. Further Observations on the Binding of Acid Phosphatase by Rat-Liver Particles." [In eng]. *Biochem J* 59, no. 3 (Mar 1955): 426-33.

Appelqvist, H., P. Waster, K. Kagedal, and K. Ollinger. "The Lysosome: From Waste Bag to Potential Therapeutic Target." *J Mol Cell Biol* 5, no. 4 (Aug 2013): 214-26.

Arfi, A., M. Richard, C. Gandolphe, and D. Scherman. "Storage Correction in Cells of Patients Suffering from Mucopolysaccharidoses Types Iiia and Vii after Treatment with Genistein and Other Isoflavones." *J Inherit Metab Dis* 33, no. 1 (Feb 2010): 61-7.

Arrasate, M., S. Mitra, E. S. Schweitzer, M. R. Segal, and S. Finkbeiner. "Inclusion Body Formation Reduces Levels of Mutant Huntingtin and the Risk of Neuronal Death." *Nature* 431, no. 7010 (Oct 14 2004): 805-10.

Avrahami, L., and H. Eldar-Finkelman. "Gsk-3 and Lysosomes Meet in Alzheimer's Disease." *Commun Integr Biol* 6, no. 5 (Sep 1 2013): e25179.

Aylward, E. H., B. F. Sparks, K. M. Field, V. Yallapragada, B. D. Shpritz, A. Rosenblatt, J. Brandt*, et al.* "Onset and Rate of Striatal Atrophy in Preclinical Huntington Disease." *Neurology* 63, no. 1 (Jul 13 2004): 66-72.

Babalola, J. O., M. Wendeler, B. Breiden, C. Arenz, G. Schwarzmann, S. Locatelli-Hoops, and K. Sandhoff. "Development of an Assay for the Intermembrane Transfer of Cholesterol by Niemann-Pick C2 Protein." *Biol Chem* 388, no. 6 (Jun 2007): 617-26.

Babiychuk, E. B., and A. Draeger. "Regulation of Ecto-5'-Nucleotidase Activity Via Ca2+-Dependent, Annexin 2-Mediated Membrane Rearrangement?" *Biochem Soc Trans* 34, no. Pt 3 (Jun 2006): 374-6.

Bach, G. "Mucolipidosis Type Iv." *Mol Genet Metab* 73, no. 3 (Jul 2001): 197-203.

Bae, M., N. Patel, H. Xu, M. Lee, K. Tominaga-Yamanaka, A. Nath, J. Geiger*, et al.* "Activation of Trpml1 Clears Intraneuronal Abeta in Preclinical Models of Hiv Infection." *J Neurosci* 34, no. 34 (Aug 20 2014): 11485-503.

Ballabio, A., and V. Gieselmann. "Lysosomal Disorders: From Storage to Cellular Damage." *Biochim Biophys Acta* 1793, no. 4 (Apr 2009): 684-96.

Baltazar, G. C., S. Guha, W. Lu, J. Lim, K. Boesze-Battaglia, A. M. Laties, P. Tyagi, U. B. Kompella, and C. H. Mitchell. "Acidic Nanoparticles Are Trafficked to Lysosomes and Restore an Acidic Lysosomal Ph and Degradative Function to Compromised Arpe-19 Cells." *PLoS One* 7, no. 12 (2012): e49635.

Bastide, M. F., W. G. Meissner, B. Picconi, S. Fasano, P. O. Fernagut, M. Feyder, V. Francardo*, et al.* "Pathophysiology of L-Dopa-Induced Motor and Non-Motor Complications in Parkinson's Disease." *Prog Neurobiol* 132 (Sep 2015): 96-168.

Belmatoug, N., A. Burlina, P. Giraldo, C. J. Hendriksz, D. J. Kuter, E. Mengel, and G. M. Pastores. "Gastrointestinal Disturbances and Their Management in Miglustat-Treated Patients." *J Inherit Metab Dis* 34, no. 5 (Oct 2011): 991-1001.

Ben-Zvi, I., S. Kivity, P. Langevitz, and Y. Shoenfeld. "Hydroxychloroquine: From Malaria to Autoimmunity." *Clin Rev Allergy Immunol* 42, no. 2 (Apr 2012): 145-53.

Bendikov-Bar, I., D. Rapaport, S. Larisch, and M. Horowitz. "Parkin-Mediated Ubiquitination of Mutant Glucocerebrosidase Leads to Competition with Its Substrates Paris and Arts." *Orphanet J Rare Dis* 9 (2014): 86.

Benktander, J., J. Angstrom, H. Karlsson, O. Teymournejad, S. Linden, M. Lebens, and S. Teneberg. "The Repertoire of Glycosphingolipids Recognized by Vibrio Cholerae." *PLoS One* 8, no. 1 (2013): e53999.

Bezprozvanny, I. "Calcium Signaling and Neurodegenerative Diseases." *Trends Mol Med* 15, no. 3 (Mar 2009): 89-100.

Bezprozvanny, I. "Presenilins: A Novel Link between Intracellular Calcium Signaling and Lysosomal Function?" *J Cell Biol* 198, no. 1 (Jul 9 2012): 7-10.

Bhutani, N., R. Piccirillo, R. Hourez, P. Venkatraman, and A. L. Goldberg. "Cathepsins L and Z Are Critical in Degrading Polyglutamine-Containing Proteins within Lysosomes." *J Biol Chem* 287, no. 21 (May 18 2012): 17471-82.

Biffi, A., E. Montini, L. Lorioli, M. Cesani, F. Fumagalli, T. Plati, C. Baldoli*, et al.* "Lentiviral Hematopoietic Stem Cell Gene Therapy Benefits Metachromatic Leukodystrophy." *Science* 341, no. 6148 (Aug 23 2013): 1233158.

Bird TD. Alzheimer Disease Overview. 1998 Oct 23 [Updated 2015 Sep 24]. In: Pagon RA, Adam MP, Ardinger HH, et al., editors. GeneReviews® [Internet]. Seattle (WA): University of Washington, Seattle; 1993-2016. Available from: http://www.ncbi.nlm.nih.gov/books/NBK1161/

Bjorkhem, I., V. Leoni, and S. Meaney. "Genetic Connections between Neurological Disorders and Cholesterol Metabolism." *J Lipid Res* 51, no. 9 (Sep 2010): 2489-503.

Blank, N., M. Schiller, S. Krienke, G. Wabnitz, A. D. Ho, and H. M. Lorenz. "Cholera Toxin Binds to Lipid Rafts but Has a Limited Specificity for Ganglioside Gm1." *Immunol Cell Biol* 85, no. 5 (Jul 2007): 378-82.

Blanz, J., F. Zunke, S. Markmann, M. Damme, T. Braulke, P. Saftig, and M. Schwake. "Mannose 6-Phosphate-Independent Lysosomal Sorting of Limp-2." *Traffic* 16, no. 10 (Oct 2015): 1127-36.

Boland, B., A. Kumar, S. Lee, F. M. Platt, J. Wegiel, W. H. Yu, and R. A. Nixon. "Autophagy Induction and Autophagosome Clearance in Neurons: Relationship to Autophagic Pathology in Alzheimer's Disease." *J Neurosci* 28, no. 27 (Jul 2 2008): 6926-37.

Boland, B., D. A. Smith, D. Mooney, S. S. Jung, D. M. Walsh, and F. M. Platt. "Macroautophagy Is Not Directly Involved in the Metabolism of Amyloid Precursor Protein." *J Biol Chem* 285, no. 48 (Nov 26 2010): 37415-26.

Braak, H., and K. Del Tredici. "Neuroanatomy and Pathology of Sporadic Parkinson's Disease." *Adv Anat Embryol Cell Biol* 201 (2009): 1-119.

Brady, R. O. "Enzyme Replacement for Lysosomal Diseases." *Annu Rev Med* 57 (2006): 283-96.

Brady, R. O., P. G. Pentchev, A. E. Gal, S. R. Hibbert, and A. S. Dekaban. "Replacement Therapy for Inherited Enzyme Deficiency. Use of Purified Glucocerebrosidase in Gaucher's Disease." *N Engl J Med* 291, no. 19 (Nov 7 1974): 989-93.

Brailoiu, E., T. Rahman, D. Churamani, D. L. Prole, G. C. Brailoiu, R. Hooper, C. W. Taylor, and S. Patel. "An Naadp-Gated Two-Pore Channel Targeted to the Plasma Membrane Uncouples Triggering from Amplifying Ca2+ Signals." *J Biol Chem* 285, no. 49 (Dec 3 2010): 38511-6.

Bras, J., A. Verloes, S. A. Schneider, S. E. Mole, and R. J. Guerreiro. "Mutation of the Parkinsonism Gene Atp13a2 Causes Neuronal Ceroid-Lipofuscinosis." *Hum Mol Genet* 21, no. 12 (Jun 15 2012): 2646-50.

Braulke, T., and J. S. Bonifacino. "Sorting of Lysosomal Proteins." *Biochim Biophys Acta* 1793, no. 4 (Apr 2009): 605-14.

Brunello, L., E. Zampese, C. Florean, T. Pozzan, P. Pizzo, and C. Fasolato. "Presenilin-2 Dampens Intracellular Ca2+ Stores by Increasing Ca2+ Leakage and Reducing Ca2+ Uptake." *J Cell Mol Med* 13, no. 9B (Sep 2009): 3358-69.

Burgunder, J. M. "Genetics of Huntington's Disease and Related Disorders." *Drug Discov Today* 19, no. 7 (Jul 2014): 985-9.

Burns, M., K. Gaynor, V. Olm, M. Mercken, J. LaFrancois, L. Wang, P. M. Mathews*, et al.* "Presenilin Redistribution Associated with Aberrant Cholesterol Transport Enhances Beta-Amyloid Production in Vivo." *J Neurosci* 23, no. 13 (Jul 2 2003): 5645-9.

Camnasio, S., A. Delli Carri, A. Lombardo, I. Grad, C. Mariotti, A. Castucci, B. Rozell*, et al.* "The First Reported Generation of Several Induced Pluripotent Stem Cell Lines from Homozygous and Heterozygous Huntington's Disease Patients Demonstrates Mutation Related Enhanced Lysosomal Activity." *Neurobiol Dis* 46, no. 1 (Apr 2012): 41-51.

Canuel, M., A. Korkidakis, K. Konnyu, and C. R. Morales. "Sortilin Mediates the Lysosomal Targeting of Cathepsins D and H." *Biochem Biophys Res Commun* 373, no. 2 (Aug 22 2008): 292-7.

Canuel, M., Y. Libin, and C. R. Morales. "The Interactomics of Sortilin: An Ancient Lysosomal Receptor Evolving New Functions." *Histol Histopathol* 24, no. 4 (Apr 2009): 481-92.

Carcel-Trullols, J., A. D. Kovacs, and D. A. Pearce. "Cell Biology of the Ncl Proteins: What They Do and Don't Do." *Biochim Biophys Acta* 1852, no. 10 Pt B (Oct 2015): 2242-55.

Carroll, J. B., A. Deik, E. Fossale, R. M. Weston, J. R. Guide, J. Arjomand, S. Kwak, C. B. Clish, and M. E. MacDonald. "Hdhq111 Mice Exhibit Tissue Specific Metabolite Profiles That Include Striatal Lipid Accumulation." *PLoS One* 10, no. 8 (2015): e0134465.

Carstea, E. D., J. A. Morris, K. G. Coleman, S. K. Loftus, D. Zhang, C. Cummings, J. Gu*, et al.* "Niemann-Pick C1 Disease Gene: Homology to Mediators of Cholesterol Homeostasis." *Science* 277, no. 5323 (Jul 11 1997): 228-31.

Castiglioni, V., M. Onorati, C. Rochon, and E. Cattaneo. "Induced Pluripotent Stem Cell Lines from Huntington's Disease Mice Undergo Neuronal Differentiation While Showing Alterations in the Lysosomal Pathway." *Neurobiol Dis* 46, no. 1 (Apr 2012): 30-40.

Cataldo, A. M., J. L. Barnett, C. Pieroni, and R. A. Nixon. "Increased Neuronal Endocytosis and Protease Delivery to Early Endosomes in Sporadic Alzheimer's Disease: Neuropathologic Evidence for a Mechanism of Increased Beta-Amyloidogenesis." *J Neurosci* 17, no. 16 (Aug 15 1997): 6142-51.

Cataldo, A. M., P. M. Mathews, A. B. Boiteau, L. C. Hassinger, C. M. Peterhoff, Y. Jiang, K. Mullaney*, et al.* "Down Syndrome Fibroblast Model of Alzheimer-Related Endosome Pathology: Accelerated Endocytosis Promotes Late Endocytic Defects." *Am J Pathol* 173, no. 2 (Aug 2008): 370-84.

Cataldo, A. M., C. M. Peterhoff, J. C. Troncoso, T. Gomez-Isla, B. T. Hyman, and R. A. Nixon. "Endocytic Pathway Abnormalities Precede Amyloid Beta Deposition in Sporadic Alzheimer's Disease and Down Syndrome: Differential Effects of Apoe Genotype and Presenilin Mutations." *Am J Pathol* 157, no. 1 (Jul 2000): 277-86.

Cattaneo, E., C. Zuccato, and M. Tartari. "Normal Huntingtin Function: An Alternative Approach to Huntington's Disease." *Nat Rev Neurosci* 6, no. 12 (Dec 2005): 919-30.

Cerny, J., Y. Feng, A. Yu, K. Miyake, B. Borgonovo, J. Klumperman, J. Meldolesi, P. L. McNeil, and T. Kirchhausen. "The Small Chemical Vacuolin-1 Inhibits Ca(2+)-Dependent Lysosomal Exocytosis but Not Cell Resealing." *EMBO Rep* 5, no. 9 (Sep 2004): 883-8.

Cesca, F., E. Bregant, B. Peterlin, M. Zadel, G. Dubsky de Wittenau, G. Siciliano, R. Ceravolo*, et al.* "Evaluating the Serca2 and Vegf Mrnas as Potential

Molecular Biomarkers of the Onset and Progression in Huntington's Disease." *PLoS One* 10, no. 4 (2015): e0125259.

Chandrachud, U., M. W. Walker, A. M. Simas, S. Heetveld, A. Petcherski, M. Klein, H. Oh*, et al.* "Unbiased Cell-Based Screening in a Neuronal Cell Model of Batten Disease Highlights an Interaction between Ca2+ Homeostasis, Autophagy, and Cln3 Protein Function." *J Biol Chem* 290, no. 23 (Jun 5 2015): 14361-80.

Chang, T. Y., C. C. Chang, N. Ohgami, and Y. Yamauchi. "Cholesterol Sensing, Trafficking, and Esterification." *Annu Rev Cell Dev Biol* 22 (2006): 129-57.

Chartier-Harlin, M. C., F. Crawford, H. Houlden, A. Warren, D. Hughes, L. Fidani, A. Goate*, et al.* "Early-Onset Alzheimer's Disease Caused by Mutations at Codon 717 of the Beta-Amyloid Precursor Protein Gene." *Nature* 353, no. 6347 (Oct 31 1991): 844-6.

Chen, C. M., C. H. Lin, H. F. Juan, F. J. Hu, Y. C. Hsiao, H. Y. Chang, C. Y. Chao*, et al.* "Atp13a2 Variability in Taiwanese Parkinson's Disease." *Am J Med Genet B Neuropsychiatr Genet* 156B, no. 6 (Sep 2011): 720-9.

Chen, F. W., C. Li, and Y. A. Ioannou. "Cyclodextrin Induces Calcium-Dependent Lysosomal Exocytosis." [In eng]. *PLoS One* 5, no. 11 (2010): e15054.

Chen, M., and J. Wang. "Gaucher Disease: Review of the Literature." *Arch Pathol Lab Med* 132, no. 5 (May 2008): 851-3.

Chevallier, J., Z. Chamoun, G. Jiang, G. Prestwich, N. Sakai, S. Matile, R. G. Parton, and J. Gruenberg. "Lysobisphosphatidic Acid Controls Endosomal Cholesterol Levels." *J Biol Chem* 283, no. 41 (Oct 10 2008): 27871-80.

Choudhury, A., D. K. Sharma, D. L. Marks, and R. E. Pagano. "Elevated Endosomal Cholesterol Levels in Niemann-Pick Cells Inhibit Rab4 and Perturb Membrane Recycling." *Mol Biol Cell* 15, no. 10 (Oct 2004): 4500-11.

Christensen, K. A., J. T. Myers, and J. A. Swanson. "Ph-Dependent Regulation of Lysosomal Calcium in Macrophages." *J Cell Sci* 115, no. Pt 3 (Feb 1 2002): 599-607.

Churchill, G. C., Y. Okada, J. M. Thomas, A. A. Genazzani, S. Patel, and A. Galione. "Naadp Mobilizes Ca(2+) from Reserve Granules, Lysosome-Related Organelles, in Sea Urchin Eggs." *Cell* 111, no. 5 (Nov 27 2002): 703-8.

Clark, L. N., A. Nicolai, S. Afridi, J. Harris, H. Mejia-Santana, L. Strug, L. J. Cote*, et al.* "Pilot Association Study of the Beta-Glucocerebrosidase N370s Allele and Parkinson's Disease in Subjects of Jewish Ethnicity." *Mov Disord* 20, no. 1 (Jan 2005): 100-3.

Coelho, D., J. C. Kim, I. R. Miousse, S. Fung, M. du Moulin, I. Buers, T. Suormala*, et al.* "Mutations in Abcd4 Cause a New Inborn Error of Vitamin B12 Metabolism." *Nat Genet* 44, no. 10 (Oct 2012): 1152-5.

Coen, K., R. S. Flannagan, S. Baron, L. R. Carraro-Lacroix, D. Wang, W. Vermeire, C. Michiels*, et al.* "Lysosomal Calcium Homeostasis Defects, Not Proton Pump Defects, Cause Endo-Lysosomal Dysfunction in Psen-Deficient Cells." *J Cell Biol* 198, no. 1 (Jul 9 2012): 23-35.

Coffey, E. E., J. M. Beckel, A. M. Laties, and C. H. Mitchell. "Lysosomal Alkalization and Dysfunction in Human Fibroblasts with the Alzheimer's Disease-Linked Presenilin 1 A246e Mutation Can Be Reversed with Camp." *Neuroscience* 263 (Mar 28 2014): 111-24.

Cornutiu, G. "The Epidemiological Scale of Alzheimer's Disease." *J Clin Med Res* 7, no. 9 (Sep 2015): 657-66.

Coutinho, M. F., L. Lacerda, and S. Alves. "Glycosaminoglycan Storage Disorders: A Review." *Biochem Res Int* 2012 (2012): 471325.

Cowan, C. M., and L. A. Raymond. "Selective Neuronal Degeneration in Huntington's Disease." *Curr Top Dev Biol* 75 (2006): 25-71.

Cox, T. M., and M. B. Cachon-Gonzalez. "The Cellular Pathology of Lysosomal Diseases." *J Pathol* 226, no. 2 (Jan 2012): 241-54.

Crumling, M. A., L. Liu, P. V. Thomas, J. Benson, A. Kanicki, L. Kabara, K. Halsey, D. Dolan, and R. K. Duncan. "Hearing Loss and Hair Cell Death in Mice Given the Cholesterol-Chelating Agent Hydroxypropyl-Beta-Cyclodextrin." *PLoS One* 7, no. 12 (2012): e53280.

Cuervo, A. M. "Autophagy and Aging: Keeping That Old Broom Working." *Trends Genet* 24, no. 12 (Dec 2008): 604-12.

Cuervo, A. M., and E. Wong. "Chaperone-Mediated Autophagy: Roles in Disease and Aging." *Cell Res* 24, no. 1 (Jan 2014): 92-104.

Cullen, P. J. "Endosomal Sorting and Signalling: An Emerging Role for Sorting Nexins." *Nat Rev Mol Cell Biol* 9, no. 7 (Jul 2008): 574-82.

Cullen, V., M. Lindfors, J. Ng, A. Paetau, E. Swinton, P. Kolodziej, H. Boston*, et al.* "Cathepsin D Expression Level Affects Alpha-Synuclein Processing, Aggregation, and Toxicity in Vivo." *Mol Brain* 2 (2009): 5.

Das, P. K., G. J. Murray, A. E. Gal, and J. A. Barranger. "Glucocerebrosidase Deficiency and Lysosomal Storage of Glucocerebroside Induced in Cultured Macrophages." *Exp Cell Res* 168, no. 2 (Feb 1987): 463-74.

Dauer, W., and S. Przedborski. "Parkinson's Disease: Mechanisms and Models." *Neuron* 39, no. 6 (Sep 11 2003): 889-909.

Davidson, C. D., N. F. Ali, M. C. Micsenyi, G. Stephney, S. Renault, K. Dobrenis, D. S. Ory, M. T. Vanier, and S. U. Walkley. "Chronic Cyclodextrin Treatment of Murine Niemann-Pick C Disease Ameliorates Neuronal Cholesterol and Glycosphingolipid Storage and Disease Progression." *PLoS One* 4, no. 9 (2009): e6951.

de Duve, C. "The Lysosome Turns Fifty." *Nat Cell Biol* 7, no. 9 (Sep 2005): 847-9.

de Duve, C., B. C. Pressman, R. Gianetto, R. Wattiaux, and F. Appelmans. "Tissue Fractionation Studies. 6. Intracellular Distribution Patterns of Enzymes in Rat-Liver Tissue." *Biochem J* 60, no. 4 (Aug 1955): 604-17.

de la Mata, M., D. Cotan, M. Oropesa-Avila, J. Garrido-Maraver, M. D. Cordero, M. Villanueva Paz, A. Delgado Pavon*, et al.* "Pharmacological Chaperones and Coenzyme Q10 Treatment Improves Mutant Beta-Glucocerebrosidase Activity and Mitochondrial Function in Neuronopathic Forms of Gaucher Disease." [In eng]. *Sci Rep* 5 (2015): 10903.

De Rosa, P., E. S. Marini, V. Gelmetti, and E. M. Valente. "Candidate Genes for Parkinson Disease: Lessons from Pathogenesis." *Clin Chim Acta* 449 (Sep 20 2015): 68-76.

Dehay, B., A. Ramirez, M. Martinez-Vicente, C. Perier, M. H. Canron, E. Doudnikoff, A. Vital*, et al.* "Loss of P-Type Atpase Atp13a2/Park9 Function Induces General Lysosomal Deficiency and Leads to Parkinson Disease Neurodegeneration." *Proc Natl Acad Sci U S A* 109, no. 24 (Jun 12 2012): 9611-6.

Dekker, N., L. van Dussen, C. E. Hollak, H. Overkleeft, S. Scheij, K. Ghauharali, M. J. van Breemen*, et al.* "Elevated Plasma Glucosylsphingosine in Gaucher Disease: Relation to Phenotype, Storage Cell Markers, and Therapeutic Response." *Blood* 118, no. 16 (Oct 20 2011): e118-27.

del Toro, D., X. Xifro, A. Pol, S. Humbert, F. Saudou, J. M. Canals, and J. Alberch. "Altered Cholesterol Homeostasis Contributes to Enhanced Excitotoxicity in Huntington's Disease." *J Neurochem* 115, no. 1 (Oct 2010): 153-67.

Delabar, J. M., D. Goldgaber, Y. Lamour, A. Nicole, J. L. Huret, J. de Grouchy, P. Brown, D. C. Gajdusek, and P. M. Sinet. "Beta Amyloid Gene Duplication in Alzheimer's Disease and Karyotypically Normal Down Syndrome." *Science* 235, no. 4794 (Mar 13 1987): 1390-2.

Denny, C. A., P. A. Desplats, E. A. Thomas, and T. N. Seyfried. "Cerebellar Lipid Differences between R6/1 Transgenic Mice and Humans with Huntington's Disease." *J Neurochem* 115, no. 3 (Nov 2010): 748-58.

Desplats, P. A., C. A. Denny, K. E. Kass, T. Gilmartin, S. R. Head, J. G. Sutcliffe, T. N. Seyfried, and E. A. Thomas. "Glycolipid and Ganglioside Metabolism Imbalances in Huntington's Disease." *Neurobiol Dis* 27, no. 3 (Sep 2007): 265-77.

Di Fonzo, A., H. F. Chien, M. Socal, S. Giraudo, C. Tassorelli, G. Iliceto, G. Fabbrini*, et al.* "Atp13a2 Missense Mutations in Juvenile Parkinsonism and Young Onset Parkinson Disease." *Neurology* 68, no. 19 (May 8 2007): 1557-62.

Di Guardo, G. "Lipofuscin, Lipofuscin-Like Pigments and Autofluorescence." *Eur J Histochem* 59, no. 1 (2015): 2485.

Di Pardo, A., V. Maglione, M. Alpaugh, M. Horkey, R. S. Atwal, J. Sassone, A. Ciammola*, et al.* "Ganglioside Gm1 Induces Phosphorylation of Mutant Huntingtin and Restores Normal Motor Behavior in Huntington Disease Mice." *Proc Natl Acad Sci U S A* 109, no. 9 (Feb 28 2012): 3528-33.

Dickson, D. W. "Parkinson's Disease and Parkinsonism: Neuropathology." *Cold Spring Harb Perspect Med* 2, no. 8 (2012).

Dodson, M. W., T. Zhang, C. Jiang, S. Chen, and M. Guo. "Roles of the Drosophila Lrrk2 Homolog in Rab7-Dependent Lysosomal Positioning." *Hum Mol Genet* 21, no. 6 (Mar 15 2012): 1350-63.

Dong, X. P., X. Cheng, E. Mills, M. Delling, F. Wang, T. Kurz, and H. Xu. "The Type Iv Mucolipidosis-Associated Protein Trpml1 Is an Endolysosomal Iron Release Channel." *Nature* 455, no. 7215 (Oct 16 2008): 992-6.

Dong, X. P., D. Shen, X. Wang, T. Dawson, X. Li, Q. Zhang, X. Cheng*, et al.* "Pi(3,5)P(2) Controls Membrane Trafficking by Direct Activation of Mucolipin Ca(2+) Release Channels in the Endolysosome." *Nat Commun* 1 (2010): 38.

Dorsey, E. R., R. Constantinescu, J. P. Thompson, K. M. Biglan, R. G. Holloway, K. Kieburtz, F. J. Marshall*, et al.* "Projected Number of People with Parkinson Disease in the Most Populous Nations, 2005 through 2030." *Neurology* 68, no. 5 (Jan 30 2007): 384-6.

Du, X., and H. Yang. "Endosomal Cholesterol Trafficking: Protein Factors at a Glance." *Acta Biochim Biophys Sin (Shanghai)* 45, no. 1 (Jan 2013): 11-7.

Eblan, M. J., S. Scholz, B. Stubblefield, U. Gutti, O. Goker-Alpan, K. S. Hruska, A. B. Singleton, and E. Sidransky. "Glucocerebrosidase Mutations Are Not Found in Association with Lrrk2 G2019s in Subjects with Parkinsonism." *Neurosci Lett* 404, no. 1-2 (Aug 14 2006): 163-5.

Edbauer, D., E. Winkler, J. T. Regula, B. Pesold, H. Steiner, and C. Haass. "Reconstitution of Gamma-Secretase Activity." *Nat Cell Biol* 5, no. 5 (May 2003): 486-8.

Edwardson, J. M., C. T. Wang, B. Gong, A. Wyttenbach, J. Bai, M. B. Jackson, E. R. Chapman, and A. J. Morton. "Expression of Mutant Huntingtin Blocks Exocytosis in Pc12 Cells by Depletion of Complexin Ii." *J Biol Chem* 278, no. 33 (Aug 15 2003): 30849-53.

Ehrlich, M. E., L. Conti, M. Toselli, L. Taglietti, E. Fiorillo, V. Taglietti, S. Ivkovic*, et al.* "St14a Cells Have Properties of a Medium-Size Spiny Neuron." *Exp Neurol* 167, no. 2 (Feb 2001): 215-26.

Erie, C., M. Sacino, L. Houle, M. L. Lu, and J. Wei. "Altered Lysosomal Positioning Affects Lysosomal Functions in a Cellular Model of Huntington's Disease." *Eur J Neurosci* 42, no. 3 (Aug 2015): 1941-51.

Escott-Price, V., C. Bellenguez, L. S. Wang, S. H. Choi, D. Harold, L. Jones, P. Holmans*, et al.* "Gene-Wide Analysis Detects Two New Susceptibility Genes for Alzheimer's Disease." *PLoS One* 9, no. 6 (2014): e94661.

Eskelinen, E. L., and P. Saftig. "Autophagy: A Lysosomal Degradation Pathway with a Central Role in Health and Disease." *Biochim Biophys Acta* 1793, no. 4 (Apr 2009): 664-73.

Evans, S. J., I. Douglas, M. D. Rawlins, N. S. Wexler, S. J. Tabrizi, and L. Smeeth. "Prevalence of Adult Huntington's Disease in the Uk Based on Diagnoses Recorded in General Practice Records." *J Neurol Neurosurg Psychiatry* 84, no. 10 (Oct 2013): 1156-60.

Faden, M. A., D. Krakow, F. Ezgu, D. L. Rimoin, and R. S. Lachman. "The Erlenmeyer Flask Bone Deformity in the Skeletal Dysplasias." *Am J Med Genet A* 149A, no. 6 (Jun 2009): 1334-45.

Fairley, C., A. Zimran, M. Phillips, M. Cizmarik, J. Yee, N. Weinreb, and S. Packman. "Phenotypic Heterogeneity of N370s Homozygotes with Type I Gaucher Disease: An Analysis of 798 Patients from the Icgg Gaucher Registry." *J Inherit Metab Dis* 31, no. 6 (Dec 2008): 738-44.

Fares, H., and I. Greenwald. "Regulation of Endocytosis by Cup-5, the Caenorhabditis Elegans Mucolipin-1 Homolog." *Nat Genet* 28, no. 1 (May 2001): 64-8.

Farfel-Becker, T., E. B. Vitner, and A. H. Futerman. "Animal Models for Gaucher Disease Research." *Dis Model Mech* 4, no. 6 (Nov 2011): 746-52.

Farfel-Becker, T., E. B. Vitner, S. N. Pressey, R. Eilam, J. D. Cooper, and A. H. Futerman. "Spatial and Temporal Correlation between Neuron Loss and Neuroinflammation in a Mouse Model of Neuronopathic Gaucher Disease." *Hum Mol Genet* 20, no. 7 (Apr 1 2011): 1375-86.

Farlow J, Pankratz ND, Wojcieszek J, et al. Parkinson Disease Overview. 2004 May 25 [Updated 2014 Feb 27]. In: Pagon RA, Adam MP, Ardinger HH, et al., editors. GeneReviews® [Internet]. Seattle (WA): University of Washington, Seattle; 1993-2016. Available from: http://www.ncbi.nlm.nih.gov/books/NBK1223/

Farg, M. A., V. Sundaramoorthy, J. M. Sultana, S. Yang, R. A. Atkinson, V. Levina, M. A. Halloran*, et al.* "C9orf72, Implicated in Amytrophic Lateral Sclerosis and Frontotemporal Dementia, Regulates Endosomal Trafficking." *Hum Mol Genet* 23, no. 13 (Jul 1 2014): 3579-95.

Farre, J. C., A. Burkenroad, S. F. Burnett, and S. Subramani. "Phosphorylation of Mitophagy and Pexophagy Receptors Coordinates Their Interaction with Atg8 and Atg11." *EMBO Rep* 14, no. 5 (May 2013): 441-9.

Fehrenbacher, N., L. Bastholm, T. Kirkegaard-Sorensen, B. Rafn, T. Bottzauw, C. Nielsen, E. Weber*, et al.* "Sensitization to the Lysosomal Cell Death Pathway by Oncogene-Induced Down-Regulation of Lysosome-Associated Membrane Proteins 1 and 2." *Cancer Res* 68, no. 16 (Aug 15 2008): 6623-33.

Feng, X., J. Xiong, Y. Lu, X. Xia, and M. X. Zhu. "Differential Mechanisms of Action of the Mucolipin Synthetic Agonist, Ml-Sa1, on Insect Trpml and Mammalian Trpml1." *Cell Calcium* 56, no. 6 (Dec 2014): 446-56.

Ficicioglu, C. "Review of Miglustat for Clinical Management in Gaucher Disease Type 1." *Ther Clin Risk Manag* 4, no. 2 (Apr 2008): 425-31.

Fuller, M., P. J. Meikle, and J. J. Hopwood. "Epidemiology of Lysosomal Storage Diseases: An Overview." In *Fabry Disease: Perspectives from 5 Years of Fos*, edited by A. Mehta, M. Beck and G. Sunder-Plassmann. Oxford: Oxford PharmaGenesis, 2006.

Gallagher, M. D., E. Suh, M. Grossman, L. Elman, L. McCluskey, J. C. Van Swieten, S. Al-Sarraj*, et al.* "Tmem106b Is a Genetic Modifier of Frontotemporal Lobar

Degeneration with C9orf72 Hexanucleotide Repeat Expansions." *Acta Neuropathol* 127, no. 3 (Mar 2014): 407-18.

Gan-Or, Z., A. Orr-Urtreger, R. N. Alcalay, S. Bressman, N. Giladi, and G. A. Rouleau. "The Emerging Role of Smpd1 Mutations in Parkinson's Disease: Implications for Future Studies." *Parkinsonism Relat Disord* (Aug 20 2015).

Gault, C. R., L. M. Obeid, and Y. A. Hannun. "An Overview of Sphingolipid Metabolism: From Synthesis to Breakdown." *Adv Exp Med Biol* 688 (2010): 1-23.

Gerasimenko, J. V., A. V. Tepikin, O. H. Petersen, and O. V. Gerasimenko. "Calcium Uptake Via Endocytosis with Rapid Release from Acidifying Endosomes." *Curr Biol* 8, no. 24 (Dec 3 1998): 1335-8.

Gerrish, A., G. Russo, A. Richards, V. Moskvina, D. Ivanov, D. Harold, R. Sims*, et al.* "The Role of Variation at Abetapp, Psen1, Psen2, and Mapt in Late Onset Alzheimer's Disease." *J Alzheimers Dis* 28, no. 2 (2012): 377-87.

Glabe, C. "Intracellular Mechanisms of Amyloid Accumulation and Pathogenesis in Alzheimer's Disease." *J Mol Neurosci* 17, no. 2 (Oct 2001): 137-45.

Goate, A., M. C. Chartier-Harlin, M. Mullan, J. Brown, F. Crawford, L. Fidani, L. Giuffra*, et al.* "Segregation of a Missense Mutation in the Amyloid Precursor Protein Gene with Familial Alzheimer's Disease." *Nature* 349, no. 6311 (Feb 21 1991): 704-6.

Goate, A., and J. Hardy. "Twenty Years of Alzheimer's Disease-Causing Mutations." *J Neurochem* 120 Suppl 1 (Jan 2012): 3-8.

Goedert, M., M. G. Spillantini, R. Jakes, D. Rutherford, and R. A. Crowther. "Multiple Isoforms of Human Microtubule-Associated Protein Tau: Sequences and Localization in Neurofibrillary Tangles of Alzheimer's Disease." *Neuron* 3, no. 4 (Oct 1989): 519-26.

Goldman, S. M. "Environmental Toxins and Parkinson's Disease." *Annu Rev Pharmacol Toxicol* 54 (2014): 141-64.

Gomez-Isla, T., R. Hollister, H. West, S. Mui, J. H. Growdon, R. C. Petersen, J. E. Parisi, and B. T. Hyman. "Neuronal Loss Correlates with but Exceeds Neurofibrillary Tangles in Alzheimer's Disease." *Ann Neurol* 41, no. 1 (Jan 1997): 17-24.

Gomez-Suaga, P., B. Luzon-Toro, D. Churamani, L. Zhang, D. Bloor-Young, S. Patel, P. G. Woodman, G. C. Churchill, and S. Hilfiker. "Leucine-Rich Repeat Kinase 2 Regulates Autophagy through a Calcium-Dependent Pathway Involving Naadp." *Hum Mol Genet* 21, no. 3 (Feb 1 2012): 511-25.

Gomez-Suaga, P., P. Rivero-Rios, E. Fdez, M. Blanca Ramirez, I. Ferrer, A. Aiastui, A. Lopez De Munain, and S. Hilfiker. "Lrrk2 Delays Degradative Receptor Trafficking by Impeding Late Endosomal Budding through Decreasing Rab7 Activity." *Hum Mol Genet* 23, no. 25 (Dec 20 2014): 6779-96.

Gondre-Lewis, M. C., R. McGlynn, and S. U. Walkley. "Cholesterol Accumulation in Npc1-Deficient Neurons Is Ganglioside Dependent." *Curr Biol* 13, no. 15 (Aug 5 2003): 1324-9.

Grabowski, G. A. "Gaucher Disease and Other Storage Disorders." *Hematology Am Soc Hematol Educ Program* 2012 (2012): 13-8.

Grabowski, G.A. "Phenotype, Diagnosis, and Treatment of Gaucher's Disease." *Lancet* 372, no. 9645 (Oct 4 2008): 1263-71.

Grabowski, G. A., and M. Horowitz. "Gaucher's Disease: Molecular, Genetic and Enzymological Aspects." *Baillieres Clin Haematol* 10, no. 4 (Dec 1997): 635-56.

Graves, A. R., P. K. Curran, C. L. Smith, and J. A. Mindell. "The Cl-/H+ Antiporter Clc-7 Is the Primary Chloride Permeation Pathway in Lysosomes." *Nature* 453, no. 7196 (Jun 5 2008): 788-92.

Grbovic, O. M., P. M. Mathews, Y. Jiang, S. D. Schmidt, R. Dinakar, N. B. Summers-Terio, B. P. Ceresa, R. A. Nixon, and A. M. Cataldo. "Rab5-Stimulated up-Regulation of the Endocytic Pathway Increases Intracellular Beta-Cleaved Amyloid Precursor Protein Carboxyl-Terminal Fragment Levels and Abeta Production." *J Biol Chem* 278, no. 33 (Aug 15 2003): 31261-8.

Grimm, M. O., H. S. Grimm, A. J. Patzold, E. G. Zinser, R. Halonen, M. Duering, J. A. Tschape*, et al.* "Regulation of Cholesterol and Sphingomyelin Metabolism by Amyloid-Beta and Presenilin." *Nat Cell Biol* 7, no. 11 (Nov 2005): 1118-23.

Grimm, M. O., V. C. Zimmer, J. Lehmann, H. S. Grimm, and T. Hartmann. "The Impact of Cholesterol, Dha, and Sphingolipids on Alzheimer's Disease." *Biomed Res Int* 2013 (2013): 814390.

Grunewald, A., B. Arns, P. Seibler, A. Rakovic, A. Munchau, A. Ramirez, C. M. Sue, and C. Klein. "Atp13a2 Mutations Impair Mitochondrial Function in Fibroblasts from Patients with Kufor-Rakeb Syndrome." *Neurobiol Aging* 33, no. 8 (Aug 2012): 1843 e1-7.

Guggilla, S. R., J. R. Senagari, P. N. Rao, and S. Madireddi. "Spectrum of Mutations in the Atp Binding Domain of Atp7b Gene of Wilson Disease in a Regional Indian Cohort." *Gene* 569, no. 1 (Sep 10 2015): 83-7.

Guha, S., E. E. Coffey, W. Lu, J. C. Lim, J. M. Beckel, A. M. Laties, K. Boesze-Battaglia, and C. H. Mitchell. "Approaches for Detecting Lysosomal Alkalinization and Impaired Degradation in Fresh and Cultured Rpe Cells: Evidence for a Role in Retinal Degenerations." *Exp Eye Res* 126 (Sep 2014): 68-76.

Gusella, J. F., and M. E. MacDonald. "Huntington's Disease: The Case for Genetic Modifiers." *Genome Med* 1, no. 8 (2009): 80.

Hackam, A. S., A. S. Yassa, R. Singaraja, M. Metzler, C. A. Gutekunst, L. Gan, S. Warby*, et al.* "Huntingtin Interacting Protein 1 Induces Apoptosis Via a Novel Caspase-Dependent Death Effector Domain." *J Biol Chem* 275, no. 52 (Dec 29 2000): 41299-308.

Halliday, G. M., and C. H. Stevens. "Glia: Initiators and Progressors of Pathology in Parkinson's Disease." *Mov Disord* 26, no. 1 (Jan 2011): 6-17.

Hamilton, J. A. "Fast Flip-Flop of Cholesterol and Fatty Acids in Membranes: Implications for Membrane Transport Proteins." *Curr Opin Lipidol* 14, no. 3 (Jun 2003): 263-71.

Hampshire, D. J., E. Roberts, Y. Crow, J. Bond, A. Mubaidin, A. L. Wriekat, A. Al-Din, and C. G. Woods. "Kufor-Rakeb Syndrome, Pallido-Pyramidal Degeneration with Supranuclear Upgaze Paresis and Dementia, Maps to 1p36." *J Med Genet* 38, no. 10 (Oct 2001): 680-2.

Hannun, Y. A., and L. M. Obeid. "Principles of Bioactive Lipid Signalling: Lessons from Sphingolipids." *Nat Rev Mol Cell Biol* 9, no. 2 (Feb 2008): 139-50.

Harada, M., S. Shakado, S. Sakisaka, S. Tamaki, M. Ohishi, K. Sasatomi, H. Koga, M. Sata, and K. Tanikawa. "Bafilomycin A1, a Specific Inhibitor of V-Type H+-Atpases, Inhibits the Acidification of Endocytic Structures and Inhibits Horseradish Peroxidase Uptake in Isolated Rat Sinusoidal Endothelial Cells." *Liver* 17, no. 5 (Oct 1997): 244-50.

Hardy, J. A., and G. A. Higgins. "Alzheimer's Disease: The Amyloid Cascade Hypothesis." *Science* 256, no. 5054 (Apr 10 1992): 184-5.

Hardy, J., and D. Allsop. "Amyloid Deposition as the Central Event in the Aetiology of Alzheimer's Disease." *Trends Pharmacol Sci* 12, no. 10 (Oct 1991): 383-8.

Hars, E. S., H. Qi, A. G. Ryazanov, S. Jin, L. Cai, C. Hu, and L. F. Liu. "Autophagy Regulates Ageing in C. Elegans." *Autophagy* 3, no. 2 (Mar-Apr 2007): 93-5.

Haughey, N. J., V. V. Bandaru, M. Bae, and M. P. Mattson. "Roles for Dysfunctional Sphingolipid Metabolism in Alzheimer's Disease Neuropathogenesis." *Biochim Biophys Acta* 1801, no. 8 (Aug 2010): 878-86.

Heinecke, K. A., B. N. Peacock, B. R. Blazar, J. Tolar, and T. N. Seyfried. "Lipid Composition of Whole Brain and Cerebellum in Hurler Syndrome (Mps Ih) Mice." *Neurochem Res* 36, no. 9 (Sep 2011): 1669-76.

Henderson, K. A., A. L. Hughes, and D. E. Gottschling. "Mother-Daughter Asymmetry of Ph Underlies Aging and Rejuvenation in Yeast." *Elife* 3 (2014): e03504.

Henderson, L. P., L. Lin, A. Prasad, C. A. Paul, T. Y. Chang, and R. A. Maue. "Embryonic Striatal Neurons from Niemann-Pick Type C Mice Exhibit Defects in Cholesterol Metabolism and Neurotrophin Responsiveness." *J Biol Chem* 275, no. 26 (Jun 30 2000): 20179-87.

Henry, A. G., S. Aghamohammadzadeh, H. Samaroo, Y. Chen, K. Mou, E. Needle, and W. D. Hirst. "Pathogenic Lrrk2 Mutations, through Increased Kinase Activity, Produce Enlarged Lysosomes with Reduced Degradative Capacity and Increase Atp13a2 Expression." *Hum Mol Genet* (Aug 6 2015).

Hirst, W. D., N. Y. Cheung, M. Rattray, G. W. Price, and G. P. Wilkin. "Cultured Astrocytes Express Messenger Rna for Multiple Serotonin Receptor Subtypes, without Functional Coupling of 5-Ht1 Receptor Subtypes to Adenylyl Cyclase." *Brain Res Mol Brain Res* 61, no. 1-2 (Oct 30 1998): 90-9.

Hockey, L. N., B. S. Kilpatrick, E. R. Eden, Y. Lin-Moshier, G. C. Brailoiu, E. Brailoiu, C. E. Futter*, et al.* "Dysregulation of Lysosomal Morphology by Pathogenic Lrrk2 Is Corrected by Tpc2 Inhibition." *J Cell Sci* 128, no. 2 (Jan 15 2015): 232-8.

Hoffman, E. P., M. L. Barr, M. A. Giovanni, and M. F. Murray. "Lysosomal Acid Lipase Deficiency." In *Genereviews(R)*, edited by R. A. Pagon, M. P. Adam, H. H. Ardinger, S. E. Wallace, A. Amemiya, L. J. H. Bean, T. D. Bird*, et al.* Seattle WA: University of Washington, Seattle, 1993.

Holemans, T., D. M. Sorensen, S. van Veen, S. Martin, D. Hermans, G. C. Kemmer, C. Van den Haute*, et al.* "A Lipid Switch Unlocks Parkinson's Disease-Associated Atp13a2." *Proc Natl Acad Sci U S A* 112, no. 29 (Jul 21 2015): 9040-5.

Holtta-Vuori, M., and E. Ikonen. "Endosomal Cholesterol Traffic: Vesicular and Non-Vesicular Mechanisms Meet." *Biochem Soc Trans* 34, no. Pt 3 (Jun 2006): 392-4.

Hopfner, F., E. C. Schulte, B. Mollenhauer, B. Bereznai, F. Knauf, P. Lichtner, A. Zimprich*, et al.* "The Role of Scarb2 as Susceptibility Factor in Parkinson's Disease." *Mov Disord* 28, no. 4 (Apr 2013): 538-40.

Horowitz, M., and A. Zimran. "Mutations Causing Gaucher Disease." *Hum Mutat* 3, no. 1 (1994): 1-11.

Huang, H. M., H. L. Chen, and G. E. Gibson. "Interactions of Endoplasmic Reticulum and Mitochondria Ca(2+) Stores with Capacitative Calcium Entry." *Metab Brain Dis* 29, no. 4 (Dec 2014): 1083-93.

Hughes, A. L., and D. E. Gottschling. "An Early Age Increase in Vacuolar Ph Limits Mitochondrial Function and Lifespan in Yeast." *Nature* 492, no. 7428 (Dec 13 2012): 261-5.

Huotari, J., and A. Helenius. "Endosome Maturation." *EMBO J* 30, no. 17 (Aug 31 2011): 3481-500.

"Induced Pluripotent Stem Cells from Patients with Huntington's Disease Show Cag-Repeat-Expansion-Associated Phenotypes." *Cell Stem Cell* 11, no. 2 (Aug 3 2012): 264-78.

Infante, R. E., M. L. Wang, A. Radhakrishnan, H. J. Kwon, M. S. Brown, and J. L. Goldstein. "Npc2 Facilitates Bidirectional Transfer of Cholesterol between Npc1 and Lipid Bilayers, a Step in Cholesterol Egress from Lysosomes." *Proc Natl Acad Sci U S A* 105, no. 40 (Oct 7 2008): 15287-92.

Ioannou, Y. A. "Guilty until Proven Innocent: The Case of Npc1 and Cholesterol." *Trends Biochem Sci* 30, no. 9 (Sep 2005): 498-505.

Isaacs, A. M., P. Johannsen, I. Holm, and J. E. Nielsen. "Frontotemporal Dementia Caused by Chmp2b Mutations." *Curr Alzheimer Res* 8, no. 3 (May 2011): 246-51.

Jefferies, H. B., F. T. Cooke, P. Jat, C. Boucheron, T. Koizumi, M. Hayakawa, H. Kaizawa*, et al.* "A Selective Pikfyve Inhibitor Blocks Ptdins(3,5)P(2) Production and Disrupts Endomembrane Transport and Retroviral Budding." [In eng]. *EMBO Rep* 9, no. 2 (Feb 2008): 164-70.

Jennings, J. J., Jr., J. H. Zhu, Y. Rbaibi, X. Luo, C. T. Chu, and K. Kiselyov. "Mitochondrial Aberrations in Mucolipidosis Type Iv." *J Biol Chem* 281, no. 51 (Dec 22 2006): 39041-50.

Jentsch, T. J., M. B. Hoegg-Beiler, and J. Vogt. "Departure Gate of Acidic Ca(2)(+) Confirmed." *EMBO J* 34, no. 13 (Jul 2 2015): 1737-9.

Ji, Z. S., K. Mullendorff, I. H. Cheng, R. D. Miranda, Y. Huang, and R. W. Mahley. "Reactivity of Apolipoprotein E4 and Amyloid Beta Peptide: Lysosomal Stability and Neurodegeneration." *J Biol Chem* 281, no. 5 (Feb 3 2006): 2683-92.

Jiang, Y., K. A. Mullaney, C. M. Peterhoff, S. Che, S. D. Schmidt, A. Boyer-Boiteau, S. D. Ginsberg*, et al.* "Alzheimer's-Related Endosome Dysfunction in Down Syndrome Is Abeta-Independent but Requires App and Is Reversed by Bace-1 Inhibition." *Proc Natl Acad Sci U S A* 107, no. 4 (Jan 26 2010): 1630-5.

Jin, L. W., F. S. Shie, I. Maezawa, I. Vincent, and T. Bird. "Intracellular Accumulation of Amyloidogenic Fragments of Amyloid-Beta Precursor Protein in Neurons with Niemann-Pick Type C Defects Is Associated with Endosomal Abnormalities." *Am J Pathol* 164, no. 3 (Mar 2004): 975-85.

Kabeya, Y., N. Mizushima, T. Ueno, A. Yamamoto, T. Kirisako, T. Noda, E. Kominami, Y. Ohsumi, and T. Yoshimori. "Lc3, a Mammalian Homologue of Yeast Apg8p, Is Localized in Autophagosome Membranes after Processing." *EMBO J* 19, no. 21 (Nov 1 2000): 5720-8.

Kasper, D., R. Planells-Cases, J. C. Fuhrmann, O. Scheel, O. Zeitz, K. Ruether, A. Schmitt*, et al.* "Loss of the Chloride Channel Clc-7 Leads to Lysosomal Storage Disease and Neurodegeneration." *EMBO J* 24, no. 5 (Mar 9 2005): 1079-91.

Kawai, A., H. Uchiyama, S. Takano, N. Nakamura, and S. Ohkuma. "Autophagosome-Lysosome Fusion Depends on the Ph in Acidic Compartments in Cho Cells." *Autophagy* 3, no. 2 (Mar-Apr 2007): 154-7.

Kempster, P. A., B. Hurwitz, and A. J. Lees. "A New Look at James Parkinson's Essay on the Shaking Palsy." *Neurology* 69, no. 5 (Jul 31 2007): 482-5.

Kilpatrick, B. S., E. R. Eden, A. H. Schapira, C. E. Futter, and S. Patel. "Direct Mobilisation of Lysosomal Ca2+ Triggers Complex Ca2+ Signals." *J Cell Sci* 126, no. Pt 1 (Jan 1 2013): 60-6.

Kim, Y. J., E. Sapp, B. G. Cuiffo, L. Sobin, J. Yoder, K. B. Kegel, Z. H. Qin*, et al.* "Lysosomal Proteases Are Involved in Generation of N-Terminal Huntingtin Fragments." *Neurobiol Dis* 22, no. 2 (May 2006): 346-56.

Kiselyov, K., G. A. Colletti, A. Terwilliger, K. Ketchum, C. W. Lyons, J. Quinn, and S. Muallem. "Trpml: Transporters of Metals in Lysosomes Essential for Cell Survival?" *Cell Calcium* 50, no. 3 (Sep 2011): 288-94.

Kiselyov, K., J. J. Jennigs, Jr., Y. Rbaibi, and C. T. Chu. "Autophagy, Mitochondria and Cell Death in Lysosomal Storage Diseases." *Autophagy* 3, no. 3 (May-Jun 2007): 259-62.

Kitatani, K., J. Idkowiak-Baldys, and Y. A. Hannun. "The Sphingolipid Salvage Pathway in Ceramide Metabolism and Signaling." *Cell Signal* 20, no. 6 (Jun 2008): 1010-8.

Kolter, T., and K. Sandhoff. "Principles of Lysosomal Membrane Digestion: Stimulation of Sphingolipid Degradation by Sphingolipid Activator Proteins and Anionic Lysosomal Lipids." *Annu Rev Cell Dev Biol* 21 (2005): 81-103.

Koo, E. H., and S. L. Squazzo. "Evidence That Production and Release of Amyloid Beta-Protein Involves the Endocytic Pathway." [In eng]. *J Biol Chem* 269, no. 26 (Jul 1 1994): 17386-9.

Korkotian, E., A. Schwarz, D. Pelled, G. Schwarzmann, M. Segal, and A. H. Futerman. "Elevation of Intracellular Glucosylceramide Levels Results in an Increase in Endoplasmic Reticulum Density and in Functional Calcium Stores in Cultured Neurons." *J Biol Chem* 274, no. 31 (Jul 30 1999): 21673-8.

Kovacs, A. D., J. M. Weimer, and D. A. Pearce. "Selectively Increased Sensitivity of Cerebellar Granule Cells to Ampa Receptor-Mediated Excitotoxicity in a Mouse Model of Batten Disease." *Neurobiol Dis* 22, no. 3 (Jun 2006): 575-85.

Kramer, M. L., and W. J. Schulz-Schaeffer. "Presynaptic Alpha-Synuclein Aggregates, Not Lewy Bodies, Cause Neurodegeneration in Dementia with Lewy Bodies." *J Neurosci* 27, no. 6 (Feb 7 2007): 1405-10.

Kreilaus, F., A. S. Spiro, C. A. McLean, B. Garner, and A. M. Jenner. "Evidence for Altered Cholesterol Metabolism in Huntington's Disease Post-Mortem Brain Tissue." *Neuropathol Appl Neurobiol* (Sep 16 2015).

Kress, G. J., K. E. Dineley, and I. J. Reynolds. "The Relationship between Intracellular Free Iron and Cell Injury in Cultured Neurons, Astrocytes, and Oligodendrocytes." *J Neurosci* 22, no. 14 (Jul 15 2002): 5848-55.

Kreutz, F., F. dos Santos Petry, M. Camassola, V. Schein, F. C. Guma, N. B. Nardi, and V. M. Trindade. "Alterations of Membrane Lipids and in Gene Expression of Ganglioside Metabolism in Different Brain Structures in a Mouse Model of Mucopolysaccharidosis Type I (Mps I)." *Gene* 527, no. 1 (Sep 15 2013): 109-14.

Kuemmerle, S., C. A. Gutekunst, A. M. Klein, X. J. Li, S. H. Li, M. F. Beal, S. M. Hersch, and R. J. Ferrante. "Huntington Aggregates May Not Predict Neuronal Death in Huntington's Disease." *Ann Neurol* 46, no. 6 (Dec 1999): 842-9.

Kunkel, G. T., M. Maceyka, S. Milstien, and S. Spiegel. "Targeting the Sphingosine-1-Phosphate Axis in Cancer, Inflammation and Beyond." *Nat Rev Drug Discov* 12, no. 9 (Sep 2013): 688-702.

Kurz, T., J. W. Eaton, and U. T. Brunk. "Redox Activity within the Lysosomal Compartment: Implications for Aging and Apoptosis." *Antioxid Redox Signal* 13, no. 4 (Aug 15 2010): 511-23.

Kwakye, G. F., D. Li, O. A. Kabobel, and A. B. Bowman. "Cellular Fura-2 Manganese Extraction Assay (Cfmea)." *Curr Protoc Toxicol* Chapter 12 (May 2011): Unit12 18.

Kwon, H. J., L. Abi-Mosleh, M. L. Wang, J. Deisenhofer, J. L. Goldstein, M. S. Brown, and R. E. Infante. "Structure of N-Terminal Domain of Npc1 Reveals Distinct Subdomains for Binding and Transfer of Cholesterol." *Cell* 137, no. 7 (Jun 26 2009): 1213-24.

Labbadia, J., and R. I. Morimoto. "Huntington's Disease: Underlying Molecular Mechanisms and Emerging Concepts." *Trends Biochem Sci* 38, no. 8 (Aug 2013): 378-85.

Lachmann, R. H., D. te Vruchte, E. Lloyd-Evans, G. Reinkensmeier, D. J. Sillence, L. Fernandez-Guillen, R. A. Dwek*, et al.* "Treatment with Miglustat Reverses the Lipid-Trafficking Defect in Niemann-Pick Disease Type C." *Neurobiol Dis* 16, no. 3 (Aug 2004): 654-8.

Lambert, J. C., C. A. Ibrahim-Verbaas, D. Harold, A. C. Naj, R. Sims, C. Bellenguez, A. L. DeStafano*, et al.* "Meta-Analysis of 74,046 Individuals Identifies 11 New Susceptibility Loci for Alzheimer's Disease." *Nat Genet* 45, no. 12 (Dec 2013): 1452-8.

Langbehn, D. R., M. R. Hayden, and J. S. Paulsen. "Cag-Repeat Length and the Age of Onset in Huntington Disease (Hd): A Review and Validation Study of Statistical Approaches." *Am J Med Genet B Neuropsychiatr Genet* 153B, no. 2 (Mar 5 2010): 397-408.

LaPlante, J. M., J. Falardeau, M. Sun, M. Kanazirska, E. M. Brown, S. A. Slaugenhaupt, and P. M. Vassilev. "Identification and Characterization of the Single Channel Function of Human Mucolipin-1 Implicated in Mucolipidosis Type Iv, a Disorder Affecting the Lysosomal Pathway." *FEBS Lett* 532, no. 1-2 (Dec 4 2002): 183-7.

Lee, J. H., W. H. Yu, A. Kumar, S. Lee, P. S. Mohan, C. M. Peterhoff, D. M. Wolfe*, et al.* "Lysosomal Proteolysis and Autophagy Require Presenilin 1 and Are Disrupted by Alzheimer-Related Ps1 Mutations." *Cell* 141, no. 7 (Jun 25 2010): 1146-58.

Lee, J. K., H. K. Jin, M. H. Park, B. R. Kim, P. H. Lee, H. Nakauchi, J. E. Carter*, et al.* "Acid Sphingomyelinase Modulates the Autophagic Process by Controlling Lysosomal Biogenesis in Alzheimer's Disease." *J Exp Med* 211, no. 8 (Jul 28 2014): 1551-70.

Lee, S., Y. Sato, and R. A. Nixon. "Primary Lysosomal Dysfunction Causes Cargo-Specific Deficits of Axonal Transport Leading to Alzheimer-Like Neuritic Dystrophy." *Autophagy* 7, no. 12 (Dec 2011): 1562-3.

Lieberman, A. P., R. Puertollano, N. Raben, S. Slaugenhaupt, S. U. Walkley, and A. Ballabio. "Autophagy in Lysosomal Storage Disorders." *Autophagy* 8, no. 5 (May 1 2012): 719-30.

Lilienbaum, A. "Relationship between the Proteasomal System and Autophagy." [In eng]. *Int J Biochem Mol Biol* 4, no. 1 (2013): 1-26.

Lim, J. P., and P. A. Gleeson. "Macropinocytosis: An Endocytic Pathway for Internalising Large Gulps." *Immunol Cell Biol* 89, no. 8 (Nov 2011): 836-43.

Lin, Y. C., J. Y. Wang, K. C. Wang, J. Y. Liao, and I. H. Cheng. "Differential Regulation of Amyloid Precursor Protein Sorting with Pathological Mutations Results in a Distinct Effect on Amyloid-Beta Production." *J Neurochem* 131, no. 4 (Nov 2014): 407-12.

Lin-Moshier, Y., T. F. Walseth, D. Churamani, S. M. Davidson, J. T. Slama, R. Hooper, E. Brailoiu, S. Patel, and J. S. Marchant. "Photoaffinity Labeling of Nicotinic Acid Adenine Dinucleotide Phosphate (Naadp) Targets in Mammalian Cells." *J Biol Chem* 287, no. 4 (Jan 20 2012): 2296-307.

Liu, Z., T. Li, P. Li, N. Wei, Z. Zhao, H. Liang, X. Ji*, et al.* "The Ambiguous Relationship of Oxidative Stress, Tau Hyperphosphorylation, and Autophagy Dysfunction in Alzheimer's Disease." *Oxid Med Cell Longev* 2015 (2015): 352723.

Lloyd-Evans, E., A. J. Morgan, X. He, D. A. Smith, E. Elliot-Smith, D. J. Sillence, G. C. Churchill*, et al.* "Niemann-Pick Disease Type C1 Is a Sphingosine Storage Disease That Causes Deregulation of Lysosomal Calcium." *Nat Med* 14, no. 11 (Nov 2008): 1247-55.

Lloyd-Evans, E., D. Pelled, C. Riebeling, and A. H. Futerman. "Lyso-Glycosphingolipids Mobilize Calcium from Brain Microsomes Via Multiple Mechanisms." *Biochem J* 375, no. Pt 3 (Nov 1 2003): 561-5.

Lloyd-Evans, E., and F. M. Platt. "Lipids on Trial: The Search for the Offending Metabolite in Niemann-Pick Type C Disease." *Traffic* 11, no. 4 (Apr 2010): 419-28.

Lloyd-Evans, E., H. Waller-Evans, K. Peterneva, and F. M. Platt. "Endolysosomal Calcium Regulation and Disease." *Biochem Soc Trans* 38, no. 6 (Dec 2010): 1458-64.

Lopez, J. J., C. Camello-Almaraz, J. A. Pariente, G. M. Salido, and J. A. Rosado. "Ca2+ Accumulation into Acidic Organelles Mediated by Ca2+- and Vacuolar H+-Atpases in Human Platelets." *Biochem J* 390, no. Pt 1 (Aug 15 2005): 243-52.

Lopez, M. E., and M. P. Scott. "Genetic Dissection of a Cell-Autonomous Neurodegenerative Disorder: Lessons Learned from Mouse Models of Niemann-Pick Disease Type C." *Dis Model Mech* 6, no. 5 (Sep 2013): 1089-100.

Love, S., L. R. Bridges, and C. P. Case. "Neurofibrillary Tangles in Niemann-Pick Disease Type C." *Brain* 118 (Pt 1) (Feb 1995): 119-29.

Luthi-Carter, R., D. M. Taylor, J. Pallos, E. Lambert, A. Amore, A. Parker, H. Moffitt*, et al.* "Sirt2 Inhibition Achieves Neuroprotection by Decreasing Sterol Biosynthesis." *Proc Natl Acad Sci U S A* 107, no. 17 (Apr 27 2010): 7927-32.

Luzio, J. P., P. R. Pryor, and N. A. Bright. "Lysosomes: Fusion and Function." *Nat Rev Mol Cell Biol* 8, no. 8 (Aug 2007): 622-32.

Lwin, A., E. Orvisky, O. Goker-Alpan, M. E. LaMarca, and E. Sidransky. "Glucocerebrosidase Mutations in Subjects with Parkinsonism." *Mol Genet Metab* 81, no. 1 (Jan 2004): 70-3.

Maccioni, R. B., G. Farias, I. Morales, and L. Navarrete. "The Revitalized Tau Hypothesis on Alzheimer's Disease." *Arch Med Res* 41, no. 3 (Apr 2010): 226-31.

Maglione, V., P. Marchi, A. Di Pardo, S. Lingrell, M. Horkey, E. Tidmarsh, and S. Sipione. "Impaired Ganglioside Metabolism in Huntington's Disease and Neuroprotective Role of Gm1." *J Neurosci* 30, no. 11 (Mar 17 2010): 4072-80.

Malakouti-Nejad, M., G. A. Shahidi, M. Rohani, S. M. Shojaee, M. Hashemi, B. Klotzle, J. B. Fan, and E. Elahi. "Identification of P.Gln858* in Atp13a2 in Two Eopd Patients and Presentation of Their Clinical Features." *Neurosci Lett* 577 (Aug 8 2014): 106-11.

Malathi, K., K. Higaki, A. H. Tinkelenberg, D. A. Balderes, D. Almanzar-Paramio, L. J. Wilcox, N. Erdeniz*, et al.* "Mutagenesis of the Putative Sterol-Sensing Domain of Yeast Niemann Pick C-Related Protein Reveals a Primordial Role in Subcellular Sphingolipid Distribution." *J Cell Biol* 164, no. 4 (Feb 16 2004): 547-56.

Malnar, M., S. Hecimovic, N. Mattsson, and H. Zetterberg. "Bidirectional Links between Alzheimer's Disease and Niemann-Pick Type C Disease." *Neurobiol Dis* 72 Pt A (Dec 2014): 37-47.

Manning-Bog, A. B., B. Schule, and J. W. Langston. "Alpha-Synuclein-Glucocerebrosidase Interactions in Pharmacological Gaucher Models: A Biological Link between Gaucher Disease and Parkinsonism." *Neurotoxicology* 30, no. 6 (Nov 2009): 1127-32.

Martina, J. A., B. Lelouvier, and R. Puertollano. "The Calcium Channel Mucolipin-3 Is a Novel Regulator of Trafficking Along the Endosomal Pathway." *Traffic* 10, no. 8 (Aug 2009): 1143-56.

Martinez-Vicente, M., Z. Talloczy, E. Wong, G. Tang, H. Koga, S. Kaushik, R. de Vries*, et al.* "Cargo Recognition Failure Is Responsible for Inefficient Autophagy in Huntington's Disease." *Nat Neurosci* 13, no. 5 (May 2010): 567-76.

Martins, C., H. Hulkova, L. Dridi, V. Dormoy-Raclet, L. Grigoryeva, Y. Choi, A. Langford-Smith*, et al.* "Neuroinflammation, Mitochondrial Defects and Neurodegeneration in Mucopolysaccharidosis Iii Type C Mouse Model." *Brain* 138, no. Pt 2 (Feb 2015): 336-55.

Marullo, M., M. Valenza, V. Leoni, C. Caccia, C. Scarlatti, A. De Mario, C. Zuccato*, et al.* "Pitfalls in the Detection of Cholesterol in Huntington's Disease Models." *PLoS Curr* 4 (2012): e505886e9a1968.

Masters, C. L., G. Simms, N. A. Weinman, G. Multhaup, B. L. McDonald, and K. Beyreuther. "Amyloid Plaque Core Protein in Alzheimer Disease and Down Syndrome." *Proc Natl Acad Sci U S A* 82, no. 12 (Jun 1985): 4245-9.

Matsuo, M., M. Togawa, K. Hirabaru, S. Mochinaga, A. Narita, M. Adachi, M. Egashira, T. Irie, and K. Ohno. "Effects of Cyclodextrin in Two Patients with Niemann-Pick Type C Disease." *Mol Genet Metab* 108, no. 1 (Jan 2013): 76-81.

Mattera, R., M. Boehm, R. Chaudhuri, Y. Prabhu, and J. S. Bonifacino. "Conservation and Diversification of Dileucine Signal Recognition by Adaptor Protein (Ap) Complex Variants." *J Biol Chem* 286, no. 3 (Jan 21 2011): 2022-30.

Maue, R. A., R. W. Burgess, B. Wang, C. M. Wooley, K. L. Seburn, M. T. Vanier, M. A. Rogers*, et al.* "A Novel Mouse Model of Niemann-Pick Type C Disease Carrying a D1005g-Npc1 Mutation Comparable to Commonly Observed Human Mutations." *Hum Mol Genet* 21, no. 4 (Feb 15 2012): 730-50.

Maulik, M., G. Thinakaran, and S. Kar. "Alterations in Gene Expression in Mutant Amyloid Precursor Protein Transgenic Mice Lacking Niemann-Pick Type C1 Protein." *PLoS One* 8, no. 1 (2013): e54605.

Mayor, S., and R. E. Pagano. "Pathways of Clathrin-Independent Endocytosis." *Nat Rev Mol Cell Biol* 8, no. 8 (Aug 2007): 603-12.

Mazzulli, J. R., Y. H. Xu, Y. Sun, A. L. Knight, P. J. McLean, G. A. Caldwell, E. Sidransky, G. A. Grabowski, and D. Krainc. "Gaucher Disease Glucocerebrosidase and Alpha-Synuclein Form a Bidirectional Pathogenic Loop in Synucleinopathies." *Cell* 146, no. 1 (Jul 8 2011): 37-52.

McKeith, I. G., D. Galasko, K. Kosaka, E. K. Perry, D. W. Dickson, L. A. Hansen, D. P. Salmon*, et al.* "Consensus Guidelines for the Clinical and Pathologic Diagnosis of Dementia with Lewy Bodies (Dlb): Report of the Consortium on Dlb International Workshop." *Neurology* 47, no. 5 (Nov 1996): 1113-24.

McKeith, I., J. Mintzer, D. Aarsland, D. Burn, H. Chiu, J. Cohen-Mansfield, D. Dickson*, et al.* "Dementia with Lewy Bodies." *Lancet Neurol* 3, no. 1 (Jan 2004): 19-28.

McKhann, G. M., D. S. Knopman, H. Chertkow, B. T. Hyman, C. R. Jack, Jr., C. H. Kawas, W. E. Klunk*, et al.* "The Diagnosis of Dementia Due to Alzheimer's Disease: Recommendations from the National Institute on Aging-Alzheimer's Association Workgroups on Diagnostic Guidelines for Alzheimer's Disease." *Alzheimers Dement* 7, no. 3 (May 2011): 263-9.

Medina, D. L., S. Di Paola, I. Peluso, A. Armani, D. De Stefani, R. Venditti, S. Montefusco*, et al.* "Lysosomal Calcium Signalling Regulates Autophagy through Calcineurin and Tfeb." *Nat Cell Biol* 17, no. 3 (Mar 2015): 288-99.

Mei, Y., M. D. Thompson, R. A. Cohen, and X. Tong. "Autophagy and Oxidative Stress in Cardiovascular Diseases." *Biochim Biophys Acta* 1852, no. 2 (Feb 2015): 243-51.

Melikian, H. E. "Neurotransmitter Transporter Trafficking: Endocytosis, Recycling, and Regulation." *Pharmacol Ther* 104, no. 1 (Oct 2004): 17-27.

Metzler, M., V. Legendre-Guillemin, L. Gan, V. Chopra, A. Kwok, P. S. McPherson, and M. R. Hayden. "Hip1 Functions in Clathrin-Mediated Endocytosis through Binding to Clathrin and Adaptor Protein 2." *J Biol Chem* 276, no. 42 (Oct 19 2001): 39271-6.

Miller, W. L. "Steroid Hormone Synthesis in Mitochondria." *Mol Cell Endocrinol* 379, no. 1-2 (Oct 15 2013): 62-73.

Mirzaian, M., P. Wisse, M. J. Ferraz, H. Gold, W. E. Donker-Koopman, M. Verhoek, H. S. Overkleeft*, et al.* "Mass Spectrometric Quantification of Glucosylsphingosine in Plasma and Urine of Type 1 Gaucher Patients Using an Isotope Standard." *Blood Cells Mol Dis* 54, no. 4 (Apr 2015): 307-14.

Mitchell, I. J., A. J. Cooper, and M. R. Griffiths. "The Selective Vulnerability of Striatopallidal Neurons." *Prog Neurobiol* 59, no. 6 (Dec 1999): 691-719.

Morgan, A. J., F. M. Platt, E. Lloyd-Evans, and A. Galione. "Molecular Mechanisms of Endolysosomal Ca2+ Signalling in Health and Disease." *Biochem J* 439, no. 3 (Nov 1 2011): 349-74.

Mousavi, S. A., L. Malerod, T. Berg, and R. Kjeken. "Clathrin-Dependent Endocytosis." *Biochem J* 377, no. Pt 1 (Jan 1 2004): 1-16.

Muench, S. P., J. Trinick, and M. A. Harrison. "Structural Divergence of the Rotary Atpases." *Q Rev Biophys* 44, no. 3 (Aug 2011): 311-56.

Mullan, M., F. Crawford, K. Axelman, H. Houlden, L. Lilius, B. Winblad, and L. Lannfelt. "A Pathogenic Mutation for Probable Alzheimer's Disease in the App Gene at the N-Terminus of Beta-Amyloid." *Nat Genet* 1, no. 5 (Aug 1992): 345-7.

Mullin, S., and A. Schapira. "The Genetics of Parkinson's Disease." *Br Med Bull* 114, no. 1 (Jun 2015): 39-52.

Murphy, K. E., L. Cottle, A. M. Gysbers, A. A. Cooper, and G. M. Halliday. "Atp13a2 (Park9) Protein Levels Are Reduced in Brain Tissue of Cases with Lewy Bodies." *Acta Neuropathol Commun* 1 (2013): 11.

Murrell, J., M. Farlow, B. Ghetti, and M. D. Benson. "A Mutation in the Amyloid Precursor Protein Associated with Hereditary Alzheimer's Disease." *Science* 254, no. 5028 (Oct 4 1991): 97-9.

Mutoh, T., N. Kawamura, Y. Hirabayashi, S. Shima, T. Miyashita, S. Ito, K. Asakura*, et al.* "Abnormal Cross-Talk between Mutant Presenilin 1 (I143t, G384a) and Glycosphingolipid Biosynthesis." *FASEB J* 26, no. 7 (Jul 2012): 3065-74.

Nalls, M. A., R. Duran, G. Lopez, M. Kurzawa-Akanbi, I. G. McKeith, P. F. Chinnery, C. M. Morris*, et al.* "A Multicenter Study of Glucocerebrosidase Mutations in Dementia with Lewy Bodies." *JAMA Neurol* 70, no. 6 (Jun 2013): 727-35.

Naylor, E., A. Arredouani, S. R. Vasudevan, A. M. Lewis, R. Parkesh, A. Mizote, D. Rosen*, et al.* "Identification of a Chemical Probe for Naadp by Virtual Screening." *Nat Chem Biol* 5, no. 4 (Apr 2009): 220-6.

Neculai, D., M. Schwake, M. Ravichandran, F. Zunke, R. F. Collins, J. Peters, M. Neculai*, et al.* "Structure of Limp-2 Provides Functional Insights with Implications for Sr-Bi and Cd36." *Nature* 504, no. 7478 (Dec 5 2013): 172-6.

Nedelsky, N. B., P. K. Todd, and J. P. Taylor. "Autophagy and the Ubiquitin-Proteasome System: Collaborators in Neuroprotection." *Biochim Biophys Acta* 1782, no. 12 (Dec 2008): 691-9.

Neely Kayala, K. M., G. D. Dickinson, A. Minassian, K. C. Walls, K. N. Green, and F. M. Laferla. "Presenilin-Null Cells Have Altered Two-Pore Calcium Channel Expression and Lysosomal Calcium: Implications for Lysosomal Function." *Brain Res* 1489 (Dec 13 2012): 8-16.

Neudorfer, O., N. Giladi, D. Elstein, A. Abrahamov, T. Turezkite, E. Aghai, A. Reches, B. Bembi, and A. Zimran. "Occurrence of Parkinson's Syndrome in Type I Gaucher Disease." *QJM* 89, no. 9 (Sep 1996): 691-4.

Nicolas, G., C. Charbonnier, D. Wallon, O. Quenez, C. Bellenguez, B. Grenier-Boley, S. Rousseau*, et al.* "Sorl1 Rare Variants: A Major Risk Factor for Familial Early-Onset Alzheimer's Disease." *Mol Psychiatry* (Aug 25 2015).

Nilius, B., G. Owsianik, T. Voets, and J. A. Peters. "Transient Receptor Potential Cation Channels in Disease." *Physiol Rev* 87, no. 1 (Jan 2007): 165-217.

Nilsberth, C., A. Westlind-Danielsson, C. B. Eckman, M. M. Condron, K. Axelman, C. Forsell, C. Stenh*, et al.* "The 'Arctic' App Mutation (E693g) Causes Alzheimer's Disease by Enhanced Abeta Protofibril Formation." *Nat Neurosci* 4, no. 9 (Sep 2001): 887-93.

Nixon, R. A. "Endosome Function and Dysfunction in Alzheimer's Disease and Other Neurodegenerative Diseases." *Neurobiol Aging* 26, no. 3 (Mar 2005): 373-82.

Nixon, R.A. "The Role of Autophagy in Neurodegenerative Disease." *Nat Med* 19, no. 8 (Aug 2013): 983-97.

Nomura, S., T. Umeda, T. Tomiyama, and H. Mori. "The E693delta (Osaka) Mutation in Amyloid Precursor Protein Potentiates Cholesterol-Mediated Intracellular Amyloid Beta Toxicity Via Its Impaired Cholesterol Efflux." *J Neurosci Res* 91, no. 12 (Dec 2013): 1541-50.

"A Novel Gene Containing a Trinucleotide Repeat That Is Expanded and Unstable on Huntington's Disease Chromosomes. The Huntington's Disease Collaborative Research Group." *Cell* 72, no. 6 (Mar 26 1993): 971-83.

Nujic, K., M. Banjanac, V. Munic, D. Polancec, and V. Erakovic Haber. "Impairment of Lysosomal Functions by Azithromycin and Chloroquine Contributes to Anti-Inflammatory Phenotype." *Cell Immunol* 279, no. 1 (Sep 2012): 78-86.

Nuytemans, K., J. Theuns, M. Cruts, and C. Van Broeckhoven. "Genetic Etiology of Parkinson Disease Associated with Mutations in the Snca, Park2, Pink1, Park7, and Lrrk2 Genes: A Mutation Update." *Hum Mutat* 31, no. 7 (Jul 2010): 763-80.

Okouchi, M., O. Ekshyyan, M. Maracine, and T. Y. Aw. "Neuronal Apoptosis in Neurodegeneration." *Antioxid Redox Signal* 9, no. 8 (Aug 2007): 1059-96.

Ottinger, E. A., M. L. Kao, N. Carrillo-Carrasco, N. Yanjanin, R. K. Shankar, M. Janssen, M. Brewster*, et al.* "Collaborative Development of 2-Hydroxypropyl-Beta-Cyclodextrin for the Treatment of Niemann-Pick Type C1 Disease." *Curr Top Med Chem* 14, no. 3 (2014): 330-9.

Ottis, P., K. Koppe, B. Onisko, I. Dynin, T. Arzberger, H. Kretzschmar, J. R. Requena*, et al.* "Human and Rat Brain Lipofuscin Proteome." *Proteomics* 12, no. 15-16 (Aug 2012): 2445-54.

Pagano, R. E. "Endocytic Trafficking of Glycosphingolipids in Sphingolipid Storage Diseases." *Philos Trans R Soc Lond B Biol Sci* 358, no. 1433 (May 29 2003): 885-91.

Pagano, R. E., V. Puri, M. Dominguez, and D. L. Marks. "Membrane Traffic in Sphingolipid Storage Diseases." *Traffic* 1, no. 11 (Nov 2000): 807-15.

Pan, L. S., Z. Wang, D. Ding, X. P. Zhu, H. L. Leng, X. B. Deng, and Y. M. Xu. "Lack of Association between the Atp13a2 A746t Variant and Parkinson's Disease Susceptibility in Han Chinese: A Meta-Analysis." *Int J Neurosci* (Jun 5 2015): 1-7.

Park, J. H., and E. H. Schuchman. "Acid Ceramidase and Human Disease." *Biochim Biophys Acta* 1758, no. 12 (Dec 2006): 2133-8.

Park, J. S., N. F. Blair, and C. M. Sue. "The Role of Atp13a2 in Parkinson's Disease: Clinical Phenotypes and Molecular Mechanisms." *Mov Disord* 30, no. 6 (May 2015): 770-9.

Park, J. S., B. Koentjoro, D. Veivers, A. Mackay-Sim, and C. M. Sue. "Parkinson's Disease-Associated Human Atp13a2 (Park9) Deficiency Causes Zinc Dyshomeostasis and Mitochondrial Dysfunction." *Hum Mol Genet* 23, no. 11 (Jun 1 2014): 2802-15.

Parkesh, R., A. M. Lewis, P. K. Aley, A. Arredouani, S. Rossi, R. Tavares, S. R. Vasudevan*, et al.* "Cell-Permeant Naadp: A Novel Chemical Tool Enabling the Study of Ca2+ Signalling in Intact Cells." *Cell Calcium* 43, no. 6 (Jun 2008): 531-8.

Pasternak, S. H., R. D. Bagshaw, M. Guiral, S. Zhang, C. A. Ackerley, B. J. Pak, J. W. Callahan, and D. J. Mahuran. "Presenilin-1, Nicastrin, Amyloid Precursor Protein, and Gamma-Secretase Activity Are Co-Localized in the Lysosomal Membrane." *J Biol Chem* 278, no. 29 (Jul 18 2003): 26687-94.

Pastores GM, Hughes DA. Gaucher Disease. 2000 Jul 27 [Updated 2015 Feb 26]. In: Pagon RA, Adam MP, Ardinger HH, et al., editors. GeneReviews® [Internet]. Seattle (WA): University of Washington, Seattle; 1993-2016.Available from: http://www.ncbi.nlm.nih.gov/books/NBK1269/

Patterson, M. C., E. Mengel, M. T. Vanier, B. Schwierin, A. Muller, P. Cornelisse, and M. Pineda. "Stable or Improved Neurological Manifestations During Miglustat Therapy in Patients from the International Disease Registry for Niemann-Pick Disease Type C: An Observational Cohort Study." *Orphanet J Rare Dis* 10 (2015): 65.

Patterson, M. C., D. Vecchio, H. Prady, L. Abel, and J. E. Wraith. "Miglustat for Treatment of Niemann-Pick C Disease: A Randomised Controlled Study." *Lancet Neurol* 6, no. 9 (Sep 2007): 765-72.

Pelled, D., S. Trajkovic-Bodennec, E. Lloyd-Evans, E. Sidransky, R. Schiffmann, and A. H. Futerman. "Enhanced Calcium Release in the Acute Neuronopathic Form of Gaucher Disease." *Neurobiol Dis* 18, no. 1 (Feb 2005): 83-8.

Penny, C. J., B. S. Kilpatrick, E. R. Eden, and S. Patel. "Coupling Acidic Organelles with the Er through Ca(2+) Microdomains at Membrane Contact Sites." *Cell Calcium* 58, no. 4 (Oct 2015): 387-96.

Petkau, T. L., and B. R. Leavitt. "Progranulin in Neurodegenerative Disease." *Trends Neurosci* 37, no. 7 (Jul 2014): 388-98.

Piotrowska, E., J. Jakobkiewicz-Banecka, A. Maryniak, A. Tylki-Szymanska, E. Puk, A. Liberek, A. Wegrzyn*, et al.* "Two-Year Follow-up of Sanfilippo Disease Patients Treated with a Genistein-Rich Isoflavone Extract: Assessment of Effects on Cognitive Functions and General Status of Patients." *Med Sci Monit* 17, no. 4 (Apr 2011): CR196-202.

Pitt, S. J., T. M. Funnell, M. Sitsapesan, E. Venturi, K. Rietdorf, M. Ruas, A. Ganesan*, et al.* "Tpc2 Is a Novel Naadp-Sensitive Ca2+ Release Channel, Operating as a Dual Sensor of Luminal Ph and Ca2+." *J Biol Chem* 285, no. 45 (Nov 5 2010): 35039-46.

Platt, F. M. "Sphingolipid Lysosomal Storage Disorders." *Nature* 510, no. 7503 (Jun 5 2014): 68-75.

Platt, F. M., B. Boland, and A. C. van der Spoel. "The Cell Biology of Disease: Lysosomal Storage Disorders: The Cellular Impact of Lysosomal Dysfunction." *J Cell Biol* 199, no. 5 (Nov 26 2012): 723-34.

Platt, F. M., G. R. Neises, G. B. Karlsson, R. A. Dwek, and T. D. Butters. "N-Butyldeoxygalactonojirimycin Inhibits Glycolipid Biosynthesis but Does Not Affect N-Linked Oligosaccharide Processing." *J Biol Chem* 269, no. 43 (Oct 28 1994): 27108-14.

Platt, F. M., C. Wassif, A. Colaco, A. Dardis, E. Lloyd-Evans, B. Bembi, and F. D. Porter. "Disorders of Cholesterol Metabolism and Their Unanticipated Convergent Mechanisms of Disease." *Annu Rev Genomics Hum Genet* 15 (2014): 173-94.

Pontikis, C. C., C. D. Davidson, S. U. Walkley, F. M. Platt, and D. J. Begley. "Cyclodextrin Alleviates Neuronal Storage of Cholesterol in Niemann-Pick C Disease without Evidence of Detectable Blood-Brain Barrier Permeability." *J Inherit Metab Dis* 36, no. 3 (May 2013): 491-8.

Popescu, A., C. F. Lippa, V. M. Lee, and J. Q. Trojanowski. "Lewy Bodies in the Amygdala: Increase of Alpha-Synuclein Aggregates in Neurodegenerative Diseases with Tau-Based Inclusions." *Arch Neurol* 61, no. 12 (Dec 2004): 1915-9.

Popugaeva, E., and I. Bezprozvanny. "Role of Endoplasmic Reticulum Ca2+ Signaling in the Pathogenesis of Alzheimer Disease." *Front Mol Neurosci* 6 (2013): 29.

Poteryaev, D., S. Datta, K. Ackema, M. Zerial, and A. Spang. "Identification of the Switch in Early-to-Late Endosome Transition." *Cell* 141, no. 3 (Apr 30 2010): 497-508.

Pryor, P. R., and J. P. Luzio. "Delivery of Endocytosed Membrane Proteins to the Lysosome." *Biochim Biophys Acta* 1793, no. 4 (Apr 2009): 615-24.

Pryor, P. R., B. M. Mullock, N. A. Bright, S. R. Gray, and J. P. Luzio. "The Role of Intraorganellar Ca(2+) in Late Endosome-Lysosome Heterotypic Fusion and in the Reformation of Lysosomes from Hybrid Organelles." *J Cell Biol* 149, no. 5 (May 29 2000): 1053-62.

Raben, N., L. Shea, V. Hill, and P. Plotz. "Monitoring Autophagy in Lysosomal Storage Disorders." *Methods Enzymol* 453 (2009): 417-49.

Radi, E., P. Formichi, G. Di Maio, C. Battisti, and A. Federico. "Altered Apoptosis Regulation in Kufor-Rakeb Syndrome Patients with Mutations in the Atp13a2 Gene." *J Cell Mol Med* 16, no. 8 (Aug 2012): 1916-23.

Ramirez, A., A. Heimbach, J. Grundemann, B. Stiller, D. Hampshire, L. P. Cid, I. Goebel*, et al.* "Hereditary Parkinsonism with Dementia Is Caused by Mutations in Atp13a2, Encoding a Lysosomal Type 5 P-Type Atpase." *Nat Genet* 38, no. 10 (Oct 2006): 1184-91.

Ramonet, D., A. Podhajska, K. Stafa, S. Sonnay, A. Trancikova, E. Tsika, O. Pletnikova*, et al.* "Park9-Associated Atp13a2 Localizes to Intracellular Acidic Vesicles and Regulates Cation Homeostasis and Neuronal Integrity.". *Hum Mol Genet* 21, no. 8 (Apr 15 2012): 1725-43.

Rauniyar, N., and J. R. Yates, 3rd. "Isobaric Labeling-Based Relative Quantification in Shotgun Proteomics." *J Proteome Res* 13, no. 12 (Dec 5 2014): 5293-309.

Raux, G., L. Guyant-Marechal, C. Martin, J. Bou, C. Penet, A. Brice, D. Hannequin, T. Frebourg, and D. Campion. "Molecular Diagnosis of Autosomal Dominant Early Onset Alzheimer's Disease: An Update." *J Med Genet* 42, no. 10 (Oct 2005): 793-5.

Ravina, B., M. Romer, R. Constantinescu, K. Biglan, A. Brocht, K. Kieburtz, I. Shoulson, and M. P. McDermott. "The Relationship between Cag Repeat Length and Clinical Progression in Huntington's Disease." *Mov Disord* 23, no. 9 (Jul 15 2008): 1223-7.

Raychowdhury, M. K., S. Gonzalez-Perrett, N. Montalbetti, G. A. Timpanaro, B. Chasan, W. H. Goldmann, S. Stahl*, et al.* "Molecular Pathophysiology of Mucolipidosis Type Iv: Ph Dysregulation of the Mucolipin-1 Cation Channel." *Hum Mol Genet* 13, no. 6 (Mar 15 2004): 617-27.

Rizzo, W. B., R. T. Leshner, A. Odone, A. L. Dammann, D. A. Craft, M. E. Jensen, S. S. Jennings*, et al.* "Dietary Erucic Acid Therapy for X-Linked Adrenoleukodystrophy." *Neurology* 39, no. 11 (Nov 1989): 1415-22.

Robinet, P., A. Fradagrada, M. N. Monier, M. Marchetti, A. Cogny, N. Moatti, J. L. Paul, B. Vedie, and C. Lamaze. "Dynamin Is Involved in Endolysosomal Cholesterol Delivery to the Endoplasmic Reticulum: Role in Cholesterol Homeostasis." *Traffic* 7, no. 7 (Jul 2006): 811-23.

Rodda, R. A. "Cerebellar Atrophy in Huntington's Disease." *J Neurol Sci* 50, no. 1 (Apr 1981): 147-57.

Roeber, S., F. Muller-Sarnowski, J. Kress, D. Edbauer, T. Kuhlmann, F. Tuttelmann, C. Schindler*, et al.* "Three Novel Presenilin 1 Mutations Marking the Wide Spectrum of Age at Onset and Clinical Patterns in Familial Alzheimer's Disease." *J Neural Transm* (Sep 8 2015).

Rosenthal, S. L., and M. I. Kamboh. "Late-Onset Alzheimer's Disease Genes and the Potentially Implicated Pathways." *Curr Genet Med Rep* 2 (2014): 85-101.

Ross, C. A. "Polyglutamine Pathogenesis: Emergence of Unifying Mechanisms for Huntington's Disease and Related Disorders." *Neuron* 35, no. 5 (Aug 29 2002): 819-22.

Rottach, K. G., R. D. von Maydell, V. E. Das, A. Z. Zivotofsky, A. O. Discenna, J. L. Gordon, D. M. Landis, and R. J. Leigh. "Evidence for Independent Feedback Control of Horizontal and Vertical Saccades from Niemann-Pick Type C Disease." *Vision Res* 37, no. 24 (Dec 1997): 3627-38.

Ruas, M., L. C. Davis, C. C. Chen, A. J. Morgan, K. T. Chuang, T. F. Walseth, C. Grimm*, et al.* "Expression of Ca(2)(+)-Permeable Two-Pore Channels Rescues Naadp Signalling in Tpc-Deficient Cells." *EMBO J* 34, no. 13 (Jul 2 2015): 1743-58.

Rub, U., F. Hoche, E. R. Brunt, H. Heinsen, K. Seidel, D. Del Turco, H. L. Paulson*, et al.* "Degeneration of the Cerebellum in Huntington's Disease (Hd): Possible Relevance for the Clinical Picture and Potential Gateway to Pathological Mechanisms of the Disease Process." *Brain Pathol* 23, no. 2 (Mar 2013): 165-77.

Rui, Y. N., Z. Xu, B. Patel, Z. Chen, D. Chen, A. Tito, G. David*, et al.* "Huntingtin Functions as a Scaffold for Selective Macroautophagy." *Nat Cell Biol* 17, no. 3 (Mar 2015): 262-75.

Ruocco, H. H., I. Lopes-Cendes, T. L. Laurito, L. M. Li, and F. Cendes. "Clinical Presentation of Juvenile Huntington Disease." *Arq Neuropsiquiatr* 64, no. 1 (Mar 2006): 5-9.

Rushton, D. J., V. B. Mattis, C. N. Svendsen, N. D. Allen, and P. J. Kemp. "Stimulation of Gaba-Induced Ca2+ Influx Enhances Maturation of Human Induced Pluripotent Stem Cell-Derived Neurons." *PLoS One* 8, no. 11 (2013): e81031.

Ryhanen, T., J. M. Hyttinen, J. Kopitz, K. Rilla, E. Kuusisto, E. Mannermaa, J. Viiri*, et al.* "Crosstalk between Hsp70 Molecular Chaperone, Lysosomes and Proteasomes in Autophagy-Mediated Proteolysis in Human Retinal Pigment Epithelial Cells." *J Cell Mol Med* 13, no. 9B (Sep 2009): 3616-31.

Saito, Y., K. Suzuki, E. Nanba, T. Yamamoto, K. Ohno, and S. Murayama. "Niemann-Pick Type C Disease: Accelerated Neurofibrillary Tangle Formation and Amyloid Beta Deposition Associated with Apolipoprotein E Epsilon 4 Homozygosity." *Ann Neurol* 52, no. 3 (Sep 2002): 351-5.

Sakai, K., C. Ishida, A. Morinaga, K. Takahashi, and M. Yamada. "Case Study: Somatic Sprouts and Halo-Like Amorphous Materials of the Purkinje Cells in Huntington's Disease." *Cerebellum* (May 12 2015).

Sands, M. S., and B. L. Davidson. "Gene Therapy for Lysosomal Storage Diseases." *Mol Ther* 13, no. 5 (May 2006): 839-49.

Sardi, S. P., S. H. Cheng, and L. S. Shihabuddin. "Gaucher-Related Synucleinopathies: The Examination of Sporadic Neurodegeneration from a Rare (Disease) Angle." *Prog Neurobiol* 125 (Feb 2015): 47-62.

Sarkar, S., and D. C. Rubinsztein. "Huntington's Disease: Degradation of Mutant Huntingtin by Autophagy." *FEBS J* 275, no. 17 (Sep 2008): 4263-70.

Saroussi, S., and N. Nelson. "The Little We Know on the Structure and Machinery of V-Atpase." *J Exp Biol* 212, no. Pt 11 (Jun 2009): 1604-10.

Scarpa, M., C. M. Bellettato, C. Lampe, and D. J. Begley. "Neuronopathic Lysosomal Storage Disorders: Approaches to Treat the Central Nervous System." *Best Pract Res Clin Endocrinol Metab* 29, no. 2 (Mar 2015): 159-71.

Schiffer, D., V. Caldera, M. Mellai, P. Conforti, E. Cattaneo, and C. Zuccato. "Repressor Element-1 Silencing Transcription Factor (Rest) Is Present in Human Control and Huntington's Disease Neurones." *Neuropathol Appl Neurobiol* 40, no. 7 (Dec 2014): 899-910.

Schmidt, K., D. M. Wolfe, B. Stiller, and D. A. Pearce. "Cd2+, Mn2+, Ni2+ and Se2+ Toxicity to Saccharomyces Cerevisiae Lacking Ypk9p the Orthologue of Human Atp13a2." *Biochem Biophys Res Commun* 383, no. 2 (May 29 2009): 198-202.

Schneider, S. A., C. Paisan-Ruiz, N. P. Quinn, A. J. Lees, H. Houlden, J. Hardy, and K. P. Bhatia. "Atp13a2 Mutations (Park9) Cause Neurodegeneration with Brain Iron Accumulation." *Mov Disord* 25, no. 8 (Jun 15 2010): 979-84.

Schondorf, D. C., M. Aureli, F. E. McAllister, C. J. Hindley, F. Mayer, B. Schmid, S. P. Sardi*, et al.* "Ipsc-Derived Neurons from Gba1-Associated Parkinson's Disease Patients Show Autophagic Defects and Impaired Calcium Homeostasis." *Nat Commun* 5 (2014): 4028.

Schroder, B. A., C. Wrocklage, A. Hasilik, and P. Saftig. "The Proteome of Lysosomes." *Proteomics* 10, no. 22 (Nov 2010): 4053-76.

Schueler, U. H., T. Kolter, C. R. Kaneski, G. C. Zirzow, K. Sandhoff, and R. O. Brady. "Correlation between Enzyme Activity and Substrate Storage in a Cell Culture Model System for Gaucher Disease." *J Inherit Metab Dis* 27, no. 5 (2004): 649-58.

Schultheis, P. J., S. M. Fleming, A. K. Clippinger, J. Lewis, T. Tsunemi, B. Giasson, D. W. Dickson*, et al.* "Atp13a2-Deficient Mice Exhibit Neuronal Ceroid

Lipofuscinosis, Limited Alpha-Synuclein Accumulation and Age-Dependent Sensorimotor Deficits." *Hum Mol Genet* 22, no. 10 (May 15 2013): 2067-82.

Schulz, A., A. Kohlschutter, J. Mink, A. Simonati, and R. Williams. "Ncl Diseases - Clinical Perspectives." *Biochim Biophys Acta* 1832, no. 11 (Nov 2013): 1801-6.

Schulze, H., and K. Sandhoff. "Lysosomal Lipid Storage Diseases." *Cold Spring Harb Perspect Biol* 3, no. 6 (Jun 2011).

Schwake, M., B. Schroder, and P. Saftig. "Lysosomal Membrane Proteins and Their Central Role in Physiology." *Traffic* 14, no. 7 (Jul 2013): 739-48.

Scott, C. C., F. Vacca, and J. Gruenberg. "Endosome Maturation, Transport and Functions." *Semin Cell Dev Biol* 31 (Jul 2014): 2-10.

Scott, C., and Y. A. Ioannou. "The Npc1 Protein: Structure Implies Function." *Biochim Biophys Acta* 1685, no. 1-3 (Oct 11 2004): 8-13.

Seehafer, S. S., and D. A. Pearce. "You Say Lipofuscin, We Say Ceroid: Defining Autofluorescent Storage Material." *Neurobiol Aging* 27, no. 4 (Apr 2006): 576-88.

Settembre, C., and A. Ballabio. "Lysosome: Regulator of Lipid Degradation Pathways." *Trends Cell Biol* 24, no. 12 (Dec 2014): 743-50.

Settembre, C., and D. L. Medina. "Tfeb and the Clear Network." *Methods Cell Biol* 126 (2015): 45-62.

Shachar, T., C. Lo Bianco, A. Recchia, C. Wiessner, A. Raas-Rothschild, and A. H. Futerman. "Lysosomal Storage Disorders and Parkinson's Disease: Gaucher Disease and Beyond." *Mov Disord* 26, no. 9 (Aug 1 2011): 1593-604.

Shao, J., and M. I. Diamond. "Polyglutamine Diseases: Emerging Concepts in Pathogenesis and Therapy." *Hum Mol Genet* 16 Spec No. 2 (Oct 15 2007): R115-23.

Shen, D., X. Wang, X. Li, X. Zhang, Z. Yao, S. Dibble, X. P. Dong*, et al.* "Lipid Storage Disorders Block Lysosomal Trafficking by Inhibiting a Trp Channel and Lysosomal Calcium Release." *Nat Commun* 3 (2012): 731.

Shoback, D., T. H. Chen, S. Pratt, and B. Lattyak. "Thapsigargin Stimulates Intracellular Calcium Mobilization and Inhibits Parathyroid Hormone Release." *J Bone Miner Res* 10, no. 5 (May 1995): 743-50.

Sidransky, E., M. A. Nalls, J. O. Aasly, J. Aharon-Peretz, G. Annesi, E. R. Barbosa, A. Bar-Shira*, et al.* "Multicenter Analysis of Glucocerebrosidase Mutations in Parkinson's Disease." *N Engl J Med* 361, no. 17 (Oct 22 2009): 1651-61.

Simpson, M. A., H. Cross, C. Proukakis, D. A. Priestman, D. C. Neville, G. Reinkensmeier, H. Wang*, et al.* "Infantile-Onset Symptomatic Epilepsy Syndrome Caused by a Homozygous Loss-of-Function Mutation of Gm3 Synthase." *Nat Genet* 36, no. 11 (Nov 2004): 1225-9.

Singh, R. D., D. L. Marks, and R. E. Pagano. "Using Fluorescent Sphingolipid Analogs to Study Intracellular Lipid Trafficking." *Curr Protoc Cell Biol* Chapter 24 (Jun 2007): Unit 24 1.

Singh, R. D., V. Puri, J. T. Valiyaveettil, D. L. Marks, R. Bittman, and R. E. Pagano. "Selective Caveolin-1-Dependent Endocytosis of Glycosphingolipids." *Mol Biol Cell* 14, no. 8 (Aug 2003): 3254-65.

Sleat, D. E., J. A. Wiseman, M. El-Banna, S. M. Price, L. Verot, M. M. Shen, G. S. Tint*, et al.* "Genetic Evidence for Nonredundant Functional Cooperativity between Npc1 and Npc2 in Lipid Transport." *Proc Natl Acad Sci U S A* 101, no. 16 (Apr 20 2004): 5886-91.

Sleegers, K., N. Brouwers, I. Gijselinck, J. Theuns, D. Goossens, J. Wauters, J. Del-Favero*, et al.* "App Duplication Is Sufficient to Cause Early Onset Alzheimer's Dementia with Cerebral Amyloid Angiopathy." *Brain* 129, no. Pt 11 (Nov 2006): 2977-83.

Snider, B. J., A. M. Fagan, C. Roe, A. R. Shah, E. A. Grant, C. Xiong, J. C. Morris, and D. M. Holtzman. "Cerebrospinal Fluid Biomarkers and Rate of Cognitive Decline in Very Mild Dementia of the Alzheimer Type." *Arch Neurol* 66, no. 5 (May 2009): 638-45.

Sparrow, J. R., and M. Boulton. "Rpe Lipofuscin and Its Role in Retinal Pathobiology." *Exp Eye Res* 80, no. 5 (May 2005): 595-606.

Spies, P. E., D. Slats, J. M. Sjogren, B. P. Kremer, F. R. Verhey, M. G. Rikkert, and M. M. Verbeek. "The Cerebrospinal Fluid Amyloid Beta42/40 Ratio in the Differentiation of Alzheimer's Disease from Non-Alzheimer's Dementia." *Curr Alzheimer Res* 7, no. 5 (Aug 2010): 470-6.

Stein, V. M., A. Crooks, W. Ding, M. Prociuk, P. O'Donnell, C. Bryan, T. Sikora*, et al.* "Miglustat Improves Purkinje Cell Survival and Alters Microglial Phenotype in Feline Niemann-Pick Disease Type C." *J Neuropathol Exp Neurol* 71, no. 5 (May 2012): 434-48.

Striessnig, J., A. Koschak, M. J. Sinnegger-Brauns, A. Hetzenauer, N. K. Nguyen, P. Busquet, G. Pelster, and N. Singewald. "Role of Voltage-Gated L-Type Ca2+ Channel Isoforms for Brain Function." *Biochem Soc Trans* 34, no. Pt 5 (Nov 2006): 903-9.

Sun, M., E. Goldin, S. Stahl, J. L. Falardeau, J. C. Kennedy, J. S. Acierno, Jr., C. Bove*, et al.* "Mucolipidosis Type Iv Is Caused by Mutations in a Gene Encoding a Novel Transient Receptor Potential Channel." *Hum Mol Genet* 9, no. 17 (Oct 12 2000): 2471-8.

Surmeier, D. J., J. N. Guzman, J. Sanchez-Padilla, and P. T. Schumacker. "The Role of Calcium and Mitochondrial Oxidant Stress in the Loss of Substantia Nigra Pars Compacta Dopaminergic Neurons in Parkinson's Disease." *Neuroscience* 198 (Dec 15 2011): 221-31.

Suzuki, M., Y. Nagai, K. Wada, and T. Koike. "Calcium Leak through Ryanodine Receptor Is Involved in Neuronal Death Induced by Mutant Huntingtin." *Biochem Biophys Res Commun* 429, no. 1-2 (Dec 7 2012): 18-23.

Taksir, T. V., J. Johnson, C. L. Maloney, E. Yandl, D. Griffiths, B. L. Thurberg, and S. Ryan. "Optimization of a Histopathological Biomarker for Sphingomyelin Accumulation in Acid Sphingomyelinase Deficiency." *J Histochem Cytochem* 60, no. 8 (Aug 2012): 620-9.

Thakur, A. K., M. Jayaraman, R. Mishra, M. Thakur, V. M. Chellgren, I. J. Byeon, D. H. Anjum*, et al.* "Polyglutamine Disruption of the Huntingtin Exon 1 N Terminus Triggers a Complex Aggregation Mechanism." *Nat Struct Mol Biol* 16, no. 4 (Apr 2009): 380-9.

Thimiri Govinda Raj, D. B., B. Ghesquiere, A. K. Tharkeshwar, K. Coen, R. Derua, D. Vanderschaeghe, E. Rysman*, et al.* "A Novel Strategy for the Comprehensive Analysis of the Biomolecular Composition of Isolated Plasma Membranes." *Mol Syst Biol* 7 (2011): 541.

Toei, M., R. Saum, and M. Forgac. "Regulation and Isoform Function of the V-Atpases." *Biochemistry* 49, no. 23 (Jun 15 2010): 4715-23.

Toogood, P. L., P. J. Harvey, J. T. Repine, D. J. Sheehan, S. N. VanderWel, H. Zhou, P. R. Keller*, et al.* "Discovery of a Potent and Selective Inhibitor of Cyclin-Dependent Kinase 4/6." *J Med Chem* 48, no. 7 (Apr 7 2005): 2388-406.

Troulinaki, K., and N. Tavernarakis. "Necrotic Cell Death and Neurodegeneration: The Involvement of Endocytosis and Intracellular Trafficking." *Worm* 1, no. 3 (Jul 1 2012): 176-81.

Trushina, E., C. A. Canaria, D. Y. Lee, and C. T. McMurray. "Loss of Caveolin-1 Expression in Knock-in Mouse Model of Huntington's Disease Suppresses Pathophysiology in Vivo." *Hum Mol Genet* 23, no. 1 (Jan 1 2014): 129-44.

Trushina, E., R. D. Singh, R. B. Dyer, S. Cao, V. H. Shah, R. G. Parton, R. E. Pagano, and C. T. McMurray. "Mutant Huntingtin Inhibits Clathrin-Independent Endocytosis and Causes Accumulation of Cholesterol in Vitro and in Vivo." *Hum Mol Genet* 15, no. 24 (Dec 15 2006): 3578-91.

Tsunemi, T., and D. Krainc. "Zn(2)(+) Dyshomeostasis Caused by Loss of Atp13a2/Park9 Leads to Lysosomal Dysfunction and Alpha-Synuclein Accumulation." *Hum Mol Genet* 23, no. 11 (Jun 1 2014): 2791-801.

Tu, H., O. Nelson, A. Bezprozvanny, Z. Wang, S. F. Lee, Y. H. Hao, L. Serneels*, et al.* "Presenilins Form Er Ca2+ Leak Channels, a Function Disrupted by Familial Alzheimer's Disease-Linked Mutations." *Cell* 126, no. 5 (Sep 8 2006): 981-93.

Turner, T. H., J. Goldstein, J. M. Hamilton, M. Jacobson, E. Pirogovsky, G. Peavy, and J. Corey-Bloom. "Behavioral Measures of Saccade Latency and Inhibition in Manifest and Premanifest Huntington's Disease." *J Mot Behav* 43, no. 4 (2011): 295-302.

Ugolino, J., S. Fang, C. Kubisch, and M. J. Monteiro. "Mutant Atp13a2 Proteins Involved in Parkinsonism Are Degraded by Er-Associated Degradation and Sensitize Cells to Er-Stress Induced Cell Death." *Hum Mol Genet* 20, no. 18 (Sep 15 2011): 3565-77.

Usenovic, M., E. Tresse, J. R. Mazzulli, J. P. Taylor, and D. Krainc. "Deficiency of Atp13a2 Leads to Lysosomal Dysfunction, Alpha-Synuclein Accumulation, and Neurotoxicity." *J Neurosci* 32, no. 12 (Mar 21 2012): 4240-6.

Vaarmann, A., S. Gandhi, and A. Y. Abramov. "Dopamine Induces Ca2+ Signaling in Astrocytes through Reactive Oxygen Species Generated by Monoamine Oxidase." *J Biol Chem* 285, no. 32 (Aug 6 2010): 25018-23.

Vaccaro, A. M., M. Tatti, F. Ciaffoni, R. Salvioli, A. Barca, and C. Scerch. "Effect of Saposins a and C on the Enzymatic Hydrolysis of Liposomal Glucosylceramide." *J Biol Chem* 272, no. 27 (Jul 4 1997): 16862-7.

Valenza, M., V. Leoni, A. Tarditi, C. Mariotti, I. Bjorkhem, S. Di Donato, and E. Cattaneo. "Progressive Dysfunction of the Cholesterol Biosynthesis Pathway in the R6/2 Mouse Model of Huntington's Disease." *Neurobiol Dis* 28, no. 1 (Oct 2007): 133-42.

Valenza, M., D. Rigamonti, D. Goffredo, C. Zuccato, S. Fenu, L. Jamot, A. Strand*, et al.* "Dysfunction of the Cholesterol Biosynthetic Pathway in Huntington's Disease." *J Neurosci* 25, no. 43 (Oct 26 2005): 9932-9.

van der Burg, J. M., M. Bjorkqvist, and P. Brundin. "Beyond the Brain: Widespread Pathology in Huntington's Disease." *Lancet Neurol* 8, no. 8 (Aug 2009): 765-74.

van Veen, S., D. M. Sorensen, T. Holemans, H. W. Holen, M. G. Palmgren, and P. Vangheluwe. "Cellular Function and Pathological Role of Atp13a2 and Related P-Type Transport Atpases in Parkinson's Disease and Other Neurological Disorders." *Front Mol Neurosci* 7 (2014): 48.

Vanha-Perttula, T., V. K. Hopsu, V. Sonninen, and G. G. Glenner. "Cathepsin C Activity as Related to Some Histochemical Substrates." *Histochemie* 5, no. 2 (Jul 27 1965): 170-81.

Vanier, M. T. "Lipid Changes in Niemann-Pick Disease Type C Brain: Personal Experience and Review of the Literature." *Neurochem Res* 24, no. 4 (Apr 1999): 481-9.

Vanier, M.T. "Niemann-Pick Disease Type C." *Orphanet J Rare Dis* 5 (2010): 16.

Vanier, M. T., and P. Latour. "Laboratory Diagnosis of Niemann-Pick Disease Type C: The Filipin Staining Test." *Methods Cell Biol* 126 (2015): 357-75.

Vanlandingham, P. A., and B. P. Ceresa. "Rab7 Regulates Late Endocytic Trafficking Downstream of Multivesicular Body Biogenesis and Cargo Sequestration." *J Biol Chem* 284, no. 18 (May 1 2009): 12110-24.

Verkhratsky, A. "The Endoplasmic Reticulum and Neuronal Calcium Signalling." *Cell Calcium* 32, no. 5-6 (Nov-Dec 2002): 393-404.

Viernes, D. R., L. B. Choi, W. G. Kerr, and J. D. Chisholm. "Discovery and Development of Small Molecule Ship Phosphatase Modulators." *Med Res Rev* 34, no. 4 (Jul 2014): 795-824.

Vincent, A. J., R. Gasperini, L. Foa, and D. H. Small. "Astrocytes in Alzheimer's Disease: Emerging Roles in Calcium Dysregulation and Synaptic Plasticity." *J Alzheimers Dis* 22, no. 3 (2010): 699-714.

Vite, C. H., J. H. Bagel, G. P. Swain, M. Prociuk, T. U. Sikora, V. M. Stein, P. O'Donnell*, et al.* "Intracisternal Cyclodextrin Prevents Cerebellar Dysfunction and Purkinje Cell Death in Feline Niemann-Pick Type C1 Disease." *Sci Transl Med* 7, no. 276 (Feb 25 2015): 276ra26.

Vitner, E. B., F. M. Platt, and A. H. Futerman. "Common and Uncommon Pathogenic Cascades in Lysosomal Storage Diseases." *J Biol Chem* 285, no. 27 (Jul 2 2010): 20423-7.

Volterra, A., N. Liaudet, and I. Savtchouk. "Astrocyte Ca(2)(+) Signalling: An Unexpected Complexity." *Nat Rev Neurosci* 15, no. 5 (May 2014): 327-35.

von Trotha, K. T., R. Heun, S. Schmitz, D. Lutjohann, W. Maier, and H. Kolsch. "Influence of Lysosomal Acid Lipase Polymorphisms on Chromosome 10 on the Risk of Alzheimer's Disease and Cholesterol Metabolism." *Neurosci Lett* 402, no. 3 (Jul 24 2006): 262-6.

Vonsattel, J. P., R. H. Myers, T. J. Stevens, R. J. Ferrante, E. D. Bird, and E. P. Richardson, Jr. "Neuropathological Classification of Huntington's Disease." *J Neuropathol Exp Neurol* 44, no. 6 (Nov 1985): 559-77.

Waelter, S., E. Scherzinger, R. Hasenbank, E. Nordhoff, R. Lurz, H. Goehler, C. Gauss*, et al.* "The Huntingtin Interacting Protein Hip1 Is a Clathrin and Alpha-Adaptin-Binding Protein Involved in Receptor-Mediated Endocytosis." *Hum Mol Genet* 10, no. 17 (Aug 15 2001): 1807-17.

Wakabayashi, K., A. M. Gustafson, E. Sidransky, and E. Goldin. "Mucolipidosis Type Iv: An Update." *Mol Genet Metab* 104, no. 3 (Nov 2011): 206-13.

Walker, M. W., and E. Lloyd-Evans. "A Rapid Method for the Preparation of Ultrapure, Functional Lysosomes Using Functionalized Superparamagnetic Iron Oxide Nanoparticles." *Methods Cell Biol* 126 (2015): 21-43.

Walkley, S. U. "Cellular Pathology of Lysosomal Storage Disorders." *Brain Pathol* 8, no. 1 (Jan 1998): 175-93.

Walkley, S. U., H. J. Baker, and M. C. Rattazzi. "Initiation and Growth of Ectopic Neurites and Meganeurites During Postnatal Cortical Development in Ganglioside Storage Disease." *Brain Res Dev Brain Res* 51, no. 2 (Feb 1 1990): 167-78.

Walkley, S. U., and L. F. James. "Locoweed-Induced Neuronal Storage Disease Characterized by Meganeurite Formation." *Brain Res* 324, no. 1 (Dec 17 1984): 145-50.

Waller-Evans, H., and E. Lloyd-Evans. "Regulation of Trpml1 Function." *Biochem Soc Trans* 43, no. 3 (Jun 2015): 442-6.

Walsh, D. M., and D. J. Selkoe. "A Beta Oligomers - a Decade of Discovery." *J Neurochem* 101, no. 5 (Jun 2007): 1172-84.

Wang, F., W. Song, G. Brancati, and L. Segatori. "Inhibition of Endoplasmic Reticulum-Associated Degradation Rescues Native Folding in Loss of Function Protein Misfolding Diseases." *J Biol Chem* 286, no. 50 (Dec 16 2011): 43454-64.

Wang, X., A. Diaz, L. Hao, B. Gancarz, J. A. den Boon, and P. Ahlquist. "Intersection of the Multivesicular Body Pathway and Lipid Homeostasis in Rna Replication by a Positive-Strand Rna Virus." *J Virol* 85, no. 11 (Jun 2011): 5494-503.

Wang, X., X. Zhang, X. P. Dong, M. Samie, X. Li, X. Cheng, A. Goschka*, et al.* "Tpc Proteins Are Phosphoinositide- Activated Sodium-Selective Ion Channels in Endosomes and Lysosomes." *Cell* 151, no. 2 (Oct 12 2012): 372-83.

Wang, Y., M. Martinez-Vicente, U. Kruger, S. Kaushik, E. Wong, E. M. Mandelkow, A. M. Cuervo, and E. Mandelkow. "Tau Fragmentation, Aggregation and Clearance: The Dual Role of Lysosomal Processing." *Hum Mol Genet* 18, no. 21 (Nov 1 2009): 4153-70.

Wang, Y., and Z. H. Qin. "Molecular and Cellular Mechanisms of Excitotoxic Neuronal Death." *Apoptosis* 15, no. 11 (Nov 2010): 1382-402.

Warby SC, Graham RK, Hayden MR. Huntington Disease. 1998 Oct 23 [Updated 2014 Dec 11]. In: Pagon RA, Adam MP, Ardinger HH, et al., editors. GeneReviews® [Internet]. Seattle (WA): University of Washington, Seattle; 1993-2016.Available from: http://www.ncbi.nlm.nih.gov/books/NBK1305/

Weiner, M. W., and D. P. Veitch. "Introduction to Special Issue: Overview of Alzheimer's Disease Neuroimaging Initiative." *Alzheimers Dement* 11, no. 7 (Jul 2015): 730-3.

White, E. "The Role for Autophagy in Cancer." *J Clin Invest* 125, no. 1 (Jan 2015): 42-6.

Williams, I. M., K. L. Wallom, D. A. Smith, N. Al Eisa, C. Smith, and F. M. Platt. "Improved Neuroprotection Using Miglustat, Curcumin and Ibuprofen as a Triple Combination Therapy in Niemann-Pick Disease Type C1 Mice." *Neurobiol Dis* 67 (Jul 2014): 9-17.

Wohlke, A., U. Philipp, P. Bock, A. Beineke, P. Lichtner, T. Meitinger, and O. Distl. "A One Base Pair Deletion in the Canine Atp13a2 Gene Causes Exon Skipping and Late-Onset Neuronal Ceroid Lipofuscinosis in the Tibetan Terrier." *PLoS Genet* 7, no. 10 (Oct 2011): e1002304.

Wolfe, D. M., J. H. Lee, A. Kumar, S. Lee, S. J. Orenstein, and R. A. Nixon. "Autophagy Failure in Alzheimer's Disease and the Role of Defective Lysosomal Acidification." *Eur J Neurosci* 37, no. 12 (Jun 2013): 1949-61.

Wong, K., E. Sidransky, A. Verma, T. Mixon, G. D. Sandberg, L. K. Wakefield, A. Morrison*, et al.* "Neuropathology Provides Clues to the Pathophysiology of Gaucher Disease." *Mol Genet Metab* 82, no. 3 (Jul 2004): 192-207.

Yang, D. S., A. Kumar, P. Stavrides, J. Peterson, C. M. Peterhoff, M. Pawlik, E. Levy, A. M. Cataldo, and R. A. Nixon. "Neuronal Apoptosis and Autophagy Cross Talk in Aging Ps/App Mice, a Model of Alzheimer's Disease." *Am J Pathol* 173, no. 3 (Sep 2008): 665-81.

Yang, D. S., P. Stavrides, M. Saito, A. Kumar, J. A. Rodriguez-Navarro, M. Pawlik, C. Huo*, et al.* "Defective Macroautophagic Turnover of Brain Lipids in the Tgcrnd8 Alzheimer Mouse Model: Prevention by Correcting Lysosomal Proteolytic Deficits." *Brain* 137, no. Pt 12 (Dec 2014): 3300-18.

Yang, N. D., S. H. Tan, S. Ng, Y. Shi, J. Zhou, K. S. Tan, W. S. Wong, and H. M. Shen. "Artesunate Induces Cell Death in Human Cancer Cells Via Enhancing Lysosomal Function and Lysosomal Degradation of Ferritin." *J Biol Chem* 289, no. 48 (Nov 28 2014): 33425-41.

Yang, X., and Y. Xu. "Mutations in the Atp13a2 Gene and Parkinsonism: A Preliminary Review." *Biomed Res Int* 2014 (2014): 371256.

Zachos, C., J. Blanz, P. Saftig, and M. Schwake. "A Critical Histidine Residue within Limp-2 Mediates Ph Sensitive Binding to Its Ligand Beta-Glucocerebrosidase." *Traffic* 13, no. 8 (Aug 2012): 1113-23.

Zampese, E., C. Fasolato, T. Pozzan, and P. Pizzo. "Presenilin-2 Modulation of Er-Mitochondria Interactions: Fad Mutations, Mechanisms and Pathological Consequences." *Commun Integr Biol* 4, no. 3 (May 2011): 357-60.

Zeitlin, S., J. P. Liu, D. L. Chapman, V. E. Papaioannou, and A. Efstratiadis. "Increased Apoptosis and Early Embryonic Lethality in Mice Nullizygous for the Huntington's Disease Gene Homologue." *Nat Genet* 11, no. 2 (Oct 1995): 155-63.

Zeng, B. J., P. A. Torres, T. C. Viner, Z. H. Wang, S. S. Raghavan, J. Alroy, G. M. Pastores, and E. H. Kolodny. "Spontaneous Appearance of Tay-Sachs Disease in an Animal Model." *Mol Genet Metab* 95, no. 1-2 (Sep-Oct 2008): 59-65.

Zerial, M., and H. McBride. "Rab Proteins as Membrane Organizers." *Nat Rev Mol Cell Biol* 2, no. 2 (Feb 2001): 107-17.

Zervas, M., K. Dobrenis, and S. U. Walkley. "Neurons in Niemann-Pick Disease Type C Accumulate Gangliosides as Well as Unesterified Cholesterol and Undergo Dendritic and Axonal Alterations." *J Neuropathol Exp Neurol* 60, no. 1 (Jan 2001): 49-64.

Zhang, F., M. Xu, W. Q. Han, and P. L. Li. "Reconstitution of Lysosomal Naadp-Trp-Ml1 Signaling Pathway and Its Function in Trp-Ml1(-/-) Cells." *Am J Physiol Cell Physiol* 301, no. 2 (Aug 2011): C421-30.

Zhang, X., X. Li, and H. Xu. "Phosphoinositide Isoforms Determine Compartment-Specific Ion Channel Activity." *Proc Natl Acad Sci U S A* 109, no. 28 (Jul 10 2012): 11384-9.

Zhu, S., Y. Wang, L. Pan, S. Yang, Y. Sun, X. Wang, and F. Hu. "Involvement of Transient Receptor Potential Melastatin-8 (Trpm8) in Menthol-Induced Calcium Entry, Reactive Oxygen Species Production and Cell Death in Rheumatoid Arthritis Rat Synovial Fibroblasts." *Eur J Pharmacol* 725 (Feb 15 2014): 1-9.

Zou, J., B. Hu, S. Arpag, Q. Yan, A. Hamilton, Y. S. Zeng, C. G. Vanoye, and J. Li. "Reactivation of Lysosomal Ca2+ Efflux Rescues Abnormal Lysosomal Storage in Fig4-Deficient Cells." *J Neurosci* 35, no. 17 (Apr 29 2015): 6801-12.

Zuccato, C., M. Tartari, A. Crotti, D. Goffredo, M. Valenza, L. Conti, T. Cataudella*, et al.* "Huntingtin Interacts with Rest/Nrsf to Modulate the Transcription of Nrse-Controlled Neuronal Genes." *Nat Genet* 35, no. 1 (Sep 2003): 76-83.

Zuccato, C., M. Valenza, and E. Cattaneo. "Molecular Mechanisms and Potential Therapeutical Targets in Huntington's Disease." *Physiol Rev* 90, no. 3 (Jul 2010): 905-81.